ORGAN SPECIFIC TOXICITY OF COPPER AND CADMIUM NANOPARTICLES ON SWISS ALBINO MICE

A THESIS SUBMITTED IN PARTIAL FULFILLMENT OF THE REQUIREMENTS FOR THE DEGREE OF DOCTOR OF PHILOSOPHY

BHANUSHREE BAISHYA

MZU REGISTRATION NO.: 2010618

Ph.D. REGISTRATION NO.: MZU/Ph.D/1540 of 04.11.2020

DEPARTMENT OF ZOOLOGY

SCHOOL OF LIFE SCIENCES

AUGUST, 2024

ORGAN SPECIFIC TOXICITY OF COPPER AND CADMIUM NANOPARTICLES ON SWISS ALBINO MICE

By

BHANUSHREE BAISHYA

Department of Zoology

Name of the Supervisor

Prof. GURUSWAMI GURUSUBRAMANIAN

Submitted

In partial fulfillment of the requirement of the Degree of Doctor of Philosophy in Zoology of Mizoram University, Aizawl.

Department of Zoology
School of Life Sciences
MIZORAM UNIVERSITY
(*A Central University*)

Dr. G. Gurusubramanian Ph.D
Professor

Phone: 09862399411 (M)
Email: gurus64@yahoo.com

CERTIFICATE

This is to certify that **Bhanushree Baishya**, Department of Zoology, Mizoram University, has completed her thesis work entitled **"Organ specific toxicity of copper and cadmium nanoparticles on Swiss albino mice"** in partial fulfillment for the Degree of Doctor of Philosophy in Zoology from November 2020-August 2024 under my guidance and supervision. No part of this dissertation has been submitted for any other degree, diploma, associateship, fellowship or other similar titles in this University or any other University or institution of higher learning.

Dated:

Place: Aizawl, Mizoram

Signature of the supervisor

(PROF. G. GURUSUBRAMANIAN)

Department of Zoology

Mizoram University

Aizawl-796004

MIZORAM UNIVERSITY
AIZAWL-796004

DECLARATION

MIZORAM UNIVERSITY

AUGUST, 2024

I **BHANUSHREE BAISHYA**, hereby declare that the subject matter of this thesis is the record of work done by me, that the contents of this thesis did not form basis of the award of any previous degree to me or to the best of my knowledge to anybody else, and that the thesis has not been submitted by me for any research degree in any other University/ Institute.

This is being submitted to the Mizoram University for the **Degree of Doctor of Philosophy** in Zoology.

Date:

Place: Aizawl, Mizoram

(BHANUSHREE BAISHYA)

Department of Zoology
Mizoram University, Aizawl-796004

(PROF. H. T LALREMSANGA)

Head
Department of Zoology
Mizoram University
Aizawl-796004

(PROF. G. GURUSUBRAMANIAN)

Supervisor
Department of Zoology
Mizoram University
Aizawl-796004

ACKNOWLEDGEMENT

At the very outset, I would like to offer my heartiest and deepest gratitude to my supervisor **Prof. G. Gurusubramanian,** Department of Zoology and Dean of Life Sciences, Mizoram University, Aizawl for his valuable guidance, support and inspiration throughout the research work. It has been a privilege working under the supervision of a hardworking, knowledgeable, and experienced person like him, who has always been a source of support and confidence. I sincerely thank him for giving me the freedom to express my thoughts and making the research work an enjoyable one.

I gratefully acknowledge **Prof. H. T Lalremsanga, HoD of Zoology,** Mizoram University, Aizawl for his moral support and helpful advice during my research work.

I would like to express my gratitude to **Dr. Vikas Kumar Roy, Dr. Amit Trivedi**, **Dr, Zothansiama, Dr. Esther Lalhmingliani, Dr. Kiran R. Kharat** and **Dr. M. Vabeiryureilai,** faculties in the department of Zoology for their endless support, blessings, and encouragement during my research work.

I want to offer my special gratitude to my teachers of my PG classes **Prof. Jogen C. Kalita** and **Prof. Dandadhar Sarma**, Department of Zoology, Gauhati University for their constant encouragement, help and support. It is my privileged and proud moment to thank all my teachers I was taught by for shaping my life.

I would like to extend my acknowledgement to the **Central Instrument Facility (CIF) IIT Guwahati** and instrumentation facility at the **Department of Chemistry, Mizoram University** for their immense help, timely support and contribution in my work.

I would like to extend my sincere thanks to all my fellow research scholars, **Bidanchi R Momin, Nisekhoto Nisa, Dr. Dinata Roy, Saeed Ahmed Laskar, Dr. Manikandan B., Pori Buragohain, Abinash Giri, Dr. Khushboo Maurya, Aarti Chettri, Abdulgani Baraka, Mimangsha Dorshan Chkravarty, Andy**

Lalremruata, Sonia Chakma, Chiranjeev Rabha and **Shruti S** for their insightful suggestions, help, cooperation and support.

A special thanks to my husband **Dr. Dhruba Jyoti Borgohain** whose unwavering motivation, inspiration and encouragement made this thesis possible.

And finally, I would like to thank the biggest motivators- my mother **Mrs. Saraswati Baishya,** my father **Mr. Nanda Baishya,** my in-laws and my all-time supportive loving family. I am deeply indebted to them for their sacrifices in shaping my life.

I pray almighty and grateful to universe for what I have.

Aizawl, Mizoram **(BHANUSHREE BAISHYA)**

Dated:

TABLE OF CONTENTS

LIST OF TABLES

values among the groups and different alphabets show significant relationship at $p < 0.05$.

Table 22 Routine observation of mean body weight, food and water consumption and loss/gain in weight, food and water consumption for the 30 days of experimental period are represented in table as mean ± SEM, significant at $p < 0.05$.

Table 23 Observations of organ and relative organ weights in mice after 30 days of CuO-NPs treatment period are represented in table as mean ± SEM, significant at $p < 0.05$.

Table 24 Accumulation of copper was detected in liver, kidney and brain tissue after 30 days of exposure in female mice. The values in the table are represented as mean ± SEM, significant at $p < 0.05$.

Table 25 Effect of CuO-NPs in lipid profiles of female mice after 30 days of treatment. All the data are represented as mean ± SEM, one-way ANOVA was performed to compare the values among the groups and different alphabets show significant relationship at $p < 0.05$.

Table 26 CuO-NPs intake triggers inflammatory response system of female mice after 30 days of treatment. All the data are represented as mean ± SEM, one-way ANOVA was performed to compare the values among the groups and different alphabets show significant relationship at $p < 0.05$.

LIST OF FIGURES

to the control mice. The figure has representation of A and B- ALT; C and D- total bilirubin, creatinine and uric acid; E and F- urea and BUN, in males and females, respectively, significant at $p < 0.05$.

Figure 6 Assessment of oxidative stress biomarker i.e., MDA levels, in five different organs namely, liver **(A)**, kidney **(B)**, brain **(C)**, testis and ovaries **(D)**, and colon **(E)** in male and female mice. All the values are presented as mean ± SEM, significant at $p < 0.05$.

Figure 7 Assessment of antioxidant enzymes status i.e., GST and GSH, in five different organs namely, liver (A), kidney (C), brain (E), testis and ovaries (G), and colon (I) for GST; and also GSH in liver (B), kidney (D), brain (F), testis and ovaries (H), and colon (J) in male and female mice. All the values are presented as mean ± SEM, significant at $p < 0.05$.

Figure 8 Assessment of antioxidant enzymes status i.e., SOD and CAT, in five different organs namely, liver **(A)**, kidney **(C)**, brain **(E)**, testis and ovaries **(G)**, and colon **(I)** for SOD; and also CAT in liver **(B)**, kidney **(D)**, brain **(F)**, testis and ovaries **(H)**, and colon **(J)** in male and female mice. All the values are presented as mean ± SEM, significant at $p < 0.05$.

Figure 9 Histopathological alteration in liver tissue of male and female mice after acute intoxication with CdO-NPs, visible after hematoxylin and eosin staining (H & E). **(A)** Control, **(B** and **F)** CdO 25 mg/kg, **(C** and **G)** CdO 50 mg/kg, **(D** and **H)** CdO 75 mg/kg, **(E)** CdO 5 mg/kg represents liver of male mice at 40X resolution and **(I)** Control (40X), **(J** and **N)** CdO 25 mg/kg (10X and 40X, respectively), **(K** and **O)** CdO 50 mg/kg (10X and 40X, respectively), **(L** and **P)** CdO 75 mg/kg (40X), **(M**) CdO 5 mg/kg (40X). Resolution at 10X and 40X are shown with scale bar 100 and 50 µm, respectively. CV- central vein; Hp- hepatocytes; S- hepatic sinusoid; BH- binucleated hepatocytes; PV- portal vein;

BD- bile duct; hA- hepatic artery; ds- dilated hepatic sinusoid; V- vacuolization; vac- extensive vacuolization; dPV- dilated portal vein; → (black arrow)- inflammatory infiltration; * (star)- multinucleated giant cell; Hem- area of haemorrhage; &- degenerative cell; N- area of necrosis; # (hash)- apoptotic nuclei; ** (double star)- congested central vein.

Figure 10 Micrographs showing histopathological alteration in kidney tissue of male and female mice after acute intoxication with CdO-NPs, visible after hematoxylin and eosin staining (H & E). **(A)** Control (at 10X resolution), **(B** and **F)** CdO 25 mg/kg (10X and 40X, respectively), **(C** and **G)** CdO 50 mg/kg kg (10X and 40X, respectively), **(D** and **H)** CdO 75 mg/kg kg (10X and 40X, respectively), **(E)** CdO 5 mg/kg (10X) represents kidney tissue of male and **(I)** Control (10X), **(J** and **N)** CdO 25 mg/kg (40X), **(K** and **O)** CdO 50 mg/kg (10X and 40X, respectively), **(L** and **P)** CdO 75 mg/kg (10X and 40X, respectively), **(M**) CdO 5 mg/kg (40X) kidney tissue of female mice. Resolution at 10X and 40X are shown with scale bar 100 and 50 µm, respectively. G- glomerulus; PT- proximal convoluted tubule; DT- distal convoluted tubule; CT- collection tubule; BV- blood vessel; dV- dilated vessel; # (hash)- glomerular degeneration with increased glomerular space; vC- vascular congestion; Hem- area of haemorrhage; &- tubular degeneration; tW- tubule with wide lumen space; Ft- fragmentation of tissue; → (black arrow)- inflammatory infiltration; Ap- apoptotic nuclei; @- tubular cast formation; N- area of necrosis.

Figure 11 Micrographs showing histopathological alteration in brain tissue of male and female mice after acute intoxication with CdO-NPs, visible after hematoxylin and eosin staining (H & E). **(A)** Control (40X resolution), **(B** and **F)** CdO 25 mg/kg (10X and 40X, respectively), **(C** and **G)** CdO 50 mg/kg kg (40X), **(D** and **H)**

CdO 75 mg/kg kg (40X), **(E)** CdO 5 mg/kg (40X) represents brain tissue of male and **(I)** Control (10X), **(J** and **N)** CdO 25 mg/kg (40X), **(K** and **O)** CdO 50 mg/kg (10X and 40X, respectively), **(L** and **P)** CdO 75 mg/kg (10X and 40X, respectively), **(M**) CdO 5 mg/kg (40X) brain tissue of female mice. Resolution at 10X and 40X are shown with scale bar 100 and 50 µm, respectively. Pn- Pyramidal neuronal cell; BV- blood vessel; → (black arrow)- inflammatory infiltration; @- darkly stained neuron; Vac- intracytoplasmic vacuolization; V- vacuolization; Ap- cellular apoptosis; N- area of necrosis; Ft- fragmentation of tissue; # (hash)- cellular degeneration; cV- congested vessel.

Figure 12 Micrographs showing histopathological alteration in testis, ovary and uterus of male and female mice after acute intoxication with CdO-NPs, visible after hematoxylin and eosin staining (H & E). **(A)** Control (40X), **(B)** CdO 5 mg/kg (40X), **(C)** CdO 25 mg/kg kg (40X), **(D)** CdO 50 mg/kg kg (40X), **(E)** CdO 75 mg/kg (40X) represents testis tissue of male, St- seminiferous tubule; LC- Leydig cell; Sg- spermatogonia; pSc- primary spermatocyte; sSc- secondary spermatocyte; Sp- spermatid; L- lumen of seminiferous tubule; * (star)- Sertoli cell; → (red arrow)- spermatozoa; V- vacuolization; Hem- haemorrhage; dLC- depletion of Leydig cell; wL- wider lumen space; &- decrease in sperm mass; # (hash)- degeneration of tubule; dSt- disorganization and depletion of seminiferous tubule by tubular necrosis; @- disorganized and sloughing of germ layer. **(F)** Control (10X), **(G)** CdO 5 mg/kg (10X), **(H)** CdO 25 mg/kg (10X), **(I)** CdO 50 mg/kg (10X), **(J)** CdO 75 mg/kg (10X) represent ovary, Pf- primary follicle; Gf- growing follicle; CL- corpus luteum; &- antrum; Gc- granulosa cell; Sf- secondary follicle; @- oocyte; ** (double star)- area of necrosis; # (hash)- follicular degeneration; → (black arrow)-

inflammatory infiltration. **(K**) Control (10X), **(L)** CdO 5 mg/kg (4X), **(M)** CdO 25 mg/kg (4X), **(N)** CdO 50 mg/kg (10X), **(O)** CdO 75 mg/kg (4X) of uterus tissue of female mice, Em- endometrium; Mm- myometrium; Pm- Perimetrium; L- lumen, ECL- epithelial cell layer; UG- uterine gland; dEm- disorganization of endometrium; N- area of necrosis; Hem- haemorrhage; Ap- apoptotic cell. Resolution of testis at 40X are shown with scale bar 50 µm whereas, ovary and uterus at 10X resolution are represented with scale bar 100 µm. Uterus at 4X resolution are shown with 250 µm scale bar.

Figure 13 Histopathological alteration in heart tissue of male and female mice after acute intoxication with CdO-NPs, visible after hematoxylin and eosin staining (H & E). **(A)** Control (4X), **(B)** CdO 5 mg/kg (10X), **(C)** CdO 25 mg/kg kg (10X), **(D)** CdO 50 mg/kg kg (10X), **(E)** CdO 75 mg/kg (10X) represents heart tissue of male, and **(F)** Control (10X), **(G)** CdO 5 mg/kg (10X), **(H)** CdO 25 mg/kg (10X), **(I)** CdO 50 mg/kg (10X), **(J)** CdO 75 mg/kg (10X) represent heart tissue of female mice. Resolution at 4X and 10X are shown with scale bar 200 and 50 µm, respectively. Mc- myocardium; BV- blood vessel; cV- congested vessel; V- vacuolization; Ft- fragmentation of tissue; &- minute tissue haemorrhage; # (hash)- inflammatory infiltration; @- wide intercellular space; Hem- extensive tissue haemorrhage.

Figure 14 Changes in the tissue architecture of lung in male and female mice were evident after histopathological analyses using hematoxylin and eosin staining (H & E). **(A)** Control (10X), **(B)** CdO 5 mg/kg (10X), **(C)** CdO 25 mg/kg kg (10X), **(D)** CdO 50 mg/kg kg (10X), **(E)** CdO 75 mg/kg (10X) represents lung tissue of male, and **(F)** Control (10X), **(G)** CdO 5 mg/kg (10X), **(H)** CdO 25 mg/kg (10X), **(I)** CdO 50 mg/kg (10X), **(J)** CdO 75 mg/kg (10X) represent lung tissue of female mice. Resolution at

performed to compare the values among the groups and different alphabets show significant relationship at $p < 0.05$.

Figure 18 CdO-NPs intake promoted oxidative stress, **(A)** MDA in liver; **(B)** MDA in kidney; **(C)** MDA in brain; and led to the depletion of antioxidant enzymes GST and non-enzymatic antioxidant i.e., GSH in **(D)** & **(G)** liver; **(E)** & **(H)** kidney and **(F)** & **(I)** brain, respectively. The data are represented as mean ± SEM, one-way ANOVA was performed to compare the values among the groups and different alphabets show significant relationship at $p < 0.05$.

Figure 19 CdO-NPs administration resulted in the depletion of enzymatic antioxidants SOD in **(A)** liver, **(C)** kidney and **(E)** brain; and CAT in **(B)** liver, **(D)** kidney and **(F)** brain, respectively. The data are represented as mean ± SEM, one-way ANOVA was performed to compare the values among the groups and different alphabets show significant relationship at $p < 0.05$.

Figure 20 Changes in tissue architecture of liver tissue after CdO-NPs intoxication in female mice for 30 days, visible after hematoxylin and eosin staining (H & E). **A, B, C, D** at 10X, and **E, F, G, H** at 40X resolution with scale bar 100 µm and 50 µm, respectively. **(A** and **E)** Control, **(B** and **F)** CdO-NPs 2 mg/kg, **(C** and **G)** CdO-NPs 5 mg/kg, **(D** and **H)** CdO-NPs 8 mg/kg. CV- congested vein; Hp- hepatocytes; S- hepatic sinusoid; BH- binucleated hepatocytes; PV- portal vein; BD- bile duct; ds- dilated hepatic sinusoid; V- vacuolization; vac- extensive vacuolization; dPV- dilated portal vein; → (black arrow)- inflammatory infiltration; &- degenerative cell; N- area of necrosis; # (hash)- apoptotic nuclei; cPV- congested portal vein.

Figure 21 Histological illustration of tissue damages in kidney after CdO-NPs intake in female mice for 30 days, visible after hematoxylin and eosin staining (H & E). **A, B, C, D** at 10X, and **E, F, G, H** at 40X resolution with scale bar 100 µm and 50 µm, respectively. **(A**

relationship at $p < 0.05$.

Figure 30 Graphs showing status of liver and kidney function biomarkers in blood serum of CuO-NPs treated and normal control group. **(A)** ALP; **(B)** ALT; **(C)** AST; **(D)** urea and blood urea nitrogen; **(E)** AST/ALT; **(F)** creatinine; **(G)** uric acid; **(H)** BUN/creatinine ratio. The data are represented as mean ± SEM, one-way ANOVA was performed to compare the values among the groups and different alphabets show significant relationship at $p < 0.05$.

Figure 31 CuO-NPs consumption triggered oxidative stress, **(A)** MDA in liver; **(D)** MDA in kidney; **(G)** MDA in brain; and led to the depletion of antioxidant enzymes GST and non-enzymatic antioxidant i.e., GSH in **(B)** and **(C)** liver; **(E)** and **(F)** kidney and **(H)** and **(I)** brain, respectively. The data are represented as mean ± SEM, one-way ANOVA was performed to compare the values among the groups and different alphabets show significant relationship at $p < 0.05$.

Figure 32 CuO-NPs consumption led to depletion of antioxidant enzymes SOD and CAT in **(A)** and **(B)** liver; **(C)** and **(D)** kidney, and **(E)** and **(F)** brain, respectively. The data are represented as mean ± SEM, one-way ANOVA was performed to compare the values among the groups and different alphabets show significant relationship at $p < 0.05$.

Figure 33 CuO-NPs intoxication resulted in alteration in tissue architecture of liver after 30 days of treatment in female mice. The alterations are visible after hematoxylin and eosin staining (H & E). **A, B, C, D** and **D1, E, F, G, H** are at 10X (scale bar =100 µm) and 40X (scale bar = 50µm) resolution, respectively. CV- congested vein; Hp- hepatocytes; S- hepatic sinusoid; BH- binucleated hepatocytes; PV- portal vein; BD- bile duct; hA- hepatic artery; ds- dilated hepatic sinusoid; V- vacuolization; vac- extensive vacuolization; dPV- dilated portal vein; → (black arrow)-

ABBREVIATIONS

NPs	Nanoparticles
CdO-NPs	Cadmium oxide nanoparticles
CuO-NPs	Copper oxide nanoparticles
nm	Nanometer
mg	Milligram
kg	Kilogram
ANOVA	Analysis of Variance
BAX	B-cell lymphoma-2-associated X
BCL-2	B cell lymphoma-2
COX-2	Cyclo-oxygenase 2
IL-6	Interleukin-6
IL-1	Interleukin-1
IL-10	Interleukin-10
TNF-α	Tumour necrosis factor α
NF-κB	Nuclear factor kappa-light-chain-enhancer of activated B cells
IL-2	Interleukin-2
P^{53}	Tumour protein P^{53}
IL-1β	Interleukin-1β
IL-4	Interleukin-4
IL-5	Interleukin-5
MPO	Myeloperoxidase
LTB4	Leukotriene B4
PG E2	Prostaglandin E2
TOAC	Total antioxidant capacity
ELISA	Enzyme linked immunosorbent assay
TGF-β	Transforming growth factor-beta
IL-12	Interleukin-12
iNOS	Inducible nitric oxide synthase

NOS-2	Nitric oxide synthase 2
PARP	Poly (ADP-ribose) polymerase
GFAP	Glial fibrillary acidic protein
PMSF	Phenylmethylsulfonyl fluoride
BBB	Blood brain barrier
MO-NPs	Metal oxide nanoparticles
ATSDR	Agency for Toxic Substances and Disease Registry
ROS	Reactive Oxygen Species
WHO	World Health Organization
Zn	Zinc
µg	Microgram
DNA	Deoxyribonucleic acid
GSH	Reduced glutathione
SOD	Superoxide dismutase
CAT	Catalase
GST	Glutathione-S-Transferase
GPx	Glutathione peroxidase
LPO	Lipid peroxidation
MDA	Malondialdehyde
LD_{50}	Medium Lethal dose
OECD	Organization for Economic Co-operation and Development
IARC	International Agency for Research on Cancer
GIT	Gastro intestinal tract
ADMET	Absorption, Distribution, Metabolism, Excretion and Toxicity
QSAR	Quantitative structure–activity relationship
ppm	Parts per million
RBCs	Red blood cells
WBCs	White blood cells

MCV	Mean corpuscular volume
MCHC	Mean corpuscular hemoglobin concentration
MCH	Mean corpuscular hemoglobin
Hb	Hemoglobin
HCT	Hematocrit
PCV	Packer cell volume
ALP	Alkaline phosphatase
AST	Aspartate aminotransferase
ALT	Alanine aminotransferase
LDH	Lactate dehydrogenase
GGT	Gamma glutamyl transferase
Nrf2	Nuclear factor erythrocyte 2-related factor 2
MAO	Monoaminoxidase
NMs	Nano-materials
FAD	Food and Drug Administration
CRP	C-reactive protein
Pb	Lead
V	Vanadium
Ni	Nickel
Kim-1	Kidney injury molecule-1
mRNA	Messenger Ribonucleic acid
NGAL	Neutrophil gelatinase-associated lipocalin
CNS	Central nervous system
MTT	3-(4,5-dimethylthiazolyl-2)-2,5 diphenyltetrazolium bromide
MNi	micronuclei
ATP	Adenosine triphosphate
HepG2	Hepatoblastoma cell line
AChE	Acetylcholinesterase
SOD1	Superoxide dismutase1
HO-1	Heme oxygenase-1

MMP	Mitochondrial membrane potential
SHRs	Spontaneously hypertensive rats
ACE	Angiotensin converting enzyme
ET-1	Endothelin-1
ICAM-1	Intercellular adhesion molecule 1
vWF	von Willebrand factor
IFN-γ	interferon-γ
MW	Molecular weight
nHA	Number of H-bond acceptor
nHD	Number of H-bond donor
nA	Number of atoms
nB	Number of bonds
nRot	Number of rotatable bonds
TPSA	Topological surface area
HSE	Heat shock factor response element
ER-LBD	Estrogen Receptor Ligand Binding Domain
nrf2/ARE	Nuclear factor (erythroid-derived 2)-like 2/antioxidant responsive element
PPAR-ɣ	Peroxisome Proliferator Activated Receptor gamma
THRα	Thyroid hormone receptor alpha
THRβ	Thyroid hormone receptor beta
NADHOX	NADH-quinone oxidoreductase
VGSC	Voltage gated sodium channel
MRTD	Maximum recommended tolerable dose
hERG	Human ether a-a-go gene
LC_{50}	Medium lethal concentration
FETEM	Field emission transmission electron microscopy
FTIR	Fourier Transform Infra-Red
HR	High resolution
SAED	Selected-area electron diffraction

XRD	X-ray diffraction
BUN	Blood urea nitrogen
HDL	High density lipoprotein
LDL	Low density lipoprotein
PBS	Phosphate buffer saline
TCA	Trichloroacetic acid
TBA	Thioburbituric acid
DTNB	5, 5-dithio-bis-(2-nitrobenzoic acid)
TNB	Thionitrobenzoic acid
NBT	Nitroblue tetrazolium
NADH	Nicotinamide adenine dinucleotide
IAEC	Institutional animal ethical committee
AAS	Atomic absorption spectrometry
ECL	Enhanced chemiluminescence
SEM	Standard error mean
VLDL	Very low-density lipoprotein
NAFLD	Non-alcoholic fatty liver disease
Caco-2	Human colorectal adenocarcinoma cell lines-2

CHAPTER- 1

INTRODUCTION

1.1 Overview

The English word **'toxic'** is a Greek derivative of the term ‘toxikon’, which in the context of medical sciences means any substance that can harm animals as well as humans. In Greek, the word 'toxon' means ‘bow’ or ‘arrow’, and later from this term came the word ‘toxikon’, which means ‘a poison in which arrows are dipped’ **(Laios et al., 2021)**. Hence, the adjective **toxicity** can be defined as the degree to which a substance can harm our environment, animals, humans, etc. The study of all noxious substances that have detrimental impacts on organisms and the environment is known as **toxicology (Naz et al., 2020)**.

Naturally occurring elements having a density at least five times greater than that of water and a high atomic weight usually 5 g cm^{-3} are known as **heavy metals**. There are more than sixty elements in the periodic table which are regarded as heavy metals **(Hocaoğlu-özyiğit** and **Genç, 2020)**. Their widespread dispersion in the environment as a result of their numerous industrial, residential, agricultural, medical, and technical applications has raised questions about their possible impacts on human health and the environment. The precise dosage, route of exposure, chemical species, as well as the age, gender, genetics, and nutritional status of the exposed individuals, all have an impact on the toxicity of these substances **(Fergusson, 1990; Tchounwou et al., 2012)**.

In the developing era of science and technology, the utilization of nanoparticles, in particular Metal Oxide Nanoparticles (MO-NPs), has received a lot of attention and relevance in recent years due to their diverse structural characteristics and special abilities that make them valuable for a number of applications **(Zhang et al., 2010; Yaqub et al., 2018)**. Electronics, energy production, industry, and environmental protection are only a few of their various uses. The nanoparticles are chemicals with a size range of 1 to 100 nm. Due to their small size and distinctive qualities, including thermal, optical, mechanical, magnetic, electrical, and electron configuration density, nanoparticles are used in these applications **(Yah et al., 2012; El Bialy et al., 2020)**.

Cadmium (Cd) is ranked as the seventh most toxic heavy metal in accordance with the rating provided by the Agency for Toxic Substances and Disease Registry (ATSDR; **Jaishankar et al., 2014; Young et al., 2019**). The first time this metal was utilized during World War I as a tin substitute and as a pigment in the paint industry. In contemporary times, it is also used to make specialized alloys, rechargeable batteries, coatings, pigments, and platings, as a plastic stabilizer, and additionally, their presence was detected in cigarette smoke **(Jaishankar et al., 2014)**. Cadmium oxide nanoparticles (CdO-NPs) were used in the initial manufacturing process of quantum dots, which are becoming more and more prominent in targeted therapeutics and medical diagnostic imaging **(Demir et al., 2020)**. This metal can cause acute and chronic intoxications in humans, with ingestion and inhalation being the main routes of exposure. Environmental Cd can build up in a variety of organs, including the liver, lungs, testes, and bones **(Micali et al., 2018)**, brain, and kidney **(Micali et al., 2018; Kini et al., 2019)**. As a result of cadmium-induced oxidative stress, mice exposed to the metal undergo weight loss, Cd accumulation in the liver, lipid peroxidation, reduced cellular antioxidant redox potential, and inflammation of the liver, kidney, and brain tissue **(Shafaei et al., 2020)**. However, the mechanism of cadmium toxicity is not known clearly **(Khan et al., 2022)**, but its effects on cells are traced in several works. The concentration of Cd may increase by 3,000fold when it binds to cysteine-rich proteins such as metallothionein. The cysteine-metallothionein complex produces hepatotoxicity in the liver before moving on to the kidney and building up in the renal tissue to create nephrotoxicity. In proteins such as cysteine, glutamate, histidine, and aspartate ligands, cadmium can imitate or replace these important metals **(Castagnetto et al., 2002; Jaishankar et al., 2014)**.

Since ancient times, **copper (Cu)** has been used for various purposes in the field of electronics technology, including semiconductors, electronic chips, metal catalysts, and heat transfer nanofluids, due to their superior thermophysical properties. Additionally, the nanoparticles of copper (CuO-NP) are used in fracture and osteoporosis-treatment drugs, additives in livestock and poultry feed, intrauterine contraceptive devices, and as an alternative antimicrobial agent in many biomedical applications **(Yang et al., 2010; Assadian et al., 2017; Bugata et al., 2018)**.

However, an excessive amount of copper can be ingested through a variety of sources, including drinking water, salt, milk, packaged foods, cosmetics, coatings, batteries, fuel additives, and diagnostic imaging materials, which can have adverse consequences like gastrointestinal issues, liver cirrhosis, multi-organ failure, shock, coma, and occasionally even death **(Araya et al., 2003; Bugata et al., 2018)** through the production of reactive oxygen species (ROS) and depletion of antioxidants **(Bugata et al., 2018; El Bialy et al., 2020)**.

The potential usage of CuO-NPs and CdO-NPs in a variety of applications has made it necessary to examine their potential harmful effects on numerous organ systems. Despite the wide range of applications for these NPs, little is known about their toxicity to organ and cellular systems, as well as the physiological and molecular mechanisms by which they manifest. Therefore, the present study was conducted to investigate the biochemical, morphological, morphometric, metal accumulation, Hematology, oxidative stress, antioxidant status, apoptosis, and their possible pathways that lead to hepato-, renal-, and neurotoxicity in female Swiss albino mice exposed to Cd and Cu NPs. Further, it has been believed that this study will be beneficial to highlight several trends and properties of the NPs that could be considered in the future to design inhibitors, either for drug discovery, therapeutics, biochemical projects, etc.

1.2 Targeted nanoparticle, their applications and concern

1.2.1 Cadmium Oxide Nanoparticles (CdO-NPs)

Cadmium (Cd) is a naturally occurring metal, that exist in the earth's crust comprising 0.1 parts per million **(Bernhoft, 2013).** Cd has a molecular weight of 112.414 g mol^{-1} **(Kadhim** and **Abbar, 2022)**. The cadmium oxide (CdO), which has both semiconductor and piezoelectric properties, is a very unique compound. CdO has a greater Exciton Binding Energy (75 meV) and Gap Energy of around 4.05 (eV) compared to other semiconductors **(Heidari** and **Brown, 2015)**.

According to the World Health Organization (WHO), cadmium (Cd) is a significant environmental contaminant that seriously harms human health and has been identified as a human carcinogen **(Mouro et al., 2019)**. Cadmium pollution in the

environment has been a source of concern since the 1960s, when Cd contamination in a region of Japan was thought to be the cause of the excruciating bone disease "itai-itai,". It was thought to be due to the consumption of rice contamination with Cd. It was discovered that individuals who ingested the contaminated rice and drank the river water over a 30-year period had accumulated significant amounts of cadmium in their bodies, which eventually was enough to cause a serious bone disease similar to osteoporosis known to the Japanese as "itai-itai byo" or "ouch-ouch disease" **(Pan et al., 2010).**

Cd and Zn share similar chemical features in terms of plant absorption and metabolic processes. However, unlike Zn, Cd has hazardous impact on plants, animals, and human beings. Synthetic insecticides and fertilizers are one of the components through which it enters the soil. The fact that it dissolves in water makes it easy to propagate in the natural world. It enters biological systems in the form of Cd^{+2} and has the ability to accumulate in both plants and marine life **(Tripathi et al., 2020; Hocaoğlu-özyiğit and Genç, 2020)**. Commercial uses for Cd include paint pigments, television screens, batteries, cosmetics, lasers, galvanizing steel, welding or soldering and, acting as a barrier in nuclear fission **(Bernhoft, 2013)**.

Depending upon the route, quantity, and rate of exposure, clinical stigmata of Cd toxicity may vary. With an elimination half-life of 10–30 years, cadmium is a common environmental contaminant with a severe harmful effect that builds up in humans as well as animals **(Nawrot et al., 2006; Zhao et al., 2019)**. In human, inhalation or ingestion are the main ways that leads to Cd exposure. Depending on the size of the particles, 10-50% of the Cd dust that is inhaled is absorbed. Skin contact has very little impact on absorption **(Bernhoft; 2020)**. Smoking of cigarette is one of the major sources of Cd exposure in human. A cigarette contains about 1-2 µg of Cd and a person smoking 20 cigarettes in a day may absorb nearly 1 µg Cd **(Taha et al., 2018; Genchi et al., 2020)**.

Cadmium oxide nanoparticles (CdO-NPs) serves as the initial material for manufacturing quantum dots, which are gaining popularity in both targeted treatments and medical diagnostic imaging **(Chan et al., 2005; Demir et al., 2020)**.

The release of Cd NPs into the environment could cause them to build up in the food chain and increase human exposure. In addition, other application of CdO-NPs includes drug delivery to tumour cells, removing cancer from living cells, attacking cancer cells, increasing the sensitivity of cancer cells to imaging, and more precise observation of them **(El Sayed et al., 2014; Heidari** and **Brown, 2015)**. The genotoxicity and cytotoxicity of CdO-NPs have been studied by several researchers. Various *in vitro* and *in vivo* experiments have been performed to determine the toxicity of CdO-NPs **(Demir et al., 2020)**. Additionally, research demonstrates that Cd is quickly absorbed, hazardous to a number of tissues, and builds up in the liver, kidney **(Dudley et al., 1984; Gathwan** and **Albir, 2020)**, testis, and pancreas, resulting in malfunctioning of these organs and severe damage **(Yang** and **Shu, 2015)**. Cd accumulation in the body leads to disturbances in the antioxidant defense system and also induces oxidative stress and tissue inflammation by increasing the amount of reactive oxygen species (ROS), altering the levels of essential components of pro- and anti-inflammatory pathways **(Cupertino et al., 2017)**.

In the era of technology and development, the application of CdO-NPs is opening new doors for researchers as it is used to treat deadly diseases, such as cancer. Although the nanoparticles have been useful to mankind in various ways, it will be ingenious to ignore the other side of the nanoparticles, which is their toxicological insight. So, there is an urgent need to understand the physiological mechanism and molecular and inflammatory pathways by which CdO-NPs induce toxicity at the cellular, tissue, and organ level. It is also thought that tracing the actual toxicological pathways may lead to the uncovering of complex effects and may help provide remedies for Cd toxicity.

1.2.2 Copper Oxide Nanoparticles (CuO-NP)

Copper is an essential trace element that is required for a number of biological activities. Among all biological functions, the most significant are the conversion of food into energy; iron metabolism; the manufacture of hormones, hemoglobin, melanin, myelin, collagen, and elastin, defense against oxidative damage **(Bhattacharya et al., 2016; Tulinska et al., 2022)**, and also helps in maintaining

homeostasis of the human body **(Naz et al., 2020)**. On the other hand, Cu is linked to the pathophysiology of many disorders and can be hazardous when present in excess **(Tulinska et al., 2022)**.

CuO-NPs have a number of interesting applications in nano-medicine, due to their outstanding antibacterial activity and promise as nosocomial infection-preventing disinfectants. These have potent antibacterial properties against several Gram +ve and Gram -ve bacterial strains, which are utilized in wound dressings **(Grigore et al. 2016; Naz et al., 2023)**. It is also known that CuO-NP have fungicidal effect against some fungal strains. For sensing glucose, dopamine, cholesterol, lactate, DNA, and other biomarkers, CuO-NPs are frequently utilized. Additionally, they could be quite helpful in the management of lung, breast, prostate, kidney, and glioma cancers due to their potential as antitumour agents (**Naz et al., 2023**). CuO-NPs are also used as one of the key elements of fertilizers **(Pelegrino et al., 2020; Tulinska et al., 2022)**, algaecide, fungicides, and herbicides, however they can also harm cells by oxidizing DNA and causing genotoxicity **(Song et al., 2012; Ghonimi et al., 2022)**. They are additionally employed to remove heavy metals from waste water **(Jain et al., 2021; Li et al., 2021; Tulinska et al., 2022)**.

Nano-forms of substantial heavy metals pose more detrimental effects as compared to their bulk ionic counterparts because of their unique properties such as smaller size, thermal, magnetic, mechanical, optical, electrical, and electron configuration density (**Yah et al., 2012; El Bialy et al., 2020; Abbasi et al., 2023**), high surface area, and reactivity **(Abbasi et al., 2023).** The particle size of the nanoparticle has played a major role in medication and drug delivery, as the smaller the size of the particle, the more efficiently it can penetrate inside the various tissues and cell **(Xu et al., 2023)**. Whereas, the same property has been challenged from the perspective of toxicity because when the same element becomes harmful for a human being, it may affect the root levels. The availability of a large number of reactive sites causes the surface-to-volume ratio of copper nanoparticles to grow, which increases reactivity or toxicity **(Naz et al., 2020)**.

Despite the various potent applications of CuO-NPs in the biomedical field, their toxic effects on several vertebrates, particularly mammalian cells and invertebrates, are a serious issue for their usage in diagnostic and therapeutic procedures. The primary causes of in vitro and in vivo toxicity of CuO-NPs are their size, surface charge, and disintegration **(Grigore et al., 2016; Naz et al., 2023)**. According to research, when NPs enter cells, they may interact with organelles and produce reactive oxygen species (ROS), which interfere with regular cellular processes. Depletion of reduced glutathione (tripeptide -glutamyl-cysteinyl-glycine, or GSH) by ROS results in oxidative stress, lipid peroxidation, and damage to cells' defensive mechanisms. Additionally, ROS raise the activity of catalase and superoxide dismutase in cells **(Tulinska et al., 2022)**.

1.3 Acute toxicity

Acute toxicity is commonly understood to be the adverse effects occurring within a short period following administration or a brief period of exposure to a substance or substances to a single dose or a number of doses given within 24 hours. Changes in the physical appearance and behavior of the dosed animals are noted during the first 24 hours and then daily for a period of 2 weeks. Acute systemic toxicity can be characterized, and its course can be shown by a variety of clinical symptoms. Accordingly, a substance that reaches the organism's body via the oral route within a short period and results in any adverse effect immediately is said to be ‘orally or acutely toxic’. However, the term ‘acute oral toxicity’ is most often used to signify the lethality and LD_{50} calculations.

The goals of acute toxicity testing are to gather data on biological activity and gain an understanding of the mode of action of a chemical. Additionally, the data on acute systemic toxicity produced by the test is used in the context of chemical manufacturing, handling, and usage to identify threats as well as regulate the risks associated with them. Government agencies are required to use the LD_{50} value, which is the basis for toxicological classification of substances, in a variety of circumstances **(Rhodes et al., 1993; Walum, 1998)**.

For the determination of the classical LD_{50} value, generally mice or rats of both the sexes are used. The classical LD_{50} determination methods demand the use of more animals (a total of 200), which has been greatly reduced by the advanced methods. The well-established and validated advanced methods were developed by the Organization for Economic Co-operation and Development (OECD), and the procedures are explained under OECD guidelines 420 (Acute oral toxicity: Fixed dose procedure) **(OECD, 1992)**, 423 (Acute oral toxicity: Acute toxic class method) **(OECD, 1996),** and 425 (Acute oral toxicity: Up-and-Down procedure) **(OECD, 2001)**.

1.4 Organ specific toxicity

The Metal Oxide NPs have promising applications in biomedicine, antimicrobial agents, diagnostics, treatment of various other complex diseases and industrial applications. However, the wide usage of NPs has put questions among the researchers due to their highly toxic nature. Human and animals getting exposed to NPs are affected adversely leading to many complexities. Human may get exposed to NPs intentionally or unintentionally. Generally, the routes of human getting exposed to NPs are through ingestion, inhalation, injection, implantation, or skin uptake **(Oberdörster et al., 2005)**. Recent studies have shown genotoxicity, cytotoxicity and immunotoxicity associated with NPs intoxication **(Naz et al., 2019)**.

According to the International Agency for Research on Cancer (IARC), Cd is recognised as the Class 1 human carcinogen **(Henson** and **Chedrese, 2004)**. The toxicity of Cd was detected in multiple organs such as, liver, kidney, brain, lung, cardiovascular system, spleen, stomach, skeletal system and reproductive system **(Joseph et al., 2001; Lopez et al., 2003; Gupta, 2019)**. Likewise, exposure to Cd in humans leads to about 30% of body Cd deposition, chiefly in the kidneys, which leads to a highly toxic effect **(Nordberg** and **Nordberg, 2002; Thévenod, 2003)**.

Liver plays a major role in determining the toxicity as it is a vital organ that involve in the metabolism, transport, and clearance of harmful foreign. Exposure to Cd were diagnosed with abnormal levels of liver function parameters, cellular necrosis, pathological degeneration, and proliferation of collagen fibres **(Zhang et al., 2022)**.

Nanodots and nanorods of Cadmium Sulfide have been reported to induce significant levels of toxicities in different organs of mice such as kidney, testis, and liver **(Liu et al., 2014)** by elevating the production of ROS **(Paesano et al., 2016)**. Earlier studies have shown that Cd has the ability to increase the permeability of the BBB and may accumulate in the brain tissue. After penetrating the brain tissue, Cd may affect the structure and function of the neuronal tissue, which leads to the degeneration and impairment of the neurons, which results in behavioural changes **(Braga et al., 2015; El-Sherbiny et al., 2022)**.

In vitro and *in vivo* studies have shown that exposure to CuO-NPs induces cytotoxicity **(Assadian et al., 2018)**, genotoxicity **(Song et al., 2012; Ghonimi et al., 2022)**, apoptosis, inflammation, oxidative damage, and histopathological changes in various organs like the liver, kidney, stomach, bone **(De Jong et al., 2019; Anreddy, 2018; Tulinska et al., 2022),** and brain **(Naz et al., 2019)**. According to **Lomer, et al. (2002)**, gastro intestinal tract (GIT) remains to be the primary route of NPs exposure hence, the oral route of intoxication has gained more importance. After being absorbed by the GIT, NPs enters in the lymphatic cells. However, entry of NPs in GIT induce ulcers by changing the lining's permeability, weakening of the tract epithelium, low absorption of nutrients, and in severe cases, continuous bleeding **(Borm et al., 2006)**.

Jong et al. (2018) have demonstrated that the rats administered with CuO-NPs at different doses are adversely affected. Hepatotoxicity and nephrotoxicity were evident from the severe inflammation, necrosis, apoptosis, and degeneration in rats exposed to CuO-NPs. It was also reported in several scientific research that once the NPs gain entry into the human body, liver is its primary target **(Xie et al., 2010)**. Harmful effects were observed on the liver, kidneys, immune system, and gastrointestinal tract when exposed to Cu intake above the biological tolerance range **(ATSDR, 2004)**. The NPs have the ability to disrupt the central nervous system as they can cross the blood brain barrier (BBB), which was evident after detecting considerable accumulation of Cu (NPs) in the hippocampus of the brain **(Li et al., 2018; Naz et al., 2019)**.

1.5 *In silico* toxicity prediction

In silico toxicology is essential to the evaluation of chemical safety and toxicity as well as the drugs discovery and development process. The term "*in silico* toxicology" refers to integrated technology that uses computers to assess the toxicity of compounds **(Parthasarathi** and **Dhawan, 2018)**. Using algorithms, software, and pertinent data, this technique offers a platform for assessment, modelling, simulation, and prediction of toxicity endpoints of different chemicals **(Pandey et al., 2022)**. The capabilities and relevance of computational techniques to predictive toxicology are still growing.

The use of computational technique is becoming way more popular in the fields of chemical toxicity testing, and drug designing and discovery, as it possesses many utilities. The technique of in silico prediction has complemented *in vivo* and *in vitro* methods by reducing labour, cost, and time and also to check the possibility of any failure in the late stage **(Madan et al., 2013; Raies** and **Bajic, 2016)**. Similarly, in the process of drug discovery, early screening of the chemical compound with the help of different in silico tools has minimized the chances of failure in the later stages. Furthermore, testing any chemicals with the computational tools also provides a basic idea about their various toxicological parameters in one go.

The field of in silico toxicology involves a broad range of computational tools, including- (i) databases that store information about chemicals, their toxicity, and their chemical properties; (ii) software that generates molecular descriptors; (iii) simulation tools for system biology and molecular dynamics; (iv) modelling techniques for toxicity prediction; (v) modelling tools like statistical packages and software that generates prediction models; (vi) expert systems that include pre-built models in web servers or standalone applications for predicting toxicity; and lastly, (vii) the visualization tools **(Raies** and **Bajic, 2016)**.

In silico screening of ADMET (Absorption, Distribution, Metabolism, Excretion and Toxicity) properties of compounds has open new door to improve quality and success rate of drugs in later stages. Moreover, computer-based screening of pharmacokinetics and toxicity of any chemicals has helped in generating the basic

toxicological profile of a compound from various aspects. Many softwares were developed for this purpose based upon the data-based approach, such as quantitative structure–activity relationship (QSAR), 3-dimentional QSAR, and similarity searches, and some with the structure-based approach, which includes protein ligand docking and pharmacophore **(Pires et al., 2015)**. Although there are many softwares available for this purpose, most of these allow paid access only; however, numerous softwares that are freely accessible for the user include pkCSM, admetSAR, ProTox-II, VEGA HUB, PASS, Toxtree, TEST, OECD QSAR toolbox, etc. and are widely in use.

1.6 Implications of heavy metals on body weight, food consumption, and water consumption

Changes in body weight, variation in consumption of food and water depends upon an array of factors, which may be related to the physiological, metabolic and various other health related issues of an individual. In general, it has been seen that infection and acute inflammation lead to weight loss in mice as well as in human **(Mendes et al., 2022).** In addition, several other reports have shown that fatigue, depression, stress, anxiety, different diseases such as diabetes **(Olson et al., 2016)**, onset of cancer and cancer treatment **(Hager, 2016)**, AIDS **(Malvy et al., 2001)**, undergoing medication etc. also leads to the loss of weight and change in pattern of feeding.

Heavy metals such as copper (Cu), cadmium (Cd), lead (Pb), magnesium (Mg), Iron (Fe), chromium (Cr), Nickel (Ni), cobalt (Co), mercury (Hg) etc. are the highly toxic elements. They are very heterogenous and highly reactive substance that may act as cofactors for various physiologic processes **(Valko et al., 2005; Padilla et al., 2010)**. **Padilla et al. (2010)** reported increase in adiposity in relation to the deficiency of copper, and increase in Cd levels was associated with the decrease in body mass index (BMI). Exposure to Cd also resulted in the reduction of body as well as brain weight **(Markiewicz-Górka et al., 2019; Vijaya et al., 2020).** Generally, weight gain or loss is related to exposure to hazardous metals and happens significantly

lower levels than those that cause apparent illness in humans or animals **(Binns et al., 2007)**.

Cu is an important trace element that is vital for various enzymes and biological processes. Adequate amount of Cu for the functioning of vital processes in human and plant are received from water and food intake **(Gaetke** and **Chow, 2003)**. In an appropriate concentration Cu helps in the growth of mice. However, excessive exposure to the chemical may lead to retarded growth **(Liu et al., 2020)**. There was a significant reduction in body weight observed in mice fed with copper sulphate as compared to the control animals **(Kumar et al., 2015)**.

1.7 Accumulation of heavy metal in organs and its concern

Persistent exposure to heavy metals can lead to their accumulation in all tissues and organs over time, causing prolonged injury to the organism because of their significant difficulties in metabolism and breakdown **(Raehsler et al., 2018)**.

The majority of Cd intake occurs by inhalation, with some also occurring through the digestive tract when dust particles are ingested together with saliva **(Ruczaj** and **Brzóska, 2023; Charkiewicz et al., 2023)**. The kidney and liver are the primary organs where Cd accumulates, however, placenta and bone **(Järup, 2002)**, lungs, liver, kidneys, pancreas, testicles, muscles, adipose tissue, and skin are the organs where this element can most frequently accumulates and inhibits the activity of enzymes that contain sulfur **(Lech** and **Sadlik, 2017; Nordberg** and **Nordberg, 2022)**. Through various means, accumulation of Cd in muscles, bones, and blood may range from 0.14 to 3.2 ppm, 1.8 ppm, and 0.0052 ppm, respectively. To maintain a healthy lifestyle, put into practice efficient preventative measures, and enhance public health, people who are most frequently exposed to heavy metals should be closely watched **(Charkiewicz et al., 2023)**.

According to **Tulinska et al. (2022)**, the mice inhaling CuO-NPs for six consecutive weeks have accumulated a 20-fold higher amount of Cu as compared to the control

group. Bio-accumulation of Cu in liver and kidney results in major damage to the hepato-renal system which ultimately affects the functioning of the organs. The same study also reported that the bio-accumulation of Cu was seen to be higher in the liver than the kidney of the rats intoxicated with CuO-NPs. Thus, suggesting that kidneys might be accumulating Cu in ionic form after in vivo exposure **(Hassanen et al., 2019)** however, liver can accumulate highest quantity of the metal, suggesting major damage to the hepatic system **(Kumar et al., 2015)**. Significant accumulation of Cu was observed on 42nd day of Cu treatment. Additionally, in those receiving high concentrations of Cu treatment, the hepatic growth index dropped, indicating that Cu overload may inhibit hepatic development **(Liu et al., 2020)**. Additionally, cadmium exposure is linked to alterations in neurotransmitters, increased lipid peroxidation, and the induction of apoptosis in brain tissues, highlighting its neurotoxic potential **(Al Kahtan, 2020)**. The presence of Cd in the environment, especially in the Carpathian region, has been associated with the accumulation of this toxic metal in the brain, contributing to dysmicroelementosis and disrupting the organism's homeostasis **(Nechytailo et al., 2023)**. Copper accumulation in brain tissues, such as the cortex, striatum, and substantia nigra, has been linked to increased levels of oxidative damage, altered protein expressions, and disruptions in antioxidant enzyme activities **(Chen et al., 2019; Kirici et al., 2019)**. Studies have highlighted that copper exposure can potentiate the degeneration of dopaminergic neurons, exacerbating conditions like Parkinson's disease when combined with other neurotoxic factors **(Cruces-Sande et al., 2019)**.

1.8 Importance of hematological and biochemical assays in toxicity study

Hematological parameters such as red blood cells (RBCs) count, white blood cells (WBCs) count and hemoglobin concentration are the important clinical indicators of health and disease conditions **(Kelada et al., 2012)**. Additionally, values beyond the normal ranges may be diagnostics for disorders such as cancer, cardiovascular diseases, immune diseases, etc. **(Lin et al., 2007)**. The main function of RBCs is to carry and supply oxygen to the cells and tissues and carbon dioxide to the lungs; thus, decreased levels of RBC signifies that an inadequate amount of oxygen and carbon dioxide return **(Isaac et al., 2013)**. Further, RBCs are vulnerable to damage

from oxidative stress. At some dosages, nanoparticles may cause oxidative stress, which ultimately results in cell toxicity and haemolysis of RBCs **(Koohi et al., 2017)**. According to past studies, high-molecular-weight proteins hold the majority of the Cd in red blood cells, and hemoglobin holding the small fraction of it **(Świergosz-Kowalewska, 2001)**. The hematopoietic process is very sensitive to the Cd toxicity, and also may lead to anaemia and various other complicacies. Administration of Cd also results in the decrease levels of RBC, hemoglobin and haematocrit in blood **(Andjelkovic et al., 2019)**.

Though Cu is a vital functional constituent of living being and also form part of 16 metalloprotein **(Özçelik et al., 2002)**, but excessive intake may result in low elimination and accumulation in tissue and organ causing Cu poisoning **(Özçelik et al., 2002; Borobia et al., 2022; Rafati et al., 2024)**. High Cu intake along with the supplement in hens leads to the elevated levels of MCV, which signifies deteriorated health condition **(Hoffbrand** and **Provan, 1997; Zhou et al., 2021)**. As reported by **Yahya et al. (2019)**, CuO-NPss treated groups showed a significant increase in WBC and a marked decrease in RBCs, Hb, and HCT counts and concentrations. Rats treated with CuO-NPs showed a significant rise in MCV and a significant decrease in MCH and platelet values, but no discernible changes in MCHC values were seen when compared to the control group. This shows that intake of nanoparticles of Cu may have a pronounced impact on the hematological parameters resulting in deteriorated health condition of animals.

Biochemical assays of different enzymes and metabolites are the clinical markers for the diagnosis of liver and kidney diseases **(Malomo, 2000; Yakubu et al., 2006)**. Generally, detection of ALP, AST, ALT, bilirubin, albumin, globulin, and other assays such as urea, uric acid, creatinine, and blood urea nitrogen are mainly performed to trace the functioning of liver and kidney, respectively. Rats exposed to CdCl for 30 consecutive days lead to increased activities of ALT, AST, ALP, and LDH **(Hamza et al., 2022)** and also the levels of serum bilirubin and transaminases were higher in mice fed with copper sulphate **(Kumar et al., 2015)**. Assessing lipid profiles in toxicity studies, is crucial for understanding mechanisms of liver injury, cardiovascular injury and potential drug-induced lipid disruptions leading to toxicity.

CuO-NPs is cytotoxic in nature and may adversely affect the liver and kidney tissues. According to the report, rats intoxicated with CuO-NPs had an elevated level of AST and ALT enzymes indicating hepato-cellular damage in the liver (**Hassanen et al., 2019; Zhou et al., 2021)**. Similarly, significant increase in the levels of BUN and creatinine in the serum sample of rats intoxicated with CuO-NPs indicated significant damages in the renal tissue **(Hassanen et al., 2019)**. Due to membrane damage, hepatic marker enzymes (AST, ALT, ALP, and GGT) are typically high in cases of liver injury. Study revealed changes in the hepatic enzymes, with an increase in the enzyme activity after $CuSO_4$ intoxication. Decrease levels of serum protein concentration is also observed after $CuSO_4$ treatment, which may be due to hepatocellular injury and inflammation caused by severe Cu toxicity **(Hashish** and **Elgaml, 2016)**.

1.9 Organ damage and histopathology mediated by toxic chemicals

The liver exposed to CdCl showed remarkable changes in the architecture of the liver tissue, which includes hypertrophy and appearance of binucleated hepatocytes, focal necrosis, dilation of the central vein, and increased in eosinophil counts **(Hamza, et al, 2022)**. Cd administration cause neuropathological as well as neurochemical alternation in the brain tissues which result in the tissue haemorrhages **(Afifa** and **Embaby, 2016)**. Exposure to cadmium (Cd) altered the gut microbiota and intestines, as evidenced by changes in intestinal microbiota and their metabolic processes, increased permeability of the intestinal barrier, local intestinal inflammation, and ultimately an increased risk of infectious diseases due to bacterial translocation, lipopolysaccharides, and endotoxins. Also, targeting organs including the liver, kidney, brain, adipose tissue, and cardiovascular system will be affected by metabolic abnormalities and systemic inflammation, raising the chance of related illnesses **(Tinkov et al., 2018; Liu et al., 2020)**. Prolonged exposure to cadmium through air, water, soil, and food can poison various organ systems, including the skeletal, urinary, reproductive, cardiovascular, central and peripheral neurological, and respiratory systems, and cause cancer **(Rafati et al., 2017)**.

Chronic Cu poisoning causes Cu to progressively build up in the liver without causing any overt symptoms or indicators. Excessive hepatic Cu storage can lead to hepatocellular lesions; subsequently, haemolysis, jaundice, and renal insufficiency are caused by Cu being released from the liver into the bloodstream **(Stogdale, 1978)**. Mice exposed to nano-copper particles exhibit obvious damage to their renal proximal tubular cells. A glomerulonephritis-related symptom in renal tissues is the swelling and shrinkage of glomerulus in the lumen of Bowman's capsules. There are further pathological alterations in the renal tubule, such as the degeneration of renal proximal convoluted tubule epithelial cells. These changes are dependent on an irreversible massive necrobiosis feature in the nano-copper particle-induced renal tissue damage, where the kidney damage in the exposed mice rapidly increases with increasing dose **(Chen et al., 2006)**.

1.10 Implications on oxidative stress and antioxidants parameters

Sarkar et al. (2011) have reported that exposure to nano-copper had increased the production of reactive oxygen species (ROS) and reactive nitrogen species (RNS) and also elevated the levels of antioxidant enzymes such as SOD, CAT, GST, GR, GPx, and also the non-enzymatic marker, GSH. It was formulated that generation of oxidative stress in tissues lead to the activation of the nuclear factor erythrocyte 2-related factor 2 (Nrf2) signalling pathways which interacts with the antioxidant response elements (ARE) and activates the transcription of antioxidant defence genes and detoxifying enzymes **(Yung et al., 2018; Du et al., 2022)**. The process of converting hydrogen peroxide into water is catalysed by GSH and catalase. SOD catalyzes the breakdown of O_2 and defends different organs from ROS-induced damage and lipoperoxidation. An imbalance in the oxidant/antioxidant system can lead to lipoperoxidation and oxidative stress, which can be caused by decreased SOD and GSH activity or increased oxygen free radical **(Weydert** and **Cullen, 2010)**. The brain is a very delicate and complex organ that controls a wide range of biological metabolic processes, resulting in it to use a lot of oxygen. A poorly developed antioxidant defense mechanism and high quantities of peroxidizable unsaturated fatty

acids make the brain tissues particularly vulnerable to harmful oxidative stress attacks **(Bondy, 1997; El-Sherbiny et al., 2022)**.

The most common events that drive Cd mediated neurotoxicity are oxidative stress and excessive free radical production. The creation of ROS, a decline in the activity of antioxidant enzymes, or decompartmentalization of metal complexes are possible mechanisms through which Cd causes lipid peroxidation **(Järup** and **Åkesson, 2009)**. Cd promotes cellular apoptosis by supressing the antioxidant defence system and also by disrupting the sulfhydryl homeostasis **(Ferlazzo et al., 2021)**. Cadmium reduces cellular resistance to oxidation and raises the generation of free radicals in the central nervous system. It might potentially cause lipid peroxidation and harm to brain cells. Oxidative deamination of monoamine neurotransmitters is brought on by its action on monoaminoxidase (MAO). Neurodegenerative illnesses including Parkinson's, Alzheimer's, and Huntington's disease, which are characterized by memory loss and behavioural abnormalities, can result from Cd poisoning **(Lopez et al., 2003; Ismail et al., 2015; Rafati et al., 2017)**. Changes in oxidative stress indicators and peroxidative damage to membrane lipids are two of the most well-known effects of excessive Cu. Oxidative stress is a condition in which the production of reactive oxygen species (ROS) surpasses the capacity of cells to protect themselves, ultimately leading to cytotoxicity. During an oxidative stress, compounds such as membrane lipids are damaged by the development of superoxide anion (O_2), hydroxyl radicals (OH), and hydrogen peroxide (H_2O_2). Lipid peroxidation is a chain process that is mediated by free radicals and is created when lipid radicals combine with oxygen to produce peroxy-radicals **(Galhardi et al., 2004)**. The majority of the studies on in vitro and in vivo systems concurred that ROS-mediated oxidative stress was the primary factor in the cytotoxic mechanism; however, in order to direct the development of more potent cytotoxic CuO-based nanodrugs or safer NMs, a deeper comprehension of the underlying toxicity pathway and the identification of the physicochemical properties triggering this mechanism are required.

1.11 Expression patterns and effects on apoptotic and inflammatory markers

"Apoptosis" is a Latin derived term which means "to fall off" **(NIH, 2023)**. It is also known as programmed cell death hence, it can be defined as the genetically determined cell death which involves condensation of nucleus, shrinkage of the cell and followed by fragmentation of the cell **(Schlesinger, 2023)**. Apoptosis is a normal process which is genetically programmed to eliminate unwanted cells from the body, which may otherwise lead to cancer. It is crucial for normal functioning and development of the immune system, normal cell turnover, chemically-induced cell death and embryonic development. However, unbefitting (too less or over) apoptosis may lead to many conditions in human **(Elmore, 2007)**. The process of apoptosis may be mediated by either mitochondrial-dependent or independent pathways. According to the report, changes in the mitochondrial membrane permeability is mediated by a BCL-2 family of proteins **(Cory** and **Adams, 2002)** and activate apoptosis by inducing oxidative stress-dependent signalling cascade **(Keeble** and **Gilmore, 2007; Sarkar et al., 2011)**. Generally, there are two groups of apoptotic regulators: one that protects the cell from apoptosis, called anti-apoptotic protein, and the other that promotes apoptosis, is called pro-apoptotic protein. BCL-2 is known for its anti-apoptotic effect, whereas BAX is a major pro-apoptotic marker **(Reed, 2006)**. Furthermore, apoptosis triggers leading to degradation of mitochondrial integrity precede the activation of caspases, which play a major role in the execution of apoptosis **(Youle** and **Strasser, 2008)**. NF-κB is a transcription factor that is widely expressed and inducible that regulates genes related to several activities, including growth, differentiation, survival, and inflammation in cells. Several environmental stressors, such as carcinogens and tumour promoters including asbestos, phorbol esters, toxic metals, UV radiation, and alcohol, can activate NF-κB **(Valko et al., 2005)**. NF-κB is activated by various stimuli like cigarette smoke and inflammatory agents, regulating genes such as COX-2 and cytokines like IL-6 and TNF-α **(Yadav et al., 2022; Alvarez et al., 2020)**. IL-6 plays a crucial role in myoblast proliferation and differentiation, modulating myogenic regulatory factors and myokine release **(Serasanambati** and **Chilakapati, 2016)**. COX-2, induced by pro-inflammatory cytokines, contributes to the production of prostaglandins and influences cell proliferation **(Tatiana, 2018)**. TNF-α, along with IL-6, affects the activity of Pax7, MyoD, and myogenin, impacting muscle

regeneration processes **(Barua et al., 2020)**. Additionally, the study on chronic hepatitis B and C infection in children highlights the diagnostic and prognostic significance of IL-6, IL-2 and TNF-α in hepatic inflammatory activity. Oncogene activation, oxidative stress, hypoxia, DNA double-strand breaks, and telomere damage, among other stress signals, stimulate cells; in response, the p53 protein is quickly activated to preserve the integrity of the cell genome by causing apoptosis, cell cycle arrest, and senescence **(Yoshida** and **Miki, 2010)**. Thus, neurological disorders can arise and progress as a result of abnormal p53 protein expression **(Tokino** and **Nakamura, 2000)**.

Cd exposure has been linked to alterations in inflammatory markers in various studies. Research has shown that Cd induces oxidative stress and inflammation by upregulating inflammatory mediators and markers such as NF-κB, IL-6, TNF-α, and COX-2 **(Ojo et al., 2023)** and similarly, Cu exposure leads to increased expression of pro-inflammatory cytokines like IL-1β, IL-6, TNF-α, and activation of NF-κB signalling pathways **(Guo et al., 2022; Pereira et al., 2016),** production of IL-12p70, IFN-γ, IL-4, and IL-5 **(Tulinska et al., 2022)**. Occupational exposure to cadmium has been associated with increased levels of pro-inflammatory cytokines like IL-6 and TNF-α, indicating immune cell activation and inflammation **(Markiewicz-Górka et al., 2022)**. Additionally, chronic cadmium exposure has been found to induce inflammatory responses in the liver, leading to increased expression of inflammatory markers like Mip-2, IL-10, IL-12, and TGF-β **(Olszowski et al., 2012)**. The mechanisms underlying copper-induced neurotoxicity involve oxidative stress, alterations in protein markers like GFAP, NF-kB, and PARP, and disturbances in cellular functions critical for neuronal health and survival. These findings collectively highlight the intricate relationship between cadmium and copper toxicity and the modulation of inflammatory markers across different organ systems by promoting oxidative stress, immune cell activation, and inflammatory responses in various tissues, highlighting the detrimental effects of toxic metals on inflammatory processes.

1.12 Rationale of the work

Heavy metals are naturally occurring toxic elements that have become more prevalent in the environment due to urbanization and industrialization, leading to serious health effects on humans, plants, and animals. The toxicity of heavy metals is influenced by various factors such as dose, route of exposure, time of exposure, concentration levels, as well as individual characteristics like age, gender, genetics, and nutritional status **(Ungureanu** and **Mustatea, 2022)**.

Research on the toxicity of CdO-NPs in various organs is crucial due to their harmful effects. Studies have shown that CdO-NPs induce haematotoxic, genotoxic, and reproductive toxicity, affecting organs like the liver, testes, and brain **(Klinova et al., 2020; Apykhtina et al., 2018; Zhou et al., 2023)**. CdO-NPs lead to oxidative stress, altered gene expression, and cell proliferation inhibition/promotion in organs like the spleen, kidney, heart, brain, and lung, indicating potential disease risks. Furthermore, CdO-NPs have been linked to cardiovascular toxicity, neurotoxicity, and nephrotoxicity, emphasizing the need for comprehensive research to understand the mechanisms underlying their toxic effects on different organ systems. Investigating the mutagenic, carcinogenic, and reproductive risks associated with CdO-NPs is essential for developing preventive measures and assessing the safety of nanomaterials containing Cd. Similarly, to ensure the safe use of CuO-NPs in diverse fields such as biomedicine, catalysis, sensors, electronics, and environmental remediation, further research is crucial to understand the long-term and chronic impacts of these nanoparticles at different concentrations **(Sajjad et al., 2023)**. Addressing the potential toxic effects of CuO-NPs is essential to enhance their suitability for various applications and mitigate the risks associated with human exposure, underscoring the need for continued investigation into their toxicological profiles and also to explore the short-term and chronic effects of CuO-NPs at different concentrations.

The present study will emphasize upon the toxic nature of Cd and Cu, significance of understanding the absorbed dose, route of exposure, and duration of exposure in determining the toxic effects, and also assess their ability to induce oxidative stress, apoptosis and inflammation in mice model. Understanding the distribution and

effects of these heavy metals is crucial for mitigating their harmful consequences on the environment, animals and human health as a whole.

CHAPTER- 2

REVIEW OF LITERATURE

A rigorous and thorough literature survey was done from the available databases such as 'PubMed', 'Mendeley', 'Google Scholar', 'ResearchGate', 'Scopus' and other online sources by applying keywords search, such as 'Heavy metals', 'Cadmium', 'Copper', 'Toxicity', 'Oxidative stress', 'Inflammatory markers', 'Histopathology', 'Hematology', 'Western blotting', 'Liver', 'Kidney', 'Brain', etc. to find out the relevant materials for the present work. Survey of various research documents helped in finding out of the past, present and future research prospect of the present study that are presented in the following sections.

2.1 Toxicological aspects CdO-NPs

According to International Agency for Research on Cancer (IARC), Cd is recognised as the Group I carcinogen **(Smoke** and **Smoking, 2004)**. It lacks necessary biological functions and is harmful to humans, animals, and plants even at low concentration **(Solenkova et al., 2014).** There are various possible routes of Cd exposure in humans, which includes inhalation (mostly from tobacco smoke), ingestion (food and water), absorption through skin, and occupational exposure. The mode of exposure affects the amount of Cd absorbed; up to 50% of it comes from inhalation, 10% from ingestion, and barely any via cutaneous contact **(Faroon et al., 2012; Das** and **Al-Naemi, 2019)**. In many countries, the human Cd levels have been found to exceed the tolerance of several organs, and this has been linked to an increased risk of chronic diseases such cancer, diabetes, and osteoporosis **(Satarug et al., 2017; Genchi et al., 2020)**. The Food and Drug Administration (FAD) has cautioned against using solutions comprising cadmium oxide nanoparticles and warned that these compounds may cause poisoning, skin discoloration, and kidney damage. The main causes of cadmium poisoning are a rise in the production of free radicals and a fall in the potency of antioxidants **(Aghababa et al., 2017)**. The main target organ of Cd toxicity is liver, kidney and bone causing major health effect such as cancer, kidney damage, bronchiolitis, emphysema, fibrosis, skeletal damage (itai-itai disease) **(Nawrot et al., 2010; Alissa** and **Ferns, 2011)**. Cd exposure can lead to changes in brain enzyme activities, oxidative DNA damage, and alterations in signal transduction pathways, showing vulnerability to the brain tissue and ultimately contributing to neurotoxicity and potential long-term behavioural consequences

(Carageorgiou and **Katramadou, 2012; Nedzvetsky et al., 2020)**. As reported earlier, Cd at a dose of 1 mg/kg body weight modulates reproductive function in male mice **(Rossman et al., 1992)**. Study performed focusing on the cytotoxic effects of different cadmium forms, including cadmium chloride ($CdCl_2$), cadmium oxide (CdO), and cadmium sulfide (CdS) in micro- and nanoparticles, on mesangial and proximal tubular kidney cells. The results showed a variability in cytotoxic responses depending on the cadmium form studied, with the toxicity strongly correlated to the cellular cadmium content. This indicated that the physico-chemical properties of the cadmium forms played a significant role in their toxic effects **(L'Azou et al., 2014)**.

2.1.1 Effects on the general observations

Toxicity can significantly impact body weight, as evidenced by various studies. Research on Bisphenol-A exposure in rats showed dose-dependent reductions in feed consumption and body weight, indicating its potential to induce anorexia **(Wang et al., 2019).** Additionally, studies on pesticides demonstrated that the longer the exposure duration, the greater the effects on body weight, with continuous declines in benchmark doses observed over time, highlighting the time-dependent nature of toxicity effects on body weight in mammals **(Zuckerman et al., 2015)**. Understanding these relationships is crucial in assessing the toxic effects of various substances on body weight and overall health. Heavy metals, such as cadmium and lead, have been shown to have a significant impact on body weight and overall health. Exposure to these toxic elements can lead to a decrease in weight gain in rats, accompanied by changes in organ size and hematological parameters **(Ungureanu** and **Mustatea, 2022)**. Furthermore, heavy metal exposure, particularly during pregnancy, has been linked to adverse effects on new-borns, including altered leukocyte telomere length and chromosomal changes that may affect birth weight and mortality **(Rajkumar** and **Gupta, 2021; Zinia et al., 2023).**

Intoxication of Wistar rats with Cd (30 mg/kg of feed) for a period of 3 months lead to the reduction in body weight, blood levels of hemoglobin, vitamin D3, antioxidant enzyme (GSH) whereas, increased in the levels of oxidative stress marker and

inflammatory marker (C-reactive protein, CRP) as compared to the control and magnesium (Mg) or/and α-lipoic acid supplemented groups **(Markiewicz-Górka et al., 2019)**. Cd intake leads to the reduction in body as well as brain weight in mice, when administered with 6 mg/kg bw of Cd at a single dose **(Vijaya et al., 2020)**. Reduction in the body weight of Wistar rats exposed to Cd 6.9-7.6 mg/kg b.w in combination with feed (30 mg/kg of feed) for 3 months was observed by **Markiewicz-Górka et al. (2019)**. According to a study, the impact of Cadmium and Lead salts was investigated on body weight gain, organ weight, and hematological parameters in rats. In the experimental groups, rats exposed to heavy metals showed a tendency towards reduced weight gain compared to the control group**.** Heavy metal intoxication led to hypo- and hypertrophy of internal organs in rats, with different metabolic rates observed. Rats in the first experimental group, exposed to cadmium, exhibited increased lung, liver, and brain weights, but decreased heart, kidney, and spleen weights relative to the control group. The study also found that heavy metal exposure resulted in changes in the morphological composition of rat blood, including decreased erythrocytes, leukocytes, and hemoglobin levels, along with increased average erythrocyte volume and content**.** Chronic heavy metal (cadmium-lead) toxicosis in rats was associated with erythrocytopenia, leukopenia, decreased hemoglobin, and increased erythrocyte volume and hemoglobin content **(Lopotych et al., 2020)**.

Synthesized cadmium nanoparticles led to an increase in hepatic enzymes concentration in the blood of rats in a dose-dependent manner after 10 days of exposure at the doses of 100 ppm, 200 ppm and 300 ppm in Wistar male rats. This increase was more pronounced in groups exposed to higher concentrations of nanoparticles, with the highest concentration group showing the most significant rise in enzyme levels **(Aghababa et al., 2017)**.

2.1.2 Metal accumulations and histopathological alterations

Exposure to cadmium nanoparticles can lead to significant accumulation in various organs, impacting both human health and the environment. Studies have shown that cadmium nanoparticles can accumulate in organs such as the kidney, lung, liver,

heart, aorta, spleen, thymus, brain, and bones, affecting their function and structure **(Lebedová et al., 2016; Apykhtina** and **Kozlov, 2017; Tai et al., 2022)**. The Cd concentrations in fish (*Sparus aurata*) tissues (muscle, gills, and liver) were monitored at different time points during the experiment. Significant Cd accumulation was observed in the gills (209.43 ng/g ww) and liver (371.72 ng/g ww) at the end of the exposure period (11 days), while muscle showed no significant accumulation **(Cirillo et al., 2012)**. Mice exposed to CdO nanoparticles for varying durations, ranging from 4 to 72 hours in acute exposure and 1 to 13 weeks in chronic exposure. TEM confirmed the distribution of nanoparticles in various organs, with a significant portion retained in the lungs initially, but gradually redistributing to secondary organs like the kidney, liver, and spleen with longer exposure. Accumulation of Cd was observed in the lung and liver after 24 hours, and in the brain, kidney, and spleen after 72 hours of exposure, with levels increasing throughout the chronic exposure period. Significant differences were noted in Cd accumulation and effects between the two exposure doses, with higher exposure leading up to a 2-fold increase in lung weight compared to the control group. Histological analyses revealed dose-dependent alterations in lung and liver morphology, tissue damage, and modulation of oxidative stress parameters, particularly after greater chronic exposure. Long-term exposure to CdO nanoparticles resulted in increased necrotic debris in the pulmonary alveoli, damage to lung tissue, and some pathological changes in the liver, while no significant changes were observed in the spleen, kidney, and brain **(Lebedová et al., 2016)**. Petroleum industry lead to accumulation of heavy metals in Plantago ovata which were consumed by goats lead to elevated levels of Pb, Cd, V, and Ni that caused injury in liver and kidney tissue, oxidative stress, and upregulation of pro-inflammatory and apoptotic markers (BAX and caspase-3) and downregulated the expression of BCL-2. Histopathological damages in the liver and kidney tissues and increased serum concentration of ALT, urea and creatinine, the markers of kidney function, were detected in the study **(Ajarem et al., 2023)**.

In a study, rats were given intraperitoneal injections of cadmium compounds over a period of time, and the harmful effects were assessed at three distinct intervals: 1.5

months after the first injection, 3 months after the second injection, and 1.5 months after the exposure stopped. The findings showed that the rats' kidneys and liver had the most cadmium accumulation, which was mostly caused by the toxico-kinetics and mode of administration of the cadmium compounds. When compared to rats exposed to cadmium chloride, rats exposed to cadmium sulphide nanoparticles had greater concentrations of cadmium in their thymus, spleen, and kidneys. It's interesting to note that after exposure to larger nanoparticles, the spleen showed more pronounced cadmium accumulation, whereas the liver, heart, aorta, and brain showed notable accumulation following exposure to cadmium chloride **(Apykhtina** and **Kozlov, 2017)**.

Pregnant CD-1 mice exposed to inhaled CdO nanoparticles (CdO NP) showed a fivefold increase in urinary kidney injury molecule-1 (Kim-1) levels without significant changes in urinary creatinine levels. Kim-1 mRNA expression peaked by gestational day 10.5, while neutrophil gelatinase-associated lipocalin (NGAL) expression increased from gestational day 10.5 to 17.5. Histological analysis revealed proximal tubular pathology at gestational day 10.5 in the exposed dams. Neonatal mice showed an increase in Kim-1 mRNA expression between postnatal days 7 and 14, with mammary glands/milk being the apparent source of cadmium for the offspring. Levels of urinary Kim-1 in pregnant mice exposed to CdO NP increased by 4.7-fold compared to control mice, with no significant change in urinary creatinine concentrations. Neutrophil gelatinase-associated lipocalin (NGAL) levels in the kidney increased due to renal cell damage caused by Cd exposure, indicating acute kidney injury. Exposure to Cd compounds, including CdO NP, leads to extensive kidney injury, oxidative stress, cellular death, and loss of renal function, ultimately resulting in kidney failure **(Blum et al., 2015)**. Chronic Cd exposure has detrimental effects on various organs and tissues, including the central nervous system (CNS), and it may be indirectly responsible for the production of reactive oxygen species (ROS). Since Cd is mostly found in the +2-oxidation state, it can enter cells by interacting with a wide variety of channels and transporters on the surface of the cell membrane. Reviewing lipid peroxidation, ROS generation, glutathione depletion, and mitochondrial dysfunction helps to better understand the

molecular processes that Cd elicits. In addition, studies have demonstrated the effects of Cd on several types of CNS cells, which may help to clarify its involvement in neurodegenerative diseases. It is true that cadmium can enhance the permeability of the blood–brain barrier (BBB) and encourage Cd entrance, which in turn activates pericytes to keep the BBB open **(Branca et al., 2020)**. Oxidative stress makes the brain very susceptible to neurodegeneration. According to the studies, Cd metal induces oxidative stress by elevation the production of ROS and also leads to disturbances in the production of antioxidant enzymes resulting to the brain damage **(Thévenod, 2009; Wang** and **Du, 2013; Alam et al., 2021)**. This oxidative stress can contribute to the destructive effects observed in the liver and kidneys of the experimental rats **(Aghababa** and **Nahid, 2017)**. ROS production and oxidative stress have been linked by numerous researchers to the mutagenicity and ecotoxicity of metals **(Yedjou** and **Tchounwou, 2006; Tchounwou et al., 2001; Sutton** and **Tchounwou, 2007; Al-Abdan et al., 2020)**.

2.1.3 Oxidative stress and antioxidant status

Cadmium toxicity is caused by a number of mechanisms, including the development of oxidative stress, which is brought on by the generation of reactive oxygen species and the depletion of the antioxidant defense complex. Research on Cd offers strong evidence, validating one of the key mechanisms of cadmium poisoning as an oxidative stress, with the liver serving as a crucial organ for acute exposure **(Matović et al., 2013)**. According to **Kong et al., (2023)**, rats administered with 5 mg/kg b.w of Cd for 4 weeks were detected with higher levels of MDA, while decreased levels of CAT, GSH and SOD in hepatic and cardiac tissues. It was reported that Cadmium sulfide nanoparticles (CdSNPs) at a dose of 10 mg/kg induced significant liver damage in rats over 45 days of exposure. Serum enzyme levels (ALT, AST, ALP) and reactive species (MDA, H_2O_2, NO) were notably elevated in rats treated with CdSNPs compared to CdS-treated rats, indicating liver injury. Histopathological examination revealed extensive parenchymal degeneration in the livers of rats exposed to CdSNPs, indicating severe tissue damage. The study concluded that the interaction between nanoparticles and cell membranes led to the generation of reactive species, causing oxidative stress, altered membrane integrity, and activation

of cell death pathways in liver cells **(Rana et al., 2021)**. Rat liver cells exposed to CdO particles showed increased toxicity over time, with the highest toxicity observed after 24 hours of exposure. The MTT assay revealed the varying effects of CdO particles on the rat liver cells at different exposure durations and concentrations **(Shelley, 2005)**.

Oreochromis mossambicus (Tilapia) exposed with sublethal concentrations of 4, 10, and 20 μg/ml selected for further investigation, where LC_{50} value was found to be 40 μg/ml. Histological analysis of blood, gills, and kidney tissues was conducted to assess oxidative stress and genotoxicity in the fish exposed to CdO-NPs. Exposure to CdO-NPss led to increased lipid peroxidation (LPO) and decreased glutathione levels in the tissues of the fish, indicating oxidative stress. Significant genotoxic effects were noted, with micronuclei (MNi) production in peripheral blood at the highest concentration on day 21 of exposure. The study revealed DNA damage in lymphocyte, gills, and kidney cells of O. mossambicus, as evidenced by an increase in the percentage of tail DNA in these tissues **(Al-Abdan et al., 2020)**. The study evaluated the cytotoxicity and genotoxicity of 10 nm CdO core-PEG stabilized nanoparticles using various assays. MTS, ATP, and LDH experiments demonstrated the concentration-dependent cytotoxicity that CdO nanoparticles generated in TK6 and HepG2 cells. Although the Ames test yielded no results for genotoxicity, the micronucleus, Comet, and mouse lymphoma assays produced positive results, demonstrating that CdO nanoparticles caused chromosomal damage, DNA breakage, and mutations. Due to the fact that very few Cd^{+2} ions were produced from the CdO nanoparticles, the toxicity of the particles was ascribed to the nanoparticles themselves. The findings indicate that CdO nanoparticles are cytotoxic and genotoxic overall, emphasizing the significance of determining the risk of human exposure and environmental protection associated with these nanoparticles **(Demir et al., 2020)**.

2.1.4 Inflammatory response mechanism

Decreases in albumin content and A/G index were seen, while an increase in organ mass was the outcome of liver damage **(Klinova et al., 2020)**. It was demonstrated that Cd causes BEAS2B cells to become less viable, accumulate reactive oxygen

species (ROS), induce apoptosis, suppress the expression of BCL-2, and increase the expression of BAX and cleaved caspase-3 protein through the mitochondria-mediated apoptotic pathway **(Cao et al., 2021; Wang et al., 2021)**. Studies also suggested that the nephrotoxicity may be possibly due to the exposure to Cd which lead to the disturbances in intracellular signalling pathway mainly by changing the expression of oxidative stress markers **(Bonizzi** and **Karin, 2004; Ajarem et al., 2023)**. Alleviating effect of Thymus serrulatus essential oil on Cd- intoxicated rats were observed after a treatment period of 7 days. The rats were divided into five different groups, of which Group 1 was considered as control (treated with 0.9% NaCl) and Group 2 received $CdCl_2$ intra peritoneally (i.p.) at a dose of 3 mg/kg. Group 3 was a positive control group and was treated with both $CdCl_2$ and silymarin (100 mg/kg, p.o). Group 4 and 5 were co-administered with $CdCl_2$ and Thymus serrulatus essential oil (100 mg/kg and 200 mg/kg, respectively) for a period of 7 consecutive days. After completion of the treatment, various markers of renal-toxicity such as urea, uric acid, and creatinine, oxidative stress markers, such as GSH and MDA levels, and also the inflammatory markers, such as NF-κB p65, iNOS and small mothers against decapentaplegic (Smad2) were assessed and were observed to be higher in concentration as compared to the normal control, positive control and Thymus serrulatus treated groups. This study showed that Cd-intoxication leads to major nephrotoxicity in rats after 7 days of treatment **(Ansari et al., 2021)**. Also, an In vivo study carried out on mice intoxicated with cadmium chloride (CdCl2) resulted in significant increase in the expression of NF-κB **(Lee** and **Lim, 2011)**.

Cd supplementation leads to the increased expression of NOS-2, NF-κB, IL-1β and TNF-α resulting in the inflammatory and apoptotic effects in mouse brain. The same study also reported that Cd intoxication enhances the expressions level of BAX, caspase-3, and decreased expression of an anti-apoptotic protein BCL-2 protein **(Alam et al., 2021)**. The rats when exposed Cd at the doses of 5 mg/kg for the period of 4 weeks showed elevated levels of pro-inflammatory cytokines such as TNF-α, IL-1β and IL-6 and also the levels of apoptotic markers including caspase-3, NF-κB and TGF-β, as compared to the control group **(Kong et al., 2023)**. Increased production of NOS-2, NF-κB, IL-1β, and TNF-α in the mouse brain is caused by

supplementation with Cd, and this has an inflammatory and apoptotic effect. The same study also found that exposure to Cd increases the expression levels of caspase-3 and BAX and decreases the expression of BCL-2, an anti-apoptotic protein **(Alam et al., 2021)**.

2.2 Toxicological aspects of CuO-NPs

Studies have shown that CuO-NPs can induce oxidative stress, cytotoxicity, genotoxicity, immunotoxicity, neurotoxicity, and inflammation in various cell lines and organisms, including bacteria, fish, and mammals **(Sajjad et al., 2023; Ramos-Zúñiga et al., 2023; Aziz** and **Abdullah, 2023)**. The entry of Cu into the body through various means can lead to adverse effects when surpassing biological tolerance levels, highlighting the importance of understanding its impact **(Al-Musawi et al., 2022)**. The toxicity mechanisms of CuO NPs involve the generation of reactive oxygen species, leaching of copper ions, coordination effects, non-homeostasis effect, autophagy, and inflammation, highlighting the complexity of their impact on biological systems**.** Factors influencing the toxicological effects of CuO NPs include their characterization, surface modification, dissolution, dosage, exposure pathways, and environmental conditions, emphasizing the importance of considering these factors in assessing their safety for various applications **(Sajjad et al., 2023)**. CuO-NPs exhibit toxicity through various mechanisms, impacting different organisms and environments. The toxicity of CuO-NPs involves reactive oxygen species generation, leaching of copper ions, protein inactivation, DNA damage, and membrane rupture, contributing to their antimicrobial properties and potential harm to living organisms **(El-Atrash et al., 2022; Moschini et al., 2023)**. Furthermore, exposure to sublethal concentrations of CuO-NPs can lead to ecotoxicological effects such as metal overload, oxidative stress, and genotoxicity, with impacts being dose, duration-dependent as well as biochemical, hematological, pathological and apoptotic organ damage in size, shape and functional group-dependent manner **(El Bailey et al., 2020)**. Additionally, CuO-NPs have been found

to induce liver and kidney tissue damage in rats, highlighting their toxic effects on mammalian systems. Understanding these toxicity mechanisms is crucial for developing safe applications of CuO-NPs and mitigating their potential risks to human health and the environment.

2.2.1 Impact on general observations

Cu NPs induce liver and kidney damage, affecting hematological parameters. Mitochondrial dysfunction and oxidative damage are key mechanisms in the hepato- and nephrotoxicity of copper nanoparticles. Based on all the data, the rats treated with 100 mg kg^{-1} d^{-1} nano-copper showed less adverse effects than the rats received 200 mg kg^{-1} d^{-1} CuNPs. CuNPs can cause overt hepatotoxicity and nephrotoxicity when exposed to a dose of 200 mg kg^{-1} d^{-1} for five days. The major mechanisms involved in this process include extensive renal proximal tubule necrosis and scattered dot hepatocytic necrosis. Furthermore, the liver and renal tissues showed markedly increased amounts of malondialdehyde, reduced thiol groups, and higher copper build up **(Lei et al., 2015)**. As reported by **Yahya et al. (2019),** significantly higher WBC in the groups treated with CuO-NPss and/or ZnONPs and decreased RBCs, Hb, and HCT concentrations were recorded in CuO-NPss, ZnONPs, and their mixture treatment groups as compared to the control group. Rats treated with CuO-NPss, ZnONPs, and their mixture showed a significant rise in MCV and decrease in MCH values and blood platelet levels, but little change in MCHC value. The study found that after administering CuO NPs to rats for 4 weeks, there were significant increases in serum ALT, AST, urea, creatinine, potassium ions, and liver and kidney tissue damage compared to the control group. Conversely, there were statistically significant decreases in serum albumin, total proteins, calcium, and sodium ions levels in the group exposed to CuO NPs compared to the control group. Additionally, the study observed changes in liver functions, including an increase in AST and ALT levels, as well as a depletion of total proteins and albumin, suggesting hepatic toxicity and dysfunction induced by CuO NPs **(El-Atrash et al., 2022; Elshamaa et al., 2022)**. CuO-NPs induced significant changes in hematological parameters and liver function in Cyprinus carpio, suggesting potential hemato- and hepatotoxicity effects **(Noureen et al., 2018)**.

Body weight significantly decreased in both CuO NPs and CuSO4 0.5 (H2O) treated groups in a concentration- and time-dependent manner compared to the control group, indicating potential toxicity. The weights of male reproductive organs, including testes, epididymis, and seminal vesicle, showed significant decreases in the treated groups compared to the control, while the average weights of the seminal vesicle and prostate increased. The same study also found abnormalities in the external appearance of new-born mice resulting from mating males treated with CuO NPs with healthy females, with the occurrence of abnormalities increasing with higher concentrations, indicating potential reproductive toxicity **(Al-Musawi et al., 2022)**.

Pulmonary exposure to copper oxide nanoparticles induces neurotoxicity, oxidative damage, and mitochondrial dysfunction in the brain, with observed lung, liver, and kidney damage. It demonstrates that CuO-NPs lead to dose-dependent brain damage in mice, highlighting the neurotoxic effects of these nanoparticles following intratracheal instillation **(Zhou et al., 2021)**.

2.2.2 Metal accumulation leading to organ toxicity

There was a 1.5 folds increase in the levels of Cu in the brain of mice intoxicated with copper sulphate whereas, highest accumulation was observed in liver (29 folds) followed by kidney (3 folds) in rats following exposure period of 30, 60 and 90 days **(Kumar et al., 2015)**. The study conducted acute and subacute toxicity assessments of copper oxide nanoparticles (CuO-NPs) in female albino Wistar rats. In the acute single high dose of 2000 mg/kg and in subacute toxicity study, multiple doses of CuO-NPs at 30, 300, and 1000 mg/kg were given daily for 28 days to the rats. Significant alterations in biochemical and antioxidant parameters were observed in the liver, kidney, and brain tissues of female albino Wistar rats exposed to copper oxide nanoparticles (CuO-NPs) in both acute and subacute toxicity studies. Higher doses of CuO-NPs led to notable changes in enzyme levels such as tissue aspartate aminotransferase, alanine aminotransferase, alkaline phosphatase, and acetylcholinesterase in the treated rats compared to the control group. Analysis of antioxidant markers like SOD, CAT, lipid malondialdehyde, and reduced glutathione

showed significant differences in the liver, kidney, and brain tissues of rats exposed to CuO-NPs. Histopathological evaluation revealed substantial abnormalities in the histoarchitecture of the liver, kidney, and brain tissues of treated rats, indicating potential toxicity induced by CuO-NPs. **(Bugata et al., 2019)**. Copper oxide nanocomposite encapsulated in arabinogalactan showed increased copper levels in liver, kidney, and brain tissues, causing morphological and neurophysiological changes, indicating organ toxicity after oral exposure **(Titov et al., 2021)**. Study concerning green-synthesized copper nanoparticles showed no toxic effects on liver function and hematological parameters in mice at doses 1000, 2000, and 5000 μg/kg for 2 weeks. However, specific effects on kidney function were not addressed in the study **(Noureen et al., 2018; Khatami et al., 2020)**.

2.2.3 Histopathological background

According to **Hassanen et al. (2019)**, rats administered with CuO-NP were found to have severe damages in their liver and kidney tissues and it was evident from the histopathological analysis. The structural deformation and swelling of the hepatocytes along with vacuolization and inflammatory infiltration of the hepatocytes were reported by **Tang et al. (2019)**, in rats intoxicated with CuNP at a dose 200 mg/kg. Following a 30-day intraperitoneal injection of 1 mg/kg of copper sulfate, **Leiva et al. (2009)** observed increased concentrations of Cu in the rat hippocampal tissue. CuO-NPs induced severe atrophy of tubular cells and glomeruli, notable necrotic tubular cells, and marked inflammatory cellular infiltration in the kidney tissues of the rats **(El-Atrash et al., 2022)**. Rats exposed to Cd for 12 weeks were diagnosed with abnormal levels of liver function parameters, cellular necrosis, pathological degeneration, and proliferation of collagen fibres **(Zhang et al., 2022)**. Mouse macrophages exposed to CuO NPs showed rapid uptake of NPs with deposition in lysosomes, leading to cell death via superoxide dismutase1 (SOD1) misfolding. CuO NPs cause mitochondrial swelling and oxidative stress in cells **(Gupta et al., 2022)**.

2.2.4 Organ toxicity mediated by oxidative stress and depleted antioxidants

Copper oxide nanoparticles induce oxidative stress, inflammation, and organ injuries, especially in individuals with cardiovascular diseases, highlighting extensive toxic effects and the need for caution **(Wang et al., 2022)**. In addition to causing oxidative damage through ROS, copper also inhibits the actions of some antioxidant enzymes that have the ability to scavenge free radicals, including SOD and CAT. Lipid damage and lipid peroxidation production were generated by copper, and the CuSO4 treated group showed a significant reduction in hepatic and renal CAT, SOD, and GSH. In order to defend against oxidative stress, the vital antioxidant defense systems CAT, SOD, and GSH are crucial. Copper shows inhibitory action on CAT, SOD, and GSH may play a role in the oxidative alteration of bio-membrane lipids and enzyme proteins by reactive oxygen species (ROS) **(Zhang et al., 2000; Hashish** and **Elgaml, 2016)**. The study demonstrates that CuO-NPs induce concentration-dependent toxicities in cells through oxidative stress mechanisms, such as the generation of reactive oxygen species (ROS), upregulation of heme oxygenase-1 (HO-1), mitochondrial dysfunction, and secretion of proinflammatory and profibrogenic cytokines, shedding light on the pathways through which CuO NPs exert their harmful effects **(Wang et al., 2022)**. Cytotoxicity of Cu-NPs was investigated in a study using human trophoblast cells and mouse reproductive organs. Mice exposed to Cu-NPs developed pathology and dysfunction of the ovary and placenta. In a time- and dose-dependent manner, these nanoparticles also produced cell cycle arrest at the G2/M phase, induced apoptosis, and inhibited the proliferation of human extra-villous trophoblast cells. The mitochondrial membrane potential (MMP) can be severely damaged by Cu-NPs, indicating that Cu-NPs may be able to initiate the signalling cascade for mitochondria-mediated death **(Zhang et al., 2018)**.

The study examined the effects of Cu on oxidative stress and apoptosis in the liver of four-week-old ICR mice treated for 21, 42 days at dosages of 0, 4, 8, and 16 mg/kg. Overexposure to Cu raised the levels of ROS and reduced antioxidant capacity, which in turn caused mitochondrial apoptosis in the liver. Cu-induced apoptosis also implicated the TNF-R1 signalling pathway. According to the study, Cu exposure triggered the TNF-R1 signalling pathway and raised the mRNA and protein

expression levels of several genes, including B-cell lymphoma-2 and Bcl-extra-large (Bcl-xL). According to the research, exposure to Cu may increase liver apoptosis and induce oxidative stress **(Liu et al., 2020)**. Four groups fed with diets containing different Cu dosages. Replacing CuCO3 with CuNPs reduced lung weight, increased Cu content in brain, kidney, and lung, intensified lipid peroxidation processes, and weakened antioxidant defense. Reducing Cu intake from 6.5 to 3.25 mg/kg improved antioxidant defense in brain and kidneys. However, these treatments negatively affected the respiratory system **(Ognik et al., 2020)**.

Numerous *in vitro* and *in vivo* studies concurred that ROS-mediated oxidative stress was the primary factor in the cytotoxic mechanism; however, in order to direct the development of more potent cytotoxic CuO-based nanodrugs or safer NMs, a deeper comprehension of the fundamental toxicity pathway and an understanding of the physicochemical properties triggering this mechanism are required **(Moschini et al., 2023)**.

2.2.5 Inflammatory response system

The study reveals significant histopathological changes in the brain, increased levels of inflammatory factors (Tnf, Il-6), and notable alterations in oxidative stress markers as a result of CuO-NPss exposure, indicating the induction of inflammation and oxidative damage in the cerebral cortex **(Zhou et al., 2021)**. In vivo experiments on spontaneously hypertensive rats (SHRs) showed that respiratory exposure to CuO NPs led to acute multiple organ injuries in the lungs, liver, kidneys, and heart, with inflammation and fibrosis being prominent. The study found that cardiac injury caused by CuO NPs was relatively less severe compared to injuries in other organs like the lungs, liver, and kidneys. After exposure to CuO NPs, there was an upregulation of various markers of inflammation and endothelial injury in SHRs, such as C-reaction protein (CRP), tumour necrosis factor α (TNF-α), intercellular adhesion molecule 1 (ICAM-1), endothelin-1 (ET-1), angiotensin converting enzyme (ACE), and von Willebrand factor (vWF), indicating systemic inflammation and potential prothrombotic effects **(Wang et al., 2022)**. Rats treated with CuNPs at the dose of 200 mg/kg have shown a significant increase in the levels of major cytokines such as TNF-α, IL-1β, IL2, MIC, MIP-1, IFN- γ and COX-2 **(Tang et al., 2019)**.

The study examined the impact of copper sulfate (CuSO4) on spleen oxidative stress, apoptosis, and inflammatory responses in mice after oral administration at doses 0, 10, 20, and 40 mg/kg for 42 days. Results showed that CuSO4 reduced antioxidant enzyme activities, increased MDA, induced apoptosis, and increased DNA damage markers. Additionally, CuSO4 caused inflammation in the spleen by upregulating the mRNA levels of various pro-inflammatory cytokines including interleukin-1β (IL-1β), IL-2, IL-4, IL-6, IL-12, TNF-α, and interferon-γ (IFN-γ) indicating its potential to cause spleen dysfunction **(Guo et al., 2022)**.

Copper sulphate pentahydrate is a common pesticide in aquaculture farming and agriculture, causing environmental contamination and affecting fish harvesting. Despite its high toxicity, copper ions remain prevalent in fish farming due to their high cytotoxicity and accumulation in sediments. The toxic effect of copper ions is attributed to oxidative stress, which affects neural tissue cells, which are crucial for organisms' vitality. A study investigated the effects of copper ions on PARP, NF-kB, and GFAP expression in Tigris scraper, *Capoeta umbla* brain tissue. Results showed that copper ions significantly downregulated GFAP expression after 72 hours of treatment, and induced changes in β-actin levels. The study also found that copper ions can suppress PARP expression in a time-dependent manner, causing astrogliosis and DNA damage in the fish brain. The findings suggest that copper sulphate has a significant effect on astrogliosis and DNA damage in the fish brain **(Kirici et al., 2019)**.

2.3 Future research perspective

The intricate interplay between oxidative stress, inflammation, and tissue damage underscores the harmful effects of Cd and Cu NPs on biological systems, emphasizing the importance of understanding and mitigating their toxic impact. Moreover, as far as the nanoparticles are concerned, they show much variability in their chemical as well as toxicological properties, with slight variations in their size, shape, and structural characteristics. In many respects, the interactions of CdO-NPs and CuO-NP with cells and tissues are unfortunately still poorly understood. Whether or not they act similarly to regular metallic forms in a living body is not

known. It is especially concerning to consider the potential effects of CdO-NPs and CuO-NPs on the liver, kidney, and brain. Although many studies have been carried out *in vivo* and *in vitro* to trace the deleterious effects and mechanisms of CuO-NPs and CdO-NPs exposure, it is the need of the hour to understand the toxic mechanisms of both the chemicals on human health and on the environment. The study on the mechanisms of toxicity at the cellular and molecular level, which investigates the effects of CdO-NPs and CuO NPs with size and dose variations, will provide valuable insights into the toxicological baseline and safe use of these chemicals.

CHAPTER- 3

OBJECTIVES

Based on the literature survey few queries have been raised for the scientific validation:

- Do CdO and CuO cause toxicity at any point to human, animals and environment?
- If they cause toxicity, what may be the lowest dose of their nano-forms that cause toxicity?
- Are there any targeted organs of toxicity? How do they affect the major organs?
- Do they modulate oxidative stress markers, antioxidant status, apoptotic and inflammatory markers?

Hence, following objectives were postulated to test the above hypotheses-

❖ **Objective 1**

Computational toxicological profiling of CdO and CuO: An *in-silico* approach.

❖ **Objective 2**

Acute oral toxicity of CdO-NPs in Swiss albino mice.

❖ **Objective 3**

To assess antioxidant status, oxidative stress parameter, histopathology, and pathways of organ toxicity induced by cadmium nanoparticles in adult mice.

❖ **Objective 4**

Evaluation of oxidative stress, antioxidant status, molecular mechanism and toxicological pathways that governs the organ specific toxicity in mice intoxicated with copper nanoparticles.

CHAPTER- 4

MATERIALS AND METHODS

I. Computational toxicological profiling of CdO and CuO: An *in-silico* approach.

4.1 Retrieval of canonical SMILES

The canonical SMILES (Simplified Molecular-Input Line-Entry System) of Copper (II) oxide (CuO; compound ID, CID: 14829) and Cadmium (II) oxide (CdO; compound ID, CID: 14782) were retrieved from PubChem (https://pubchem.ncbi.nlm.nih.gov/) database.

4.2 LD_{50} dose and pathway prediction by using ProTox-II online software

ProTox-II provides us with the information on organ toxicity, toxicity endpoints, nuclear receptors signaling pathways, stress response pathways, molecular initiating events and metabolism of a chemical. The software is freely accessible for the users at http://tox.charite.de/protox_II **(Banerjee et al., 2018)**. The simple procedure to use the software is to click on the link that takes us to the homepage of the software. Then clicking on the TOX PREDICTION dialogue box, paste either PubChem name or canonical SMILES followed by clicking on the parameters that we would like to predict and finally on Tox-prediction. The results for the prediction parameters will appear on the screen.

Prediction of general physical properties such as molecular weight (MW), number of H-bond acceptor (nHA, optimal range is 0-12), number of H-bond donor (nHD, optimal range is 0-7), number of atoms (nA), number of bonds (nB), number of rotatable bonds (nRot, optimal range is 0-11) **(Xiong et al., 2021)**, medium Lethal dose (LD_{50}) and toxicity class was predicted using ProTox-II software.

The ratio of a neutral compound's concentrations in the organic and aqueous phases of a two-compartment system at equilibrium is known as the octanol–water partition coefficient P (logP, optimal range is 0 to 3 log mol/L) **(Xiong et al., 2021)**. Most often, logP, its logarithmic form, is employed **(Mannhold et al., 2009)**. Topological surface area (TPSA, optimal rage is 0-140 $Å^2$ based on Veber rule) **(Xiong et al., 2021)** is the measurement of total amount of polar atoms' contributions to their

molecular surface area, which is typically van der Waals, includes oxygen, nitrogen, and the hydrogen atoms they are linked to **(Prasanna** and **Doerksen, 2009)**.

Pathway prediction using ProTox-II for various toxicity pathways and endpoints, including hepatotoxicity, neurotoxicity, nephrotoxicity, respiratory toxicity, cardiotoxicity, immunotoxicity, cytotoxicity, carcinogenicity, mutagenicity, and acute toxicity, BBB-barrier, ecotoxicity, clinical toxicity, nutritional toxicity, androgen receptor (AR), aromatase, estrogen Receptor Alpha (ER), estrogen Receptor Ligand Binding Domain (ER-LBD), Peroxisome Proliferator Activated Receptor gamma (PPAR-Gamma), Nuclear factor (erythroid-derived 2)-like 2/antioxidant responsive element (nrf2/ARE), heat shock factor response element (HSE), mitochondrial membrane potential (MMP), phosphoprotein (Tumour Suppressor) p53, thyroid hormone receptor alpha (THRα), thyroid hormone receptor beta (THRβ), acetylcholinesterase (AChE), NADH-quinone oxidoreductase (NADHOX), voltage gated sodium channel (VGSC), cytochrome CYP1A2, cytochrome CYP2C19, cytochrome CYP2C9, cytochrome CYP2D6, cytochrome CYP3A4, cytochrome CYP2E1. These parameters help to predict potentiality of a drug to induce toxicity at various levels. It also integrates pharmacophores, fragment propensities, and machine learning models (Tox21). The data used to build the predictive models comes from both *in vivo* cases (such as carcinogenicity and hepatotoxicity) and *in vitro* experiments (such as Tox21, AMES bacterial mutation, hepG2 cytotoxicity, and immunotoxicity assays). The predicted results appear as active (positive) or inactive (negative) with their confidence score for each pathway and endpoint predictions **(Banerjee et al., 2018)**.

4.3 ADMET profiling using pkCSM online software

pkCSM, a graph-based signature was used to know about the absorption, distribution, metabolism, excretion, and toxicity (ADMET) properties of CdO and CuO. The pkCSM is a freely usable software and it was accessed using the https://biosig.lab.uq.edu.au/pkcsm/prediction **(Pires et al., 2015)**. The canonical SMILES format was pasted in the input file section and after that clicking on the predict gave us with a link, which further showed the result of the predictions.

Water solubility (LogS) represents the solubility of a compound in water at 25ºC. The optimal range in -4 to 0.5 log mol/L which indicated proper water solubility of a chemical. Caco-2 or human colorectal adenocarcinoma cell lines-2 permeability value represents absorption efficacy of orally administered drug and the high permeability is indicated by Papp > 8 x 10^{-6} cm/s. Intestinal absorption (human) is parameters representing human intestinal permeability or absorption of a drug and ≥ 30% are highly absorbed by the intestine. Human skin permeability (log Kp) value > -2.50 is considered as having low skin permeability. P-glycoprotein (Pgp) substrate is an ATP-binding transporter that binds to toxins and help them remove out of the body hence, acting as a biological barrier for any toxin or xenobiotics entering the body.

Blood brain barrier (BBB) permeability (log BB) is an important parameter that helps to predict the probability of a drug to cross the BBB and reach the brain. Prediction of this parameter helps to reduce the side effect of any drug or chemical hence, helps in neuro-toxicity prediction. The value log BB > 0.3 and log BB< -1 are considered readily and poorly permeable, respectively. CNS (central nervous system) permeability (log PS) at the range log PS > -2 in considered to penetrate CNS while, log PS < -3 are unable to penetrate the CNS. Cytochrome P450 is a crucial detoxifying enzyme mainly found in liver that oxidizes toxins and facilitates their excretion. Cytochrome P450 inhibitor, CYP1A2, CYP2C19, CYP2C9, CYP2D6, and CYP3A4 inhibitor prediction helps to determine the ability of a drug weather it is going to act as an inhibitor or not. CYP2D6 substrate and CYP3A4 substrate helps to determine the ability of Cytochrome to metabolize a drug or not. If a drug act as a substrate to cytochrome P450 then it can be metabolized by the enzyme.

Excretion rate of a chemical is determined by the test parameter total clearance (log mL/min/kg), which is a combination of hepatic metabolism and excretion via kidneys. Assessment of total clearance is important to determine the safe dose of any chemical.

AMES test was performed to predict the probable mutagenicity of the chemicals in bacteria. The results are shown as yes (positive) or no (negative). Maximum

recommended tolerable dose (MRTD) provides information on the threshold toxic dose of a chemical in human. The chemical with MRTD value ≤ 0.477 log (mg/kg/day) is considered as low tolerance and > 0.477 is considered high tolerance. Human ether a-a-go gene (hERG I and II) is a potassium channel encoding gene, inhibition of which may lead various complicacies such as, QT syndrome (fatal ventricular arrhythmia). Rat LD_{50} value in mol/kg and minnow toxicity (LC_{50}) are predicted to determine the acute toxicity dose. LC50 < 0.5 mM (log LC_{50} < -0.3) are regarded as highly acute toxic **(Pires et al., 2015)**.

II. *In vivo* study

4.4 Animal ethics

This study was performed in strict accordance with the guiding principles approved by ARRIVE guidelines **(Du Sert et al., 2020)** for the care and use of Laboratory animals. The whole experimental procedure of using animal was approved by the Institutional Animal Ethical Committee, Mizoram University, Aizawl, Mizoram, India, bearing Approval No. MZU/IAEC/2021-22/07 dt. September 03, 2021. All the necessary measures and care were taken during and prior to the experiment to reduce the suffering and distress of the animals.

4.5 Test Chemical

4.5.1 Cadmium oxide nanoparticle (CdO-NPs)

CdO nano powder (size < 50 nm) was commercially purchased from Nanoshel, India (CAS No: 1306-19-0; Purity 99.9%). The particles were crystalline in structures and brown colour in appearance.

4.5.2 Copper oxide nanoparticle (CuO-NPs)

CuO-NPs purchased as black powder from Sigma-Aldrich (St. Louis, MO 63103, USA), product number 544868 and CAS number 1317-38-0. The particles were crystalline in structures having average particle size range < 50 nm (TEM).

4.6 Characterization of NPs

Fourier Transform Infra-Red (FTIR) spectrometry was performed using IR Affinity 1s (00703, Shimadzu, Japan) to study about the functional group **(Raul et al., 2014)**, elements and molecular structure analysis of the compound **(Manyasree et al., 2017; Karthik et al., 2018)**.

The characterization of the purchased chemical was done to further confirm its structure, size, shape, purity, and surface morphology. Particle size and shape of the compound was studied by generating high resolution (HR) images under Field Emission Transmission Electron Microscopy (FETEM) **(Vijayakumar et al., 2022)** (JEOL 2100 F HR, Japan) at 200kV. Selected-area electron diffraction (SAED) pattern was investigated to find out the physical nature of the particle using TEM **(Balamurugan et al., 2016)**.

The structure of the test compound was studied using X-ray diffraction (XRD-Smartlab, Rigaku, Japan) with Cu Kα radiation operating at a wavelength (λ) of 1.5406 Å, and at a voltage (V) of 40 kV and current (A) 125 mA setting.

4.7 Preparation of test solution

The test solution was prepared by dissolving required amount of the test chemical in 0.9% saline solution. The solution was vigorous sonicated (PCI Analytics, India, model: 500F) so as to suspend the test chemical uniformly. Every day prior to the treatment, the test solution was sonicated for 10-15 minutes.

4.8 Animal maintenance

Swiss albino mice, weighing 25±5 g of the age group 2-3 weeks old and a total of thirty male and eighty female mice, were collected from the Animal Care and Housing facility, Mizoram University, Aizawl, Mizoram. The male and female mice were housed separately, five per cages, in clean and hygienic polypropylene cages and maintained in the air-conditioned set up at a temperature range of 20 ± 2 ºC, 50-70% relative humidity and under a 12-hour dark/12-hour light cycle. The mice were fed daily at regular interval with a standard commercial mouse pellet feed and ultra-pure water ad libitum. Cleaning of the cages and housing area, and monitoring of the heath conditions of mice were performed daily.

Experiment-I- Acute oral toxicity of CdO-NPs in Swiss albino mice

Acute oral toxicity test was performed in accordance with the guiding principle described by the OECD 423 guidelines **(**Acute Oral Toxicity-Acute Toxic Class Method) **(OECD, 2001)**. The acute toxic class method is a stepwise procedure that was introduced to reduce the number of animals used in the test and their sufferings. Test compounds may not necessarily need to be given at dosages that are known to produce significant suffering and pain because of their corrosive or extremely irritating properties. Animals who exhibit signs of severe and persistent suffering or those are morbidly obese must be killed humanely. The test results will be interpreted similarly for these animals as for those that perished during the test. This test procedure may be repeated if needed and provides ranking of the test chemical similar to other Acute toxicity testing guidelines (OECD 420 and OECD 425; **OECD, 2001**). The animals were monitored at regular interval for any sign of discomfort, distress, behavioral changes and mortality after the administration of single dose of test chemical.

4.9 Dosage selection, experimental groups and LD_{50} calculation

In compliance with the OECD 423 Guidelines **(OECD, 2001)**, the starting dose was selected as 5 mg/kg b.w, one of the doses from the four fixed doses (5, 50, 300 and 2000 mg/kg b.w). Prior to the administration of the test compound, all the experimental animals were fasted for 3-4 hours, during fasting only food was withheld but not water. Animals were weighed individually and administered with CdO-NPs orally by using ball tipped oral gavage in accordance to their body weight. Animals were treated with a single dose of CdO-NPs in different groups having administered with initial low dose in day 1 and doses were increased sequentially based upon the observation of previous doses. All the experimental animals were allocated in five different groups, having both male and female (1:1 ratio), based upon their mean body weight and were orally treated with the following doses-

Group	Dose (p.o., 1 mL/100 g b.w)	Male + Female (number; n)
I (Control)	Vehicle only	06 + 06

II	CdO-NPs 5 mg/kg b.w	06 + 06
III	CdO-NPs 25 mg/kg b.w	06 + 06
IV	CdO-NPs 50 mg.kg b.w	06 + 06
V	CdO-NPs 75 mg/kg b.w	06 + 06

After the single dose of oral treatment, the mice were fasted for 2 hours followed by monitoring of general behavior and any indicators of toxicity continuously for 1 hour, then sporadically for 4 hours, and finally over a period of 24 hours. Mice were further monitored once a day for a total of 14 days to look for any behavioral changes, signs of toxicity or/and mortality, and the latency of death. The doses of CdO-NPs were increased based on the behavioral changes and moribund status of the subsequent lower doses. The acute oral toxicity for calculating lethal dose 50 (LD_{50}) was done using probit analysis **(Finney, 1971)**.

4.10 Sample collection

After the completion of 14^{th} day, mice were fasted for 3-4 hours and sacrificed after application of mild anesthesia, 90 mg/kg Ketamine (50-150 mg/kg b.w) and 5 mg/kg Xylazine (5-10 mg/kg b.w) with a 27G needle IP **(Shojaei et al., 2014)**. Blood sample (approximately 0.8 to 1.0 mL from each mouse) were collected after decapitation and a portion of it was immediately mixed with the anticoagulant **(Andjelkovic et al., 2019)** and used for the hematological analysis, and another part of the blood sample were kept undisturbed at room temperature for 20 minutes allowing it to clot. Later, serum sample were obtained by centrifugation at 3000 × g for 15 minutes at 4°C and preserved at -20°C for the biochemical analyses. All the vital orans such as, liver, kidney, brain, heart, lung, spleen, colon, ovaries, uterus and testis were immediately excised, weighed separately from each individual (both male and female) and washed 2 times in ice-cold saline buffer (20 mM Tris –HCl, 0.14 M NaCl buffer, pH 7.4). A part of the tissue samples was fixed in Bouin's fixative containing saturated picric acid (75%), formaldehyde (25%) and glacial acetic acid (5%), and others kept for the estimation of oxidative stress, antioxidant parameters and inflammatory markers at -20°C.

4.11 Daily monitoring-clinical signs and symptoms, body weight, food and water consumption, rectal temperature, and organ indices

Animals were monitored closely just after treatment for 30 mins then for 4 hrs and 6-8 hrs for any sign or symptom of abnormality. And then, monitoring was done in every 24 hrs for remaining 14 days. During the period of treatment, from 1st day to day 14th, body weight (g), food consumption (g), water consumption (mL) and rectal temperature (°C) of each individual of the groups were measured once daily between 06:00 am to 06:00 pm. Rectal temperature was computed using a greased metallic thermocouple (2 mm in diameter), connected with a digital probe was inserted about 2 cm depth of the rectum and hold for 1 minutes to get a stable reading. Any sign of distress, discomfort and behavioral anomaly were observed daily at a regular interval. All the observed data were immediately documented and stored for further analyses.

Gain/loss (%) of body weight was calculated using the formula

$$\left[\frac{\text{Final body weight (g)} - \text{Initial body weight (g)}}{\text{Initial body weight (g)}}\right] \times 100$$

Relative organ weight (g/100g) was calculated as

$$\frac{\text{Organ weight (g)}}{\text{Body weight (g)}} \times 100 \text{ (g)}$$

(Bidanchi et al., 2022).

4.12 Hematological analysis

Blood levels of hemoglobin (Hb) was estimated by acid hematin method using Sahli's hemoglobinometer. Total red blood cell (RBC), total white blood cell (WBC) and packed cell volume (PVC) were computed using hemocytometer **(Thrall** and **Weiser, 2002)**. Additionally, RBC related indices such as mean corpuscular volume (MCV), mean corpuscular hemoglobin concentration (MCHC), and mean corpuscular hemoglobin (MCH) were calculated by following standard formulas.

4.13 Serum biochemical analyses

Serum sample stored at -20 °C were used for the analysis of various markers of hepato-renal functions and lipid profiles. The sample were thawed to the room temperature and various serological assays were performed both for male and female separately in triplet. Serum levels of total protein **(Gornall et al., 1949)**, albumin **(Doumas et al., 1971)**, alkaline phosphatase (ALP, **Kind** and **King, 1954)**, alanine amino-transferase (ALT, **Reitman** and **Frankel, 1957)**, aspartate amino-transaminase (AST, **Reitman** and **Frankel, 1957)**, creatinine **(Bonsnes** and **Taussky, 1945)**, urea **(Berthelot, 1859)**, uric acid **(Yahia, 2019)** were estimated using commercially available kits (Coral Clinical systems, Goa, India) and, total and direct bilirubin **(Garber, 1981)** were quantified using diagnostic kit manufactured by Asritha Diatech India Pvt. Ltd (Euro Diagnostic systems, Chennai, India), according to the manufacturer protocol. Blood urea nitrogen (BUN), and globulin levels were computed by using equations [BUN= urea × 0.467] and [total protein (g/dL) - albumin], respectively. Similarly, ratios of AST and ALT and albumin and globulin were also measured by diving former by the latter. The above-mentioned parameters were evaluated to figure out the status of hepato-renal functions in all the treatment groups in comparison to the control group. Further, the markers of lipid profile such as triglycerides **(Trinder, 1969a)**, cholesterol **(Trinder, 1952)**, high density lipoprotein (HDL) cholesterol **(Mire** and **Snow, 1986)**, were estimated by using commercial diagnostic kits (Coral Clinical systems, Goa, India), where as low density lipoprotein (LDL) cholesterol was calculated in accordance to the formula by **Freidewald et al. (1972)**, where

$$\text{LDL cholesterol} = (\text{Total cholesterol}) - [\text{HDL Cholesterol} + \frac{\text{Triglyceride}}{5}]$$

Levels of blood glucose **(Trinder, 1969b)**, calcium ion **(Gitelman, 1967)**, sodium ion **(Maruna, 1957)**, potassium ion **(Teeri** and **Sesin, 1958)** and chloride ion **(Schoenfeld** and **Lewellen, 1964)** were also assessed individually in all the groups using Coral clinical kits (Coral Clinical systems, Goa, India) following the manufacturer protocol.

4.14 Oxidative stress and antioxidant enzyme status

Tissue and cellular level of reactive oxygen species (ROS) generation and oxidative stress was assessed by detecting the levels of malondialdehyde (MDA) and antioxidant enzymes status. Biomarkers of oxidative stress was measured in liver, kidney, brain, colon, testis and ovary of all the groups.

4.14.1 Tissue homogenate preparation

Tissue samples were homogenized in ice cold 1× phosphate buffer saline (PBS) constituting 137 mM sodium chloride (NaCl), 2.7 mM potassium chloride (KCl), 10 mM sodium phosphate dibasic (Na_2HPO_4), and 1.8 mM potassium phosphate monobasic (KH_2PO_4) dissolved in distilled water to produce 10% homogenate (w/v).

4.14.2 Quantification of protein in the tissue sample

Protein quantification was done by Bradford's method **(Bradford, 1976)**. The assay was performed by diluting 1µL of 10% tissue homogenate to 99 µL distilled water, and then to it 500 µL of Bradford's reagent was added. The absorbance was recorded immediately under a UV-VIS spectrophotometer (Eppendorf, BioPhotometer) at 595 nm against a blank containing everything except, additionally, 1 µL of distilled water instead of a tissue sample. The concentration of protein in the sample was express in µg.

4.14.3 Measurement of tissue lipid peroxidation (LPO) and malondialdehyde (MDA) levels

MDA is the end product of LPO at cellular or tissue level, therefore the levels of LPO is directly proportionate to the concentration of MDA. The presence of MDA was detected according to the procedure described by **Ohkawa et al. (1979)**. The basic principle of the method is to allow MDA to react with Thioburbituric acid (TBA) after precipitating the protein of the sample with Trichloroacetic acid (TCA). 10 % tissue homogenate (in 1 × PBS, w/v) and freshly prepared 15% TCA was mixed in the ratio of 1:1 and result in the precipitation of the proteins present in the sample. The mixture was centrifuged at 10,000 × g for 30 minutes and the supernatant was collected carefully. Then 0.8% TBA was prepared freshly and mixed

with the supernatant (1:1) and allowed to boil at 95 ºC for 25 minutes. The resultant was allowed to cool to the room temperature and the optical density was read at 532 nm against a blank, devoid protein lysate. MDA concentration was expressed as nmol/mg of protein.

4.14.4 Glutathione reduced (GSH) assay

GSH was estimated based on a method described earlier by **Moron et al. (1979)** with a slight modification. The basic working principle of the assay is that the thiol reagent [5, 5-dithio-bis-(2-nitrobenzoic acid), DTNB] reacts with GSH to form 5-thionitrobenzoic acid (TNB) chromophore. The concentration of formation of TNB is proportionate to the concentration of GSH present in the sample. The assay in brief, 900 µL of 0.2 M Na_2HPO_4, 20 µL of DTNB and 80 µL of 10% tissue homogenate (w/v) was mixed together and after incubation for 2 minutes, optical density was measured at 412 nm against the blank and expressed as Unit (U)/mg of protein. The blank contained everything of the assay mixture except for the tissue homogenate, which was replaced with the same quantity of distilled water so as to maintain the homogeneity.

4.14.5 Glutathione-S-Transferase (GST) assay

GST assay was performed by adding 100 µL of 0.1 M phosphate buffer, pH 6.7 (containing 0.1 M dipotassium hydrogen phosphate, K_2HPO_4 and 0.1 M potassium dihydrogen phosphate, KH_2PO_4) and 20 µL of 20 mM 1-chloro, 2,4-dinitobenzene (CDNB) followed by incubation at 37 ºC for 10 minutes. After incubation 60 µL of 20 mM GSH and 10 µL of 10% tissue homogenate (w/v) was added and after the incubation for 5 minutes at room temperature optical density was measured at 340 nm against distilled water serving as the blank. An assay mixture devoid of enzyme was taken as the assay control **(Habig et al., 1974)**. Concentration of the GST was expressed as U/mg of protein.

4.14.6 Catalase (CAT) assay

The catalase assay was carried out based on the method and principle described earlier by **Hadwan (2018)**, a slight modification from the method of **Aebi et al.**

(1984). At first, H_2O_2 in the assay mixture was dissociated by CAT, present in the tissue homogenate (10%, w/v), and it occurred after mixing 10 µL of tissue homogenate with 100 µL of 10 mM hydrogen peroxide (H_2O_2), followed by incubation for 2 minutes at 37 ºC. Then the working solution containing 110 mM cobalt nitrate [$Co(NO_3)_2$], 10 mM sodium hexametaphosphate [$(Na(PO_3)]_6$; Graham salt], and 2.14 M sodium bicarbonate ($NaHCO_3$) was added to the assay mixture and incubated for 10 minutes at room temperature in the dark, which resulted in the formation of carbonato-cobaltate [$Co(CO_3)_3Co$] after the reaction of $Co(NO_3)_2$ with left-over H_2O_2. It gave olive green coloured complex, giving clear absorbance peak at 440 nm, which was measured against distilled water, serving as a blank. A standard devoid of tissue lysate was also prepared to quantify the presence of initial H_2O_2 in the assay mixture. CAT was expressed as U/ mg of protein.

4.14.7 Superoxide dismutase (SOD) assay

The tissue level of SOD was quantified based on the procedure formulated by **Kakkar et al. (1984)**. In a nutshell, to 50 µL of 10% tissue homogenate (w/v) 60 µL of 25 mM sodium pyrophosphate ($Na_4P_2O_7$) buffer (pH 8.3), 25 µL of 186 µM phenazine methosulphate (PMS), 75 µL of 300 µM nitroblue tetrazolium (NBT) were added. The reaction was initiated by adding 50 µL of 760 µM nicotinamide adenine dinucleotide (NADH), which resulted in the formation of NADH-phenazine methosulphate-nitroblue tetrazolium complex after incubation at 30 ºC for 90 sec. The reaction was immediately stopped by adding 250 µL of acetic acid and 500 µL of n-butanol to the assay mixture. Then the mixture was centrifuge at 10,000 × g for 10 minutes at room temperature which resulted in the extraction of the coloured complex by n-butanol. An assay mixture devoid of tissue homogenate was used as assay control. The colour intensity of the supernatant was measured at 560 nm against n-butanol serving as a blank. Value of SOD was expressed as U/mg of protein.

4.15 Histopathological analysis

The tissue sample, pre-fixed in Bouin's fixative for 24 hours and preserved in 70% alcohol (v/v) were processed for the histopathological study. Liver, kidney, brain,

heart, lung, spleen, colon, ovaries, uterus and testis were cut into small sections, dehydrated with the grades of alcohol, embedded in paraffin block and cut into sections of 5 µm thickness (Leica, RM 2125 RTS, Leica systems, Mumbai, India). Further, the cut tissue sections were allowed to adhere to the pre-coated microscope slides, cleared with xylene, dipped in descending grades of alcohol, stained with hematoxylin solution, followed by counterstaining with eosin solution, and finally properly dehydrated, cleared with xylene, and mounted with DPX (dibutylphthalate polystyrene xylene) **(Jensen, 2008)**. All the tissue sections were assessed under a microscope (Leica DM 2500, Leica Microsystems, Wetzlar, Germany) fitted with a computerized digital camera (DFC 450C, Leica Microsystems, Wetzlar, Germany) and compared with the control group to find out the occurrence of any degree of organ damage in the treatment group.

Experiment-II To assess antioxidant status, oxidative stress parameter, histopathology, and pathways of organ toxicity induced by cadmium nanoparticles in adult mice.

4.16 Experimental design, dosages selection, animal treatment

In this experiment, a total of 24 female Swiss albino mice in the age group of 2-3 months, weighing 25 ± 5 g, were allocated into four different groups (n = 6) by random sampling method. As mentioned earlier, CdO-NPs was prepared in 0.9% saline solution and sonicated vigorously for proper mixing in the solution. The animals were administered with the test chemical orally (p. o.) by a bulb-pointed oral gavage fitted with a 1 ml syringe. The first group was treated with the saline solution while the other three groups received different doses of CdO-NPs solution daily for a period of 30 days. In the previous experiment of acute toxicity test, the LD_{50} dose in female was calculated to be 58.12 mg/kg hence, the doses lower than LD_{50} were selected for the 30 days treatment. The dosage selected for the experiment are mentioned below-

Group	Dose (p.o., 1 mL/100 g b.w)	Female (number; n)
I (Control)	Vehicle only	06
II	CdO-NPs 2 mg/kg b.w	06

III	CdO-NPs 5 mg/kg b.w	06
IV	CdO-NPs 8 mg/kg b.w	06

Prior to the treatment, all the experimental animals were fasted for 12 hours. During fasting, food was withdrawn but was provided with sufficient water. The procedure and guidelines approved by the Institutional Animal Ethical Committee, Mizoram University, Aizawl, Mizoram, India, were strictly followed during the time of whole experiment.

4.17 Daily monitoring- body weight, food and water consumption

Body weight of each individual animals were recorded every day before the treatment. In the similar way every day, the animals were fed with a 100 mL of ultrapure water and 50 g of food (dry weight). The next day, measurement of the left-over food and water was recorded to find out the food and water consumption, respectively, and was expressed as average intake per group.

4.18 Sample collection and organ weight

At the end of the 30^{th} day, all the animals were fasted for 12 hours followed by weighing each animal individually and finally anaesthetized with intra-peritoneally (IP) injection of Ketamine (90 mg/kg b.w)/Xylazine (5 mg/kg bw) mixture **(Shojaei et al., 2014)**. All the animals were sacrificed by following the IAEC guidelines. Blood samples were collected by decapitation; a part of it was kept undisturbed at room temperature and allowed to clot, and the other part was used for the hematological analysis according to the earlier-mentioned procedure **(4.10)**. Then, all the samples were centrifuged at 3000 × g for 15 minutes at 4 ºC, serum were collected carefully, labelled and stored at -20 ºC for serum biochemical assay. Immediately after sacrificing the animals, all the organs were excised and washed in ice-cold saline buffer. Weight of each organs were recorded and later, relative organ weights were computed based on the earlier mentioned formula. Liver, kidney and brain tissue were cut into equal parts carefully, a part of it were fixed in Bouin's

fixative for histopathological study and the other parts were stored at -20 ºC for western blotting.

4.19 Hematological assay

The various hematological parameters namely, total RBC, total WBC, concentration of haemoglobin and PCV were measured using the procedure mentioned in earlier section **(4.12)**. From the above computed values, various other related hematological parameters (MCV, MCHC and MCH) were calculated.

4.20 Estimation of metal accumulation in tissue

Heavy metal accumulation in liver, kidney and brain (cortex) tissue was estimated by using atomic absorption spectrometry (AAS). For the analysis, wet digestion of the tissue sample in nitric acid (HNO_3) and H_2O_2 medium was carried out based on the earlier described method by **Jia et al. (2017**) with minor modification. Briefly, 100 mg of frozen tissue sample was weight and minced, thawed at room temperature. 500 µL of HNO_3 and 500 µL of H_2O_2 was added to the tissue sample. Then, it was boiled at 80 ºC until a clear solution without any trace of tissue sample was achieved. The solution was again diluted to 3 mL with 30% HNO_3. After digestion, the tissue suspension was stored in properly sealed tubes at 4 ºC until analysis in AAS.

4.21 Liver and kidney function test, lipid profiles

The markers related to the liver and kidney functions including ALP, AST, ALT, total protein, bilirubin (total and direct), albumin, globulin, urea, uric acid and creatinine were estimated in the serum sample. Other parameters such as A/G ratio, AST/ALT ratio and BUN were computed using standard formula. Lipid profiles parameters including triglyceride, cholesterol, HDL cholesterol and LDL cholesterol, and blood glucose, Na^+, K^+, Cl^+ and Ca^+ ion concentrations were also assessed. All the tests were performed using commercially available kits according to the manufacturer protocol as cited in the aforementioned section **(4.13)**.

4.22 Quantification of inflammatory markers

Different biomarkers of inflammatory response were assayed by Enzyme linked immunosorbent assay in serum sample. Various interleukins (IL) namely IL-1, IL-6

and IL-10, leukotriene B4 (LTB4), Prostaglandin E2 (PG E2) and additionally myeloperoxidase (MPO) and total antioxidant capacity (TOAC) were measured using commercially available ELISA kits (Bioassay Technology Laboratory, China) by following manufacturer instructions.

4.23 Oxidative stress and antioxidant enzyme assay

Levels of antioxidant and oxidative stress biomarkers were evaluated in liver, kidney, and brain tissues. For the liver and kidney, whole tissue was used, while only the cortex of the brain was used for the analysis of the markers. Enzymatic antioxidant assays such as SOD, CAT, and GST and non-enzymatic antioxidant biomarkers that include GSH and LPO (lipid peroxidation) were assessed using standard protocols as mentioned in the earlier section **(4.14)**.

4.24 Histopathological study

Histological studies were carried out on liver, kidney and brain (cortex) tissues, based on the protocol mentioned in the above section **(4.15)**. The paraffin wax embedded tissue sections were cut into 5 µm thick sections, stained with hematoxylin-eosin and observed under microscope for any toxicity related tissue architectural damage.

4.25 Western blotting

4.25.1 Preparation of tissue homogenate

Tissue homogenate was prepared for the protein estimation and western blot analysis in a sample buffer (lysis buffer) containing 100µL of 100 mM sodium chloride (NaCl), 10 µL of 10 mM Tris-Hydrochloric acid (Tris HCl; pH 7.6), 10 µL of 1 mM Ethylenediaminetetraacetic acid (EDTA; pH 8.0), 10µL of 1 mM Phenylmethylsulfonyl fluoride (PMSF), 10 µL of 1 µg/mL aprotinin and finally the volume was adjusted to 1mL. Then, the tissue samples were thawed to the room temperature and 10% homogenate (w/v) was prepared in the lysis buffer. The sample mixture was centrifuged at 10,000 × g for 15 minutes at 4 ºC.

4.25.2 Protein estimation

Protein estimation in the above prepared lysate was done by the Bradford's method **(Bradford, 1979)**. The detailed method is described in the previous section.

4.25.3 Quantification of apoptotic, anti-apoptotic and inflammatory response markers

The protein sample were mixed with SDS gel loading buffer containing 100 mM Tris HCl (pH 6.8), 2% (v/v) β-mercaptoethanol, 4% sodium dodecyl sulfate, 0.02% Bromophenol blue and 20% Glycerol followed by boiling to denature the protein. The proteins of equal amount i.e., 50 µg/well was run in 10% SDS-polyacrylamide gel electrophoresis (PAGE) along with the standard protein marker to separate the proteins based upon their molecular weight. The current was turned on and voltage was set at 100 V and allowed to separate the proteins completely. Electrophoresed gel containing separated protein were transferred to the nitrocellulose (NC) membrane (0.45 µm; Cat# 1620115, Bio-Rad Laboratories, Germany) by the semi dry transfer method (Medox-Bio, Mini Semi Dry Blotting, MX-1295-01) for a period of 20-30 minutes. The membranes were then blocked for any non-specific binding of antibodies using blocking solution containing 0.05% Tween 20 prepared in 1 x PBS (PBST) and 10% skimmed milk (Cat# GRM1254, HiMedia Private Ltd. Mumbai, India) for 1 hour at room temperature. After blocking membranes were applied with primary antibodies and incubated under humidified chambers for overnight (or at least 12 hour) at 4 ºC followed by washing with PBST in the next morning. Then, again specific HRP (Horseradish peroxidase) conjugated secondary antibodies were probed and incubated at room temperature for at least 4 hours. Membranes were again washed with PBST at room temperature and then Enhanced chemiluminescence (ECL; Cat# 1705061, BioRad, Hercules, USA) was applied over it according to the manufacturer's instructions, and incubated for 5 minutes. The membranes were kept under X-ray cassette and developed onto X-ray film under the application of X-ray developer and fixer in a dark room. The developed X-ray films were analysed quantitatively by volume densitometry using ImageJ software (imagej.nih.gov/).

Separate films were developed with polyclonal β-Tubulin (Cat# E-AB-20070, Elabscience Biotechnology Inc. USA) for all samples as loading control and all the targeted antibodies were normalized against it. All the western blots were performed in triplicates **(Annie et al., 2019)**.

BAX, BCL-2 and Active caspase-3

The membranes, just after blocking were probe with pro-apoptotic markers, a monoclonal mouse BAX at dilution 1:1000 (23 kDa; Cat# sc-7480, Santa Cruz Biotechnology, Inc. USA) and a monoclonal mouse active caspase-3 at dilution 1:2000 (17 kDA; Cat# E-AB-22115, Elabscience Biotechnology Inc. USA) and anti-apoptotic marker, a monoclonal mouse BCL-2 (26 kDa; Cat# sc-7382, Santa Cruz Biotechnology, Inc. USA) for overnight. The membranes were washed thoroughly in PBST with constant agitation. The primary BAX, BCL-2 or active caspase-3 binding was confirmed after probing with HRP-conjugated goat anti-mouse IgG secondary antibody (1:4000; Cat# E-AB-1001, Elabscience Biotechnology Inc. USA) for 4 hours and detection with ECL followed by volume densitometric quantification.

NF-κB, TNF-α, IL-6, iNOS, COX-2, P^{53} and PPAR-ɣ

The expression of a monoclonal mouse P^{65} NF-κB, a pro-inflammatory marker (65 kDa; 1:2000; Cat# E-AB-22066, Elabscience Biotechnology Inc. USA), a pro-inflammatory cytokine polyclonal rabbit TNF-α (16 kDa; 1:1000; Cat# E-AB-33121, Elabscience Biotechnology Inc. USA), and other inflammatory response markers such as polyclonal rabbit IL-6 (23kDa; 1:1000; Cat# BS-0872R, Bioss Antibodies, USA) and polyclonal rabbit iNOS (130 kDa; 1:1000; Cat# BS-2072R, Bioss Antibodies, USA) and a tumour suppressor polyclonal rabbit P^{53} (44 kDa; 1:1000; Cat# E-AB-32468, Elabscience Biotechnology Inc. USA) and a promoter of tumourigenesis polyclonal rabbit COX-2 (80 kDa; 1:1000; Cat# E-AB-31012, Elabscience Biotechnology Inc. USA) and a polyclonal rabbit PPAR-ɣ (57 kDa; 1:1000; Cat# E-AB-32647, Elabscience Biotechnology Inc. USA) were quantified by probing the blocked membranes in desired antibodies for overnight followed by washing in PBST and detection by probing conditionally with HRP-conjugated goat anti-mouse IgG and goat anti-rabbit IgG secondary antibody (1:4000; Cat# E-AB-

1001, Elabscience Biotechnology Inc. USA). Finally, volume densitometric quantification of the ECL developed film was done by using ImageJ software.

Experiment-III Evaluation of oxidative stress, antioxidant status, molecular mechanism and toxicological pathways that governs the organ specific toxicity in mice intoxicated with copper nanoparticles.

4.26 Experimental design and study plan

Twenty-four female Swiss albino mice (2-3 months old, weighing 25 ± 5 g) were randomly distributed into four groups (n = 6) of which, one group was control and other three were treated with CuO-NPs. The period of experiment was 30 days and during that period all the animals were treated daily with the test solution orally (p.o.), according to the plan mentioned below-

Group	Dose (p.o., 1 mL/100 g b.w)	Female (number; n)
I (Control)	Vehicle only	06
II	CuO-NPs 1 mg/kg b.w	06
III	CuO-NPs 5 mg/kg b.w	06
IV	CuO-NPs 10 mg/kg b.w	06

All the animals were observed routinely and body weight, food and water consumption were recorded daily. At the end of the experiment all the animals were sacrificed by decapitation after the intra peritoneal (IP) application of mild anesthesia.

4.27 Sample collection, relative organ weight and hematological assay

Blood samples were collected immediately after sacrificing the animals following decapitation. Hematological parameters were studied immediately following the procedures mentioned in the earlier sections **(4.12)**. All the organs were immediately excised, washed in the saline buffer and weights were recorded for the computation of relative organ weight. Half portion of the organs were fixed in Bouin's solution for histological studies and others kept at -20 ºC for the AAS analysis, antioxidant

assay and western blotting. Blood serum was also collected and stored at -20 ºC for further analysis.

4.28 Assessment of metal accumulation by AAS

Accumulation of the Cu metal in the liver, kidney and brain (cortex) was assayed under AAS. Digestion of 100 mg of tissue sample was performed using HNO_3 and H_2O_2 using the protocol mentioned in the previous **section 4.20**.

4.29 Serological assays and ELISA

Biomarkers of hepato-renal functions such as ALP, ALT, AST, total protein, albumin, globulin, urea, creatinine and uric acid were assessed using commercial kits according to manufacturer protocol, as mentioned in the above **section 4.13**. Additionally, concentration of Ca, K, Na and Cl ions were assessed with the help of ready to use commercial kits (Coral Clinical systems, Goa, India). Cellular inflammatory markers such as IL-1, IL-6, IL-10, LTB4 and PG E2 and TAOC and MPO were assessed by using ELISA kits as mentioned earlier **(section 4.22)**.

4.30 Oxidative stress and antioxidant status

In accordance to the afore-mentioned detailed protocols **(section 4.14)**, levels of antioxidant and oxidative stress biomarkers were evaluated in liver, kidney, and brain (cortex) tissues. Enzymatic antioxidant assays such as SOD, CAT, and GST and non-enzymatic antioxidant biomarkers that include GSH and LPO (lipid peroxidation) were assessed.

4.31 Histology of liver, kidney and brain

Liver, kidney and cortex of brain tissue were prepared for the study of any architectural changes and toxicity related damages. The histology of tissue was performed according to the protocol described above **(section 4.15)**.

4.32 Western blotting

Western blotting was performed in 10% tissue homogenate of liver, kidney and brain (cortex). The antibodies targeting BAX, BCL-2, caspase-3, NF-κB, TNF-α, P^{53},

COX-2, PPAR-ɣ, IL-6 and iNOS were probed into membranes separately and detected by using HRP-conjugated secondary antibodies followed by ECL detection method. The detailed protocol for western blotting analyses is mentioned in the above **section 4.25**.

4.33 Statistical analyses

The analysis of all the statistical data were performed in SPSS software (Windows version 20.0, USA) and presented as the mean ± standard error of the mean (SEM). The results for normality and homogeneity were evaluated by the Kolmogorov and Smirnoff test and the Levene test, respectively. A One factor analysis of variance (ANOVA) was performed for the data with a normal distribution for inter-group comparison. ANOVA was followed by Tukey's test if it showed significant difference between the groups. For the variances not showing a normal and homogenous distribution, a non-parametric test was performed. Probability value less than 0.05 ($p < 0.05$) was considered statistically significant. The data showing significance difference were labelled with different alphabets while the similar alphabet depicted that the data were not significant.

CHAPTER- 5

RESULTS

I. Computational toxicological profiling of CdO and CuO: An *in-silico* approach.

5.1 LD_{50} dose and pathway prediction using ProTox-II online software

5.1.1 CdO

Prediction of general physical properties of CdO such as, nHA, nHD, nRot, and TPSA had shown in the safety range however, logP (-0.12 log mol/L) value representing permeability pattern of biomolecules below the range. LD_{50} in animal was predicted to be very low (67 mg/kg) with 100% average similarity and prediction accuracy, and came under the toxicity class III ($50 < LD50 \leq 300$, toxic if swallowed).

Pathway prediction using ProTox-II for various toxicity pathways and endpoints showed that CdO is active for neurotoxicity (0.52), BBB barrier (0.99), ecotoxicity (0.77) and Cytochrome CYP2C9 (0.68). It was found to be inactive for other pathways and toxicity endpoints.

Table 1 General characteristics and LD_{50} prediction of CdO using ProTox-II online server.

Parameters	Value
Canonical SMILE	O=[Cd]
Molecular weight (MW)	128.41
No. H-bond acceptor (nHA)	2
No. H-bond donor (nHD)	0
No. of Atoms (nA)	2
No. of bonds (nB)	1
No. of rotatable bonds (nRot)	0
Topological polar surface area (TPSA)	17.07 $Å^2$
Octanol/Water partition coefficient (logP)	-0.12 log mol/L
Predicted LD_{50}	67 mg/kg
Class	Class III: toxic if swallowed (50 < LD50

	≤ 300)

Table 2 Target pathway prediction of CdO for various toxicity parameters using ProTox-II online server.

Classification	**Target**	**Prediction**	**Probability**
Organ toxicity	Hepatotoxicity	Inactive	0.97
	Neurotoxicity	Active	0.52
	Nephrotoxicity	Inactive	0.80
	Respiratory toxicity	Inactive	0.80
	Cardiotoxicity	Inactive	0.98
Toxicity end points	Carcinogenicity	Inactive	0.66
	Immunotoxicity	Inactive	0.99
	Mutagenicity	Inactive	0.59
	Cytotoxicity	Inactive	0.79
	BBB-barrier	Active	0.99
	Ecotoxicity	Active	0.77
	Clinical toxicity	Inactive	0.85
	Nutritional toxicity	Inactive	0.59
Tox21-Nuclear receptor signalling pathways	Androgen Receptor (AR)	Inactive	
	Aromatase	Inactive	0.93
	Estrogen Receptor Alpha (ER)	Inactive	0.94
	Estrogen Receptor Ligand Binding Domain (ER-LBD)	Inactive	0.86
	Peroxisome Proliferator Activated Receptor Gamma (PPAR-Gamma)	Inactive	0.86
Tox21-Stress response pathways	Nuclear factor (erythroid-derived 2)-like	Inactive	0.79

	2/antioxidant responsive element (nrf2/ARE)		
	Heat shock factor response element (HSE)	Inactive	0.79
	Mitochondrial Membrane Potential (MMP)	Inactive	0.95
	Phosphoprotein (Tumour Suppressor) p53	Inactive	0.89
Molecular Initiating Events	Thyroid hormone receptor alpha (THRα)	Inactive	0.90
	Thyroid hormone receptor beta (THRβ)	Inactive	0.78
	Acetylcholinesterase (AChE)	Inactive	0.97
	NADH-quinone oxidoreductase (NADHOX)	Inactive	0.97
	Voltage gated sodium channel (VGSC)	Inactive	0.95
Metabolism	Cytochrome CYP1A2	Inactive	0.96
	Cytochrome CYP2C19	Inactive	0.95
	Cytochrome CYP2C9	Active	0.68
	Cytochrome CYP2D6	Inactive	0.88
	Cytochrome CYP3A4	Inactive	0.93
	Cytochrome CYP2E1	Inactive	0.94

5.1.2 CuO

Prediction of physical properties of CuO such as, nHA, nHD, nRot, and TPSA had shown in the safety range however, logP (-0.12 log mol/L) value representing

permeability pattern of biomolecules below the range. LD_{50} in animal was predicted to be 413 mg/kg with 33.33% average similarity and 23% prediction accuracy and fell under the toxicity class IV ($300 < LD50 \leq 2000$, harmful if swallowed).

Similar to CdO, CuO pathway prediction using ProTox-II for various toxicity pathways and endpoints showed that CuO is active for neurotoxicity (0.52), BBB barrier (0.99), ecotoxicity (0.77) and Cytochrome CYP2C9 (0.68). It was found to be inactive for other pathways and toxicity endpoints.

Table 3 General characteristics and prediction of LD_{50} value of CuO using ProTox-II online server.

Parameters	Value
Canonical SMILE	O=[Cu]
Molecular weight (MW)	79.55
Number of hydrogen bond acceptors (nHA)	2
Number of hydrogen bond donors (nHD)	0
Number of atoms (nA)	2
Number of bonds (nB)	1
Number of rotatable bonds (nRot)	0
Topological Polar Surface Area (TPSA)	17.07
Octanol/water partition coefficient (logP)	-0.12 log mol/L
Predicted LD50	413 mg/kg
Class	Class IV: harmful if swallowed ($300 < LD50 \leq 2000$)

Table 4 Target Pathway Prediction of CuO for various toxicity parameters using ProTox-II online server.

Classification	Target	Prediction	Probability
Organ toxicity	Hepatotoxicity	Inactive	0.97
	Neurotoxicity	Active	0.52
	Nephrotoxicity	Inactive	0.80
	Respiratory toxicity	Inactive	0.80

	Cardiotoxicity	Inactive	0.98
Toxicity end points	Carcinogenicity	Inactive	0.66
	Immunotoxicity	Inactive	0.99
	Mutagenicity	Inactive	0.59
	Cytotoxicity	Inactive	0.79
	BBB-barrier	Active	0.99
	Ecotoxicity	Active	0.77
	Clinical toxicity	Inactive	0.85
	Nutritional toxicity	Inactive	0.59
Tox21-Nuclear receptor signalling pathways	Androgen Receptor (AR)	Inactive	1.00
	Aromatase	Inactive	0.93
	Estrogen Receptor Alpha (ER)	Inactive	0.94
	Estrogen Receptor Ligand Binding Domain (ER-LBD)	Inactive	0.86
	Peroxisome Proliferator Activated Receptor Gamma (PPAR-Gamma)	Inactive	0.86
Tox21-Stress response pathways	Nuclear factor (erythroid-derived 2)-like 2/antioxidant responsive element (nrf2/ARE)	Inactive	0.79
	Heat shock factor response element (HSE)	Inactive	0.79
	Mitochondrial Membrane Potential (MMP)	Inactive	0.95
	Phosphoprotein (Tumour Suppressor) p53	Inactive	0.89
Molecular Initiating Events	Thyroid hormone receptor alpha (THRα)	Inactive	0.90

	Thyroid hormone receptor beta (THRβ)	Inactive	0.78
	Acetylcholinesterase (AChE)	Inactive	0.97
	NADH-quinone oxidoreductase (NADHOX)	Inactive	0.97
	Voltage gated sodium channel (VGSC)	Inactive	0.95
Metabolism	Cytochrome CYP1A2	Inactive	0.96
	Cytochrome CYP2C19	Inactive	0.95
	Cytochrome CYP2C9	Active	0.68
	Cytochrome CYP2D6	Inactive	0.88
	Cytochrome CYP3A4	Inactive	0.93
	Cytochrome CYP2E1	Inactive	0.94

5.2 ADMET profiling of CdO and CuO pkCSM online software

5.2.1 CdO

ADMET profiling of CdO was performed in various parameters to predict its potential toxicity. Under the property of absorption, water solubility value of 0.43, Caco2 value of 1.49 X 10^{-6} cm/s, 100% intestinal absorption, and skin permeability value -2.89 were predicted for CdO. CdO is also predicted as the substrate of P-glycoprotein. The BBB permeability (log BB) value of -0.070 and CNS permeability (log PS) value of -2.393 were assessed under the drug distribution property. CdO was predicted negative all the cytochrome P450 inhibitors (CYP1A2, CYP2C19, CYP2C9, CYP2D6, and CYP3A4), as well as for the cytochrome P450 substrate (CYP2D6 and CYP3A4). Total clearance was found to be 0.86 log mL/min/kg, which is a very low value. Additionally, it was showing negative for AMES test (mutagenic potential). Maximum tolerated dose in human is 1.22 (log mg/kg/day),

oral Rat acute toxicity value is 2.22 (mol/kg) and Minnow Toxicity value is 2.23 (log mM). Further, as per the prediction CdO is not a hERG I and II inhibitor.

Table 5 ADMET properties of CdO predicted by pkCSM online server.

Property	Model name	Predicted value
Absorption	Water solubility (logS) (log mol/L)	0.43
	Caco2 permeability (log Papp in 10^{-6} cm/s)	1.49
	Intestinal absorption (% absorbed)	100
	Skin permeability (log Kp)	-2.89
	P-glycoprotein substrate (Yes/No)	Yes
Distribution	BBB permeability (log BB)	-0.07
	CNS permeability (log PS)	-2.39
Metabolism	CYP2D6 substrate (Yes/No)	No
	CYP3A4 substrate (Yes/No)	No
	CYP1A2 inhibitor (Yes/No)	No
	CYP2C19 inhibitor (Yes/No)	No
	CYP2C9 inhibitor (Yes/No)	No
	CYP2D6 inhibitor (Yes/No)	No
	CYP3A4 inhibitor (Yes/No)	No
Excretion	Total clearance (log mL/min/kg)	0.86
Toxicity	AMES toxicity (Yes/No)	No
	Maximum tolerated dose in human (log mg/kg/day)	1.22
	hERG I inhibitor (Yes/No)	No
	hERG II inhibitor (Yes/No)	No
	Oral Rat Acute Toxicity (mol/kg)	2.22
	Minnow Toxicity (log mM)	2.23

5.2.2 CuO

To estimate the possible toxicity of CuO, ADMET profiling was carried out in a number of parameters. CuO was predicted to have the following absorption properties: 100% intestinal absorption, a skin permeability value of -2.90, a water solubility value of 0.58, and a Caco2 value of 1.49 X 10^{-6} cm/s. It is also anticipated that CuO serves as P-glycoprotein's substrate. The drug distribution property was evaluated by the BBB permeability (log BB) value of -0.06 and the CNS permeability (log PS) value of -2.40. For both the cytochrome P450 substrate (CYP2D6 and CYP3A4) and all cytochrome P450 inhibitors (CYP1A2, CYP2C19, CYP2C9, CYP2D6, and CYP3A4), CuO was anticipated to be negative. A low value of 0.75 log mL/min/kg was found to be the total clearance. The AMES test showed negative mutagenic potentiality of CuO. The oral rat acute toxicity value is 2.28 (mol/kg), the minnow toxicity value is 2.49 (log mM), and the maximum tolerated dose in humans is 1.24 (log mg/kg/day). Moreover, CuO is not a hERG I and II inhibitor according to the prediction.

Table 6 ADMET properties of CuO predicted by pkCSM online server.

Property	Model name	Predicted value
Absorption	Water solubility (log/mol)	0.58
	Caco2 permeability (log Papp in 10^{-6} cm/s)	1.49
	Intestinal absorption (% absorbed)	100
	Skin permeability (log Kp)	-2.90
	P-glycoprotein substrate (Yes/No)	Yes
Distribution	BBB permeability (log BB)	-0.06
	CNS permeability (log PS)	-2.40
Metabolism	CYP2D6 substrate (Yes/No)	No
	CYP3A4 substrate (Yes/No)	No
	CYP1A2 inhibitor (Yes/No)	No
	CYP2C19 inhibitor (Yes/No)	No
	CYP2C9 inhibitor (Yes/No)	No
	CYP2D6 inhibitor (Yes/No)	No
	CYP3A4 inhibitor (Yes/No)	No
Excretion	Total clearance (log mL/min/kg)	0.75
Toxicity	AMES toxicity (Yes/No)	No
	Maximum tolerated dose in	1.24

	human (log mg/kg/day)	
	hERG I inhibitor (Yes/No)	No
	hERG II inhibitor (Yes/No)	No
	Oral Rat Acute Toxicity (mol/kg)	2.28
	Minnow Toxicity (log mM)	2.49

II. *In vivo* study

5.3 Characterization of CdO-NPs and CuO-NPs

5.3.1 CdO-NPs

FTIR is a very effective technique that helps to gather information on the functional group, elements and molecular structure of a compound under study. **Figure 1A** is a FTIR image of CdO-NPs, peaks observed at 401.19 cm^{-1}, 447.47 cm^{-1}, 601.79 cm^{-1}, 671.23 cm^{-1}, 771.53 cm^{-1}, 1381.03 cm^{-1} and 3240.41 cm^{-1}. The peak 447.47 cm^{-1} corresponds to stretching vibration of pure Cd-O. Wagging vibration of CdO was observed at 1381.03 cm^{-1}. The broad spectrum at 3240.41 cm^{-1} shows the presence of O-H stretching vibration. All the functional groups of CdO were recorded between 400 cm^{-1} to 4000 cm^{-1}.

XRD analysis has revealed the crystallized structure of CdO-NPs (**Figure 1B)**. The XRD peaks were observed at 2θ values 33.02, 38.32, 55.30, 65.92 and 96.28 were indexed to miller indices (hkl) at planes (1 1 1), (2 0 0), (2 2 0), (3 1 1) and (2 2 2), respectively that are well matched with the JCPDS (Joint Committee on Powder Diffraction Standards) card no: 75-0592 for peaks and attributed to JCPDS #:00-005-0640 for indices.

The FETEM image **(Figure 1C)** revealed that the CdO-NPs are predominantly spherical in shape, without any physical contact with each other and the size ranges from 5-50 nm. **Figure 1D** is the image showing SAED pattern of the CdO-NPs, which shows clear concentric rings with intermittent dots. This pattern of SAED indicates that the particles are crystalline in nature **(Venugopal et al., 2017)**.

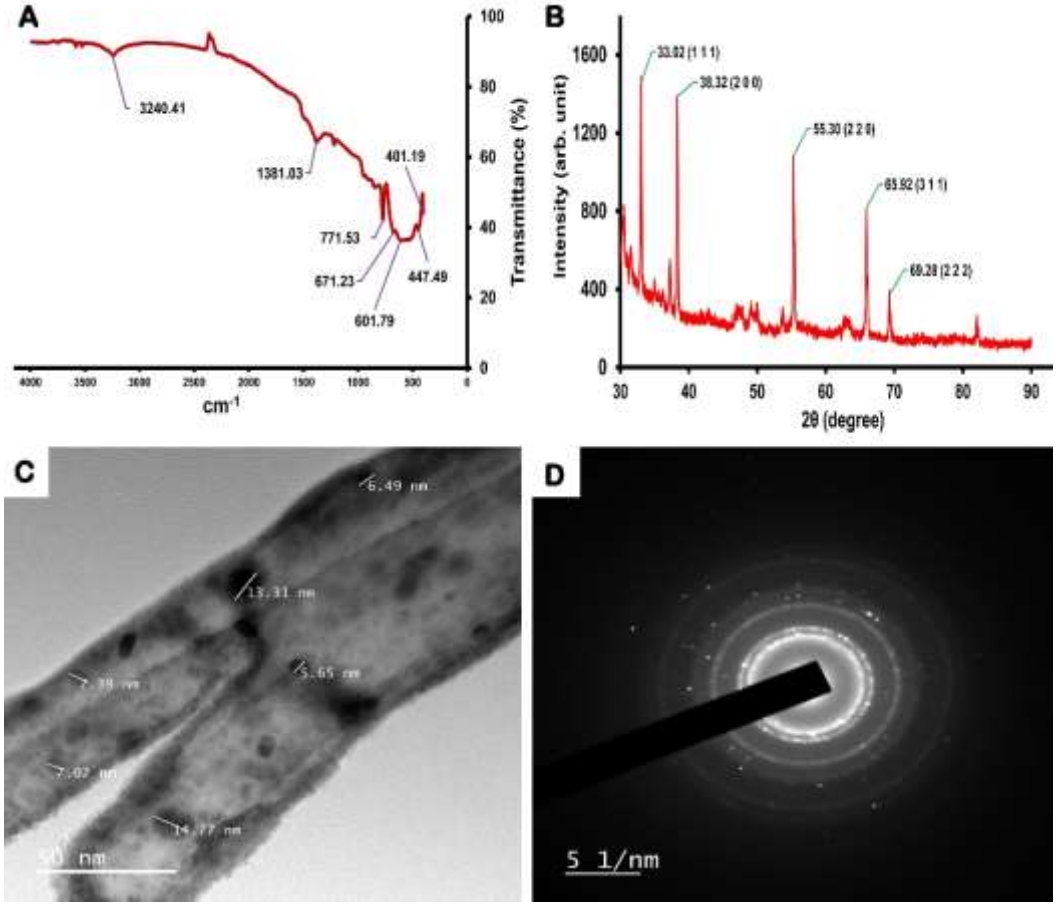

Figure 1 Characterization of CdO-NPs. **A**- FTIR spectrum; **B**- XRD pattern; **C**- FETEM image showing shape and size range; **D**- SAED pattern showing concentric rings with intermittent dots.

5.3.2 CuO-NPs

FTIR spectrum of CuO-NPs is shown in **Figure 2A.** The peaks were observed at 416.61 cm^{-1}, 487.35 cm^{-1}, 601.70 cm^{-1} and 771.53 cm^{-1} indicating stretching vibration of Cu-O **(Manyasree et al., 2017)**.

Figure 2B is showing the XRD peaks and miller indices (hkl) of CuO-NPs. According to JCPDS data no. 80-1916, the exhibited diffraction peaks at 2θ values 32.6, 35.58, 38.80, 48.82, 53.50, 58.42, 61.66, 66.32, 68.18 and 72.44 indexed at (1 1 0), (-1 1 1), (1 1 1), (-1 1 2), (-2 0 2), (0 2 0), (2 0 2), (-1 1 3), (-3 1 1) and (2 2 0), respectively

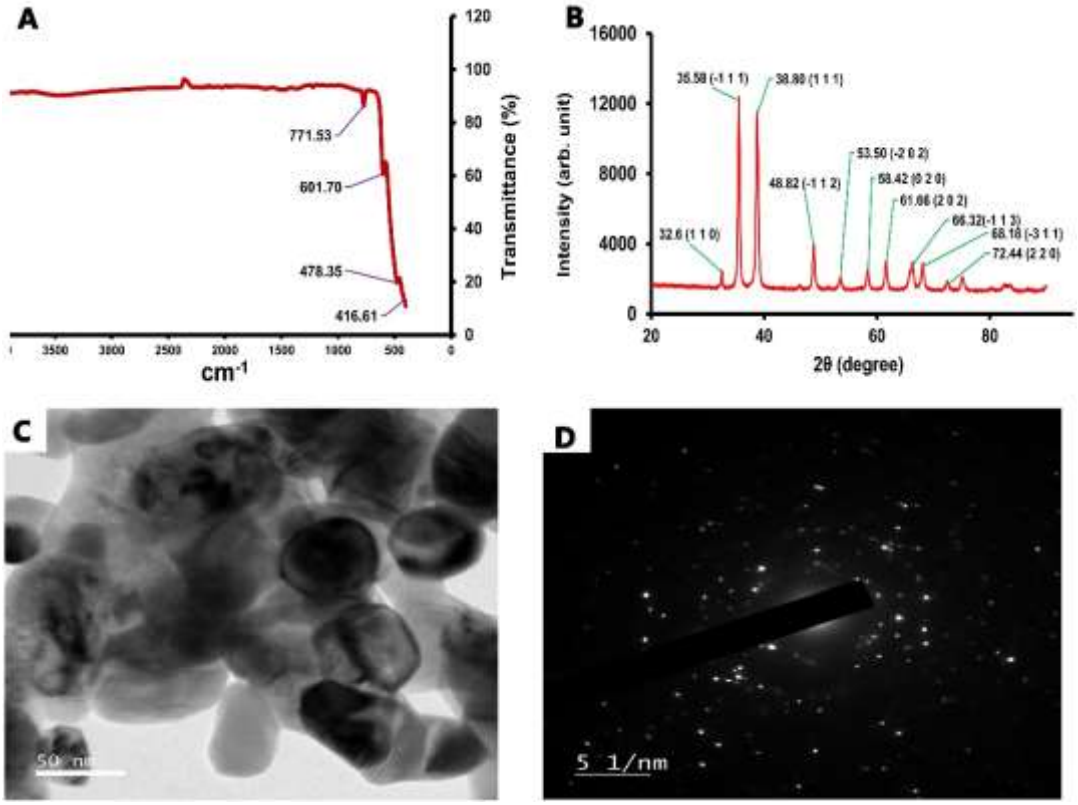

Figure 2 Characterization of CuO-NPs. **A**- FTIR spectrum; **B**- XRD pattern; **C**- FETEM image shows spherical shape and size range; **D**- SAED pattern.

corresponds to different planes of crystalline monoclinic structure of CuO-NPs **(Awwad et al., 2015)**. The largest peaks were seen at 2θ = 35.58 (-1 1 1) and 38.80 (1 1 1), which again attributed to the crystalline structure of CuO-NPs.

FETEM image of CuO-NPs is represented in **Figure 2C**. The TEM imaging revealed that the particles are in nano range (≤ 50 nm) and spherical in shape. SAED pattern **(Figure 2D**) showing concentric rings with many intermittent dots attributing crystalline nature of CuO-NPs.

Experiment-I Acute oral toxicity of CdO-NPs in Swiss albino mice.

5.4 Mortality, clinical signs and symptoms, and LD_{50} calculation

Any sign of toxicity and changes in behaviour was monitored routinely just after the treatment. **Table 7** and **Table 8** listed various parameters observed during the regular monitoring in different treatment groups of male and female mice, respectively. Mortality percentage of 33.33% and 66.67% was observed in both male and female at doses 50 mg/kg bw and 75 mg/kg bw, respectively. Additionally, in females, 16.67% was seen in the treatment group with 25 mg/kg bw dose. Dose-wise group mortality data were recoded and used to calculate the LD_{50} values for both and male and female Swiss albino mice. Following OECD 423 guidelines and performing probit analysis (SPSS software, Windows version 20.0, USA) according to **Finney (1971)**, LD_{50} of 63.82 mg/kg in male and 58.21 mg/kg in female were determined.

Clinical signs and symptoms such as loose stool, paleness of urine, slow somato-motor activity, diarrhoea, drowsiness, aggressiveness, dyspnea, tremors, and swollen stomach were observed in male and female animal groups at higher dose. The symptoms were more prominently seen in the case of females, with few symptoms such as loose stool, paleness of urine, slow somato-motor activity, appearance of black spots in the stomach region, aggressiveness, and swollen stomach being visible from the medium dose itself (25 mg/kg bw) in case of female.

Table 7: Clinical signs and symptoms in male mice after treatment with four different doses of CdO-NPs.

Clinical signs/Wellness parameters	**Control group**	**CdO-NPs 5 mg/kg**	**CdO-NPs 25 mg/kg**	**CdO-NPs 50 mg/kg**	**CdO-NPs 75 mg/kg**
Faecal matter consistency	Normal	Normal	Normal	Normal	Loose stool

Urination and Urine appearance	Normal	Normal	Normal	Paleness of urine	Paleness of urine
Red tear (oozing of blood from eyes, and haemorrhage)	Normal	Normal	Normal	Normal	Normal
Change in skin (Fur loss, spots, colour change, and infestation)	Normal	Normal	Normal	Normal	Appearance of black spots on the stomach
Somato-motor activity	Active	Active	Active	Slow	Slow
Ear bleeding	Absent	Absent	Absent	Absent	Absent
Eye colour change	No change	No change	No change	No change	No change
Diarrhoea	No signs	No signs	No signs	No signs	Observed
Coma	Absent	Absent	Absent	Absent	Absent
Drowsiness	Absent	Absent	Absent	Absent	Observed
Aggression	Normal	Normal	Normal	Aggressive	Aggressive
Dyspnea	Absent	Absent	Absent	Absent	Observed
Convulsions and tremors	Absent	Absent	Absent	Tremor observed	Tremor observed
Salivation	Absent	Absent	Absent	Absent	Absent
Sedation	Absent	Absent	Absent	Absent	Absent
Swollen	Absent	Absent	Absent	Observed	Observed

stomach					
Paralysis	Absent	Absent	Absent	Absent	Absent
Mortality/ Death	No mortality	No mortality	No mortality	2 out of 6 mice dead (33.33%)	4 out of 6 mice dead (66.67%)

Table 8: Clinical signs and symptoms in female mice after treatment with four different doses of CdO-NPs.

Clinical signs/Wellness parameters	**Control**	**CdO-NPs 5 mg/kg**	**CdO-NPs 25 mg/kg**	**CdO-NPs 50 mg/kg**	**CdO-NPs 75 mg/kg**
Faecal matter consistency	Normal	Normal	Normal	Normal	Loose stool
Urination and Urine appearance	Normal	Normal	Normal	Normal	Paleness of urine
Red tear (oozing of blood and haemorrhage)	Normal	Normal	Normal	Normal	Normal
Change in skin (Fur loss, spots and colour change)	Normal	Normal	Normal	Appearance of black spots on the stomach	Appearance of black spots on the stomach
Somato-motor activity	Active	Active	Slow	Slow	Slow
Ear bleeding	Absent	Absent	Absent	Absent	Absent
Eye colour	No change	No change	No change	No change	No change

change					
Diarrhoea	No signs	No signs	No signs	No sings	Observed
Coma	Absent	Absent	Absent	Absent	Absent
Drowsiness	Absent	Absent	Absent	Absent	Observed
Aggression	Normal	Normal	Aggressive	Aggressive	Aggressive
Dyspnea	Absent	Absent	Absent	Observed	Observed
Convulsions and tremors	Absent	Absent	Absent	Absent	Absent
Salivation	Absent	Absent	Absent	Absent	Absent
Sedation	Absent	Absent	Absent	Absent	Absent
Swollen stomach	Absent	Absent	Observed	Observed	Observed
Paralysis	Absent	Absent	Absent	Absent	Absent
Mortality/ Death	No mortality	No mortality	1 out of 6 mice dead (16.67%)	2 out of 6 mice dead (33.33%)	4 out of 6 mice dead (66.67%)

5.5 Body weight, food and water consumption, rectal temperature

The mean body weight **(Figure 3A** and **B)**, food consumption **(Figure 3C** and **D)** and water consumption **(Figure 3E** and **F)** in male and female mice were observed to be decreased in the treatment groups as compared to the control. To be more specific, in male, dose 5 mg/kg bw didn't show variation in mean body weight however, in case of female significant decrease in mean body weight was observed in all the treatment groups as compared to the control. Elevated levels of rectal temperature were observed among males and females as compared to the control groups and significant increase was observed at higher doses (50 mg/kg bw and 75 mg/kg bw) **(Figure 3C** and **D)**. Food and water consumption observed during the experimental period were depicting a decreasing trend in the treatment groups. Further, there were significant differences in

percentage mean body weight, food and water consumption, and rectal temperature in male and female mice of different groups as compared to the control groups **(Table 9** and **10)**. Different alphabet in the **Figure 3** indicated significant difference at $p < 0.05$ among the groups.

5.6 Relative organ weight

In the case of male, reduction in relative organ weight of liver, kidney, stomach, colon, pancreas, testis, and caput and cauda were observed in high dose group as compared to the control **(Table 11)**. **Table 12** represented the relative organ weight of different organs of female mice. Significant reduction in relative organ weight of liver, kidney, spleen stomach, colon, ovaries and uterus were observed in case of female mice. However, no significant changes were observed in brain, heart and pancreas of both male and female.

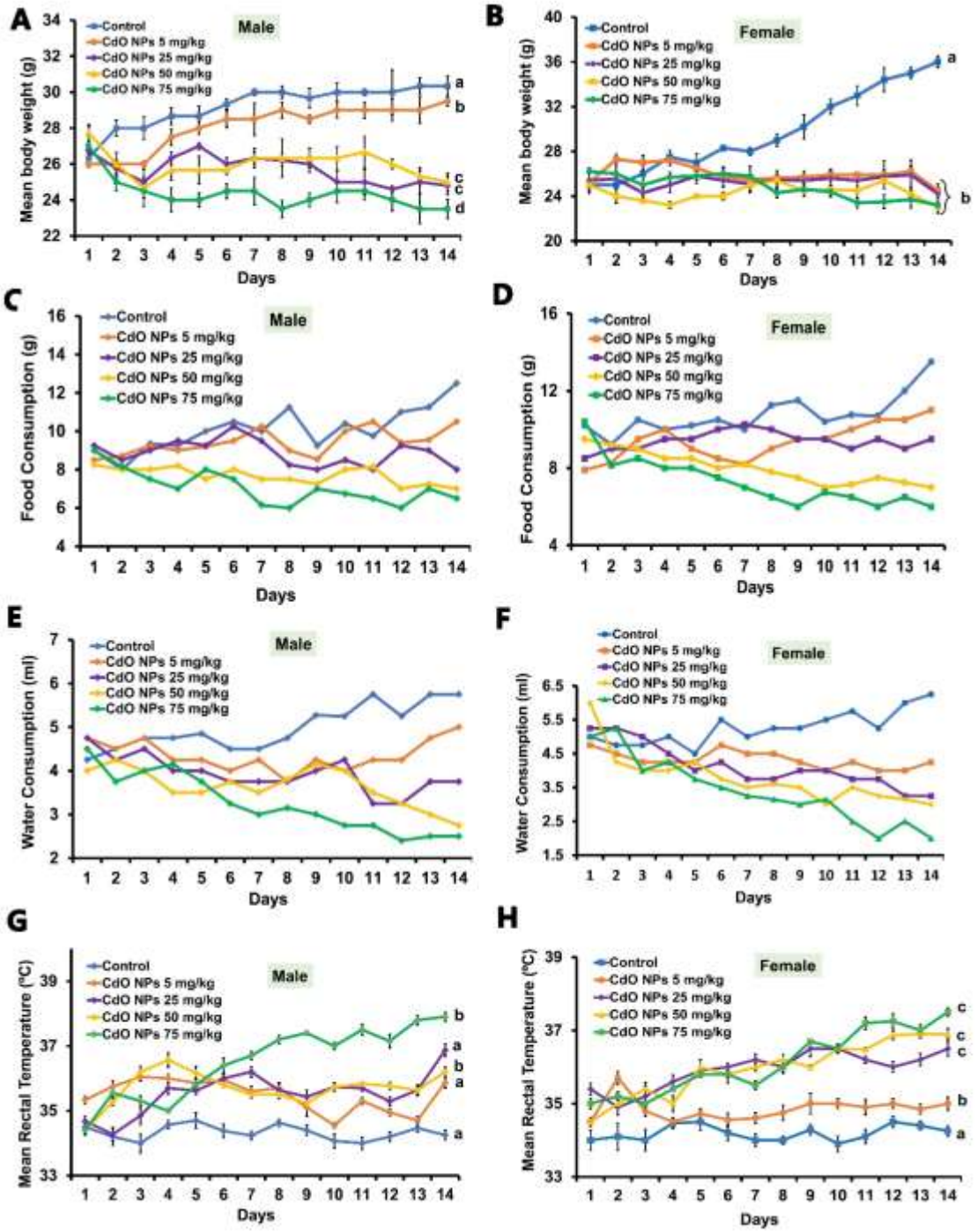

Figure 3 Changes in body weight, food consumption, water consumption and rectal temperature during the treatment period in different treatment groups. **A, C, E** and **G**-mean body weight, mean food consumption, mean water consumption and rectal

temperature in male, respectively; **B, D, F** and **G** mean body weight, food consumption and water consumption and rectal temperature in female, respectively. Data are represented as mean ± SEM (only mean in case of food and water consumption), statistically significant at $p < 0.05$. Significance values are indicated with different alphabets.

5.7 Effects on hematological parameters

Intoxication with single dose of CdO-NPs led to the changes in hematological parameters in male and female mice of different dose groups **(Table 13** and **Table 14)**. Significant reduction in total counts of RBC and concentration of hemoglobin was observed in case both male and female mice at higher doses (50 mg/kg bw and 75 mg/kg bw). Additionally, in comparison to the control groups, percentage of packer cell volume (PCV) was found to be decreased significantly all the groups of male and female. Meanwhile, a significant increase in the total WBC counts was seen in the medium dose to high dose groups of male and female as compared to the control group. Moreover, at higher doses, RBC indices such as MCV, MCHC and MCH were observed to be higher as compared to the control.

Table 9 Daily observations in male mice were recoded and tabulated as mean ± SEM

Daily observations	**Treatment Group (mg/kg bw)**				
	Control	**CdO-NPs 5 mg/kg**	**CdO-NPs 25 mg/kg**	**CdO-NPs 50 mg/kg**	**CdO-NPs 75 mg/kg**
Mean body weight/day (g)	29.23 ± 0.31 a	28.10 ± 0.33 b	25.70 ± 0.27 c	25.98 ± 0.21 c	24.35 ± 0.24 d
Body weight gain/loss (%)	15.19 ± 0.18 a	13.46 ± 0.12 b	-7.29 ± 0.11 c	-9.91 ± 0.22 d	-12.96 ± 0.21 e
Mean Food consumption/day (g)	10.11 ± 0.31 a	9.42 ± 0.18 a, b	8.9 ± 0.18 b	7.69 ± 0.12 c	7.1 ± 0.23 c
Food consumption gain/loss (%)	38.89 ± 0.69 a	23.53 ± 0.22 b	-13.51 ± 0.14 c	-15.15 ± .45 c	-27.78 ± 0.28 d
Mean Water consumption/day (g)	4.99 ± 0.14 a	4.36 ± 0.10 b	3.93 ± 0.12 b, c	3.64 ± 0.12 c, d	3.25 ± 0.18 d
Water consumption gain/loss (%)	35.29 ± 0.25 a	5.26 ± 0.18 b	-21.05 ± 0.12 c	-31.25 ± 0.19 d	-44.44 ± 0.14 e
Mean rectal temperature/day (°C)	34.67 ± 0.21 a	35.37 ± 0.14 a	35.79 ± 0.22 b	35.91 ± 0.20 b	36.01 ± 0.27 b

Rectal temperature gain/loss (%)	0.09 ± 0.01 a	1.53 ± 0.11 b	6.17 ± 0.08 c	5.23 ± 0.1 d	7.99 ± 0.15 e

Table 10 Daily observations in female mice were recoded and tabulated as mean ± SEM, significant at $p < 0.05$.

Daily observations	**Treatment Group (mg/kg bw)**				
	Control	**CdO-NPs 5 mg/kg**	**CdO-NPs 25 mg/kg**	**CdO-NPs 50 mg/kg**	**CdO-NPs 75 mg/kg**
Mean body weight/day (g)	29.75 ± 0.99 a	26.00 ± 0.21 b	25.30 ± 0.13 b	24.31 ± 0.20 b	24.83 ± 0.30 b
Body weight gain/loss (%)	36 ± 0.24 a	-2.77 ± 0.11b	-4.72 ± 0.14 c	-8.00 ± 0.14 d	-11.45 ± 0.21 e
Mean Food consumption/day (g)	10.80 ± 0.27 a	9.40 ± 0.25 b	9.41 ± 0.12 b	8.00 ± 0.22 c	7.27 ± 0.33 c
Food consumption gain/loss (%)	32.35 ± 0.24 a	34.83 ± 0.50 b	11.76 ± 0.21 c	-26.32 ± 0.28 d	-42.31 ± 0.19 e
Mean Water consumption/day (g)	5.26 ± 0.13 a	4.32 ± 0.07 b	4.12 ± 0.18 b	3.76 ± 0.20 b	3.37 ± 0.27 c

Water consumption gain/loss (%)	25 ± 0.15 a	-10.50 ± 0.48 b	-38.10 ± 0.12 c	-50.00 ± 0.28 d	-60.00 ± 0.49 e
Mean rectal temperature/day (°C)	34.20 ± 0.06 a	34.84 ± 0.08 b	35.96 ± 0.13 c	35.97 ± 0.20 c	36.13 ± 0.24 c

Table 11 Relative organ weight of different organs of male mice of five different groups. Data represented as mean ± SEM, significant at $p < 0.05$.

Relative Organ weight	**Treatment Group (mg/kg bw)**				
	Control	**CdO-NPs 5 mg/kg**	**CdO-NPs 25 mg/kg**	**CdO-NPs 50 mg/kg**	**CdO-NPs 75 mg/kg**
Liver	5.30 ± 0.23 a	5.16 ± 0.19 b	4.95 ± 0.21 b	4.32 ± 0.17 b	4.02 ± 0.15 b
Kidney	1.55 ± 0.12 a	1.51 ± 0.02 a	1.51 ± 0.03 a	1.30 ± 0.02 b	1.12 ± 0.01 b
Brain	1.55 ± 0.01a	1.52 ± 0.05 a	1.48 ± 0.03 a	1.47 ± 0.04 a	1.45 ± 0.02 a
Spleen	0.45 ± 0.01 a	0.44 ± 0.01 a	0.43 ± 0.01 a	0.42 ± 0.01 a	0.37 ± 0.02 b
Stomach	0.72 ± 0.01 a	0.70 ± 0.01 a	0.64 ± 0.01 b	0.63 ± 0.01 b	0.58 ± 0.01 c
Colon	0.96 ± 0.02 a	0.87 ± 0.01 b	0.85 ± 0.01 b	0.62 ± 0.01 c	0.64 ± 0.01 c
Pancreas	0.61 ± 0.01 a	0.60 ± 0.01 a	0.58 ± 0.01 a	0.59 ± 0.01 a	0.60 ± 0.01 a

Heart	0.48 ± 0.01 a	0.44 ± 0.01 a	0.44 ± 0.01 a	0.43 ± 0.01 a	0.42 ± 0.01 a
Lungs	0.98 ± 0.02 a	0.95 ± 0.02 a	0.84 ± 0.01 b	0.77 ± 0.01 c	0.79 ± 0.01 c
Testis	0.48 ± 0.02 a	0.47 ± 0.01 a	0.43 ± 0.01 a	0.40 ± 0.01 b	0.37 ± 0.01 b
Caput and Cauda	0.28 ± 0.01 a	0.25 ± 0.01 a	0.24 ± 0.01 a	0.23 ± 0.01 b	0.20 ± 0.01 b
Seminal vesicle	0.54 ± 0.02 a	0.47 ± 0.01 b	0.47 ± 0.01 b	0.48 ± 0.01 a	0.34 ± 0.01 c

Table 12 Relative organ weights of different organs of female mice of five different groups. Data are represented as mean ± SEM, significant at $p < 0.05$.

Relative organ weight	**Treatment Group (mg/kg bw)**				
	Control	**CdO-NPs 5 mg/kg bw**	**CdO-NPs 25 mg/kg**	**CdO-NPs 50 mg/kg**	**CdO-NPs 75 mg/kg**
Liver	7.64 ± 0.55 a	5.06 ± 0.64 b	6.15 ± 0.38 a	4.87 ± 0.44 b	4.38 ± 0.31 b
Kidney	1.08 ± 0.03 a	0.98 ± 0.01 a	1.10 ± 0.04 a	0.74 ± 0.04 b	0.78 ± 0.02 b
Brain	1.60 ± 0.02 a	1.56 ± 0.04 a	1.47 ± 0.03 b	1.56 ± 0.02 a	1.50 ± 0.02 b
Spleen	0.58 ± 0.01 a	0.44 ± 0.01 b	0.37 ± 0.02 c	0.28 ± 0.02 d	0.30 ± 0.01 d
Stomach	0.94 ± 0.03 a	0.73 ± 0.01 a	1.05 ± 0.12 a	0.69 ± 0.01 b	0.61 ± 0.02 b
Colon	1.98 ± 0.09 a	1.79 ± 0.14 a	1.99 ± 0.07 a	1.12 ± 0.18 b	1.22 ± 0.08 b

Pancreas	0.88 ± 0.01 a	0.89 ± 0.01 a	0.89 ± 0.02 a	0.87 ± 0.02 a	0.86 ± 0.01 a
Heart	0.48 ± 0.01 a	0.47 ± 0.02 a	0.51 ± 0.01 a	0.50 ± 0.02 a	0.47 ± 0.01 a
Lungs	1.48 ± 0.02 a	0.84 ± 0.04 a	0.70 ± 0.01 b	0.77 ± 0.01 a	0.63 ± 0.01 b
Ovaries	0.07 ± 0.01 a	0.07 ± 0.01 a	0.07 ± 0.01 a	0.06 ± 0.01 b	0.04 ± 0.01 c
Uterus	0.69 ± 0.02 a	0.91 ± 0.01 b	0.54 ± 0.01 c	0.27 ± 0.01 d	0.30 ± 0.01 d

Table 13 Effect of CdO-NPs intoxication led to the changes in different hematological parameters in male mice. Data are represented as mean ± SEM, significant at $p < 0.05$. Different alphabets attributes to the significant relationship among the groups.

Hematological parameters	**Control**	**CdO-NPs 5 mg/kg**	**CdO-NPs 25 mg/kg**	**CdO-NPs 50 mg/kg**	**CdO-NPs 75 mg/kg**
RBC (10^6/µl)	12.21 ± 0.91 a	10.02 ± 0.72 a	9.82 ± 0.57 a	8.80 ± 0.64 b	8.01 ± 0.38 b
WBC (10^3/µl)	6.06 ± 0.61 a	6.27 ± 0.53 a	8.68 ± 0.77 b	9.12 ± 0.29 c	10.88 ± 0.31 c
Hemoglobin (g/dL)	12.53 ± 0.88 a	9.84 ± 0.39 b	10.40 ± 0.65 a	8.68 ± 0.31 b	8.15 ± 0.45 b
PCV (%)	44.50 ± 1.06 a	36.27 ± 1.00 a	35.14 ± 0.73 a	25.64 ± 0.59 b	23.54 ± 0.61 b
MCV (fL)	36.45 ± 0.66 a	36.20 ± 0.48 a	35.78 ± 0.55 a	29.14 ± 0.84 b	29.39 ± 0.56 b
MCHC (g/dL)	28.16 ± 0.68 a	27.13 ± 0.49 a	29.60 ± 0.34 a	33.85 ± 0.15 b	34.62 ± 0.47 b
MCH (pg)	10.26 ± 0.25 a	9.82 ± 0.05 a	10.59 ± 0.16 b	9.86 ± 0.13 a	10.17 ± 0.19 a, b

Table 14 Effect of CdO-NPs intoxication led to the changes in different hematological parameters in female mice. Data are represented as mean ± SEM, significant at $p < 0.05$. Different alphabets attributes to the significant relationship among the groups.

Hematological parameters	**Control**	**CdO-NPs 5 mg/kg**	**CdO-NPs 25 mg/kg**	**CdO-NPs 50 mg/kg**	**CdO-NPs 75 mg/kg**
RBC (10^6/µl)	10.81 ± 0.68 a	10.23 ± 0.81 a	8.44 ± 0.37 a	7.12 ± 0.52 b	5.34 ± 0.57 b

WBC (10^3/µl)	6.15 ± 0.55 a	6.39 ± 0.70 a	8.97 ± 0.62 b	8.55 ± 0.59 a, b	11.12 ± 0.48 c
Hemoglobin (g/dL)	11.56 ± 0.63 a	10.29 ± 0.57 a, b	8.64 ± 0.41 b, c	8.22 ± 0.29 c	7.14 ± 0.35 c
PCV (%)	41.68 ± 1.29 a	36.87 ± 1.37 a	31.92 ± 1.73 b	27.66 ± 1.60 b	21.42 ± 1.58 c
MCV (fL)	38.56 ± 0.32 a	36.04 ± 0.51b	37.82 ± 0.64 a	38.85 ± 0.41 a, c	40.11 ± 0.56 c
MCHC (g/dL)	27.74 ± 0.48 a	27.91 ± 0.25 a	27.07 ± 0.45 a	29.72 ± 0.28 b	33.33 ± 0.53 c
MCH (pg)	10.69 ± 0.28 a, b	10.06 ± 0.37 a	10.24 ± 0.28 a, b	11.54 ± 0.19 b	13.37 ± 0.51 c

5.8 Effects on hepatic and renal function biomarkers, lipid profiles and ion concentration

CdO-NPs intoxication resulted in deterioration of liver and kidney function that were evident from the analyses performed on blood serum for different liver and kidney function biomarkers and metabolites. A significant, dose-dependent decrease in serum total protein, albumin, globulin and A/G ratio were observed in males and females of treatment groups as compared to the normal control mice **(Figure 4A, B, C** and **D)**. Additionally, the concentration of ALP, AST **(Figure 4 E** and **F)**, ALT **(Figure 5 A** and **B)**, total bilirubin, creatinine, uric acid **(Figure 5 C** and **D)** and urea **(Figure 5 E** and **F)** were recorded to be significantly higher in the treatment groups as compared to the control groups. The levels of BUN **(Figure 5 E** and **F)** were significantly higher in females while insignificant increase was recorded in males, as compared to the normal control group.

The serum level detection of lipid profiles, serum glucose level and ion concentration in males and females are represented in **Table 15** and **Table 16**, respectively. Significant

elevation of total cholesterol and triglycerides were observed in dose-dependent manner as compared to the control. Moreover, decrease in HDL and increase in LDL levels were observed in treatment groups. However, there was no significant changes observed in the blood serum glucose levels. Additionally, detection of various crucial ion concentration has revealed that there was increase in chloride and potassium ion concentrations while, decrease concentration of calcium and sodium levels were seen in the treatment group mice as compared to the control mice.

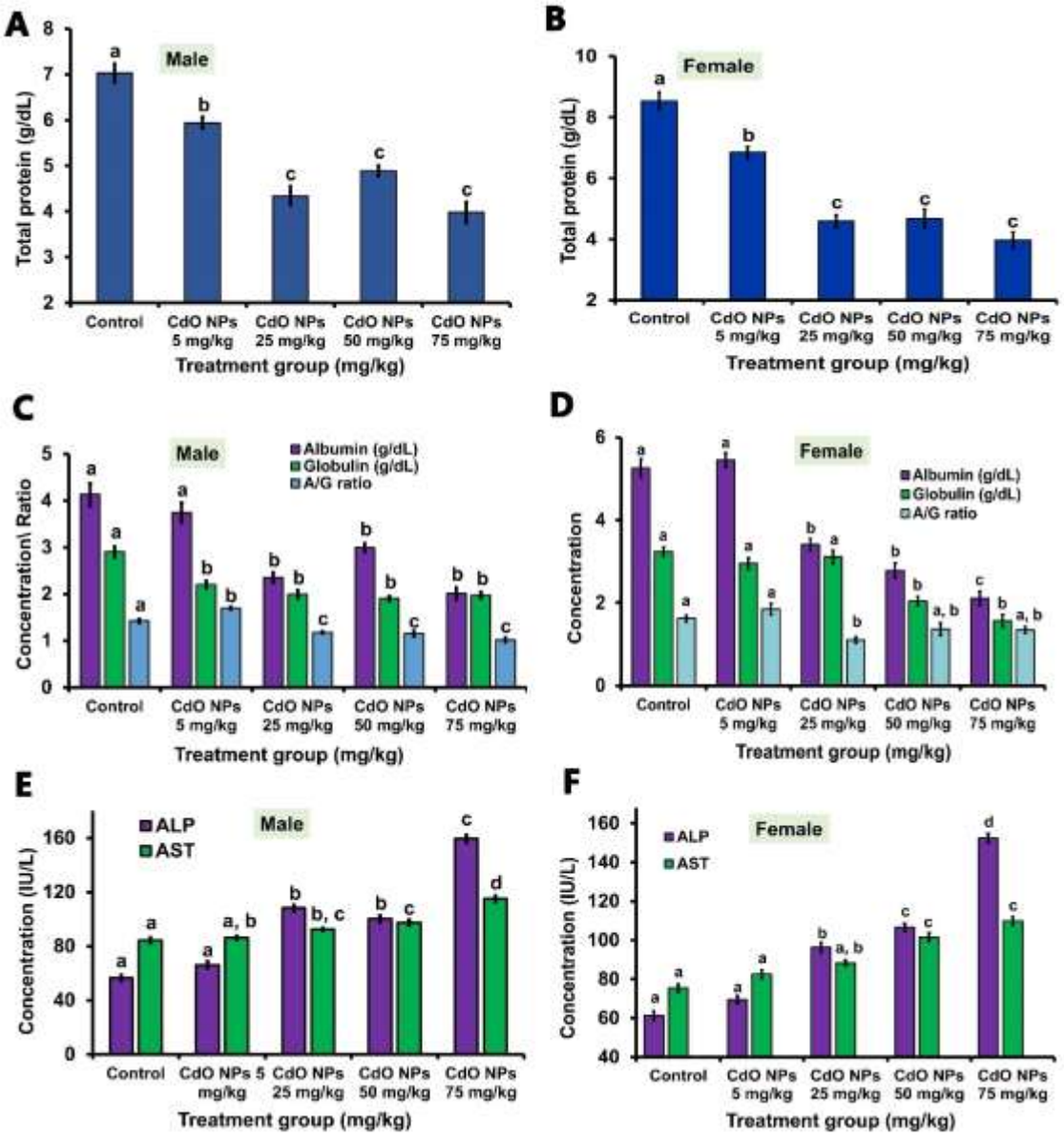

Figure 4 Acute exposure to CdO-NPs led to significant effects on serum level concentration of total protein, albumin, globulin, A/G ratio, ALP and AST in male and female mice after 14 days as compared to the control mice. The figure has representation of **A** and **B**- total protein; **C** and **D**- Albumin, globulin and A/G ratio; **E** and **F**- ALP and AST, in males and females, respectively, significant at $p < 0.05$.

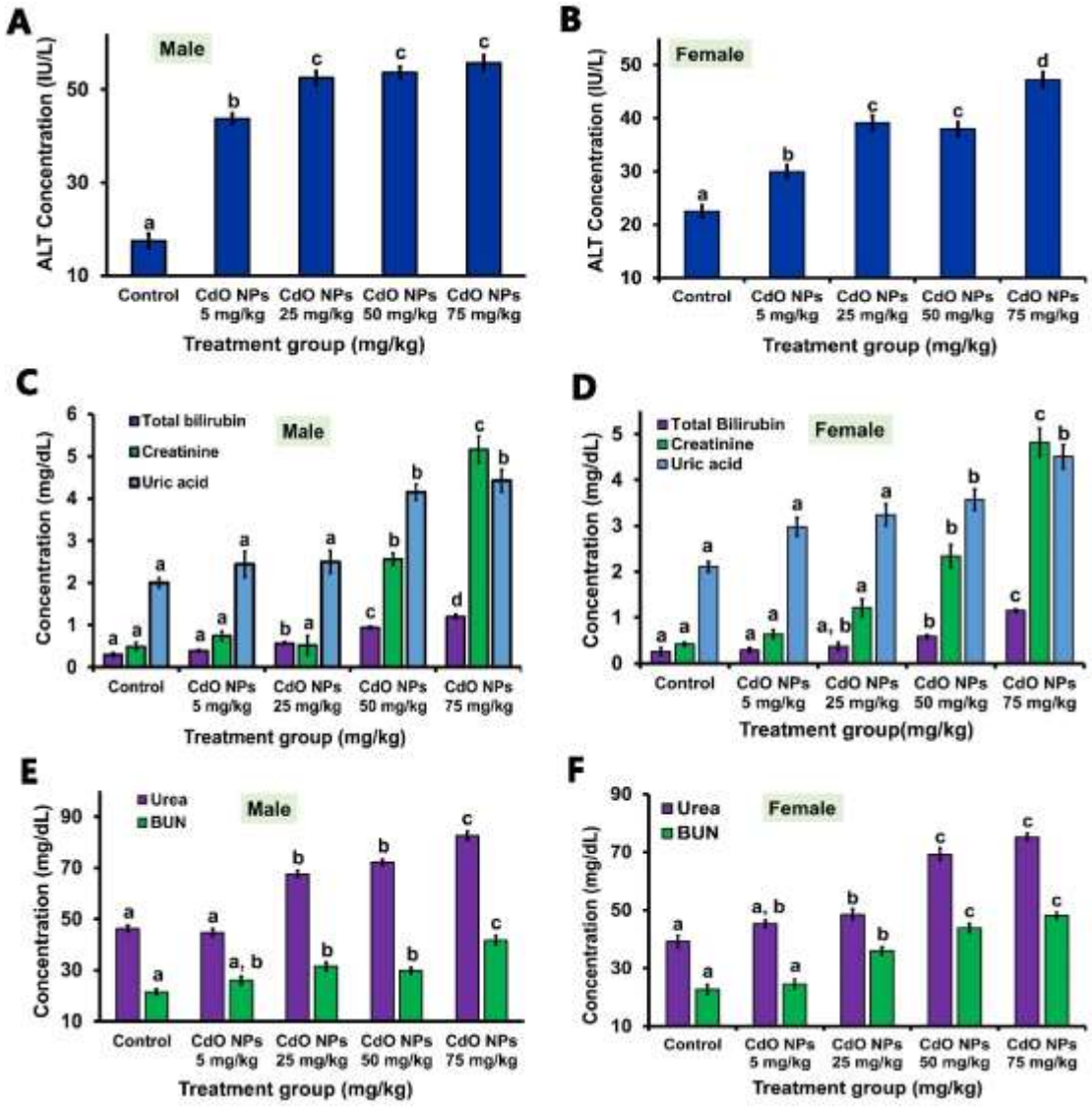

Figure 5 Acute exposure to CdO-NPs led to significant effects on serum level concentration of ALT, total bilirubin, creatinine, uric acid, urea and BUN in male and female mice after 14 days as compared to the control mice. The figure has representation of **A** and **B**- ALT; **C** and **D**- total bilirubin, creatinine and uric acid; **E** and **F**- urea and BUN, in males and females, respectively, significant at $p < 0.05$.

Table 15 Representation of lipid profiles, blood serum glucose level and major ion concentrations in CdO-NPs treatment as well as control group male mice. Data were presented as mean ± SEM which were significant at $p < 0.05$.

Lipid Profiles/ Blood serum glucose level/ Ion concentration	**Treatment Group (mg/kg bw)**				
	Control	**CdO-NPs 5 mg/kg**	**CdO-NPs 25 mg/kg**	**CdO-NPs 50 mg/kg**	**CdO-NPs 75 mg/kg**
Total Cholesterol (mg/dL)	98.99 ± 1.78 a	104.02 ± 1.49 a	113.56 ± 1.97 b	135.00 ± 1.57 c	149.24 ± 1.84 d
Triglycerides (mg/dL)	111.90 ± 2.17 a	133.33 ± 1.89 b	154.25 ± 1.35 c	215.07± 1.79 d	225.39 ± 2.81 e
HDL Cholesterol (mg/dL)	72.00 ± 1.07 a	70.97 ± 1.21 a	62.50 ± 1.03 b	65.67 ± 1.21 b	64.61 ± 1.49 b
LDL Cholesterol (mg/dL)	4.61 ± 0.87 a	6.39 ± 1.02 a	19.95 ± 1.11 b	26.49 ± 1.26 c	39.54 ± 1.48 d
Glucose (mg/dL)	72.90 ± 1.69 a	75.80 ± 1.71 a	70.58 ± 1.22 a	73.74 ± 1.18 a	79.83 ± 1.55 a
Calcium (mg/dL)	9.79 ± 0.31 a	9.48 ± 0.22 a	8.99 ± 0.28 a	8.82 ± 0.19 a	5.14 ± 0.09 b
Chloride (mmol/L)	118.60 ± 1.25 a	119.39 ± 1.54 a	120.73 ± 1.48 b	123.07 ± 1.19 c	123.74 ± 1.78 c
Sodium (mmol/L)	157.99 ± 1.87 a	152.76 ± 1.49 a	141.70 ± 1.62 b	128.83 ± 1.25 b	105.12 ± 1.33 c

Potassium (mmol/L)	7.40 ± 0.54 a	8.15 ± 0.62 a	13.66 ± 0.41 b	10.02 ± 0.38 a	12.29 ± 0.89 b

Table 16 Representation of lipid profiles, blood serum glucose level and major ion concentrations in CdO-NPs treatment as well as control group female mice. Data were presented as mean ± SEM which were significant at $p < 0.05$.

Lipid Profiles/ Blood serum glucose level/ Ion concentration	**Treatment Group (mg/kg bw)**				
	Control	**CdO-NPs 5 mg/kg**	**CdO-NPs 25 mg/kg**	**CdO-NPs 50 mg/kg**	**CdO-NPs 75 mg/kg**
Total Cholesterol (mg/dL)	85.11 ± 1.48 a	98.54 ± 1.75 b	125.02 ± 1.23 c	139.78 ± 1.07 d	155.19 ± 1.25 e
Triglycerides (mg/dL)	98.90 ± 1.98 a	112.30 ± 2.15 b	149.80 ± 1.68 c	195.26 ± 1.97 d	237.14 ± 2.33 e
HDL Cholesterol (mg/dL)	64.25 ± 1.27 a	62.31 ± 1.06 a	60.97 ± 1.00 b	55.48 ± 1.48 b	52.19 ± 1.67 b
LDL Cholesterol (mg/dL)	6.12 ± 1.24 a	6.48 ± 1.34 a	21.52 ± 1.08 b	29.34 ± 2.17 c	41.27 ± 1.92 d
Glucose (mg/dL)	73.12 ± 1.04 a	74.21 ± 1.12 a	72.67 ± 1.28 a	76.45 ± 1.33 a, b	82.78 ± 2.10 b

Calcium (mg/dL)	8.52 ± 0.58 a	8.61 ± 0.49 a	7.21 ± 0.32 a	6.55 ± 0.14 b	5.08 ± 0.27 b
Chloride (mmol/L)	112.34 ± 1.67 a	115.27 ± 2.17 a	113.09 ± 1.56 a	125.47 ± 1.28 b	129.97 ± 1.67 b
Sodium (mmol/L)	148.26 ± 1.41 a	150.56 ± 1.20 a	140.87 ± 1.38 a, b	137.00 ± 1.08 b	122.40 ± 1.54 c
Potassium (mmol/L)	7.58 ± 0.92 a	8.12 ± 0.54 a	7.97 ± 1.04 a	14.02 ± 0.33 b	16.55 ± 1.19 b

5.9 Effects CdO-NPs exposure on oxidative stress biomarker and antioxidant defence mechanism on liver, kidney, brain, testis, ovary and colon

Intoxication with CdO-NPs in male and female mice in the treatment group showed changes in the tissue oxidative stress marker i.e., MDA levels. Significant increase in the concentration of MDA was observed in liver **(Figure 6A)**, kidney **(Figure 6B)** and brain **(Figure 6C)** of the treatment mice as compared to the control mice however, female mice had shown more prominent effects than the male mice. Further, significant elevation of MDA level was also noted in testis of male and ovary of female **(Figure 6D)** mice as well as in colon of the CdO-NPs treated mice.

Assessment of antioxidant enzymes such as GSH, GST, SOD and CAT, revealed poor antioxidant status in mice intoxicated with CdO-NPs. Significant depletion of GSH, GST, SOD and CAT were observed in liver, kidney, brain, testis, ovary and colon in the treatment groups as compared to the normal control group mice **(Figure 7** and **Figure 8)**. However, effects were prominently observed in the high dosages of CdO-NPs intoxicated mice.

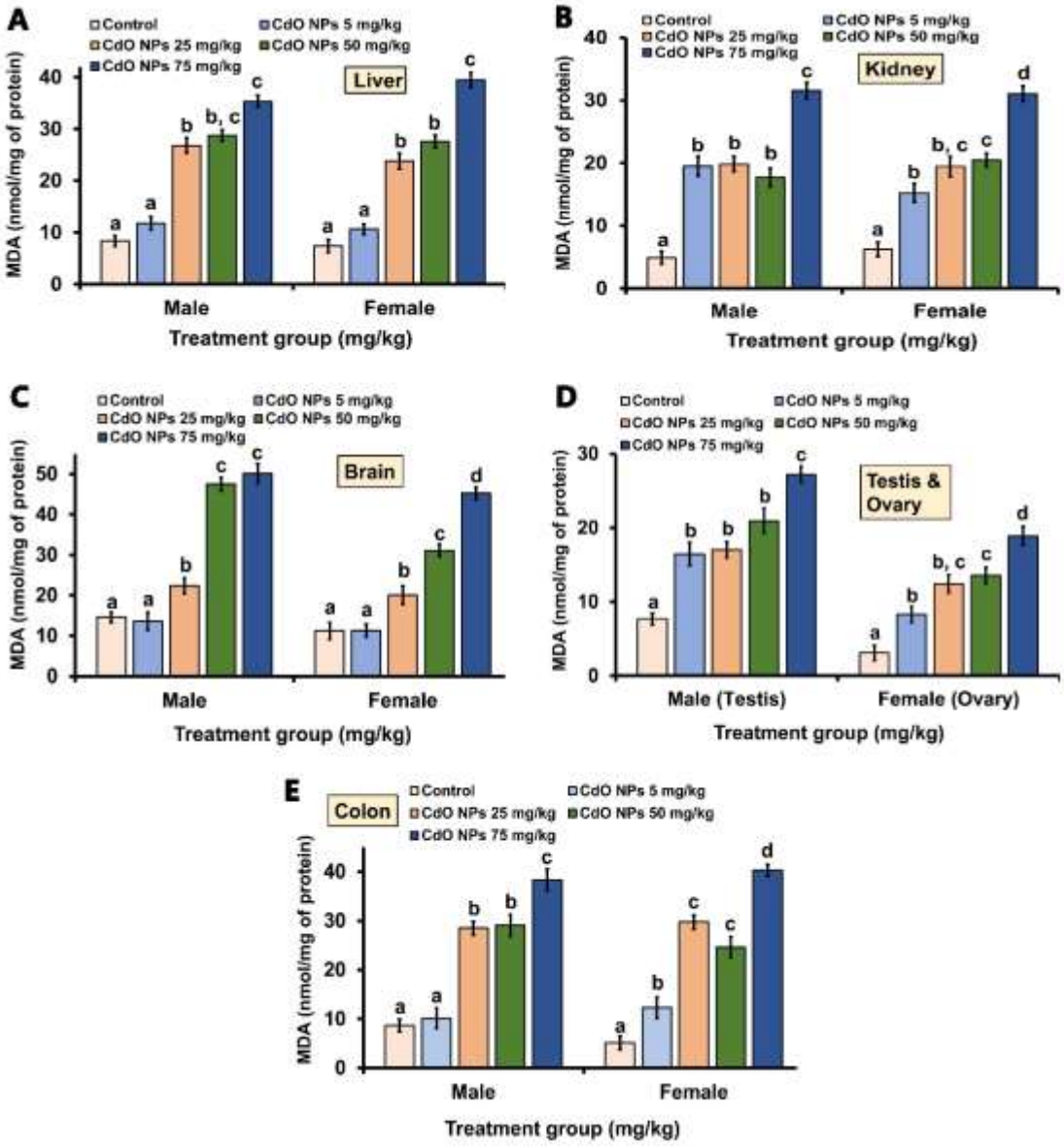

Figure 6 Assessment of oxidative stress biomarker i.e., MDA levels, in five different organs namely, liver **(A)**, kidney **(B)**, brain **(C)**, testis and ovaries **(D)**, and colon **(E)** in male and female mice. All the values are presented as mean ± SEM, significant at $p < 0.05$.

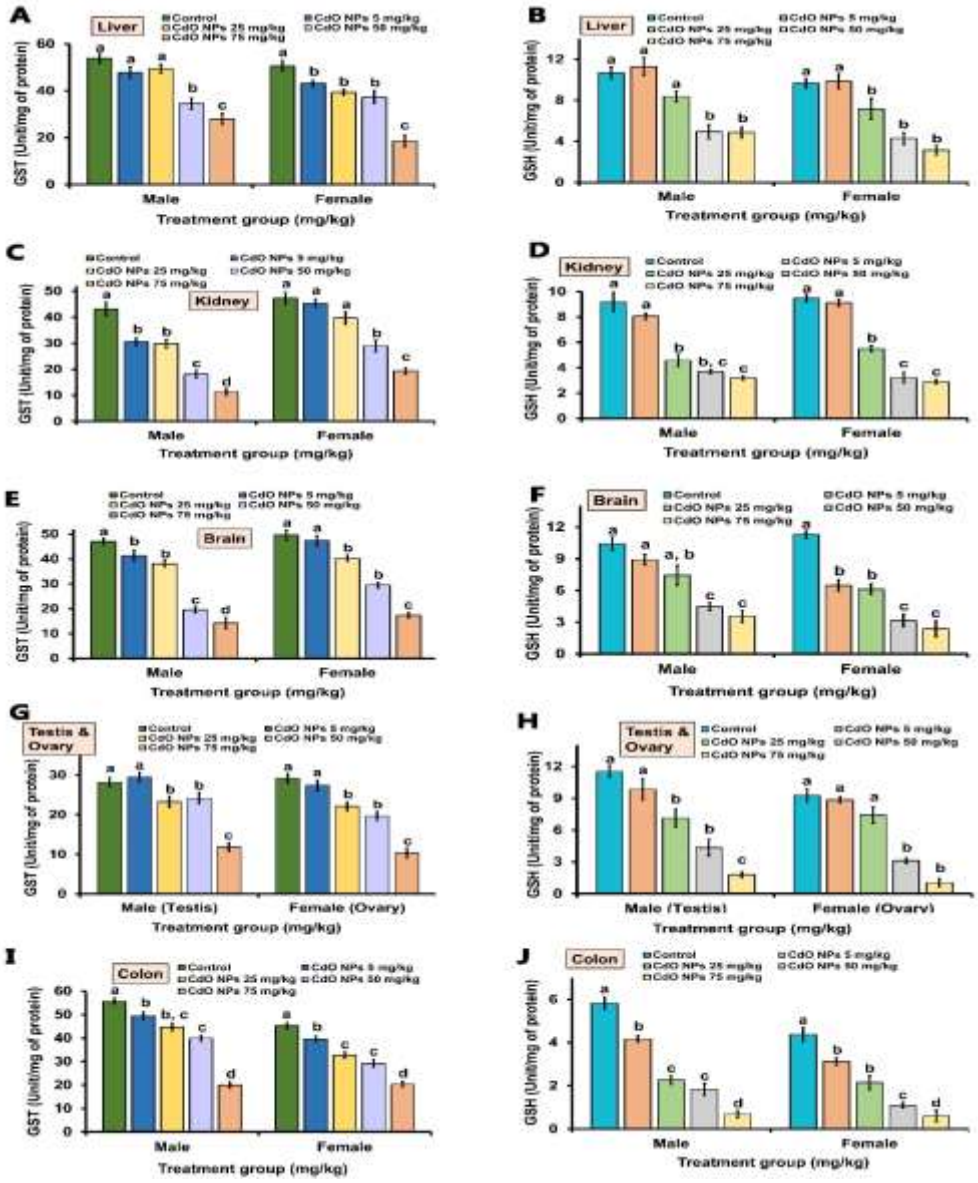

Figure 7 Assessment of antioxidant enzymes status i.e., GST and GSH, in five different organs namely, liver **(A)**, kidney **(C)**, brain **(E)**, testis and ovaries **(G)**, and colon **(I)** for GST; and also GSH in liver **(B)**, kidney **(D)**, brain **(F)**, testis and ovaries **(H)**, and colon **(J)** in male and female mice. All the values are presented as mean ± SEM, significant at $p < 0.05$.

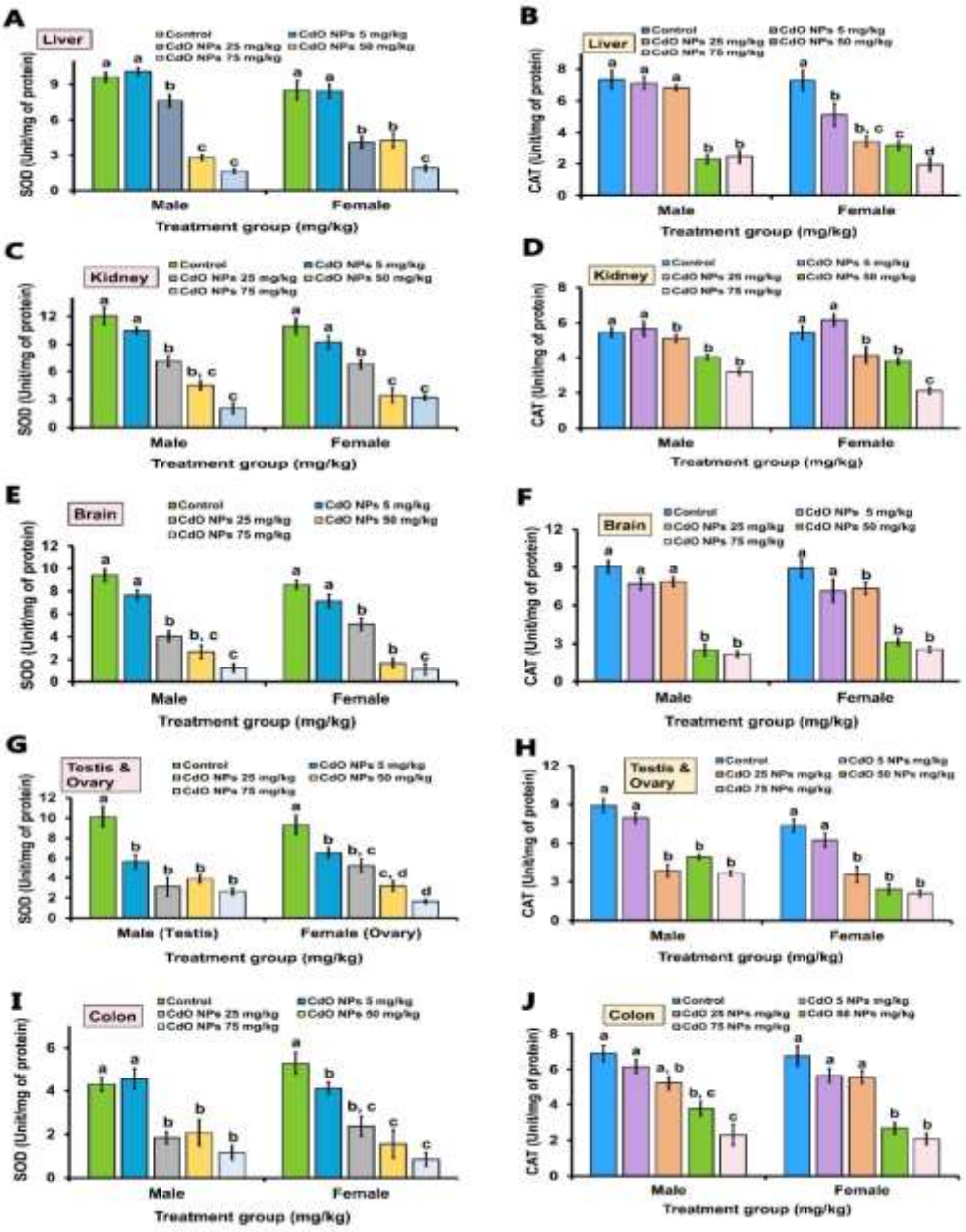

Figure 8 Assessment of antioxidant enzymes status i.e., SOD and CAT, in five different organs namely, liver **(A)**, kidney **(C)**, brain **(E)**, testis and ovaries **(G)**, and colon **(I)** for SOD; and also CAT in liver **(B)**, kidney **(D)**, brain **(F)**, testis and ovaries **(H)**, and colon **(J)** in male and female mice. All the values are presented as mean ± SEM, significant at $p < 0.05$.

5.10 Histopathological analyses revealed alteration in tissue architecture

5.10.1 Histopathology of liver

Normal architecture of liver with well-organized structure of central vein (CV), hepatocytes (Hp), binucleated hepatocyte (BH), hepatic sinusoids (S) were clearly visible in control mice in both male and female **(Figure 9A** and **I)**. In case of male, inflammatory infiltration (→) was evident in 5 mg/kg bw group **(Figure 9E)** and inflammatory infiltration with dilated sinusoid (ds) and multinucleated cells (*) were seen in group treated with 25 mg/kg bw **(Figure 9B** and **F)**. Further, in groups treated with 50 mg/kg bw **(Figure 9C** and **G)**, tissue haemorrhage (Hem), inflammatory infiltration (→), tissue vacuolization (V), degenerative cells (&) whereas, in addition to inflammatory infiltration (→), dilated portal veins (dPV) with tissue necrosis (N) were clearly evident in the histological sections of group treated with 75 mg/kg bw **(Figure 9D** and **H)**. In case of female mice, congestion of central vein (**), vacuolization (V), inflammatory infiltration (→), dilated portal vein (dPV), extensive vacuolization (vac) and apoptotic nuclei (#) were visible in the treatment groups **(Figure 9I, J, K, L, M, N, O** and **P)**.

5.10.2 Histopathology of kidney

The histological sections of control animals were showing normal structure of glomerulus (G) with compact organization, proximal convoluted tubule (PT), distal convoluted tubule (DT), collecting tubule/duct (CT) and normal blood vessels in both the sexes **(Figure 10A** and **I)**. Pathological changes such as dilated vessel (dV), glomerular degeneration with increased glomerular space (#), vascular congestion (vC) area of haemorrhage (Hem), tubular degeneration (&), tubule with wide lumen space (tW), fragmentation of tissue (Ft), inflammatory infiltration (→), apoptotic nuclei (Ap), tubular cast formation (@) were evident in both male and female experimental groups with severe tissue necrosis (N) were visible in groups 50 mg/kg b.w and 75 mg/kg b.w of female animals **(Figure 10J, K, L, M, N, O** and **P)**. Furthermore, prominent changes in tissue architecture was seen from the low dose itself in case of female mice.

5.10.3 Histopathology of brain

Pyramidal neurons (Pn) and blood vessels with normal tissue architecture could be seen in the histological sections of brain in control mice **(Figure 11A** and **I)**. The animals treated with CdO-NPss were found to have cellular vacuolization (V), inflammatory infiltration (→), darkly stained neurons (@), intracellular vacuolization (Vac), vascular congestion (vC), cellular apoptosis (Ap), cellular degeneration (#), fragmentation of tissue (Ft) and necrotic area (N) were clearly visible in male and female of different groups.

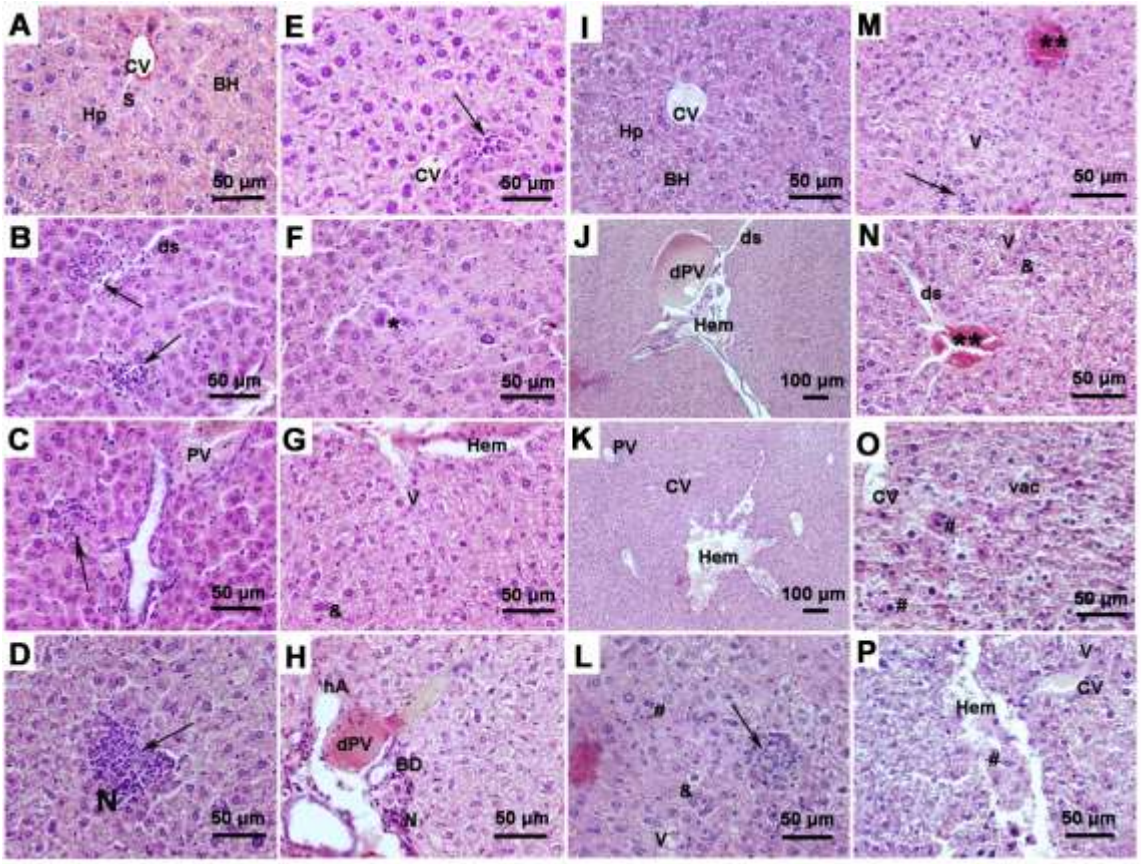

Figure 9 Histopathological alteration in liver tissue of male and female mice after acute intoxication with CdO-NPs, visible after hematoxylin and eosin staining (H & E). **(A)** Control, **(B** and **F)** CdO 25 mg/kg, **(C** and **G)** CdO 50 mg/kg, **(D** and **H)** CdO 75 mg/kg,

(E) CdO 5 mg/kg represents liver of male mice at 40X resolution and **(I)** Control (40X), **(J** and **N)** CdO 25 mg/kg (10X and 40X, respectively), **(K** and **O)** CdO 50 mg/kg (10X and 40X, respectively), **(L** and **P)** CdO 75 mg/kg (40X), **(M**) CdO 5 mg/kg (40X). Resolution at 10X and 40X are shown with scale bar 100 and 50 µm, respectively. CV- central vein; Hp- hepatocytes; S- hepatic sinusoid; BH- binucleated hepatocytes; PV- portal vein; BD- bile duct; hA- hepatic artery; ds- dilated hepatic sinusoid; V- vacuolization; vac- extensive vacuolization; dPV- dilated portal vein; → (black arrow)- inflammatory infiltration; * (star)- multinucleated giant cell; Hem- area of haemorrhage; &- degenerative cell; N- area of necrosis; # (hash)- apoptotic nuclei; ** (double star)- congested central vein.

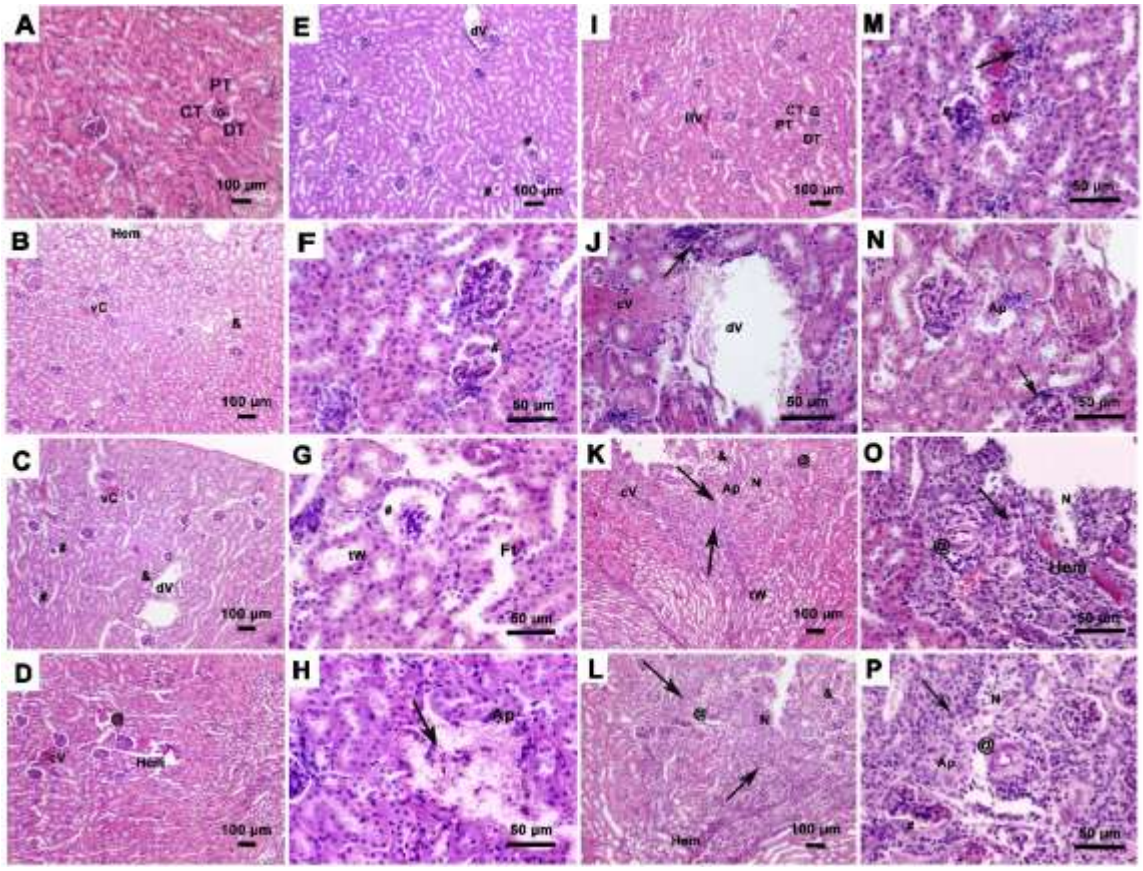

Figure 10 Micrographs showing histopathological alteration in kidney tissue of male and female mice after acute intoxication with CdO-NPs, visible after hematoxylin and

eosin staining (H & E). **(A)** Control (at 10X resolution), **(B** and **F)** CdO 25 mg/kg (10X and 40X, respectively), **(C** and **G)** CdO 50 mg/kg kg (10X and 40X, respectively), **(D** and **H)** CdO 75 mg/kg kg (10X and 40X, respectively), **(E)** CdO 5 mg/kg (10X) represents kidney tissue of male and **(I)** Control (10X), **(J** and **N)** CdO 25 mg/kg (40X), **(K** and **O)** CdO 50 mg/kg (10X and 40X, respectively), **(L** and **P)** CdO 75 mg/kg (10X and 40X, respectively), **(M**) CdO 5 mg/kg (40X) kidney tissue of female mice. Resolution at 10X and 40X are shown with scale bar 100 and 50 µm, respectively. G- glomerulus; PT- proximal convoluted tubule; DT- distal convoluted tubule; CT- collection tubule; BV- blood vessel; dV- dilated vessel; # (hash)- glomerular degeneration with increased glomerular space; vC- vascular congestion; Hem- area of haemorrhage; &- tubular degeneration; tW- tubule with wide lumen space; Ft- fragmentation of tissue; → (black arrow)- inflammatory infiltration; Ap- apoptotic nuclei; @- tubular cast formation; N- area of necrosis.

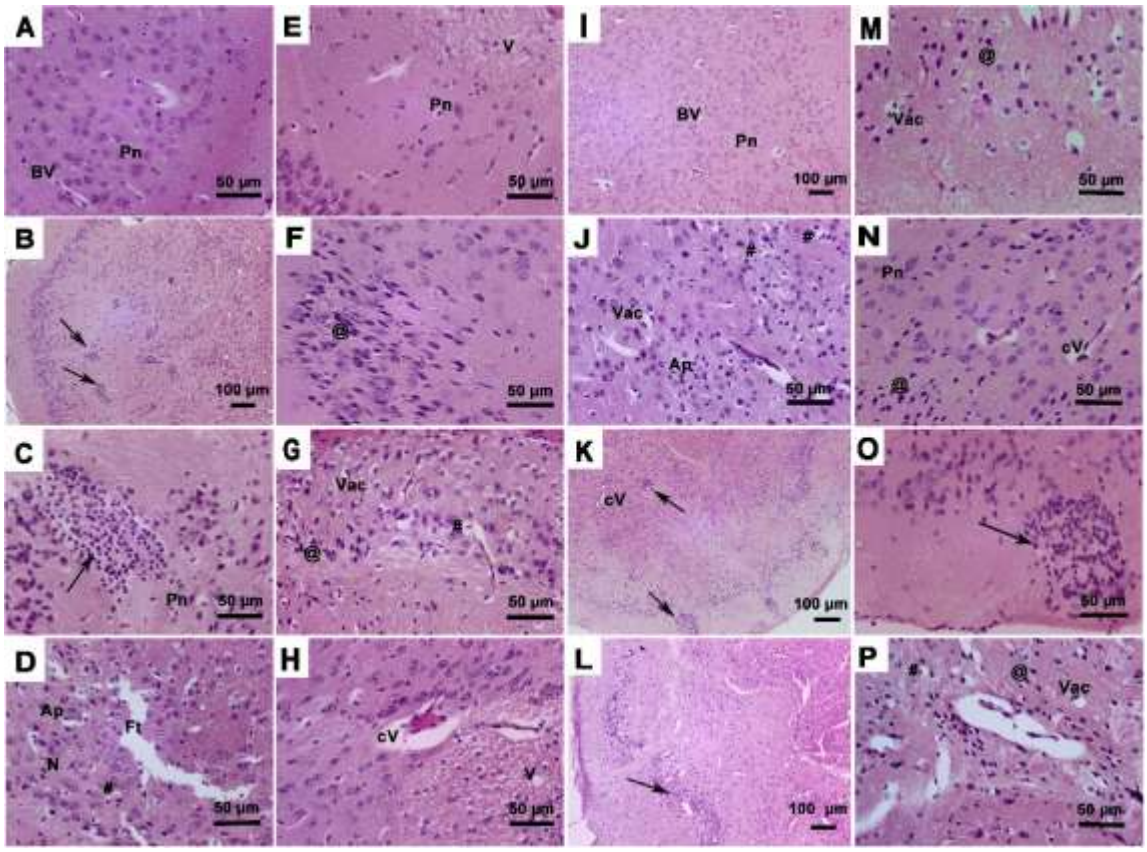

Figure 11 Micrographs showing histopathological alteration in brain tissue of male and female mice after acute intoxication with CdO-NPs, visible after hematoxylin and eosin staining (H & E). **(A)** Control (40X resolution), **(B** and **F)** CdO 25 mg/kg (10X and 40X, respectively), **(C** and **G)** CdO 50 mg/kg kg (40X), **(D** and **H)** CdO 75 mg/kg kg (40X), **(E)** CdO 5 mg/kg (40X) represents brain tissue of male and **(I)** Control (10X), **(J** and **N)** CdO 25 mg/kg (40X), **(K** and **O)** CdO 50 mg/kg (10X and 40X, respectively), **(L** and **P)** CdO 75 mg/kg (10X and 40X, respectively), **(M**) CdO 5 mg/kg (40X) brain tissue of female mice. Resolution at 10X and 40X are shown with scale bar 100 and 50 µm, respectively. Pn- Pyramidal neuronal cell; BV- blood vessel; → (black arrow)- inflammatory infiltration; @- darkly stained neuron; Vac- intracytoplasmic vacuolization; V- vacuolization; Ap- cellular apoptosis; N- area of necrosis; Ft- fragmentation of tissue; # (hash)- cellular degeneration; cV- congested vessel.

5.10.4 Histopathology of testis, ovary and uterine horn

Histopathological study of testis, ovary and uterine horn of control groups revealed normal tissue architecture **(Figure 12A, F** and **K)**. The sections of testis showed normal structure of seminiferous tubule (St), Leydig cells (LC), lumen of seminiferous tubule (L), and formation of spermatogonia (Sg), primary spermatocyte (pSc), secondary spermatocyte (sSc), Sp- spermatid (Sp), Sertoli cell (*) and spermatozoa (→). Likewise, ovary of control group was found with normal formation of primary follicle (Pf), secondary follicle (Sf) and corpus luteum (CL) and uterine horn with normal architecture of endometrium (Em), myometrium (Mm), perimetrium Pm), lumen (L), epithelial cell layer (ECL) and uterine glands (UG) were also evident in control mice.

Testis of the treatment mice were found with wide space in the lumen of seminiferous tubule (wL), depletion of Leydig cells (dLC), vacuolization (V), tissue haemorrhage (Hem), decrease in sperm mass (&) in the lumen of the seminiferous tubule, degeneration of tubule (#), disorganization and depletion of seminiferous tubule by tubular necrosis (dSt) and disorganized and sloughing of germ layer (@) **(Figure 12B, C, D** and **E)**. Normal ovarian tissue architecture was seen in mice treated with 5 mg/kg

bw and 25 mg/kg bw **(Figure 12G** and **H)**, except for a small sign of follicular degeneration in the later. However, high doses of CdO-NPs in mice resulted in several area of tissue necrosis (**), follicular degeneration (#) and inflammatory infiltration (→) in the testis tissue **(Figure 12I** and **J)**. The testis sections of high dose group showed severe depletion of seminiferous tubules. The sections of uterine horn had disorganization of endometrium (dEm), area of tissue necrosis (N), tissue haemorrhage (Hem) and apoptotic cell (Ap) after treatment with the test chemical **(Figure 12L, M, N** and **O)**.

5.10.5 Histopathology of heart

Histological sections of heart with normal organization of myocardium (Mc) was seen in case of normal control in both male and female animals **(Figure 13A** and **F)**. The sections of heart of CdO-NPs treated mice were seen with congested vessels (cV), vacuolization (V), fragmentation of tissue (Ft), minute tissue haemorrhage (&), inflammatory infiltration (#), wide intercellular space (@) and extensive tissue haemorrhage (Hem) in male and female of different dose groups **(Figure 13B, C, D, E, G, H, I** and **J)**.

5.10.6 Histopathology of lung

Normal organisation of alveolus (AV), blood vessel (BV) and bronchiole (Bc) were evident in the groups treated with normal saline solution (control) **(Figure 14A** and **F)** however, sign of tissue haemorrhage (Hem), inflammatory infiltration (→), dilated blood vessel (dBV), congestion of vessel (cV) and depleted bronchiole (dBc) were found in the differently dosed CdO-NPs treated groups **(Figure 14B, C, D, E, G, H, I** and **J)**.

5.10.7 Histopathology of spleen

Histological analyses of spleen tissue from different group of experimental animals revealed normal architecture of white pulp (wP), red pulp (rP) and germinal centre (Gc) in case of control mice **(Figure 15A** and **F)** whereas, large numbers of megakaryocytes (Mg), vacuolization (V) in splenic tissue, congestion of tissue (Ct) tissue fragmentation (Ft) and presence of apoptotic nuclei (Ap) were found in the spleen sections of both male and female of treatment groups **(Figure 15B, C, D, E, G, H, I** and **J)**.

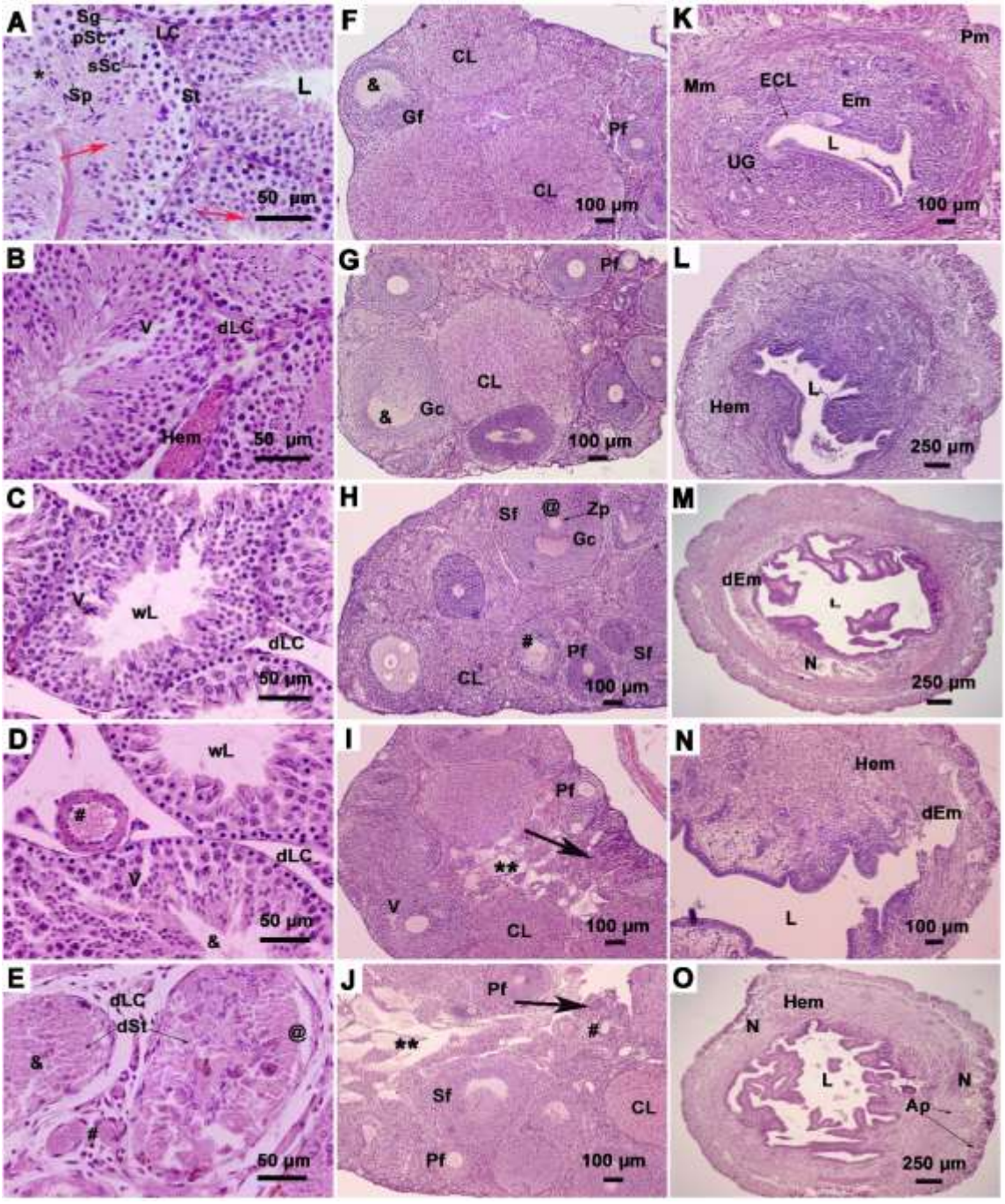

Figure 12 Micrographs showing histopathological alteration in testis, ovary and uterus of male and female mice after acute intoxication with CdO-NPs, visible after hematoxylin and eosin staining (H & E). **(A)** Control (40X), **(B)** CdO 5 mg/kg (40X), **(C)** CdO 25 mg/kg kg (40X), **(D)** CdO 50 mg/kg kg (40X), **(E)** CdO 75 mg/kg (40X)

represents testis tissue of male, St- seminiferous tubule; LC- Leydig cell; Sg- spermatogonia; pSc- primary spermatocyte; sSc- secondary spermatocyte; Sp- spermatid; L- lumen of seminiferous tubule; * (star)- Sertoli cell; → (red arrow)- spermatozoa; V- vacuolization; Hem- haemorrhage; dLC- depletion of Leydig cell; wL- wider lumen space; &- decrease in sperm mass; # (hash)- degeneration of tubule; dSt- disorganization and depletion of seminiferous tubule by tubular necrosis; @- disorganized and sloughing of germ layer. **(F)** Control (10X), **(G)** CdO 5 mg/kg (10X), **(H)** CdO 25 mg/kg (10X), **(I)** CdO 50 mg/kg (10X), **(J)** CdO 75 mg/kg (10X) represent ovary, Pf- primary follicle; Gf- growing follicle; CL- corpus luteum; &- antrum; Gc- granulosa cell; Sf- secondary follicle; @- oocyte; ** (double star)- area of necrosis; # (hash)- follicular degeneration; → (black arrow)- inflammatory infiltration. **(K**) Control (10X), **(L)** CdO 5 mg/kg (4X), **(M)** CdO 25 mg/kg (4X), **(N)** CdO 50 mg/kg (10X), **(O)** CdO 75 mg/kg (4X) of uterus tissue of female mice, Em- endometrium; Mm- myometrium; Pm- Perimetrium; L- lumen, ECL- epithelial cell layer; UG- uterine gland; dEm- disorganization of endometrium; N- area of necrosis; Hem- haemorrhage; Ap- apoptotic cell. Resolution of testis at 40X are shown with scale bar 50 µm whereas, ovary and uterus at 10X resolution are represented with scale bar 100 µm. Uterus at 4X resolution are shown with 250 µm scale bar.

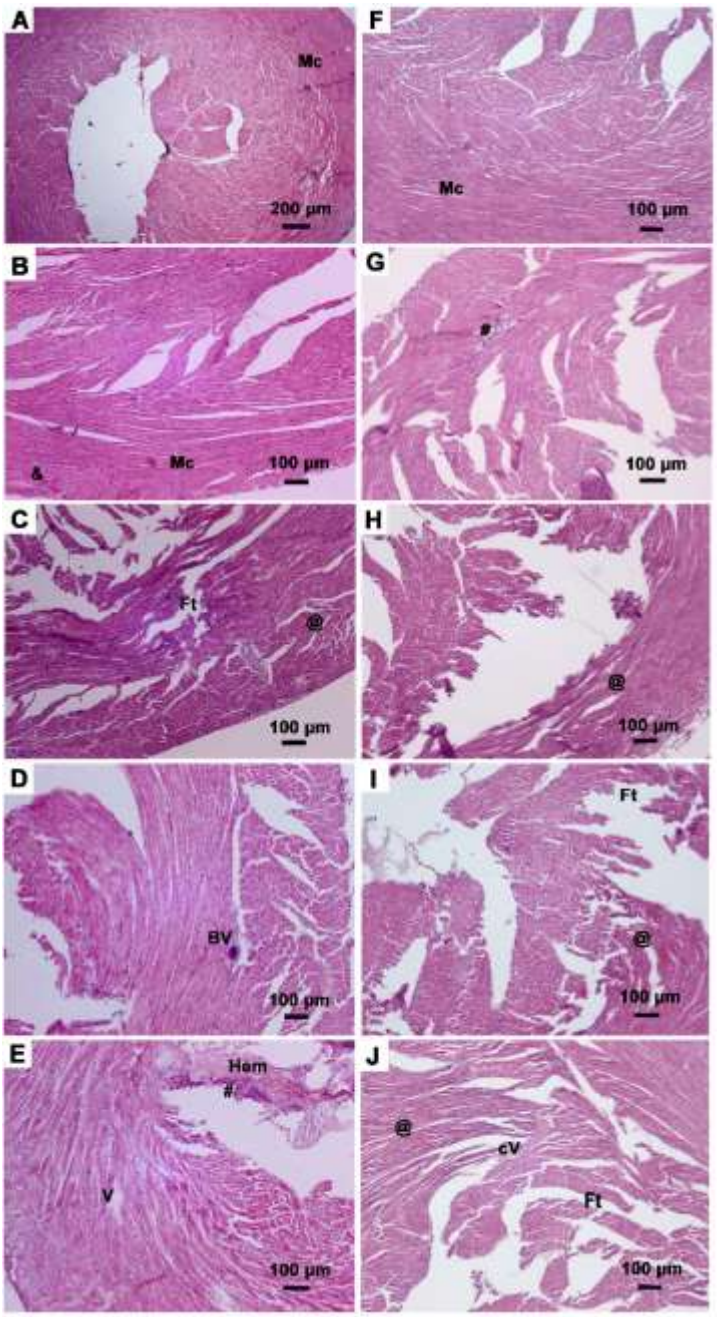

Figure 13 Histopathological alteration in heart tissue of male and female mice after acute intoxication with CdO-NPs, visible after hematoxylin and eosin staining (H & E). **(A)** Control (4X), **(B)** CdO 5 mg/kg (10X), **(C)** CdO 25 mg/kg kg (10X), **(D)** CdO 50 mg/kg kg (10X), **(E)** CdO 75 mg/kg (10X) represents heart tissue of male, and **(F)** Control (10X), **(G)** CdO 5 mg/kg (10X), **(H)** CdO 25 mg/kg (10X), **(I)** CdO 50 mg/kg

(10X), **(J)** CdO 75 mg/kg (10X) represent heart tissue of female mice. Resolution at 4X and 10X are shown with scale bar 200 and 50 µm, respectively. Mc- myocardium; BV- blood vessel; cV- congested vessel; V- vacuolization; Ft- fragmentation of tissue; &- minute tissue haemorrhage; # (hash)- inflammatory infiltration; @- wide intercellular space; Hem- extensive tissue haemorrhage.

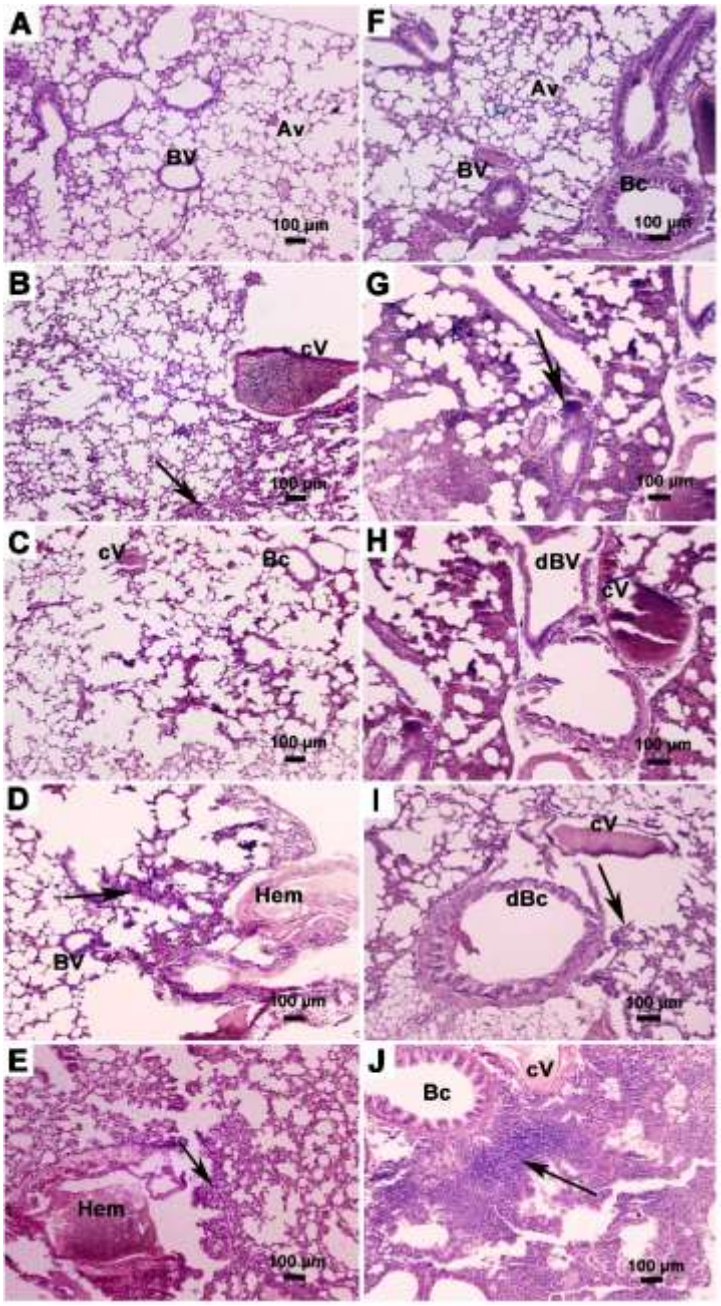

Figure 14 Changes in the tissue architecture of lung in male and female mice were evident after histopathological analyses using hematoxylin and eosin staining (H & E). **(A)** Control (10X), **(B)** CdO 5 mg/kg (10X), **(C)** CdO 25 mg/kg kg (10X), **(D)** CdO 50 mg/kg kg (10X), **(E)** CdO 75 mg/kg (10X) represents lung tissue of male, and **(F)** Control (10X), **(G)** CdO 5 mg/kg (10X), **(H)** CdO 25 mg/kg (10X), **(I)** CdO 50 mg/kg

(10X), **(J)** CdO 75 mg/kg (10X) represent lung tissue of female mice. Resolution at 10X are shown with scale bar 100 µm. Av- alveolus; BV- blood vessel; Bc- bronchiole; Hem- haemorrhage; → (black arrow)- inflammatory infiltration; dBV- dilated blood vessel; cV- congested vessel; dBc- depleted bronchiole.

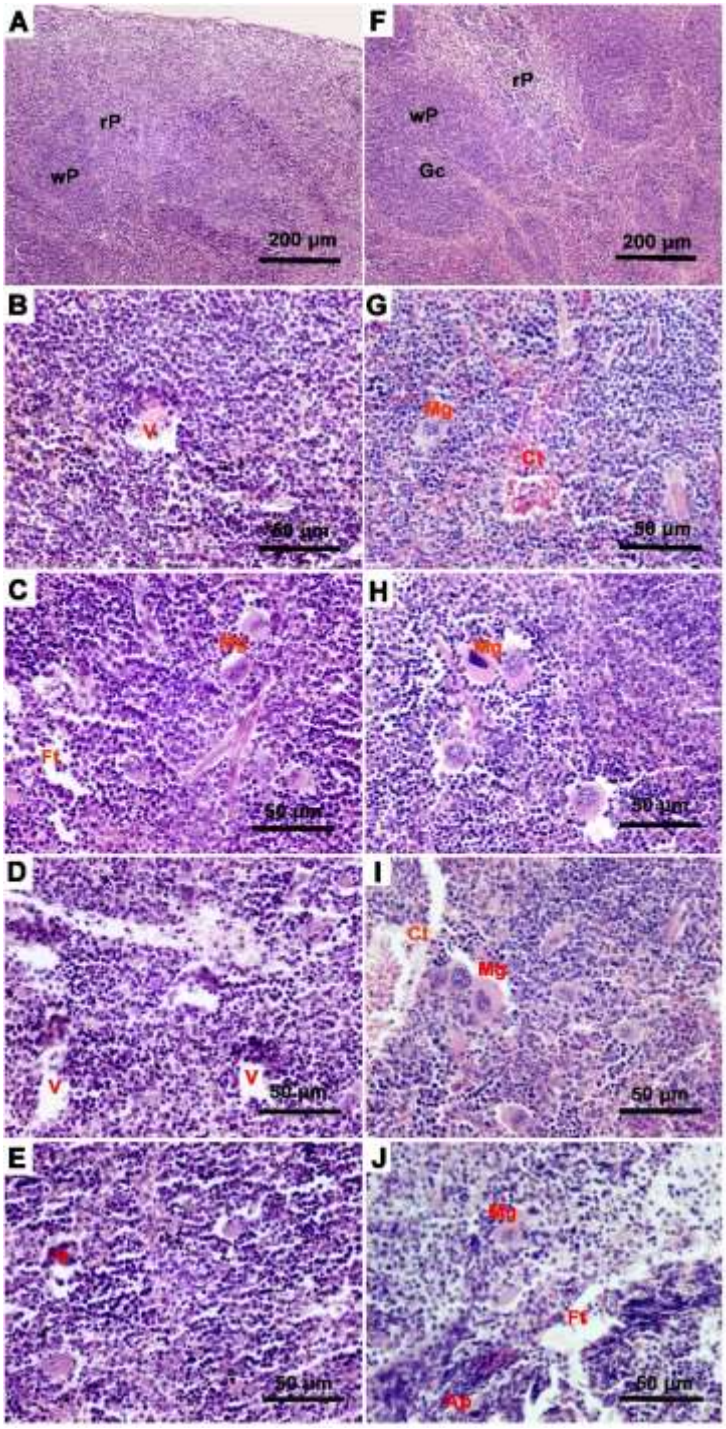

Figure 15 Changes in the tissue architecture of spleen in male and female mice were evident after histopathological analyses using hematoxylin and eosin staining (H & E). **(A)** Control (10X), **(B)** CdO 5 mg/kg (40X), **(C)** CdO 25 mg/kg kg (40X), **(D)** CdO 50

mg/kg kg (40X), **(E)** CdO 75 mg/kg (40X) represents spleen tissue of male, and **(F)** Control (10X), **(G)** CdO 5 mg/kg (40X), **(H)** CdO 25 mg/kg (40X), **(I)** CdO 50 mg/kg (40X), **(J)** CdO 75 mg/kg (10X) represent spleen tissue of female mice. Resolution at 10X and 40X are shown with scale bar 200 µm and 50 µm. wP- white pulp; rP- red pulp; Gc- germinal centre; Mg- megakaryocytes; V- vacuolization; Ct- congestion of tissue; Ft- fragmentation of tissue; Ap- apoptotic nuclei.

Experiment-II To assess antioxidant status, oxidative stress parameter, histopathology, and pathways of organ toxicity induced by cadmium nanoparticles in adult mice.

CdO-NPs intoxication effects on body weight, daily food and water consumption

After 30 days of CdO-NPs administration, significant decrease in the mean body weight of mice were observed in a dose-dependent manner in all the treatment groups as compared to the normal control group **(Figure 16A)**. The pattern of feeding and water consumptions were also showing significant decrease among the control and treated groups **(Figure 16B** and **C)**. The loss/gain percentage of mean body weight, food and consumption are tabulated in **Table 17**, which shows significant gain of mean body weight, food and water consumption in control group and loss of the same in the treatment groups.

5.11 CdO-NPs intake impacts upon the organ weight and relative organ weight

CdO-NPs intake had prevailing impact upon the organ weights of the treated female mice. The measurement of organ weights and calculation of relative organ weight is shown in **Table 18**. The significant effect of the test compound was observed in liver, kidney, spleen, colon, lung, ovary and uterus however, effects on the relative weights of brain, stomach, pancreas and heart were insignificant.

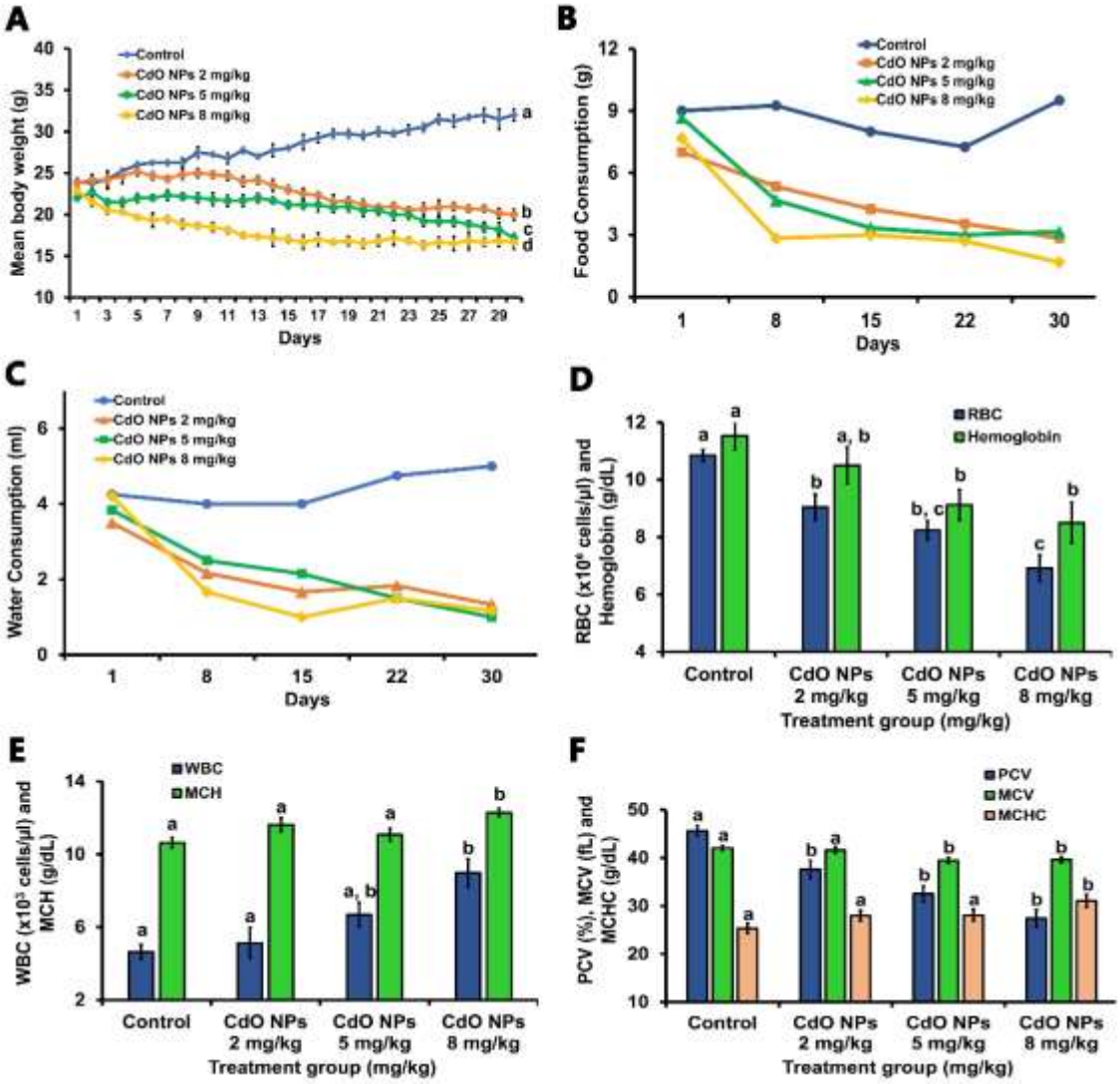

Figure 16 Graphs depicting the changes in mean body weight, food and water consumption, and variation in different hematological parameters in the CdO-NPs treated mice as compared to the control group. **(A)** mean body weight; **(B)** mean food consumption; **(C)** mean water consumption; **(D)** RBC counts and hemoglobin concentration; **(E)** WBC counts and MCH; **(F)** PCV, MCV and MCHC. The data are represented as mean ± SEM, one-way ANOVA was performed to compare the values among the groups and different alphabets show significant relationship at $p < 0.05$.

Table 17 Routine observation of mean body weight, food and water consumption and loss/gain in weight, food and water consumption for the 30 days of experimental period are represented in table as mean ± SEM, significant at $p < 0.05$.

Daily Observation (Mean body weight/Food and water consumption)	**Treatment group (mg/kg bw/day) and exposure period (30 days, p.o.)**			
	Control	**CdO-NPs 2 mg/kg**	**CdO-NPs 5 mg/kg**	**CdO-NPs 8 mg/kg**
Mean body weight/day (g)	28.38 ± 0.45 a	22.68 ± 0.33 b	20.79 ± 0.26 c	17.93 ± 0.31 d
Mean gain/loss in body weight (%)	33.33 ± 0.72 a	-16.07 ± 0.57 b	-21 ± 0.29 c	-26.98 ± 0.42 d
Mean food consumption/day (g)	8.37 ± 0.21 a	4.30 ± 0.20 b	4.21 ± 0.35 b	3.16 ± 0.26 c
Mean gain/loss in food consumption (%)	5.56 ± 0.27 a	-59.52 ± 0.41 b	-63.67 ± 0.35 c	-78.26 ± 0.24 d
Mean water consumption (ml)	4.33 ± 0.10 a	2.16 ± 0.13 b	2.00 ± 0.13 b, c	1.66 ± 0.14 c
Mean gain/loss in water consumption (%)	17.65 ± 0.82 a	-61.90 ± 0.51 b	-73.91 ± 0.43 c	-72.22 ± 0.33 c

5.12 Effects on hematological parameters

Analysis of hematological parameters on all the experimental as well as control group had revealed major effects of CdO-NPs intoxication in female mice. Depletion of total RBCs count and hemoglobin concentration **(Figure 16D)** whereas, increase in total WBCs count **(Figure 16E)** were seen in the treatment groups that were more significantly variable in the high dose groups as compared to the control mice. RBC indices, MCH **(Figure 16E)**, MCV and MCHC were showing an increasing trend from control to the high dose group with significant difference only between control and high dose group, however, PCV had decreased significantly among control and the treated groups (**Figure 16F)**.

Table 18 Routine observation of relative organ weight for the 30 days of experimental period are represented in table as mean ± SEM, one-way ANOVA was performed to compare the value among the groups and different alphabets show significant relationship at $p < 0.05$.

Organ (Relative organ weight)	**Treatment Group (mg/kg bw/day) and exposure period (30 days, p.o.)**			
	Control	**CdO-NPs 2 mg/kg**	**CdO-NPs 5 mg/kg**	**CdO-NPs 8 mg/kg**
Liver	5.82 ± 0.15 a	5.70 ± 0.11 a	4.28 ± 0.20 b	4.41 ± 0.14 b
Kidney	1.35 ± 0.02 a	1.32 ± 0.05 a	1.33 ± 0.01 a	1.17 ± 0.01b
Brain	2.58 ± 0.07 a	2.57 ± 0.02 a	2.48 ± 0.02 a	2.55 ± 0.03 a
Spleen	0.86 ± 0.02 a, b	0.88 ± 0.05 a	0.72 ± 0.01 b	0.74 ± 0.03 b
Stomach	1.14 ± 0.05 a	1.12 ± 0.01 a	1.18 ± 0.02 a	1.15 ± 0.04 a
Colon	1.14 ± 0.02 a	1.09 ± 0.02 b	1.04 ± 0.03 b	1.12 ± 0.01 b
Pancreas	0.74 ± 0.02 a	0.76 ± 0.02 a	0.59 ± 0.01 b	0.69 ± 0.01 a
Heart	0.62 ± 0.02 a	0.59 ± 0.02 a	0.60 ± 0.01 a	0.63 ± 0.02 a
Lungs	2.10 ± 0.08 a	1.80 ± 0.15 a	1.22 ± 0.08 b	1.25 ± 0.05 b
Ovaries	0.09 ± 0.01 a	0.09 ± 0.01 a	0.06 ± 0.01 b	0.06 ± 0.01 b
Uterus	0.30 ± 0.01 a	0.28 ± 0.01 a	0.16 ± 0.01 b	0.16 ± 0.01 b

5.13 Cadmium concentration increased in major organs with regular exposure

Significant increase in the quantity of cadmium heavy metal was observed in liver, kidney and brain tissues of treatment groups as compare to the normal control mice **(Table 19)**. Additionally, results also displayed that the accumulation was highest in liver followed by kidney and less in case of brain tissue.

Table 19 Accumulation of Cadmium metal in target organ was analysed using AAS and are represented as mean ± SEM, significant at $p < 0.05$.

Accumulation of cadmium (ppm)	**Treatment group (mg/kg bw /day) and exposure period (30 days, p.o.)**			
	Control	**CdO-NPs 2 mg/kg**	**CdO-NPs 5 mg/kg**	**CdO-NPs 8 mg/kg**
Liver	0.002 ± 0.02 a	0.095 ± 0.07 a, b	0.289 ± 0.05 b	0.628 ± 0.07 c
Kidney	0.005 ± 0.02 a	0.097 ± 0.05 a, b	0.184 ± 0.02 b	0.417 ± 0.04 c
Brain	0.001 ± 0.00 a	0.049 ± 0.01 a	0.066 ± 0.02 b	0.109 ± 0.01 c

5.14 Effect on liver and kidney function, and degradation of lipid profiles

Significant depletion of total protein, albumin, globulin **(Figure 17A** and **B)** and significant increase in A/G ratio, total and direct bilirubin **(Figure 17C** and **D)** were observed in all the treated groups as compared to the normal control mice. Further, increase in the concentration of different kidney function biomarkers such as creatinine, uric acid, urea and blood urea nitrogen were observed in the treatment groups **(Figure 17C, D** and **E)**. Significant increase in ALP **(Figure 17F)** was seen in all the treatment group whereas, AST and ALT **(Figure 17G** and **H)** concentrations were seen to be significantly elevated in in the high dose groups as compared to the control group.

Deterioration in the lipid profile was noted after the treatment with CdO-NPs and it was evident from the significant increase in the levels of total cholesterol, triglycerides, LDL cholesterol and decrease the concentration of HDL cholesterol in the blood serum of CdO-NPs intoxicated mice **(Table 20)**. Further, significant decrease in the concentration of calcium, chloride, and potassium whereas, decrease in the level of sodium was observed in the treatment groups as compared to the normal control. However, no change was seen the serum glucose level.

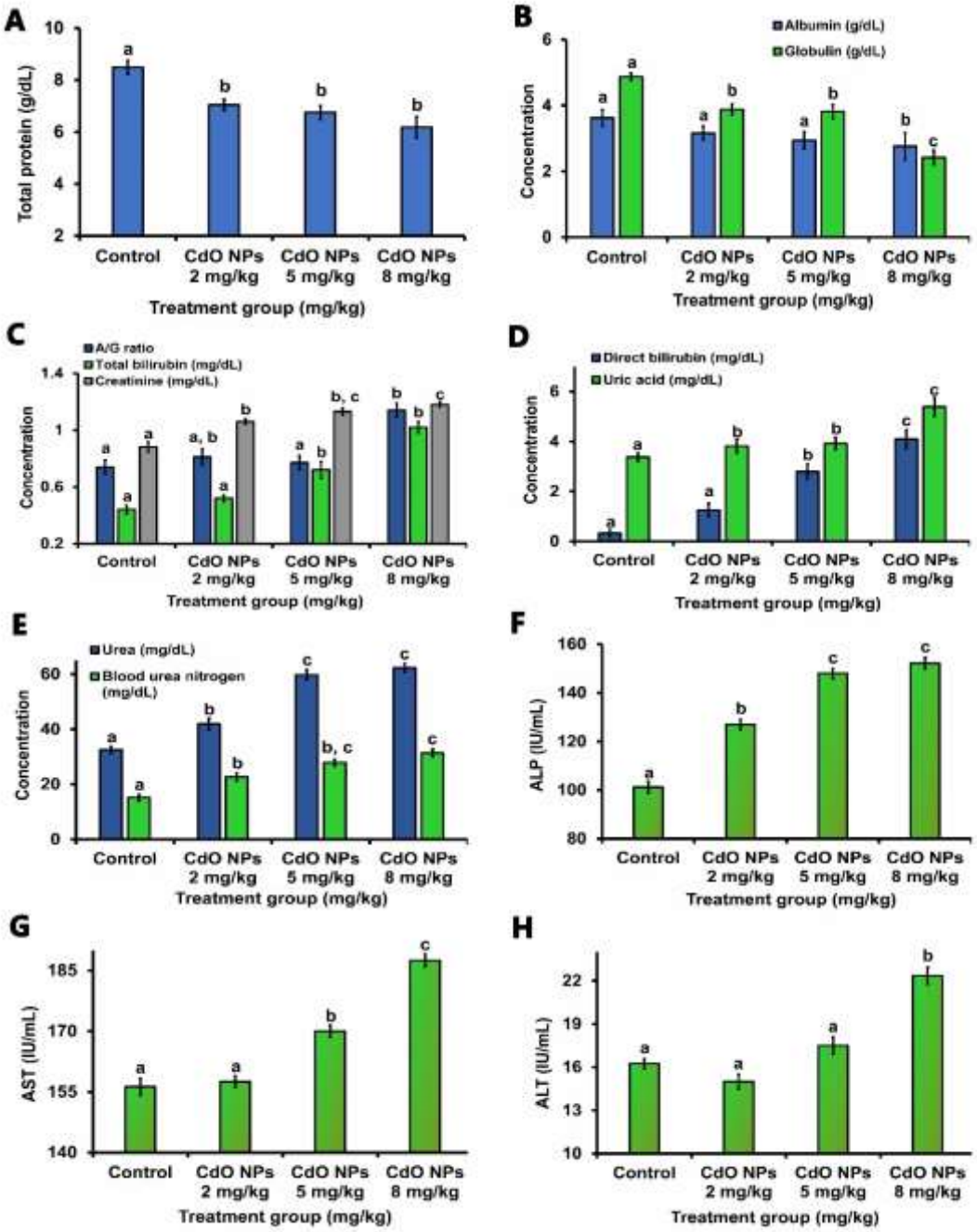

Figure 17 Graphs depicting the liver and kidney functions biomarkers. **(A)** total protein; **(B)** albumin and globulin; **(C)** A/G ratio, total bilirubin and creatinine; **(D)** direct bilirubin and uric acid; **(E)** urea and blood urea nitrogen; **(F)** ALP; **(G)** AST; **(H)** ALT. The data are represented as mean ± SEM, one-way ANOVA was performed to compare the values among the groups and different alphabets show significant relationship at $p < 0.05$.

Table 20 Effect of CdO-NPs in lipid profiles of female mice after 30 days of treatment. All the data are represented as mean ± SEM, one-way ANOVA was performed to compare the values among the groups and different alphabets show significant relationship at $p < 0.05$.

Lipid Profiles	**Treatment group (mg/kg bw /day) and exposure period (30 days, p.o.)**			
	Control	**CdO-NPs 2 mg/kg**	**CdO-NPs 5 mg/kg**	**CdO-NPs 8 mg/kg**
Total Cholesterol (mg/dL)	68.87 ± 1.33 a	73.85 ± 1.14 b	97.51 ± 1.17 c	95.23 ± 1.23 c
Triglycerides (mg/dL)	108.43 ± 1.64 a	122.89 ± 1.11 b	123.59 ± 1.29 b	119.81 ± 1.41 b
HDL Cholesterol (mg/dL)	13.90 ± 0.44 a	10.04 ± 0.58 b	8.60 ± 0.81 b	9.50 ± 0.54 b
LDL Cholesterol (mg/dL)	33.29 ± 1.15 a	39.24 ± 1.08 b	63.80 ± 1.22 c	61.58 ± 1.01 c
Glucose (mg/dL)	88.35 ± 0.91 a	85.33 ± 1.35 a	82.09 ± 0.86 a	83.30 ± 1.06 a
Calcium (mg/dL)	10.05 ± 0.53 a	9.20 ± 0.75 a	9.39 ± 0.48 a	8.30 ± 0.72 b
Chloride (mmol/L)	186.95 ± 1.21 a	173.91 ± 1.34 b, c	177.39 ± 1.14 b	169.13 ± 2.08 c
Sodium (mmol/L)	107.55 ± 1.91 a	105.41 ± 2.67 a	123.15 ± 1.72 b	148.36 ± 2.48 c
Potassium (mmol/L)	10.48 ± 0.38 a	8.08 ± 0.19 b	7.01 ± 0.12 c	7.45 ± 0.21 b, c

5.15 Impact of CdO-NPs intake on inflammatory response system

CdO-NPs promoted inflammation, which is evidenced by a significant increase in the serum is pro-inflammatory markers, including IL-1, IL-6, LTB4, prostaglandin E-2, FAD, MPO and a significant decrease in the anti-inflammatory marker, IL-10, and TAOC compared to the control group **(Table 21)**.

Table 21 Impact of CdO-NPs intake on inflammatory response system of female mice after 30 days of treatment. All the data are represented as mean ± SEM, one-way ANOVA was performed to compare the values among the groups and different alphabets show significant relationship at $p < 0.05$.

Inflammatory markers	**Treatment group (mg/kg bw / day) and exposure period (30 days, p. o.)**			
	Control	**CdO-NPs 2 mg/kg**	**CdO-NPs 5 mg/kg**	**CdO-NPs 8 mg/kg**
FAD (ng/L)	142.26 ± 2.33 a	195.45 ± 2.51 b	245.65 ±1.85 c	287.12 ± 1.62 d
IL-10 (pg/ml)	16.91 ± 1.12 a	13.7 ± 1.35 a, b	11.45 ±1.22 b, c	6.93 ± 1.26 c
IL-6 (ng/L)	1.01 ± 0.23 a	1.87 ± 0.14 b	2.01 ± 0.19 b	3.10 ± 0.21 c
MPO (ng/ml)	1.35 ± 0.36 a	3.85 ± 0.17 b	4.05 ± 0.24 b	4.73 ± 0.41 b
IL-1 (pg/ml)	15.09 ± 1.21 a	18.17 ± 1.54 a	32.41 ± 1.48 b	37.07 ± 1.27 b
Prostaglandin E-2 (ng/ml)	0.09 ± 0.02 a	0.46 ± 0.04 b	0.48 ± 0.02 b	0.96 ± 0.03 c
Leukotriene B4 (ng/ml)	1.45 ± 0.21 a	2.98 ± 0.56 b	3.38 ± 0.34 b	5.20 ± 0.15 c
TAOC (U/ml)	6.50 ± 0.33 a	4.68 ± 0.25 b	4.20 ± 0.19 b	2.80 ± 0.45 c

5.16 CdO-NPs promoted oxidative stress and depleted the antioxidant enzymes

Administration of CdO-NPs for 30 days in female mice induced significant level of oxidative stress in liver **(Figure 18A)**, kidney **(Figure 18B)** and brain **(Figure 18C)** tissue which was validated by significant increase in the concentration of tissue level malondialdehyde (MDA) in CdO-NPs treated animals as compared to the control group.

The enzymatic anti-oxidant, SOD **(Figure 19A, C** and **E)**, CAT **(Figure 19B, D** and **F)**, GST **(Figure 18D, E** and **F** in liver, kidney and brain, respectively) and non-enzymatic anti-oxidant, GSH reserve was significantly depleted in liver, kidney and brain tissues after CdO-NPs intake in all the treated groups as compared to the normal control female mice after 30 days of intoxication.

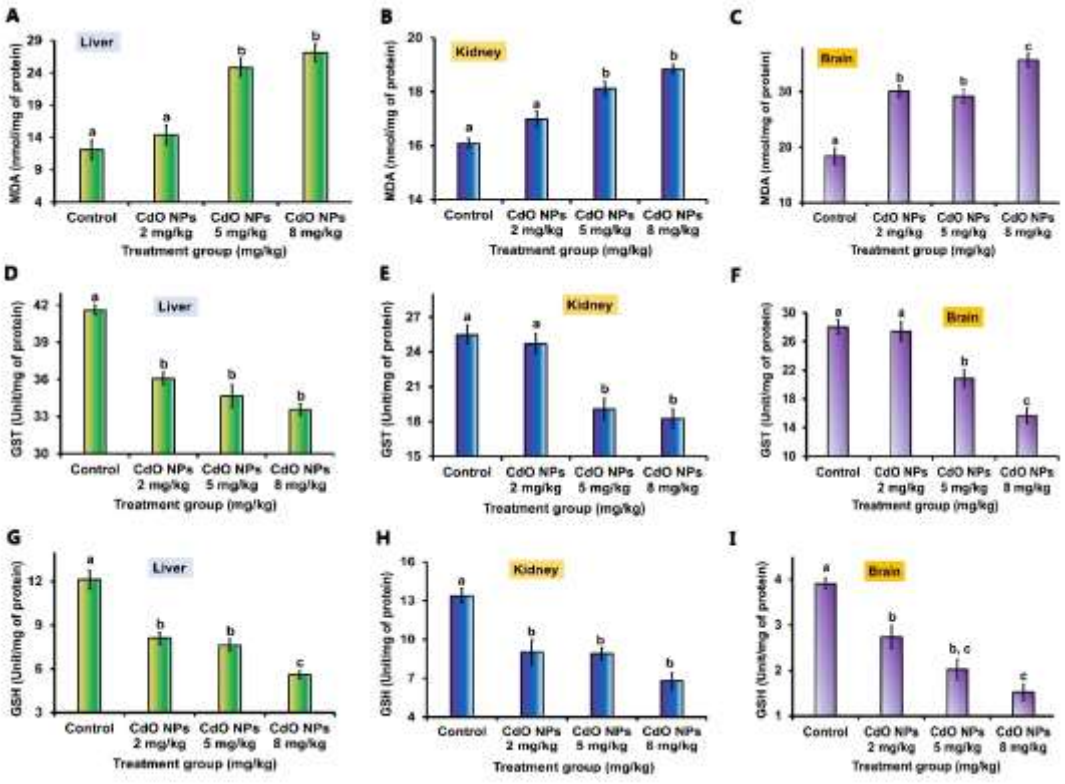

Figure 18 CdO-NPs intake promoted oxidative stress, **(A)** MDA in liver; **(B)** MDA in kidney; **(C)** MDA in brain; and led to the depletion of antioxidant enzymes GST and non-enzymatic antioxidant i.e., GSH in **(D)** & **(G)** liver; **(E)** & **(H)** kidney and

(F) & **(I)** brain, respectively. The data are represented as mean ± SEM, one-way ANOVA was performed to compare the values among the groups and different alphabets show significant relationship at $p < 0.05$.

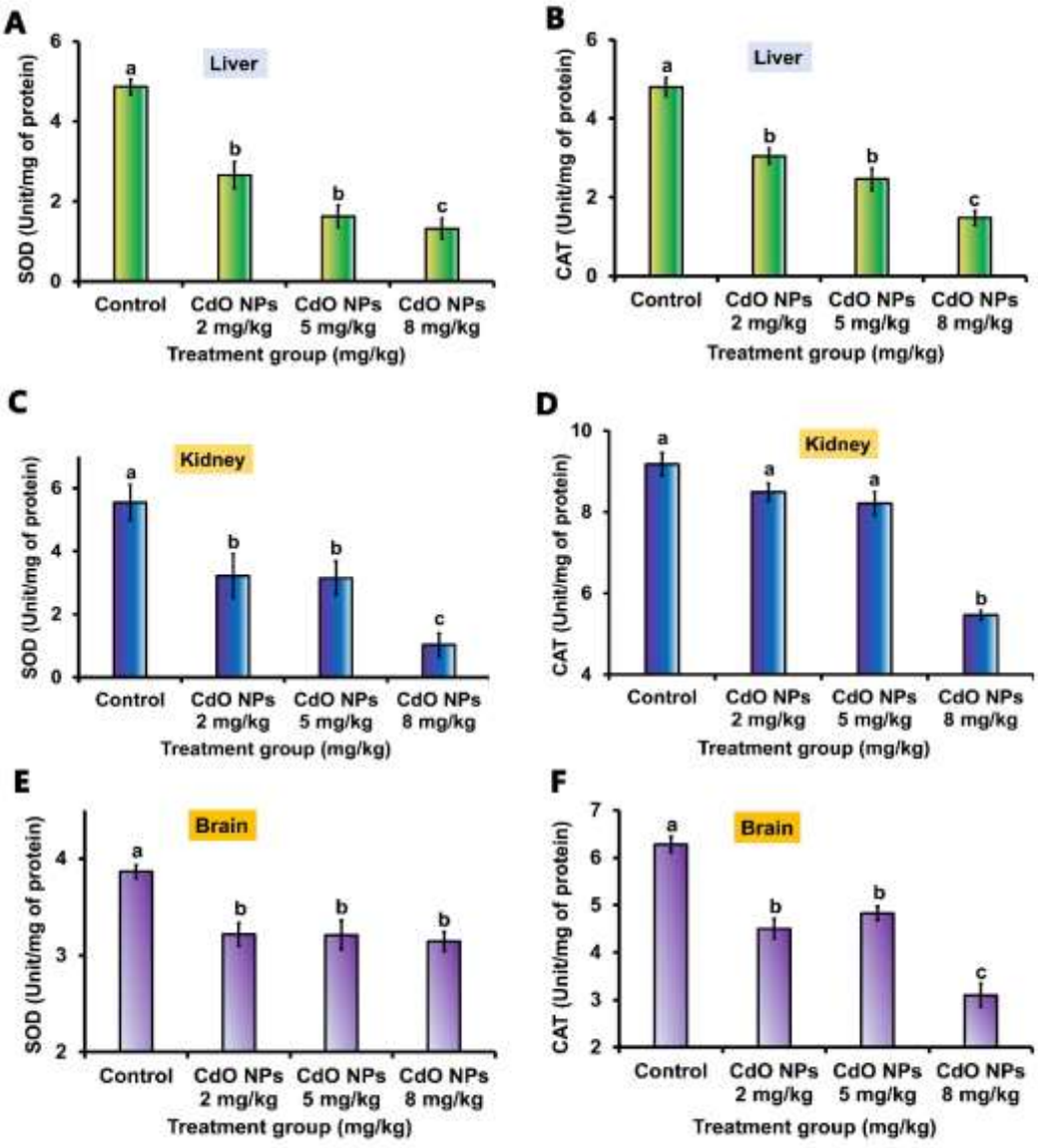

Figure 19 CdO-NPs administration resulted in the depletion of enzymatic antioxidants SOD in **(A)** liver, **(C)** kidney and **(E)** brain; and CAT in **(B)** liver, **(D)** kidney and **(F)** brain, respectively. The data are represented as mean ± SEM, one-way ANOVA was performed to compare the values among the groups and different alphabets show significant relationship at $p < 0.05$.

5.17 CdO-NPs intake induce histopathological alteration

5.18.1 Histopathological changes in liver

Normal hepatocytes (Hp), portal vein (PV), central vein (CV), bile duct (BD) and hepatic sinusoids (S) were seen in the control mice **(Figure 20A** and **E)**. The treatment of CdO-NPs led to the alteration of hepatic tissue architecture, which was evident from the appearance of portal vein congestion (cPV), cellular vacuolization (V) and formation of apoptotic nuclei (#) in the group treated with 2 mg/kg bw **(Figure 20B** and **F)**. In addition to the cellular vacuolization, the medium dosed group showed dilation of portal vein (dPV), dilation of sinusoid (ds), a few inflammatory infiltration (→) and cellular degeneration (&) **(Figure 20C** and **G)**. Intoxication of CdO-NPs at a dose of 8 mg/kg bw (for 30 days) had resulted in severe tissue necrosis (N) with marked inflammatory infiltration, dilation of sinusoid at various point and vacuolization **(Figure 20D** and **H)**.

5.18.2 Alteration of tissue architecture of kidney

Kidney tissue sections of CdO-NPs treated animals outlined glomerular degeneration with increase glomerular space (#), dilation of renal blood vessels (dV), vascular congestion (vC), cellular vacuolization (V), area of haemorrhage (Hem), tubular degeneration (&), renal tubule with wide luminal space (tW), tissue fragmentation (Ft), inflammatory infiltration (→), apoptotic nuclei (Ap) and area of necrosis (N) **(Figure 21B, C, D, F, G** and **H)** whereas, control mice exhibited balanced structure of renal cortex (C), medulla (M), glomerulus (G), proximal convoluted tubule (PT), distal convoluted tubule (DT), collection tubule (CT), blood vessel (BV) and Bowman's capsule (BC) **(Figure 21A** and **E)**.

5.18.3 Impact on the brain tissue architecture

Histological sections of brain tissue showed normal pyramidal neuronal cell (Pn) and blood vessels (BV) with compact tissue organization in control mice after 30 days of treatment with normal saline solution **(Figure 22A** and **E)**. However, CdO-NPs treatment led to the inflammatory infiltration (→), appearance of darkly stained neuron (@), intracytoplasmic vacuolization (Vac), cellular vacuolization (V), cellular

apoptosis (Ap, tissue necrosis (N), fragmentation of tissue (Ft), cellular degeneration (#) and congested vessel (cV) in the differently dosed groups of animals. The degree of histopathological alterations was more severe at the higher doses **(Figure 22C, G** and **D, H)**. However, fragmentation of tissue and intracytoplasmic vacuolization (vac) were seen at the dose of 2 mg/kg bw **(Figure 22B** and **F)**.

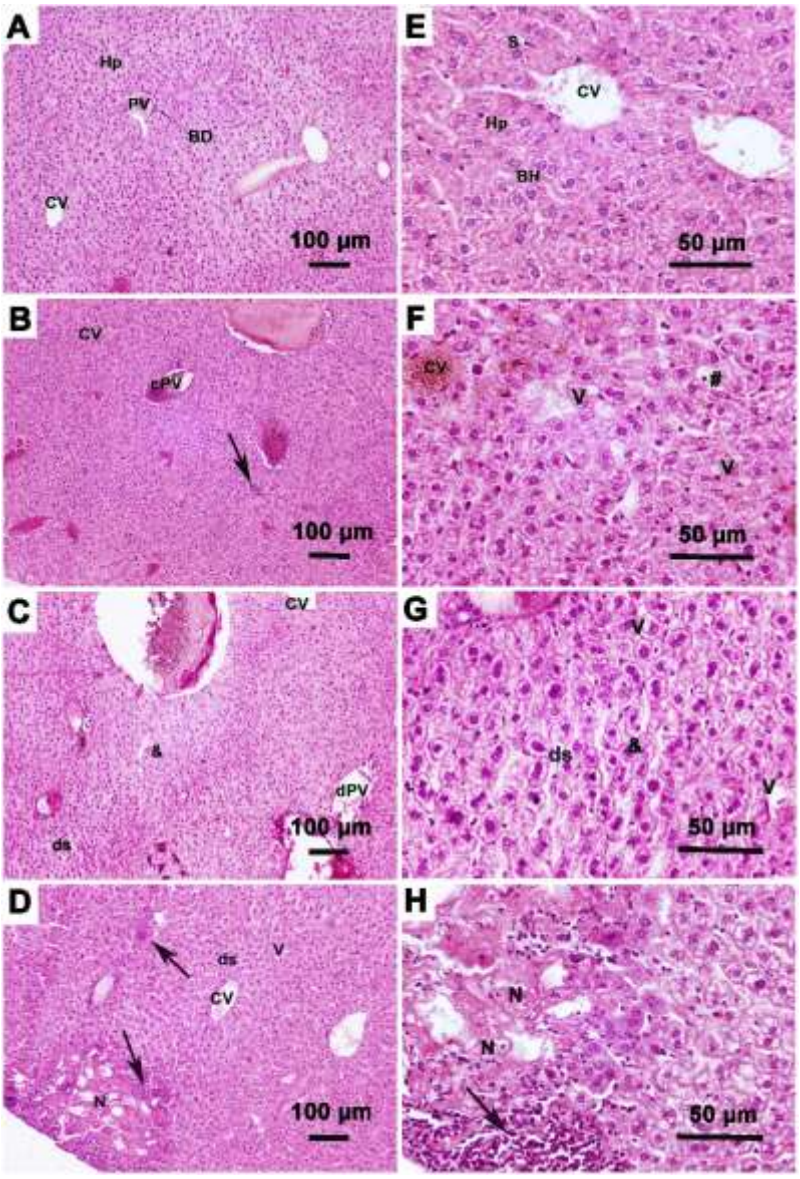

Figure 20 Changes in tissue architecture of liver tissue after CdO-NPs intoxication in female mice for 30 days, visible after hematoxylin and eosin staining (H & E). **A, B, C, D** at 10X, and **E, F, G, H** at 40X resolution with scale bar 100 µm and 50 µm, respectively. **(A** and **E)** Control, **(B** and **F)** CdO-NPs 2 mg/kg, **(C** and **G)** CdO-NPs 5

mg/kg, **(D** and **H)** CdO-NPs 8 mg/kg. CV- congested vein; Hp- hepatocytes; S- hepatic sinusoid; BH- binucleated hepatocytes; PV- portal vein; BD- bile duct; ds- dilated hepatic sinusoid; V- vacuolization; vac- extensive vacuolization; dPV- dilated portal vein; → (black arrow)- inflammatory infiltration; &- degenerative cell; N- area of necrosis; # (hash)- apoptotic nuclei; cPV- congested portal vein.

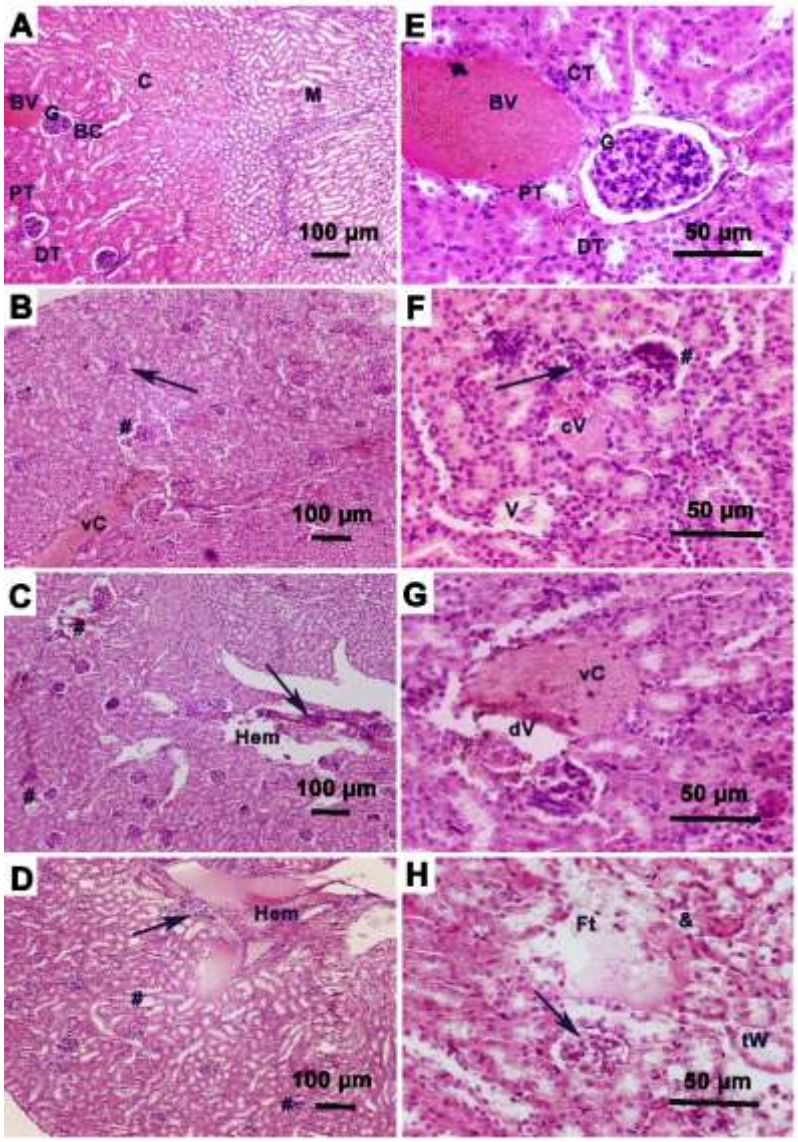

Figure 21 Histological illustration of tissue damages in kidney after CdO-NPs intake in female mice for 30 days, visible after hematoxylin and eosin staining (H & E). **A, B, C, D** at 10X, and **E, F, G, H** at 40X resolution with scale bar 100 µm and 50 µm, respectively. **(A** and **E)** Control, **(B** and **F)** CdO-NPs 2 mg/kg, **(C** and **G)** CdO-NPs 5 mg/kg, **(D** and **H)** CdO-NPs 8 mg/kg. C- cortex; M- medulla; G- glomerulus; PT-

proximal convoluted tubule; DT- distal convoluted tubule; CT- collection tubule; BV- blood vessel; BC- Bowman's capsule; dV- dilated vessel; # (hash)- glomerular degeneration with increased glomerular space; vC- vascular congestion; V- vacuolization; Hem- area of haemorrhage; &- tubular degeneration; tW- tubule with widened space; Ft- fragmentation of tissue; → (black arrow)- inflammatory infiltration; Ap- apoptotic nuclei; N- area of necrosis.

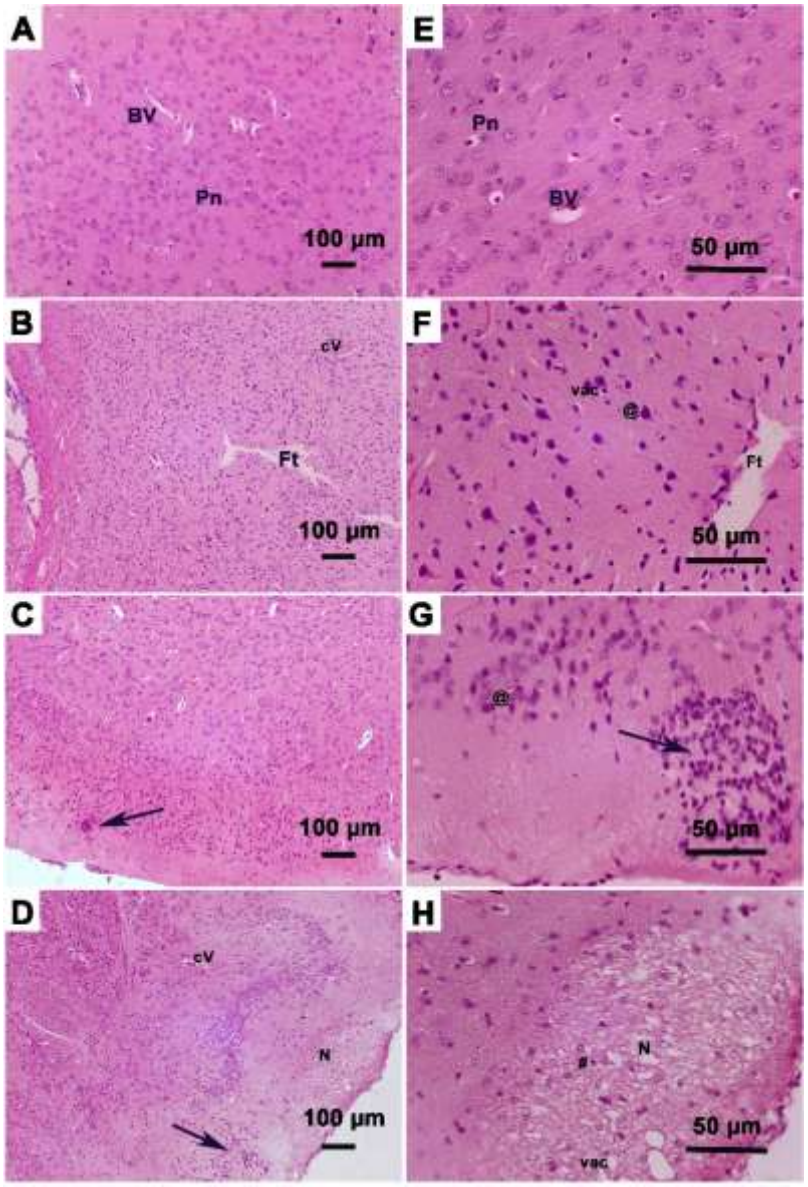

Figure 22 Micrographs of brain tissue showing effects of CdO-NPs intoxication in female mice, visible after hematoxylin and eosin staining (H & E). **A, B, C, D** at 10X, and **E, F, G, H** at 40X resolution with scale bar 100 µm and 50 µm,

respectively. **(A** and **E)** Control, **(B** and **F)** CdO-NPs 2 mg/kg, **(C** and **G)** CdO-NPs 5 mg/kg, **(D** and **H)** CdO-NPs 8 mg/kg. Pn- Pyramidal neuronal cell; BV- blood vessel; → (black arrow)- inflammatory infiltration; @- darkly stained neuron; Vac- intracytoplasmic vacuolization; V- vacuolization; Ap- cellular apoptosis; N- area of necrosis; Ft- fragmentation of tissue; # (hash)- cellular degeneration; cV- congested vessel.

5.18 Expression pattern of pro-apoptotic, anti-apoptotic, inflammatory markers and tumour suppressor protein in liver, kidney and brain tissues after CdO-NPs intoxication

Expression patterns of apoptotic and anti-apoptotic markers, different inflammatory markers and tumour related protein were changed dramatically in liver, kidney and brain tissues after CdO-NPs treatment. More specifically, the expression levels of pro-apoptotic markers such as BAX **(Figure 23A, C** and **E)** and active caspace-3 **(Figure 24A, C** and **E)** had increased significantly whereas, there was a significant decline in the expression of anti-apoptotic marker, BCL-2 **(Figure 23A, C** and **E)** as compared to the control group.

Furthermore, CdO-NPs intoxication had significantly elevated the expression of inflammatory markers including COX-2 **(Figure 24B, D** and **F)**, TNF-α **(Figure 26A, C** and **E)**, NF-κB **(Figure 26B, D** and **F)**, IL-6 **(Figure 25A, C** and **E)**and iNOS **(Figure 25B, D** and **F)**in the liver, kidney and brain tissues as compared to the normal mice, indicating its drastic effect upon the inflammatory response system. Additionally, analysis of tumour suppressor protein P^{53} **(Figure 27A, C** and **E)** revealed that CdO-NPs intoxication led to rise in its expression indicating possible role in the development of cancer. Moreover, liver, kidney and brain tissues had shown a significant decline in the expression of PPAR-ɣ in treatment mice as compared to the control group **(Figure 27B, D** and **F)**.

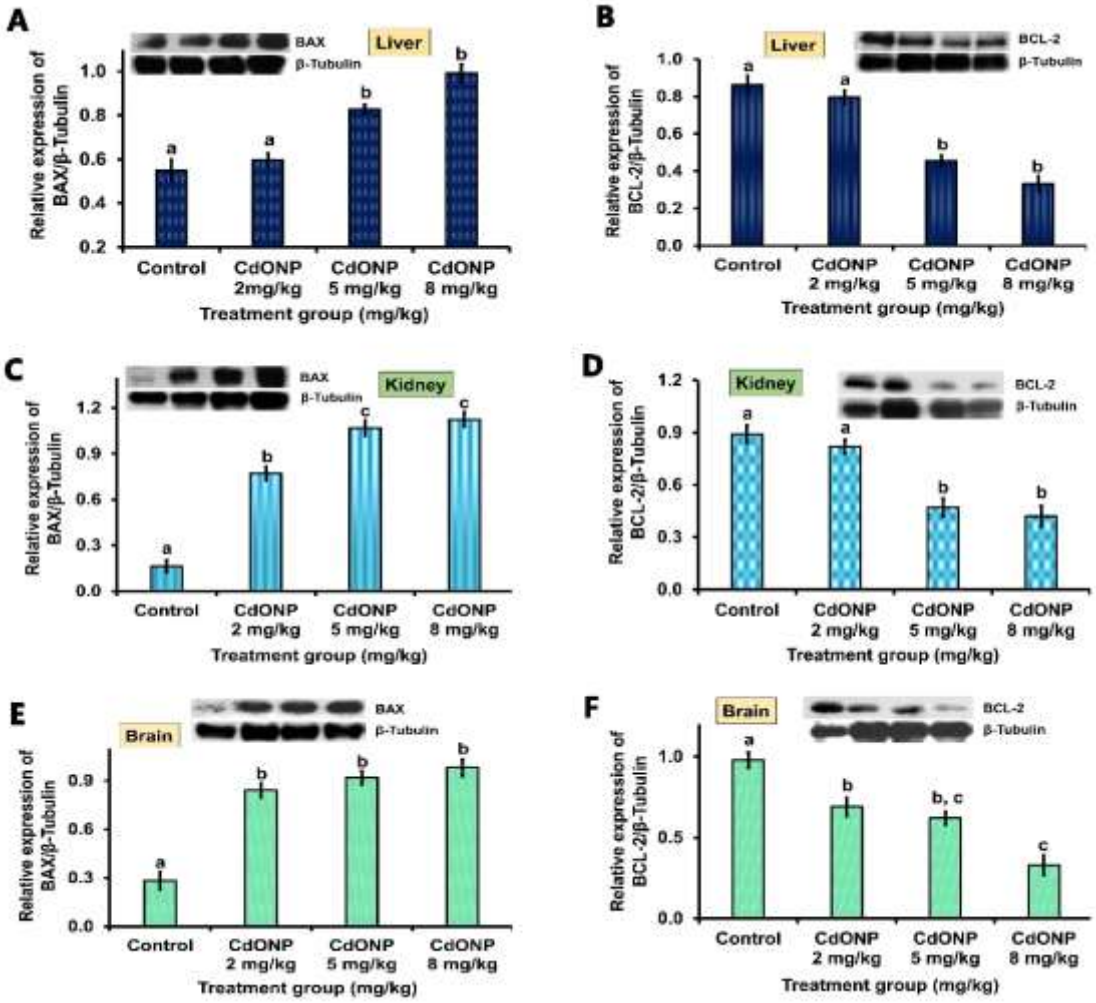

Figure 23 CdO-NPs triggers the expression of pro-apoptotic marker, BAX and depletion of anti-apoptotic marker, BCL-2 in treatment mice. The bar graph signifies densitometric analysis of BAX and BCL-2 in liver **(A** and **B**, respectively**)**, kidney **(C** and **D**, respectively**)** and brain tissues **(E** and **F**, respectively**)** (mean ± SEM, significant at $p < 0.05$).

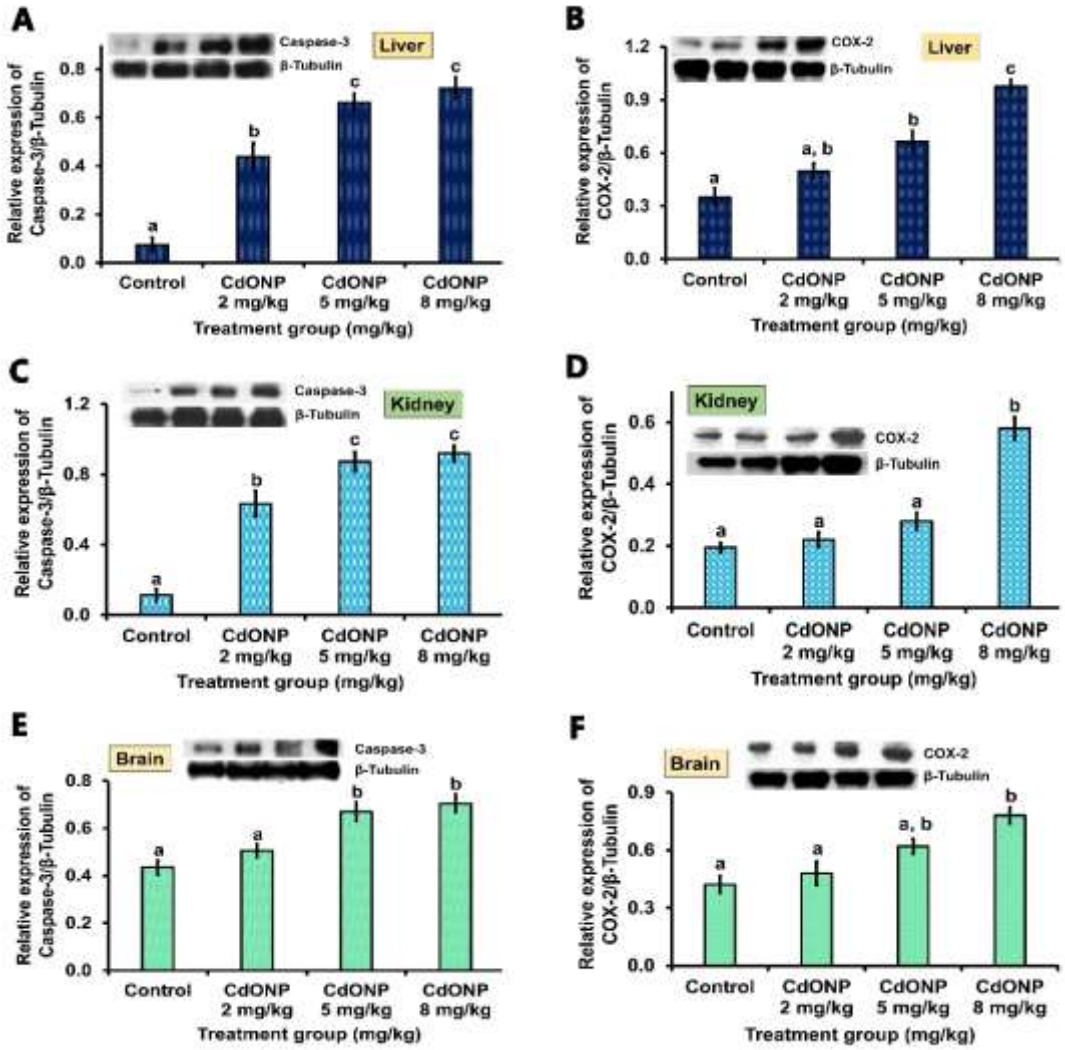

Figure 24 CdO-NPs triggers the expression of pro-apoptotic marker, active cascape-3 and inflammatory marker, COX-2 in treatment mice. The bar graph signifies densitometric analysis of active caspace-3 and COX-2 in liver (**A** and **B**, respectively), kidney (**C** and **D**, respectively and brain tissues (**E** and **F**, respectively) (mean ± SEM, significant at $p < 0.05$).

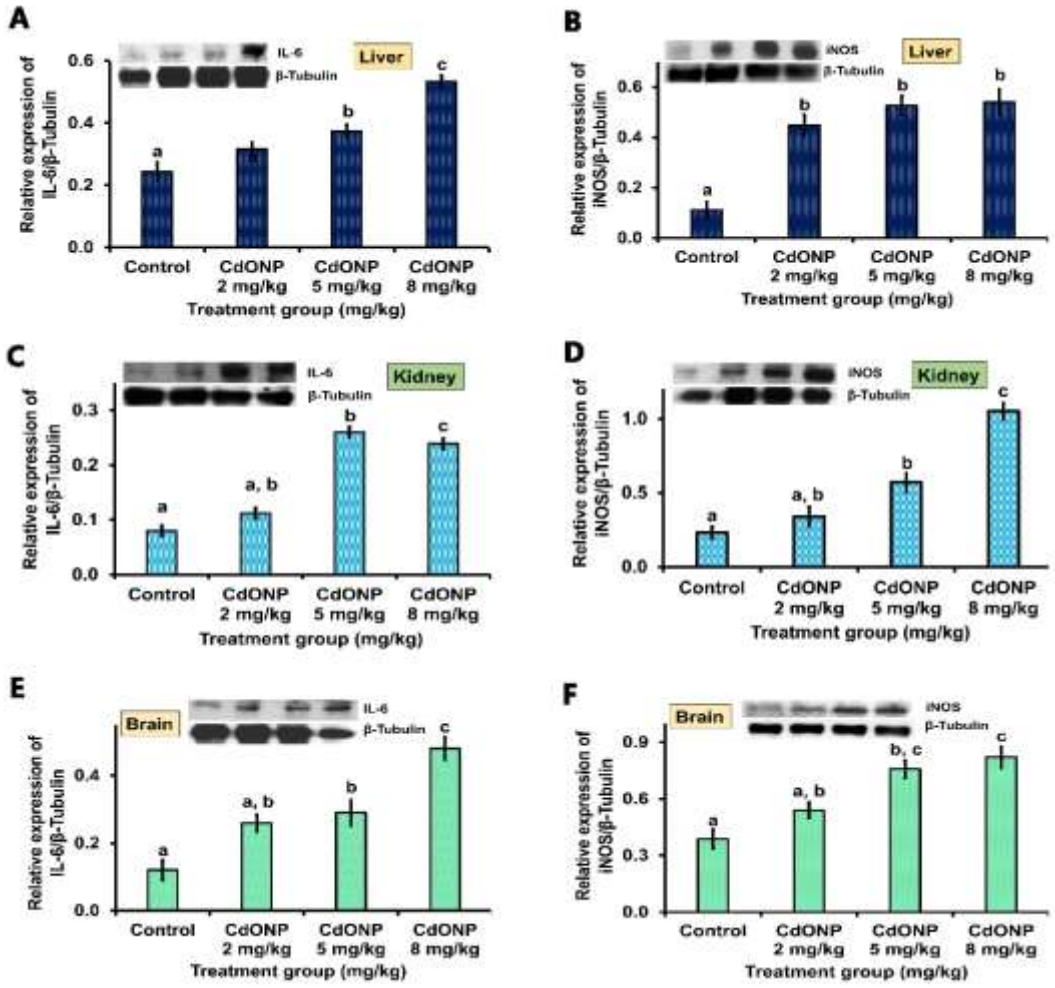

Figure 25 CdO-NPs triggers the expression of inflammatory marker, IL-6 and iNOS in treatment mice. The bar graph signifies densitometric analysis of IL-6 and iNOS in liver (**A** and **B**, respectively), kidney (**C** and **D**, respectively and brain tissues (**E** and **F**, respectively) (mean ± SEM, significant at $p < 0.05$).

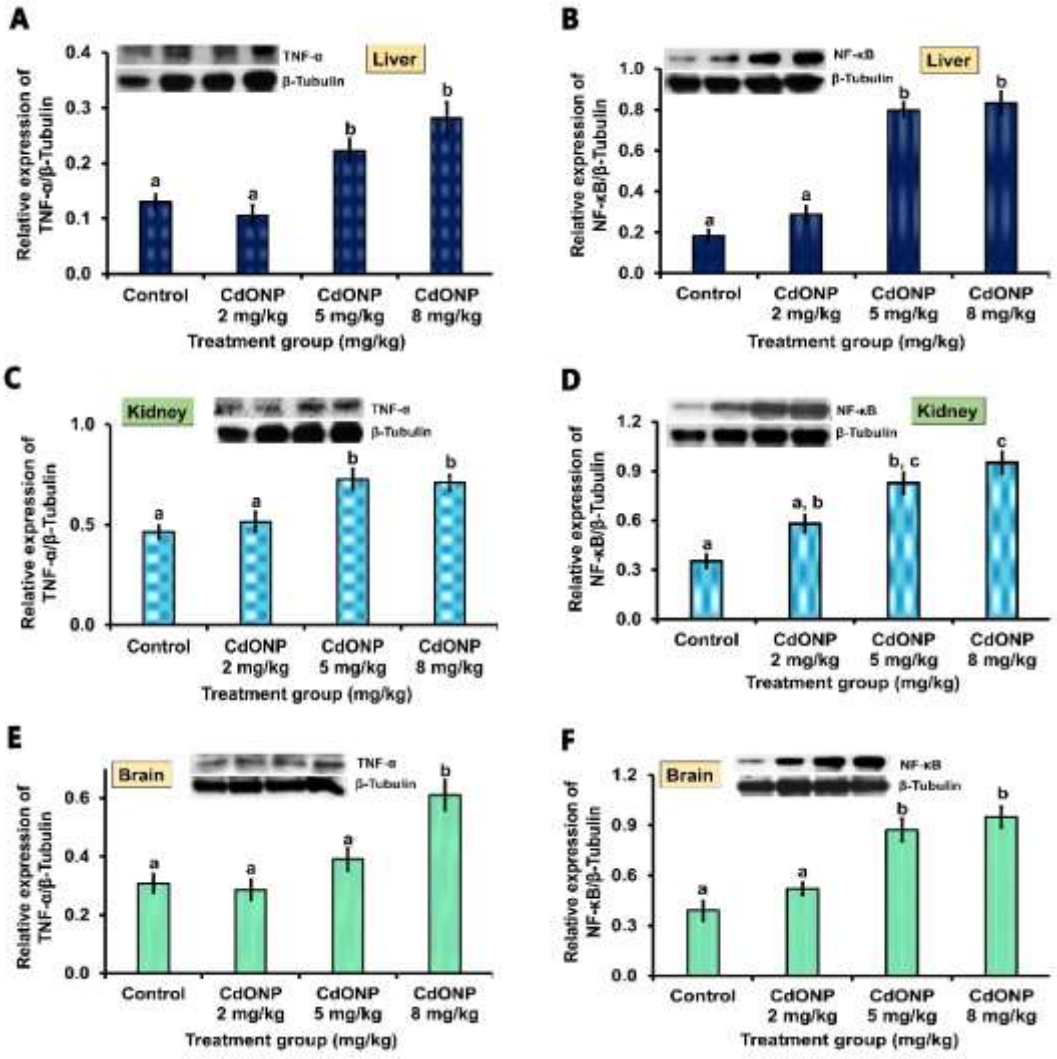

Figure 26 CdO-NPs triggers the expression of inflammatory marker, TNF-α and NF-κB in treatment mice. The bar graph signifies densitometric analysis of TNF-α and NF-κB in liver (**A** and **B**, respectively), kidney (**C** and **D**, respectively and brain tissues (**E** and **F**, respectively) (mean ± SEM, significant at $p < 0.05$).

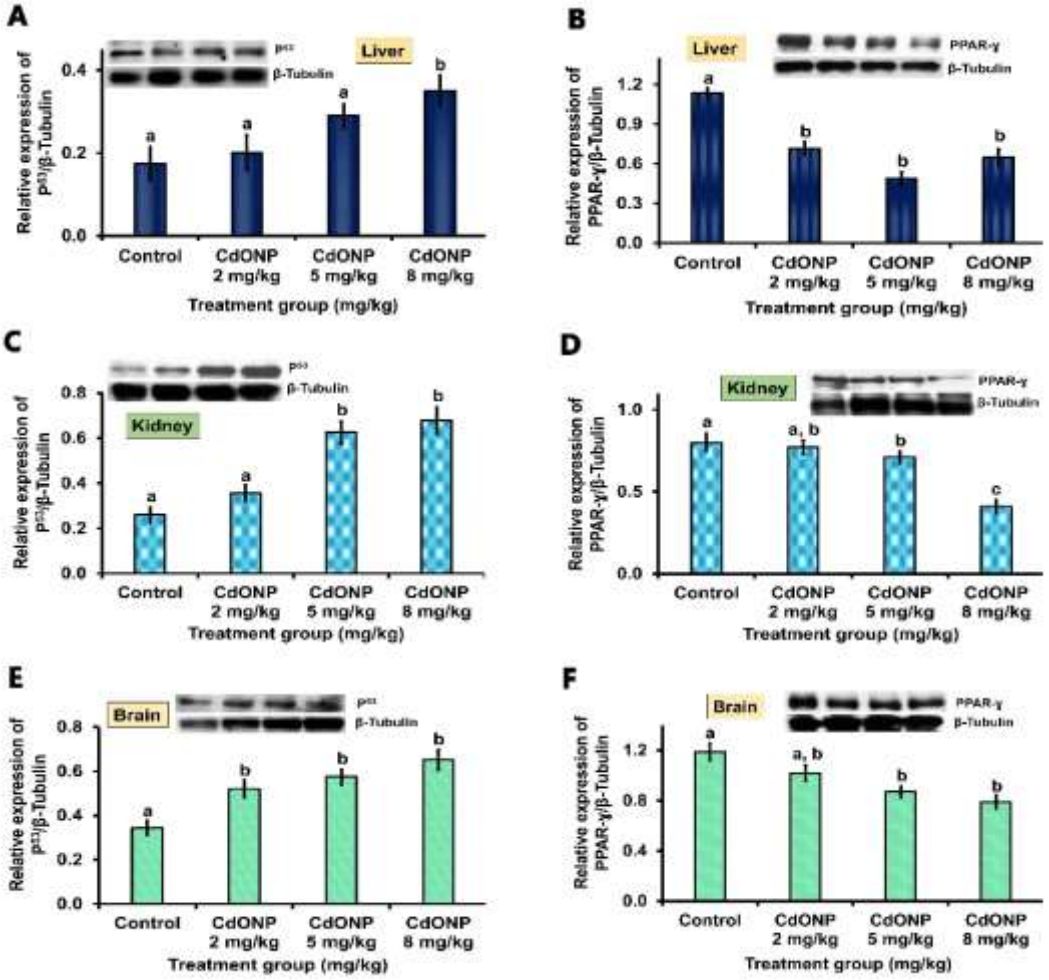

Figure 27 CdO-NPs triggers the expression of tumour suppressor, P^{53}, and PPAR-ɣ in treatment mice. The bar graph signifies densitometric analysis of P^{53} and PPAR-ɣ in liver (**A** and **B**, respectively), kidney (**C** and **D**, respectively and brain tissues (**E** and **F**, respectively) (mean ± SEM, significant at $p < 0.05$).

.

Experiment-III Evaluation of oxidative stress, antioxidant status, molecular mechanism and toxicological pathways that governs the organ specific toxicity in mice intoxicated with copper nanoparticles

5.19 Effect on body weight, food and water consumption and organ indices

CuO-NPs intoxication had impact upon the body weight and feeding pattern **(Figure 28)** in female mice. A significant decrease in body weight, food and water consumption were recorded during the period of experiment in treatment groups as compared to the normal control. In normal control group, an increasing trend of body weight, rate of food and water consumptions were observed from day 1 to day 30 whereas, in treated groups same were showing a decreasing trend. There was a significant loss of body weight, food and water consumption from initial to the final day of the experiment **(Table 22)**.

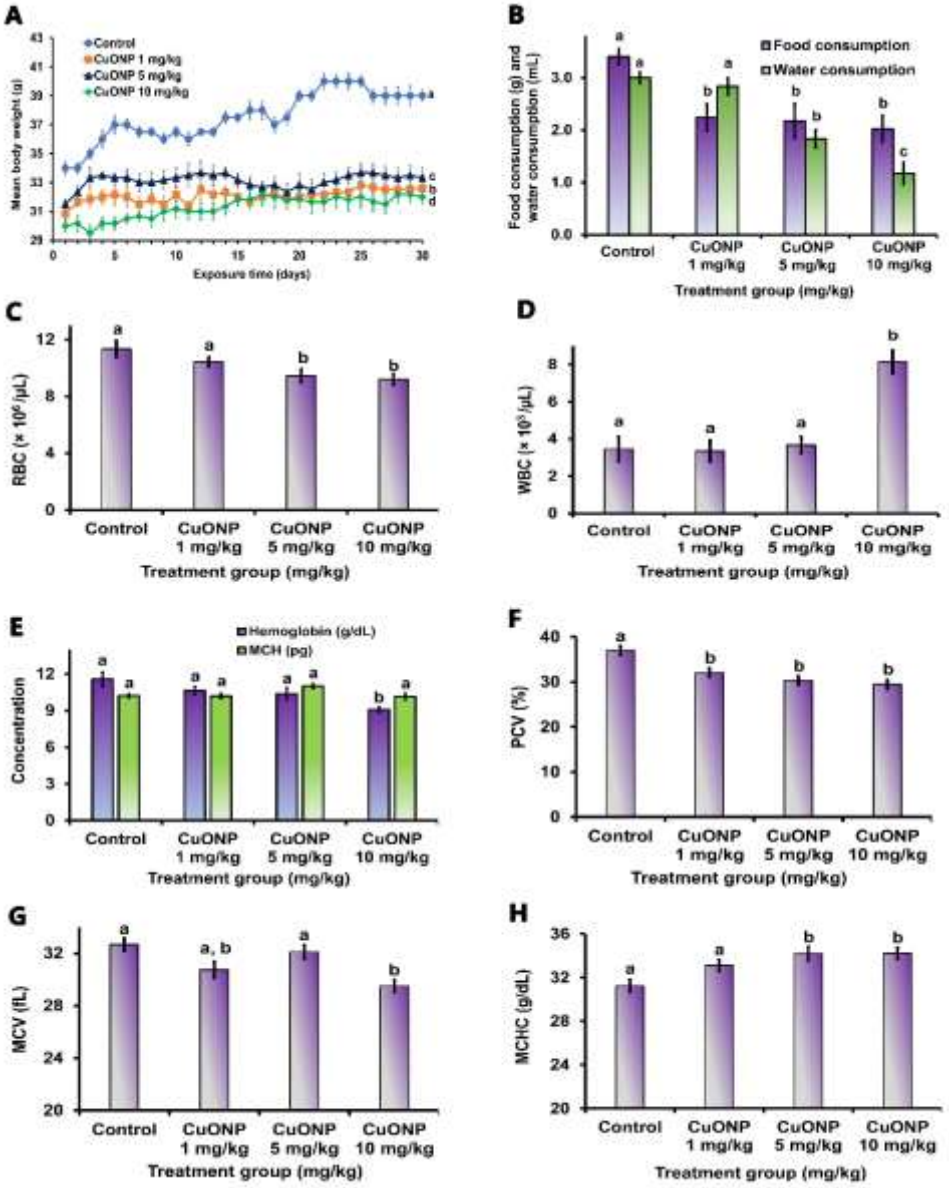

Figure 28 Graphs showing mean body weight, food and water consumption, and hematological parameters in the experimental groups. **(A)** mean body weight; **(B)** mean food and mean water consumption, respectively; **(C)** RBC counts; **(D)** WBC counts; **(E)** hemoglobin concentration and MCH; **(F)** PCV; **(G)** MCV and **(H)** MCHC. The data are represented as mean ± SEM, one-way ANOVA was performed to compare the values among the groups and different alphabets show significant relationship at $p < 0.05$.

Table 22 Routine observation of mean body weight, food and water consumption and loss/gain in weight, food and water consumption for the 30 days of experimental period are represented in table as mean ± SEM, significant at $p < 0.05$.

Daily observation (Body weight/Food and water consumption)	**Treatment group (mg/kg bw / day) and exposure period (30 days, p. o.)**			
	Control	**CuO-NPs 1 mg/kg**	**CuO-NPs 5 mg/kg**	**CuO-NPs 10 mg/kg**
Mean body weight/day (g)	37.53 ± 0.31 a	32.07 ± 0.08 b	33.13 ± 0.09 c	31.27 ± 0.13 d
Mean gain/ loss in body weight (%)	14.82 ± 0.05 a	-5.62 ± 0.06 b	-5.20 ± 0.07 c	-6.13 ± 0.17 d
Mean Food consumption/day (g)	3.40 ± 0.15 a	2.24 ± 0.26 b	2.17 ± 0.33 b	2.02 ± 0.26 b
Mean gain/loss in food consumption (%)	17.31 ± 0.28 a	-14.28 ± 0.37 b	-48.65 ± 0.26 c	-63.41 ± 0.21 d
Mean Water consumption/day (ml)	3.00 ± 0.11 a	2.83 ± 0.16 a	1.83 ± 0.17 b	1.17 ± 0.21 c
Mean gain/loss in water consumption (%)	18.46 ± 0.38 a	-34.64 ± 0.49 b	-43.40 ± 0.28 c	-67.47 ± 0.37 d

There was significant decrease in relative weight of liver, kidney, stomach, spleen, lung, ovary and uterus signifying decrease in organ as well as body weight. Whereas,

increased in the relative weight of the brain indicated that the only body weight had decreased not the brain weight in the treatment group as compared to the normal female **(Table 23)**.

Table 23 Observations of organ and relative organ weights in mice after 30 days of CuO-NPs treatment period are represented in table as mean ± SEM, significant at $p < 0.05$.

Organ (relative organ weight)	**Treatment group (mg/kg bw / day) and exposure period (30 days, p. o.)**			
	Control	**CuO-NPs 1 mg/kg**	**CuO-NPs 5 mg/kg**	**CuO-NPs 10 mg/kg**
Liver	4.15 ± 0.03 a	4.84 ± 0.15 b	3.60 ± 0.21 a, c	3.43 ± 0.17 c
Kidney	0.87 ± 0.02 a	0.95 ± 0.04 a	0.81 ± 0.03 a	0.63 ± 0.03 b
Brain	1.28 ± 0.06 a	1.47 ± 0.05 b	1.41 ± 0.02 b	1.45 ± 0.05 b
Stomach	0.64 ± 0.01 a, b	0.68 ± 0.01 b	0.60 ± 0.03 a, c	0.57 ± 0.01 c
Heart	0.39 ± 0.01 a	0.40 ± 0.02 a	0.38±0.01 a	0.35 ± 0.01 a
Spleen	0.45 ± 0.03 a	0.46 ± 0.01 a	0.36 ± 0.04 a, b	0.31 ± 0.01 b
Ovary	0.08 ± 0.01 a, b	0.09 ± 0.00 a	0.06 ± 0.01 b	0.06 ± 0.00 b
Uterus	0.41 ± 0.01 a	0.36 ± 0.02 b	0.30 ± 0.01 b, c	0.28 ± 0.01 c
Lung	0.72 ± 0.01 a	0.76 ± 0.01 a	0.69 ± 0.02 a	0.65 ± 0.01 b
Pancreas	0.69 ± 0.03 a	0.70 ± 0.02 a	0.67 ± 0.03 a	0.66 ± 0.02 a

5.20 CuO-NPs consumption effects hematological parameters

Hematological parameters were evaluated to know about the health and functioning of blood. In the analyses, decrease in the RBC counts **(Figure 28C)**, hemoglobin concentration **(Figure 28E)** and PCV **(Figure 28E)** were observed significantly in the high dose group (10 mg/kg bw) as compared to the control groups. The WBC counts were also significantly higher in in high dose group indicating probability of inflammation **(Figure 28D)**. Further, decline in MCV **(Figure 28G)**, elevation in MCHC **(Figure 28H)** and no significant change was noted in MCH **(Figure 28E)** concentration in treatment groups as compared to the normal control group.

5.21 Accumulation of copper in target organs

Copper concentration was quantified in target organs i.e., liver, kidney and brain, to evaluate the organ load and metabolism of the metal after consumption. It was found that concentration of the metal increased significantly in all the organs and mostly higher accumulation was observed at high dose as compared to the normal control group **(Table 24)**.

Table 24 Accumulation of copper was detected in liver, kidney and brain tissue after 30 days of exposure in female mice. The values in the table are represented as mean ± SEM, significant at $p < 0.05$.

Concentration of accumulated Copper (ppm)	**Treatment group (mg/kg bw / day) and exposure period (30 days, p. o.)**			
	Control	**CuO-NPs 1 mg/kg**	**CuO-NPs 5 mg/kg**	**CuO-NPs 10 mg/kg**
Liver	0.004 ± 0.02 a	0.048 ± 0.01 a	0.177 ± 0.03 b	0.347 ± 0.06 c
Kidney	0.002 ± 0.05a	0.084 ± 0.02 a	0.134 ± 0.03 a	0.215 ± 0.02 b
Brain	0.002 ± 0.01 a	0.057 ± 0.01 a	0.123 ± 0.01 a, b	0.198 ± 0.02 b

5.22 Serological assays demonstrated deterioration of liver, kidney and lipid profiles

Serological assays on liver and kidney functions biomarkers demonstrated that, there was depletion of total protein, globulin, albumin and increased production of total bilirubin, direct bilirubin, ALP, ALT, AST, urea, blood urea nitrogen, uric acid and creatinine in treatment groups as compared to the control, indicating deterioration of liver and kidney profiles **(Figure 29** and **Figure 30)**. Further, there was an elevation of albumin/globulin, AST/ALT, and BUN/creatinine ratio **(Figure 29D, Figure 30C** and **Figure 30H)**.

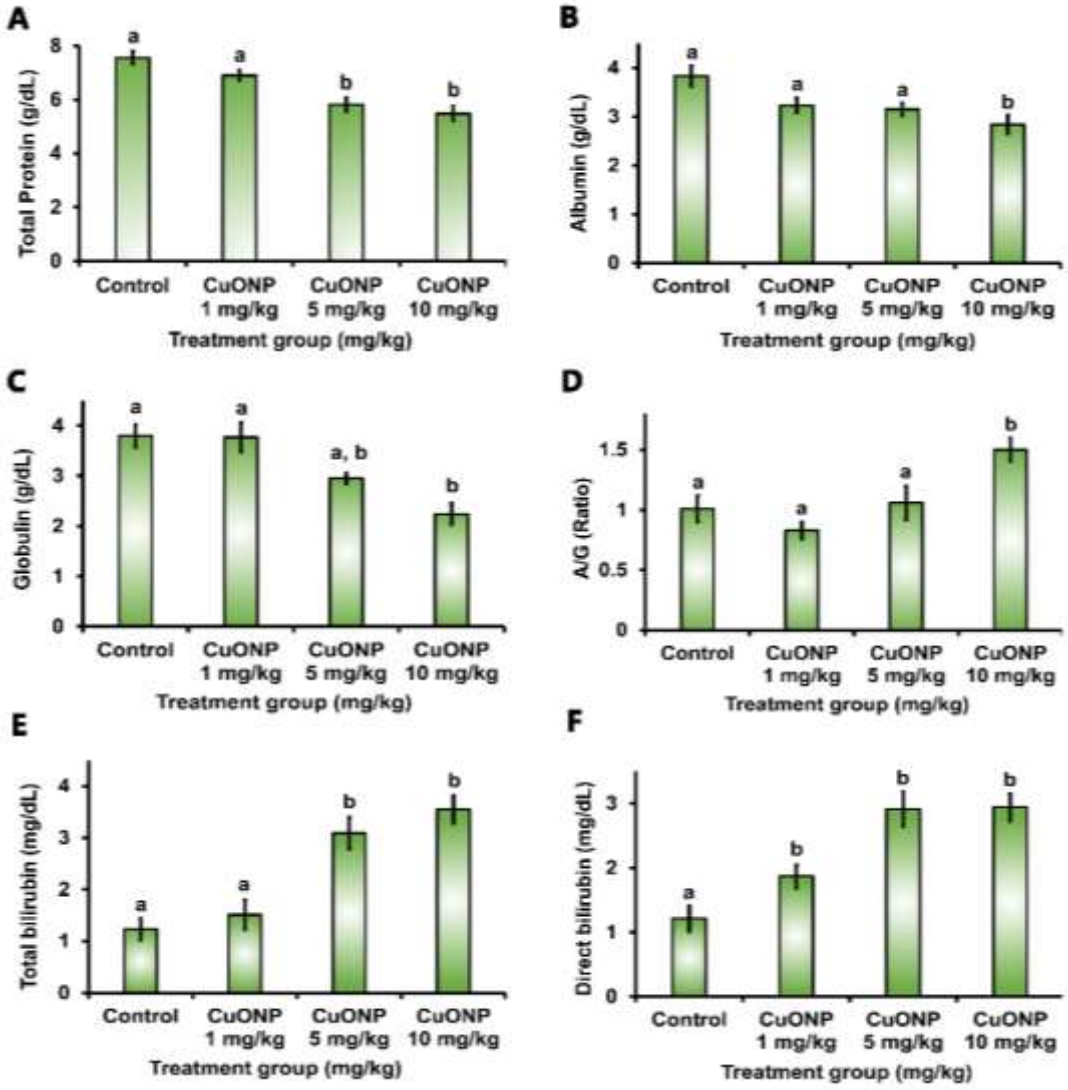

Figure 29 Graphs showing status of liver function biomarkers in blood serum of CuO-NPs treated and normal control group. **(A)** total protein; **(B)** albumin; **(C)** globulin; **(D)** A/G ratio; **(E)** total bilirubin; **(F)** direct bilirubin. The data are represented as mean ± SEM, one-way ANOVA was performed to compare the values among the groups and different alphabets show significant relationship at $p < 0.05$.

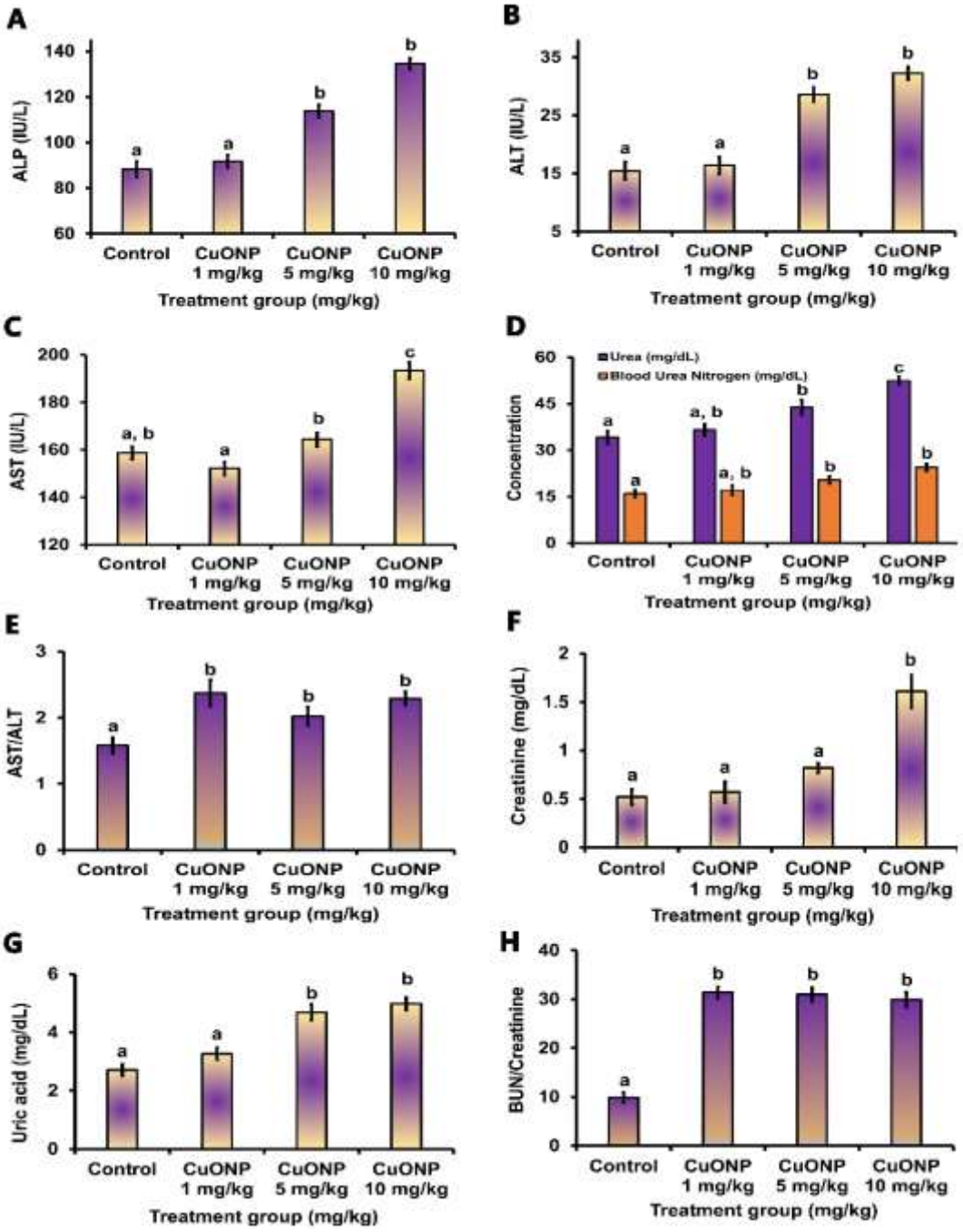

Figure 30 Graphs showing status of liver and kidney function biomarkers in blood serum of CuO-NPs treated and normal control group. **(A)** ALP; **(B)** ALT; **(C)** AST; **(D)** urea and blood urea nitrogen; **(E)** AST/ALT; **(F)** creatinine; **(G)** uric acid; **(H)** BUN/creatinine ratio. The data are represented as mean ± SEM, one-way ANOVA was performed to compare the values among the groups and different alphabets show significant relationship at $p < 0.05$.

Significant increase in the concentration of total cholesterol and LDL cholesterol while decline in the concentration of HDL cholesterol were observed in the treatment group as compare to the control group. However, no significant changes were noticed in triglycerides and serum glucose concentration. Decline in the concentration of chloride, potassium and elevated levels of sodium were observed in the treatment groups as compared to the control. Calcium concentration didn't show much variation across the group **Table 25**.

Table 25 Effect of CuO-NPs in lipid profiles of female mice after 30 days of treatment. All the data are represented as mean ± SEM, one-way ANOVA was performed to compare the values among the groups and different alphabets show significant relationship at $p < 0.05$.

Lipid Profiles	**Treatment Group (mg/kg bw / day) and exposure period (30 days, p.o.)**			
	Control	**CuO-NPs 1 mg/kg**	**CuO-NPs 5 mg/kg**	**CuO-NPs 10 mg/kg**
Total Cholesterol (mg/dL)	60.11 ± 1.49 a	69.32 ± 1.11 b	72.68 ± 1.37 b	92.37 ± 2.31 c
Triglycerides (mg/dL)	115.57 ± 1.22 a	112.33 ± 0.98 b	118.02 ± 1.08 a	118.97 ± 1.12 a
HDL Cholesterol (mg/dL)	12.29 ±0.75 a	11.08 ± 0.89 a	10.37 ± 1.13 a, b	7.25 ± 0.87 b
LDL Cholesterol (mg/dL)	38.11 ± 2.01 a, b	35.22 ± 1.78 a	45.19 ± 2.07 b	52.07 ± 1.19 c
Glucose (mg/dL)	85.21 ± 1.08 a	89.14 ± 1.11 a	84.09 ± 1.15 a,	82.07 ± 1.28 a
Calcium (mg/dL)	9.08 ± 0.88 a	10.97 ± 0.91 a	7.12 ± 0.78 b	7.37 ± 1.09 a, b

Chloride (mmol/L)	185.18 ± 2.21 a	188.93 ± 1.58 a	170.27 ± 2.07 b	172.09 ± 1.67 b
Sodium (mmol/L)	98.21 ± 1.77 a	112.08 ± 2.61 b	129.87 ± 1.38 c	135.59 ± 2.01 c
Potassium (mmol/L)	11.67 ± 0.61 a	11.29 ± 0.71 a	9.18 ± 0.53 a	8.79 ± 0.67 b

5.23 CuO-NPs intoxication triggers inflammatory response system

Inflammatory and oxidative stress response systems were triggered after regular consumption of CuO-NPs and it was evident from the elevated levels of IL-6, IL-1, FAD, MPO, prostaglandin, leukotriene, and decline in the concentration of IL-10 and TAOC **(Table 26)**.

Table 26 CuO-NPs intake triggers inflammatory response system of female mice after 30 days of treatment. All the data are represented as mean ± SEM, one-way ANOVA was performed to compare the values among the groups and different alphabets show significant relationship at $p < 0.05$.

Inflammatory markers	**Treatment group (mg/kg bw / day) and exposure period (30 days, p. o.)**			
	Control	**CuO-NPs 1 mg/kg**	**CuO-NPs 5 mg/kg**	**CuO-NPs 10 mg/kg**
FAD (ng/L)	164.13 ± 2.13 a	204.16 ± 2.04 b	235.23 ± 1.21 c	240.44 ± 1.65 c
IL-10 (pg/ml)	20.99 ± 1.54 a	16.89 ± 1.20 b	11.15 ± 1.08 c	13.86 ± 1.17 c
IL-6 (ng/L)	1.29 ± 0.24 a	3.08 ± 0.29 b	2.85 ± 0.17 b	4.69 ± 0.31 c
MPO (ng/ml)	1.78 ± 0.14 a	1.19 ± 0.23 a	3.04 ± 0.31 b	3.85 ± 0.28 b
IL-1 (pg/ml)	18.17 ± 1.07 a	24.82 ± 1.33 b	23.67 ± 1.12 b	35.26 ± 1.24 c
Prostaglandin E-2 (ng/ml)	0.24 ± 0.02 a	0.30 ± 0.01 b	0.33 ± 0.03 b	0.34 ± 0.01 b
Leukotriene B4 (ng/ml)	1.89 ± 0.67 a	3.15 ± 0.45 b	4.85 ± 0.39 b, c	6.29 ± 0.37 c

TAOC (U/ml)	4.40 ± 0.15 a	3.26 ± 0.42 b	2.65 ± 0.34 b, c	1.04 ± 0.65 c

5.24 Stimulation of oxidative stress response and depletion of antioxidants in targeted organs

Consumption of CuO-NPs was linked with the stimulation of oxidative stress and depletion of enzymatic and non-enzymatic antioxidants. This was evident from the elevated levels of MDA in liver, kidney and brain tissues of all the treatment groups as compared to the control group **(Figure 31A, D and G)**. The levels of non-enzymatic antioxidants i.e., GSH was lowered significantly in liver only at high dose (10 mg/kg bw) **(Figure 31C)**, whereas, in kidney and brain it was significantly depleted in both 5 mg/kg bw and 10 mg/kg bw group as compared to the control **(Figure 31F and I)**.

Enzymatic antioxidants GST, showed significant depletion at high doses (5 mg/kg bw and 10 mg/kg bw) in liver and kidney and in brain depletion was significant only at a dose of 10 mg/kg bw **(Figure 31B, E and H)**. SOD showed marked depletion at 1 mg/kg bw and 10 mg/kg bw doses in liver tissue and at both the higher doses (5 mg/kg bw and 10 mg/kg bw) in kidney and brain **(Figure 31A, C and E)**. Depletion of CAT was observed in all the tissues (liver, kidney and brain) but more significantly in liver tissues of all the treated groups as compared to the control group **(Figure 31B, D and F)**.

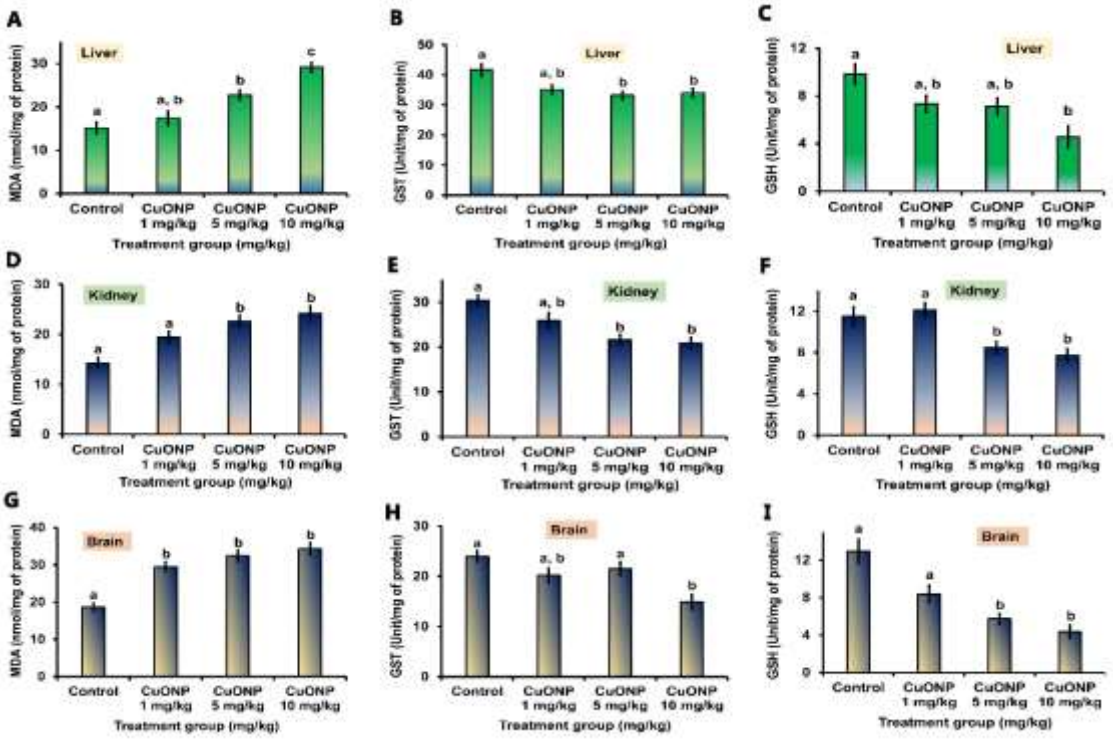

Figure 31 CuO-NPs consumption triggered oxidative stress, **(A)** MDA in liver; **(D)** MDA in kidney; **(G)** MDA in brain; and led to the depletion of antioxidant enzymes GST and non-enzymatic antioxidant i.e., GSH in **(B)** and **(C)** liver; **(E)** and **(F)** kidney and **(H)** and **(I)** brain, respectively. The data are represented as mean ± SEM, one-way ANOVA was performed to compare the values among the groups and different alphabets show significant relationship at $p < 0.05$.

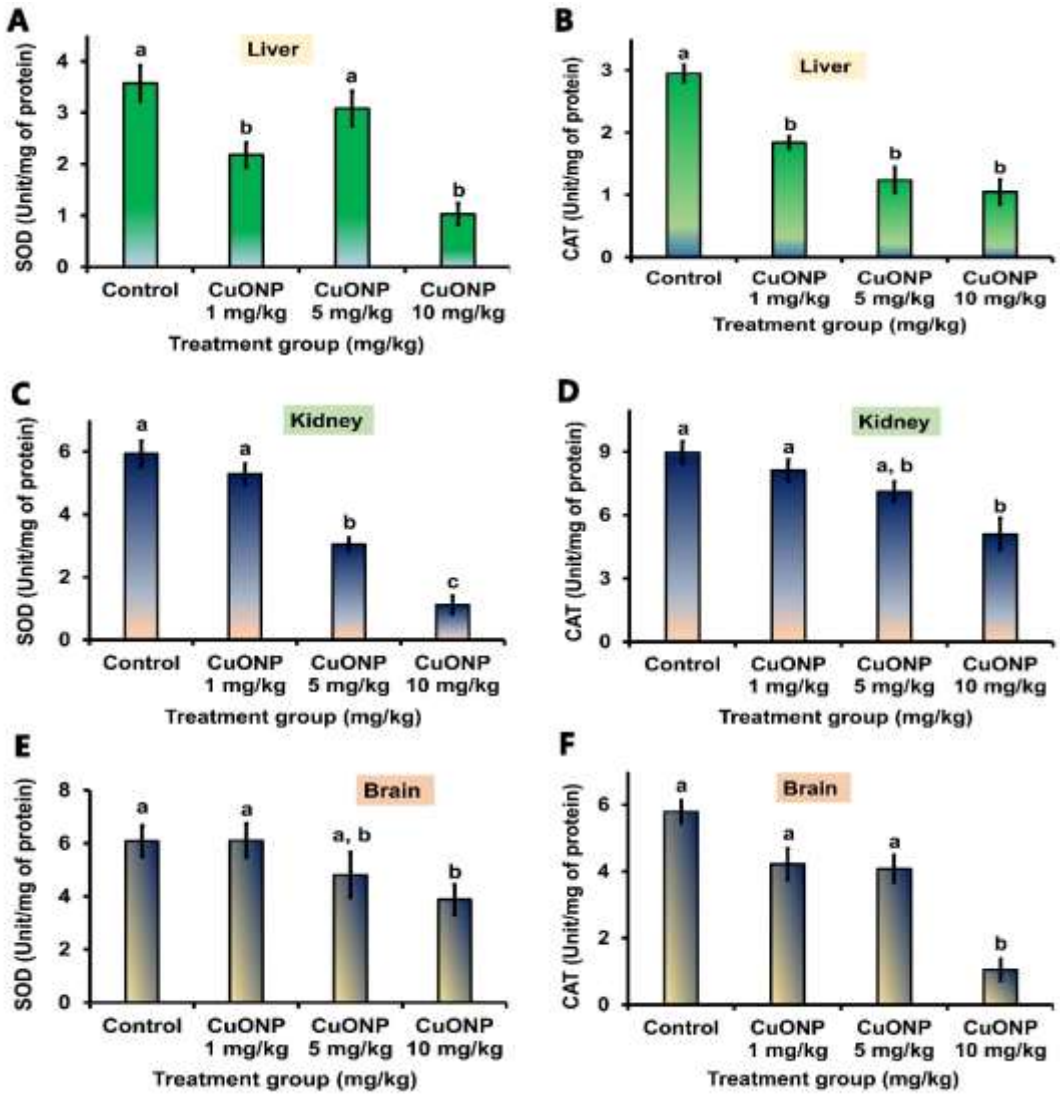

Figure 32 CuO-NPs consumption led to depletion of antioxidant enzymes SOD and CAT in **(A)** and **(B)** liver; **(C)** and **(D)** kidney, and **(E)** and **(F)** brain, respectively. The data are represented as mean ± SEM, one-way ANOVA was performed to compare the values among the groups and different alphabets show significant relationship at $p < 0.05$.

5.25 CuO-NPs induce histopathological alteration in tissue

5.26.1 Histological changes in liver tissue after CdO-NPs intake

Histopathological examination of liver tissue showed dilation of central vein (dCV), dilation of sinusoid (ds), presence of apoptotic nuclei (#), degeneration of hepatocytes (&), tissue fragmentation (Ft), congestion of central vein (**), infiltration of inflammatory cells (→), congestion of portal vein (cPV), and tissue

haemorrhage (Hem) in the CuO-NPs treated animals **(Figure 33B, C, D, F, G and H)**. The structure of hepatocytes (Hp) with binucleated cell (BH), central vein (CV), portal vein (PV, hepatic artery (hA), bile duct (BD), and hepatic sinusoid (S) was found to be normal in architecture in the control group **(Figure 33A and E)**. Alterations were markedly increased in the high-dose CuO-NPs intoxicated group **(Figure 33D and H)**.

5.26.2 Alteration of renal tissue architecture after CuO-NPs intoxication

Control mice treated with normal saline **(Figure 34A and E)** showed a normal structure of glomerulus (G), proximal convoluted tubule (PT), distal convoluted tubule (DT), collection tubule/duct (CT), and Bowman's capsule (BC) in the kidney, whereas, glomerular degeneration with increased glomerular space (#), area of haemorrhage (Hem), inflammatory infiltration (→), and presence of apoptotic nuclei (Ap) were reported in mice administered with CuO-NPs in dose-dependent manner **(Figure 34B, C, D, F, G and H)**.

5.26.3 CuO-NPs administration revealed histopathological changes in brain tissue

Histopathological analysis on brain tissue revealed that administration of CuO-NPs at sub-acute levels in mice had resulted in alteration of tissue architecture, displaying darkly stained neuron (@), inflammatory infiltration (→), cellular vacuolization (V) and apoptosis (Ap), area of necrosis (N), cellular degeneration (#), congestion of blood vessels (cV), and fragmentation of tissue (Ft) in the treatment groups in a dose-dependent manner **(Figure 35B, C, D, F, G and H)**. Control mice exhibited normal tissue architecture **(Figure 35A and E)**.

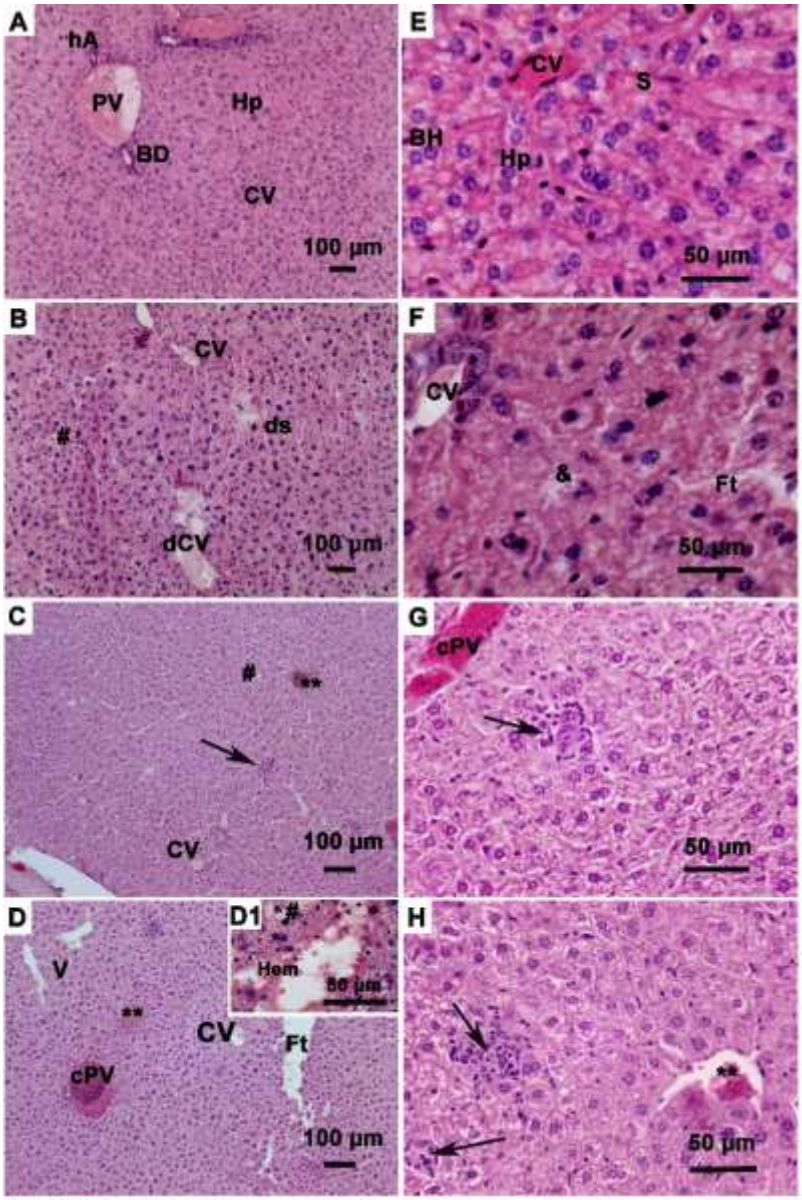

Figure 33 CuO-NPs intoxication resulted in alteration in tissue architecture of liver after 30 days of treatment in female mice. The alterations are visible after hematoxylin and eosin staining (H & E). **A, B, C, D** and **D1, E, F, G, H** are at 10X (scale bar =100 µm) and 40X (scale bar = 50µm) resolution, respectively. CV- congested vein; Hp- hepatocytes; S- hepatic sinusoid; BH- binucleated hepatocytes; PV- portal vein; BD- bile duct; hA- hepatic artery; ds- dilated hepatic sinusoid; V- vacuolization; vac- extensive vacuolization; dPV- dilated portal vein; → (black arrow)- inflammatory infiltration; Hem- area of haemorrhage; &- degenerative cell;

N- area of necrosis; # (hash)- apoptotic nuclei; ** (double star)- congested central vein; cPV- congested portal vein.

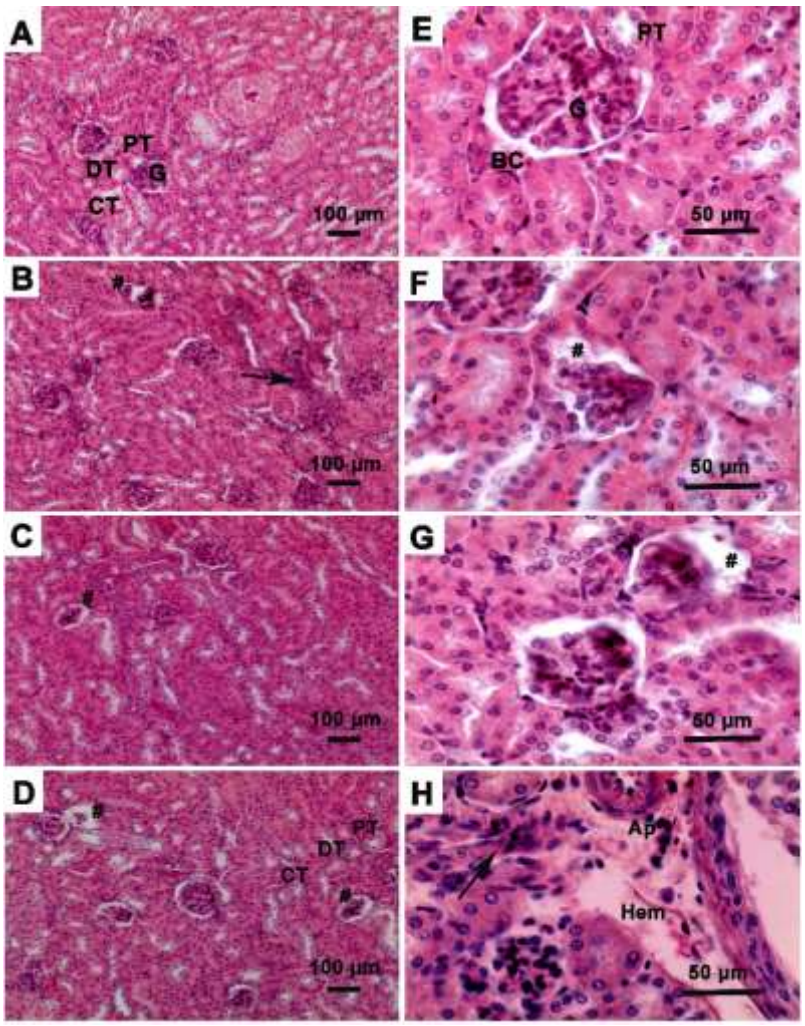

Figure 34 Alteration in tissue architecture of kidney in female mice was revealed after 30 days of CuO-NPs treatment. Hematoxylin and eosin staining was done for the histopathological study. **A, B, C, D** at 10X (scale bar = 100 µm) and **E, F, G, H** at 40X (scale bar = 50 µm) resolution, respectively. G- glomerulus; PT- proximal convoluted tubule; DT- distal convoluted tubule; CT- collection tubule; BC- Bowman's capsule; # (hash)- glomerular degeneration with increased glomerular space; Hem- area of haemorrhage; → (black arrow)- inflammatory infiltration; Ap- apoptotic nuclei.

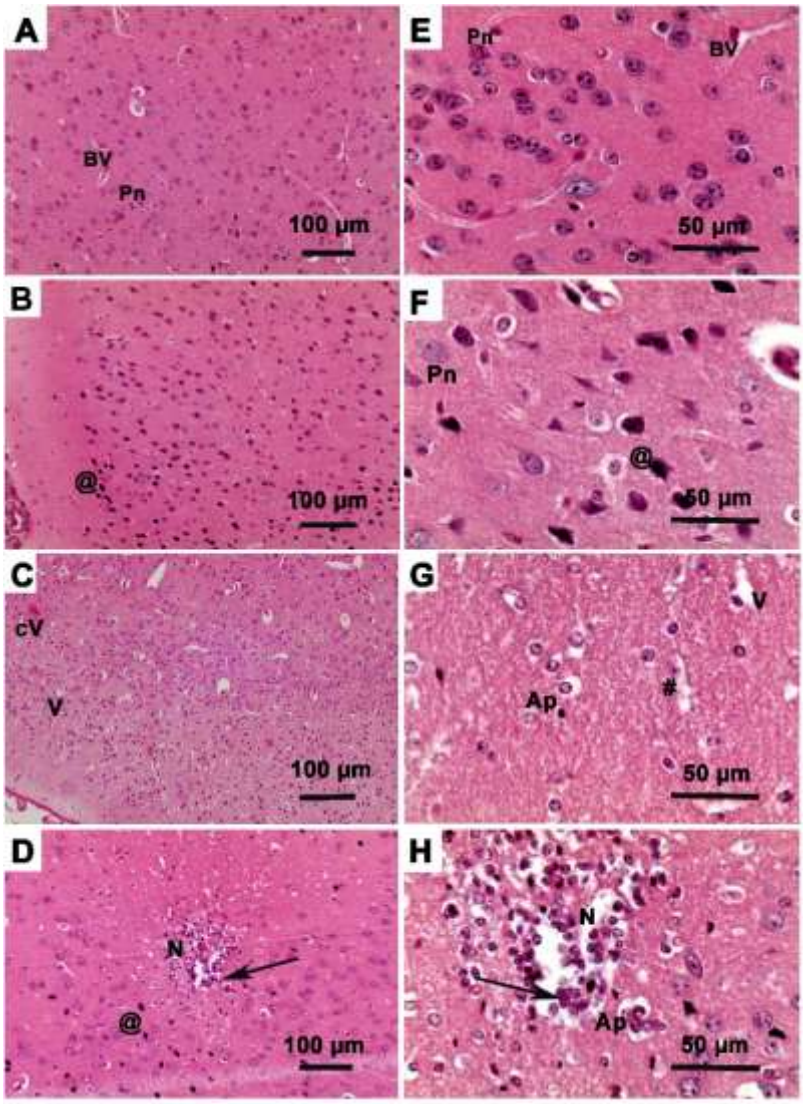

Figure 35 Effect of CuO-NPs intoxication in the brain of female mice, studied after hematoxylin and eosin staining (H & E). **A, B, C, D** at 10X (scale bar = 100 µm) and **E, F, G, H** at 40X (scale bar = 50 µm) resolution, respectively. Pn- Pyramidal neuronal cell; BV- blood vessel; → (black arrow)- inflammatory infiltration; @- darkly stained neuron; V- vacuolization; Ap- cellular apoptosis; N- area of necrosis; # (hash)- cellular degeneration; cV- congested vessel; Ft- fragmentation of tissue.

5.26 Expression of pro-apoptotic, anti-apoptotic and inflammatory markers in liver, kidney and brain tissue of CuO-NPs intoxicated mice

Expression of pro-apoptotic, anti-apoptotic and inflammatory markers were accessed to investigate their role in CuO-NPs intoxicated female mice. In the study, it was

found that expression of pro-apoptotic markers BAX and active caspace-3 had increased in liver, kidney and brain of the treatment groups, and more significantly in the high dosed groups (5 mg/kg bw and 10 mg/kg bw) (**Figure 36A, C and E** and **Figure 37A, C and E)**.

Inflammatory markers, COX-2 **(Figure 37B, D and F)**, IL-6 (**Figure 38A, C and E)**, iNOS **(Figure 38B, D and F)**, TNF-α (**Figure 39A, C and E)**and NF-κB (**Figure 39B, D and F)**were observed and found to have increasing trends in the treatment groups as compared to the normal control mice. This result was the evident that CuO-NPs intoxication triggered inflammation in liver, kidney and brain tissue of the mice.

CuO-NPs intoxication also led to changes in the expression pattern of P^{53}, a tumour suppressor protein and PPAR-ɣ. Increased in the expression of P^{53} **(Figure 40A, C, and E)** whereas decline in the expression of PPAR-ɣ **(Figure 40B, D, and F)** were observed in the liver, kidney and brain tissues of CuO-NPs intoxicated mice as compared to the normal control group. However, changes in the pattern of expression of all the analysed markers were more prominent in the high dosed groups signifying that with increasing doses the effects of CuO-NPs intoxication may get more severe.

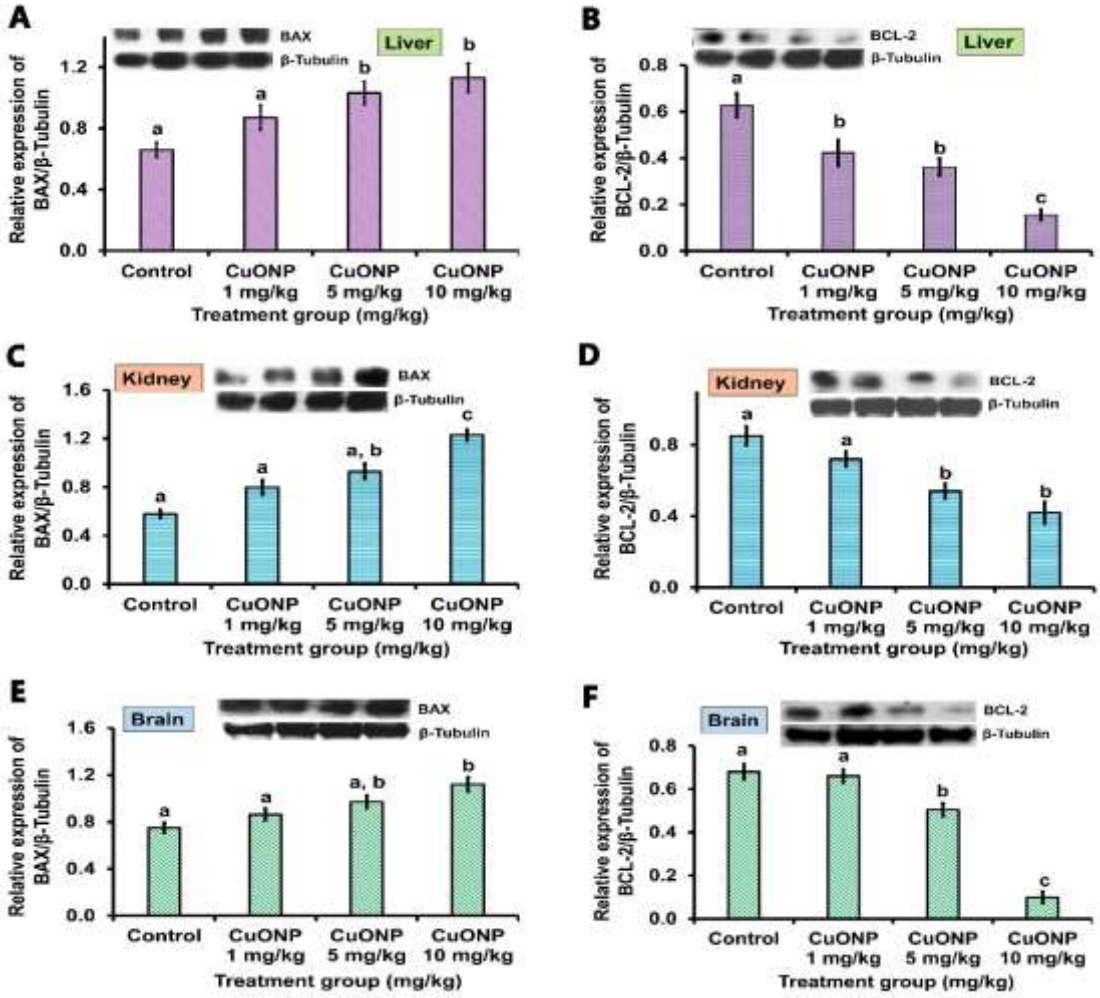

Figure 36 CuO-NPs intake triggers the expression of pro-apoptotic marker, BAX and decrease the expression of anti-apoptotic marker, BCL-2 in treatment mice as compared to the normal control group. The bar graph signifies densitometric analysis of BAX and BCL-2 in liver (**A and B**, respectively), kidney (**C and D**, respectively and brain tissues (**E and F**, respectively) (mean ± SEM, significant at $p < 0.05$).

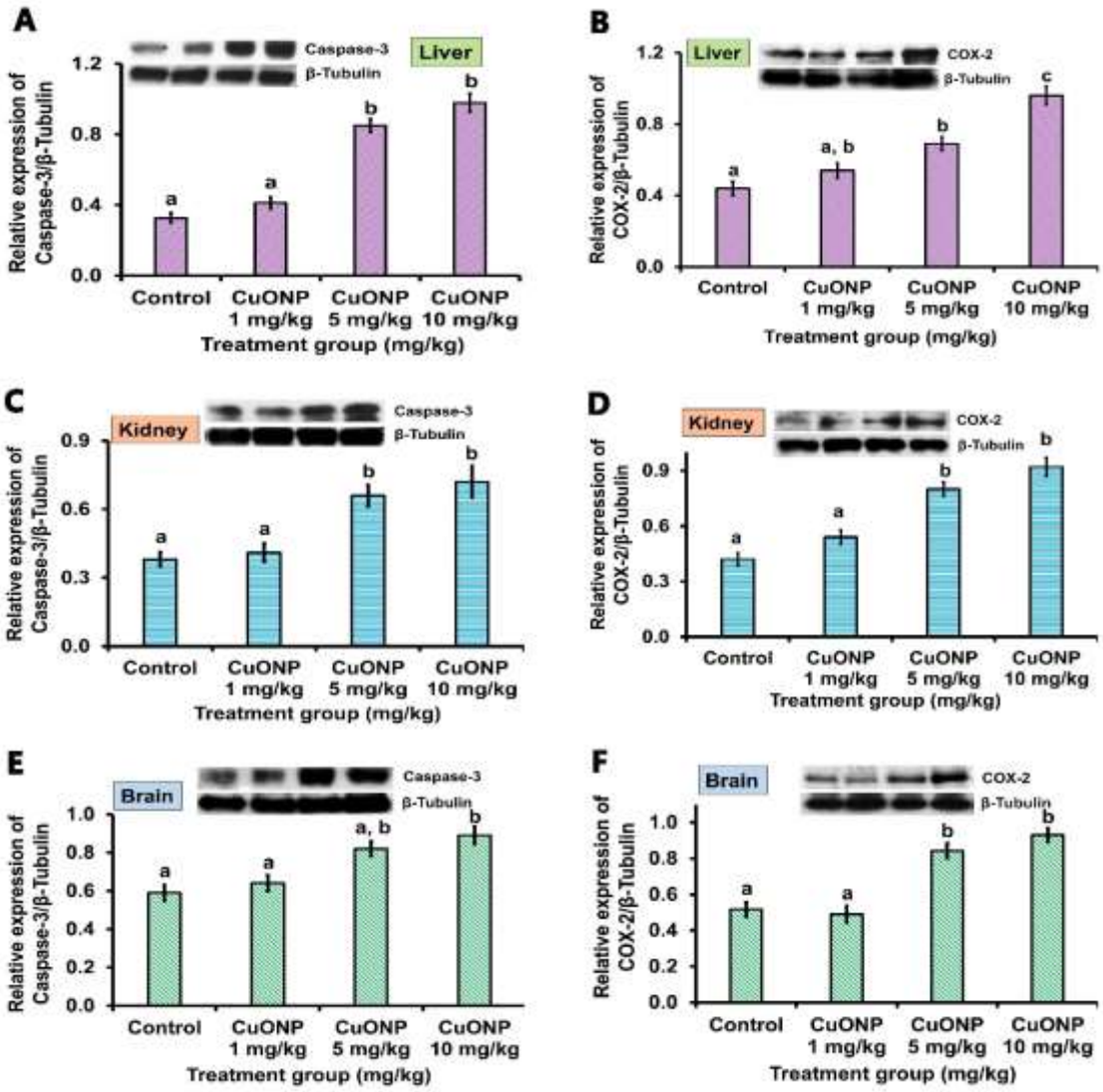

Figure 37 CuO-NPs triggers the expression of pro-apoptotic marker, active cascape-3 and inflammatory marker, COX-2 in treatment mice. The bar graph signifies densitometric analysis of active caspace-3 and COX-2 in liver (**A and B**, respectively), kidney (**C and D**, respectively and brain tissues (**E and F**, respectively). The values are represented as mean ± SEM, significant at $p < 0.05$, one-way ANOVA was performed to compare between different experimental groups.

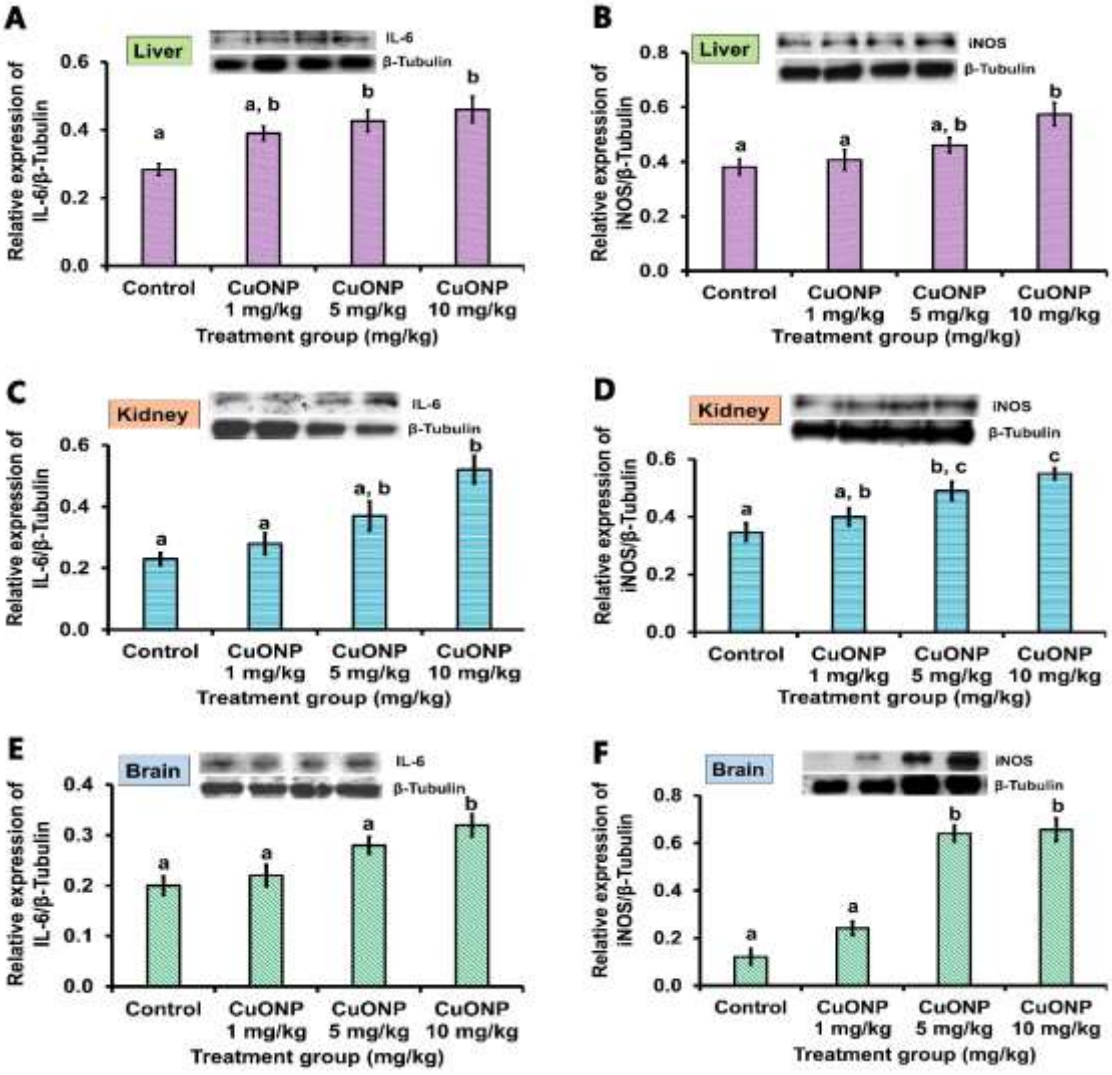

Figure 38 CuO-NPs triggers the expression of inflammatory marker, IL-6 and iNOS in treatment mice. The bar graph signifies densitometric analysis of IL-6 and iNOS in liver (**A and B**, respectively), kidney (**C and D**, respectively and brain tissues (**E and F**, respectively). The values are represented as mean ± SEM, significant at $p < 0.05$, one-way ANOVA was performed to compare between different experimental groups.

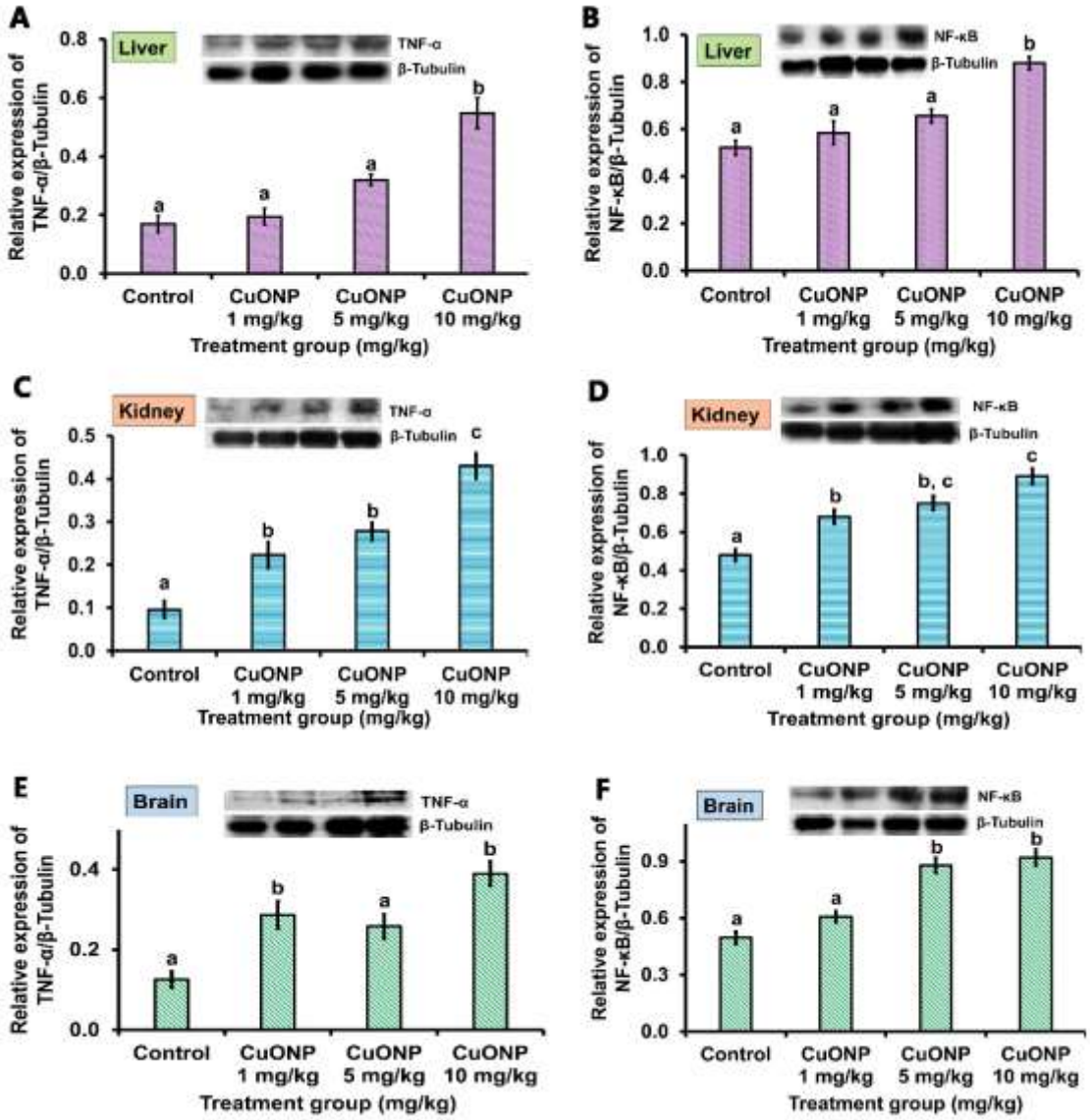

Figure 39 Regular consumption of CuO-NPs for 30 days stimulates the expression of inflammatory marker, TNF-α and NF-κB in treatment mice. The bar graph signifies densitometric analysis of TNF-α and NF-κB in liver (**A and B**, respectively) kidney (**C and D**, respectively and brain tissues (**E and F**, respectively). All the values are represented as mean ± SEM, significant at $p < 0.05$, one-way ANOVA was performed to compare between different experimental groups.

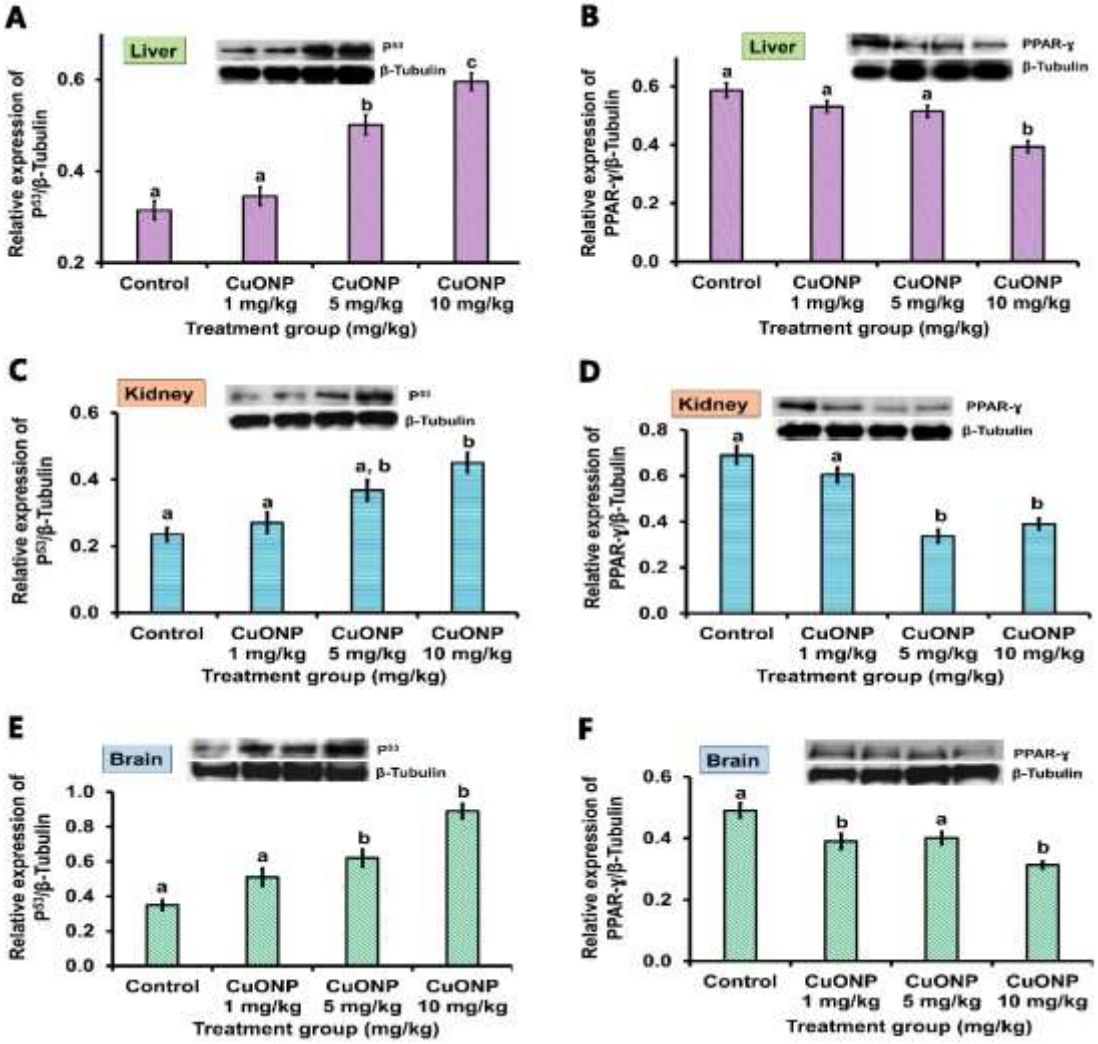

Figure 40 CuO-NPs triggers the expression of tumour suppressor, P^{53}, and PPAR-ɣ in treatment mice. The bar graph signifies densitometric analysis of P^{53} and PPAR-ɣ in liver (**A and B**, respectively), kidney (**C and D**, respectively and brain tissues (**E and F**, respectively). All the values are represented as mean ± SEM, significant at $p < 0.05$, one-way ANOVA was performed to compare between different experimental groups.

CHAPTER- 6

DISCUSSION

Heavy metals are dangerous because of many detrimental consequences. They have the potential to cause cancer and teratogenic consequences in addition to chronic degenerative alterations, especially in the kidneys, liver, and brain system **(Ibrahim et al., 2006; IARC, 1987)**. Cd is a very toxic heavy metal and is ranked as the seventh most toxic heavy metal in accordance with the rating provided by the Agency for Toxic Substances and Disease Registry (ATSDR; **Jaishankar et al., 2014; Young et al., 2019**). Reports have shown that, in many countries, the human Cd levels have been found to exceed the tolerance levels of several organs, and this has been linked to an increased risk of chronic diseases such cancer, diabetes, and osteoporosis **(Satarug, et al., 2017; Genchi et al., 2020)**. The Cd poisoning is mainly due to the production of free radicals and a fall in the potency of antioxidants **(Aghababa et al., 2017)**, the main target organs being liver, kidney and bone causing major health effect such as cancer, kidney damage, bronchiolitis, emphysema, fibrosis, skeletal damage (itai-itai disease) **(Nawrot et al., 2010; Alissa** and **Ferns, 2011)**. Numerous additional harmful health consequences, such as hypertension, type 2 diabetes mellitus, and cancer, were observed in studies of populations that were persistently exposed to low concentrations of Cd **(Matović et al., 2011; Matović et al., 2015)**.

Cu, that fulfils the minimal requirement of atomic weight under the range of heavy metals. It has been used for various applications since many years. It is also an essential element crucial for normal physiological functions, including drug metabolism, carbohydrate metabolism, and antioxidant defense systems **(Al-Musawi et al., 2022)**. However, it has health benefits for the body, when consumed in excess of what the body can metabolize, it builds up in the body and causes harmful effects such as immune system, liver, kidney, and gastrointestinal system dysfunction, neurological illnesses, and reproductive dysfunction **(Jomova et al., 2022; Hassan et al., 2024)**. CuO-NPs induced severe atrophy and colour change in the spleen, as well as morphological alterations, necrosis, and malfunction in the kidney, stomach, and liver. They also disrupted the epithelial lining of the gastrointestinal system **(Abudayyak et al., 2020)**. After multiple oral exposures to CuO NPs, significant organ toxicity was observed in the liver, kidney, and brain. Studies have shown that

CuO NPs induce pathomorphological changes in the liver, such as necrosis and degeneration, while in the kidney, proliferation of mesangial cells and tubule brush border loss were noted **(Stepankov et al., 2021)**. As a redox-active element, copper can alternate between the states Cu^{++} and Cu^{+}. When both of these forms are present inside cells and intracellular enzymes are active, several ROS are produced. These ROS then interact with proteins, lipids, and DNA resulting in both autophagy as well as apoptosis **(Perelshtein et al., 2015; Laha et al., 2014)**.

6.1 *In silico* LD_{50} and pathway prediction, and ADMET profiling

The negative value of logP signifies that the chemicals have more affinity toward aqueous phase (more hydrophilic) **(Mannhold et al., 2009)**. In the study of drug transport characteristics such intestinal absorption and blood-brain barrier (BBB) penetration, TPSA has been a frequently employed molecular descriptor **(Prasanna** and **Doerksen, 2009)**. In our study, both CdO and CuO reflected high affinity towards water; hence, these compounds are hydrophilic, which could readily mix with water and increase its permeability in the animal body. However, TPSA, nHA, and nHD were within the optimal range. The LD_{50} predicted for CdO and CuO was 67 and 413 mg/kg, respectively were very low which indicated high toxic potentiality of the chemicals. Therefore, research focusing on the *in vivo* and *in vitro* toxicity of need.

ProTox-II was used to predict various toxicity pathways and endpoints, including hepatotoxicity, neurotoxicity, nephrotoxicity, respiratory toxicity, cardiotoxicity, immunotoxicity, cytotoxicity, carcinogenicity, mutagenicity, and acute toxicity, BBB-barrier, ecotoxicity, clinical toxicity, nutritional toxicity, androgen receptor (AR), aromatase, estrogen Receptor Alpha (ER), estrogen Receptor Ligand Binding Domain (ER-LBD), Peroxisome Proliferator Activated Receptor gamma (PPAR-Gamma), Nuclear factor (erythroid-derived 2)-like 2/antioxidant responsive element (nrf2/ARE), heat shock factor response element (HSE), mitochondrial membrane potential (MMP), phosphoprotein (Tumour Suppressor) p53, thyroid hormone receptor alpha (THRα), thyroid hormone receptor beta (THRβ), acetylcholinesterase (AChE), NADH-quinone oxidoreductase (NADHOX), voltage gated sodium channel

(VGSC), cytochrome CYP1A2, cytochrome CYP2C19, cytochrome CYP2C9, cytochrome CYP2D6, cytochrome CYP3A4, cytochrome CYP2E1. These parameters help to predict potentiality of a drug to induce toxicity at various levels. The data used to build the predictive models comes from both *in vivo* cases (such as carcinogenicity and hepatotoxicity) and *in vitro* experiments (such as Tox21, AMES bacterial mutation, hepG2 cytotoxicity, and immunotoxicity assays). The predicted results appear as active (positive) or inactive (negative) with their confidence score for each pathway and endpoint predictions **(Banerjee et al., 2018)**. The Test chemicals, CdO and CuO are inactive for all other pathways except for neurotoxicity, BBB-barrier permeability, ecotoxicity and Cytochrome P450 (CYP2C9) pathways, according to the prediction. The present results indicated that these may be the possible target pathway for toxicity induced by the test chemicals.

LogS represents the solubility of a compound in water at 25ºC. The value obtained for CdO (0.432 log mol/L) and CuO (0.58 log mol/L) indicated high water-soluble property of the chemicals.

Caco-2 or human colorectal adenocarcinoma cell lines-2 permeability value represents absorption efficacy of orally administered drug and the high permeability is indicated by Papp > 8 x 10^{-6} cm/s. In the present study, both CdO and CuO showed Caco2 permeability value of 1.49 x 10^{-6}, which indicated less permeability through the Caco-2. Conversely, both the chemicals have the potentiality of high absorption by the intestinal (human) cells as the result indicated 100% absorption value. Human skin permeability (log Kp) of CdO and CuO are more negative (> -2.50), therefore it is considered to have high skin permeability. The results showed potentiality of P-glycoprotein (Pgp) to remove CdO and CuO out of the body hence, could act as a biological barrier for any toxin or xenobiotics entering the body.

Blood brain barrier (BBB) permeability (log BB) of CdO (-0.070) and CuO (-0.055) were found to be within the optimum range (optimum -1.0 to 0.30), however, the values were less negative which indicated their potentiality to cross the BBB and induce neuro-toxicity. It is interpreted that these chemicals may cross the BBB and induce brain toxicity important parameter that helps to predict the probability of a

drug to cross the BBB and reach the brain. Prediction of this parameter helps to reduce the side effect of any drug or chemical hence, helps in neuro-toxicity prediction. The value log BB > 0.3 and log BB < -1 are considered readily and poorly permeable, respectively **(Xiong et al., 2021)**. CNS (central nervous system) permeability (log PS) value for both CdO and CuO (-2.40) were predicted to be higher than > -2, hence, it is considered to penetrate CNS. Result showed that CdO and CuO are not a substrates or inhibitors of Cytochrome P450. Although, these chemicals will not inhibit the Cyt P450 functions but they will also not be metabolised by the same. Therefore, the results showed probability of health risk associated with exposure to these chemicals **(Pires et al., 2015)**.

Excretion rate of CdO (0.86 log mL/min/kg) and CuO (0.75 log mL/min/kg) are low as per the predictions of total clearance, which is a combination of hepatic metabolism and excretion via kidneys. The low clearance of a chemical may lead to bioaccumulation, which may cause damage to the major organs (kidney, liver, brain, heart etc.).

CdO and CuO, both the chemicals showed negative for AMES test. Though the Maximum recommended tolerable dose (MRTD) calculated for the given chemicals were below the tolerance level but the difference from the tolerable dose was very low. Therefore, the chemicals may cause harm to human if exposed regularly. However, both the chemicals were found to be negative for Human ether a-a-go gene (hERG I and II) inhibitor. Both the chemicals are highly toxic to rat as the predicted LD_{50} for CdO (2.22 mol/kg) and CuO (2.28 mol/kg) were at very low dose. However, minnow toxicity (LC_{50}) were predicted to be negative as the LC_{50} values were higher than 0.5 mM.

6.2 Acute oral toxicity of CdO-NPs

Acute oral toxicity testing plays a crucial role in assessing the potential harm of substances when orally administered. Various methods exist for determining acute toxicity, such as the LD_{50} test, which is commonly used **(Li et al., 2024)**. Analysis of body weight, food and water consumption and rectal temperature plays a crucial role in monitoring toxicity of any substance. Moreover, body weight, feeding and

drinking are the interlinked parameters **(Bachmanov et al., 2002)**. One of the markers of the harmful effects of the test material during toxicological testing may be changes in body weight. Data on the amount of food and water consumed by experimental animals serve as reliable markers of their rate of growth **(Stevens, 1982)**. In our experiment, clinical signs and changes in behaviour was observed after treatment of higher doses (50 and 75 mg/kg bw) indicating health complicacies in animals. Further, there was a decrease in body weight, food and water consumption and increase in rectal temperature of male and female animals after exposure to the CdO-NPs, which signifies that acute exposure to the chemical has potential effects on metabolism, growth and thermoregulation. Additionally, analysing food and water consumption in acute toxicity tests provides valuable insights into the test substance's effects on growth and health of experimental animals, aiding in toxicity assessment **(Todić et al., 2003)**. Cd exposure was associated with reduced body weight in the study, indicating a potential link between toxic metal exposure and weight changes. Substantial decrease in the food and water consumption observed more significantly at the higher doses shed light on the functioning of specific organs such as, liver and kidneys after Cd exposure **(Mitra et al., 2021)**. Decline food and water intake also signifies endogenous intoxication after acute CdO-NPs exposure. Measurement of relative organ weights provide a valuable indication of toxicity. In the present study, decrease in the relative organ weight of specific organs such as, liver, kidney, stomach, colon, lungs, testis and ovary in male and female mice may be due to the toxicity induced by CdO-NPs.

Hematological parameters such as red blood cells (RBCs) count, white blood cells (WBCs) count and hemoglobin concentration are the important clinical indicators of health and disease conditions **(Kelada et al., 2012)**. Hematological analysis in our experiment showed decreased concentration of RBC and hemoglobin which puts insight into the CdO-NPs induced oxidative stress caused in different organs led to anaemia and lose of RBC membrane function as well as degradation of RBC indices such as MCV, MCH and MCHC. Additionally, increase in the concentration of WBCs in blood indicates leucocytes hypersensitivity **(Adeyomoye** and **Adewumi, 2019)** and inflammatory response to the heavy metals.

Biochemical assays of different enzymes and metabolites are the clinical markers for the diagnosis of liver and kidney diseases **(Malomo, 2000; Yakubu et al., 2006)**. Generally, detection of ALP, AST, ALT, bilirubin, albumin, globulin, and other assays such as urea, uric acid, creatinine, and blood urea nitrogen are mainly performed to trace the functioning of liver and kidney, respectively. We found that exposure to acute CdO-NPs at higher doses in male and female mice led to decline in the concentration of protein, and elevated levels of albumin, globulin, ALP, AST, ALT, bilirubin, urea, creatinine and uric acid at high doses revealed potentiality of CdO-NPs to induce liver and kidney injury mediated by toxicity and impairment of their normal functioning.

Assessing lipid profiles is crucial in toxicity studies as they provide a molecular snapshot of cellular status, aiding in early detection of adverse drug effects, such as hepatotoxicity, renal toxicity potential etc. **(Goracci et al., 2019)**. Moreover, lipid profiling provides valuable information on organ function, nutritional status, metabolic effects, and dose response relation **(Bedia, 2022)**. Degradation of lipid profiles with increased levels of total cholesterol, triglycerides, LDL-cholesterol and decrease levels of HDL-cholesterol were the evident of CdO-NPs induced organ toxicity reported in our present study. However, CdO-NPs don't have any significant effects on the glucose metabolism as no changes in blood glucose levels were detected in both male and female after CdO-NPs treatment as per our study.

Analyses on the blood ion concentration revealed decline levels of calcium and sodium. Conversely, increase in the concentration of chloride and potassium were detected in our study. Changes in the serum ion concentrations help to provide insight into the effects of toxic chemicals on electrolyte balance, metabolic functions, nutritional status, bone health and organ functions **(Kesari** and **Noel, 2022)**. Our study provides valuable evidence to the CdO-NPs induced toxicity that potentially modulates the electrolyte balance, organ function and metabolism.

Production of ROS surpasses the capacity of cells to protect themselves, ultimately leading to cytotoxicity. During an oxidative stress, compounds such as membrane lipids are damaged by the development of superoxide anion (O_2), hydroxyl radicals

(OH), and hydrogen peroxide (H_2O_2). Lipid peroxidation is a chain process that is mediated by free radicals and is created when lipid radicals combine with oxygen to produce peroxy-radicals **(Galhardi et al., 2004)**. GSH, GST, SOD, and CAT are crucial antioxidant enzymes that play a vital role in combating oxidative stress **(Wu et al., 2019)**. Assessment of MDA level in major organs after acute exposure to CdO-NPs showed significant increase, indicating potential oxidative stress induced by Cd toxicity. Additionally, GSH, GST, SOD and CAT levels have declined after significantly in liver, kidney, brain, testis, ovary and colon tissue after CdO-NPs treatment revealing organ-specific toxicity after acute Cd exposure.

Oxidative stress plays a crucial role in various clinical pathologies, impacting histopathology through gene regulation, antioxidant response, and potential therapeutic interventions with natural antioxidants **(Saha et al., 2022)** and leads to histopathological changes in organs like the nervous system, cardiovascular system, lung, liver, and kidney, causing cellular and tissue damage **(Palipoch** and **Koomhin, 2015)**. In our study, we have found that liver, kidney, brain, testis and ovary tissue underwent significant alterations in tissue architecture after Cd exposure. However, changes in tissue architectures of heart, lung and spleen tissues were also noticed indicating organ specific cellular toxicity induced by Cd intoxication. The histopathological changes observed may be due to the involvement of oxidative stress that underscores the importance of understanding and managing redox imbalance in Cd mediated organ toxicity.

6.3 Organ toxicity induced by CdO-NPs and CuO-NPs

In the present study, CdO-NPs and CuO-NPs of size < 50 nm were used to evaluated the organ toxicity in mice model. Earlier studies have shown that exposure to toxic heavy metals such as Cd can lead to decreased weight gain in rats, accompanied by internal organ changes and hematological alterations **(Lopotych et al., 2020; Ungureanu** and **Mustatea, 2022)**. Research on *Tilapia guineensis* and *Tympanotonus fuscatus* showed that exposure to Cu resulted in reduced weight gains or weight loss in the test species **(Oyewo** and **Don-Pedro, 2006)**. Research indicates that exposure to CuO-NPs can lead to changes in body weight, with significant

decreases observed in treated groups compared to controls **(Al-Musawi et al., 2022; Stepankov et al., 2021)**. In the current study, it was found that the toxic effects of CdO-NPs and CuO-NPs has led to the decrease in body weight, food and water consumption in mice as recorded after acute (CdO-NPs) and short-term (both CdO-NPs and CuO-NPs) exposure as compared to the normal control mice, which could be due to endogenous intoxication **(Lopotych et al., 2020)**. Subacute exposure to CdO nanoparticles led to decreased body weight gain in rats **(Papp et al., 2012)** indicating toxicity **(Klinova et al., 2021)**. In mice, long-term exposure to Cu as a dietary supplement led to increased body weight initially, but later caused hepatotoxic effects, including structural changes in the liver such as vacuolar degeneration, necrosis, karyorrhexis, and endolysis potentially due to lipid peroxidation and free radicals **(Wang et al., 2014)**. An alternative explanation for the alterations and weight loss is the build-up of metals in the organs **(Kong et al., 2014; Al-Bairuty et al., 2016; Song et al., 2017)**. Reduction in the relative organ weight of liver and kidney indicates Cd and Cu induced organ-specific toxicity in our present study.

Studies have shown that Cu and Cd intoxication can induce alterations in hematological parameters, such as increased WBCs and decreased RBCs, hemoglobin, and platelet count **(Yaqub et al., 2018; Nikolić et al., 2015; Gluhcheva et al., 2011)**. WBC, RBC and hemoglobin concentrations were decreased significantly while increase in MCH was observed in copper mine workers than in the control group **(Lotfi** and **Rezazadeh, 2018)**. Present results are also in agreement with previous reports indicating decrease in the levels of RBCs, hemoglobin, PCV and increase in the levels of WBCs after treatment with both CuO-NPs and CdO-NPs. As a result of oxidative damage caused by Cd on different organs, RBCs lose the function of its membrane, resulting in anaemia from a decrease in RBCs, hemoglobin and haematocrit values, and iron levels in the blood **(Kostić et al., 1993)**. Leucocyte hypersensitivity to heavy metals may be indicated by this rise, and the alterations may be the consequence of immune responses that generate antibodies to counteract the stress that heavy metals impose **(Adeyomoye** and **Adewumi, 2019)**.

Studies have shown that Cd accumulation in organs like the liver and kidneys is influenced by the method of administration and the presence of chelating agents **(Engström, 1981)**. Research on rats exposed to Cd through drinking water or intraperitoneal injections demonstrated significant differences in Cd accumulation in various organs, with higher levels found in the liver and kidneys **(Nwokocha et al., 2011; Winiarska-Mieczan** and **Kwiecień, 2016)**. Furthermore, the distribution of Cd in organs like the liver, kidneys, brain, lungs, heart, and spleen was influenced by the source of exposure, whether through feed or water **(Winiarska-Mieczan** and **Kwiecień, 2016)**. Additionally, Cd accumulation in tissues was found to be sex-dependent, with variations observed between male and female rats as proposed by **Nwokocha et al. (2011),** showing higher Cd content in the kidney, stomach, and blood compared of female as compared to males**.** The study suggests a lower accumulation of Cu in other tissues compared to the kidneys, liver, brain, and heart indicates a selective ability of these organs to accumulate Cu from the administered nanocomposite **(Titov et al., 2021)**. Metal accumulation in organs after oral treatment varies depending on the route and duration of exposure. A dose-dependent increase in the concentration of Cd and Cu metals were estimated in liver, kidney and brain tissues of female mice after 30 days of exposure. However, highest concentration being observed in liver, indicating rapid bioaccumulation as compared to kidney and brain. Further, Cd had shown higher bioaccumulation rate in fishes which may lead to Cd build-up in human through food chain **(FAO/WHO, 2015; Zaghloul et al., 2024)**. Polyuria, severe tubular dysfunction, and decreased glomerular filtration rate are the results of cadmium build-up in the kidney. Toxicants, xenobiotics, and endogenous wastes accumulate as a result of a decrease in glomerular filtration rate **(Orr** and **Bridges, 2017)**. These findings highlight the complexity of heavy metal (both Cd and Cu) accumulation in organs following oral treatment, emphasizing the importance of considering factors such as route of exposure, duration, and sex differences. The accumulation of CdO-NPs was higher in all the three targeted organs revealing its higher bioaccumulation and low metabolism in animal body.

One of the main mechanisms of Cd-induced hepatic toxicity is thought to be oxidative stress, which is caused by the body's build-up of Cd and negatively impacts liver function by producing ROS **(Sanjeev et al., 2019; Oyinloye et al., 2016; Liu et al., 2017; Matović et al., 2015)**. Elevations in serum AST, ALT, and ALP activity are typically indicative of hepatic damage. A high risk of liver failure and liver dysfunction may be indicated by hyperbilirubinemia. The conditions outlined above could be detected to accurately diagnose liver damage **(Jagadeesan, 2006; Ahmadi, 2020; Han et al., 2020)**. It was found in the present study that CdO-NPs and CuO-NPs can potentially lead to the hepatotoxicity that was evident from the degradation of proteins, albumin, and globulin and the elevation of bilirubin levels in the blood serum. Additionally, increased serum levels of ALP, ALT and AST in the current study also attributed to the hepatocellular injury and inflammation caused by severe Cd and Cu toxicity **(Hashish** and **Elgaml, 2016)**. However, among the two test chemicals the effects on the liver function biomarkers were seen to have higher in case of CdO-NPs.

The kidney is the target organ of chronic Cd poisoning, with a half-life of around thirty years for cadmium. Cd-induced nephrotoxicity in mice revealed altered protein expression related to kidney metabolism, oxidative damage, and cell migration **(Sun et al., 2021; Yan** and **Allen, 2021)**. It was reported that excessive Cu could induce animal hepatotoxicity, nephrotoxicity, cardiomyopathy, hepatocyte apoptosis, and body condition decline **(Zhou et al., 2021)**. The present study satisfies the past finding showing elevation in the concentration of serum urea, creatinine, uric acid, and BUN indicating nephrotoxicity induced by CdO-NPs, however, in case of CuO-NPs, significant elevation was recorded with intoxication at higher dose which shows tolerance in the lower doses. Rise in the serum level of uric acid (hyperuricemia) is linked with the systemic oxidative stress, inflammation, activation of renin-angiotensin system and endothelial dysfunction **(Kanbay et al., 2014; Mazzali et al., 2002; Inaba et al., 2013; Hahn et al., 2017)**. Exposure to toxic chemicals lead to the abrupt loss of kidney function due to the accumulates toxic end products of nitrogen metabolism and creatinine in the blood, reduces urine production, or both is the hallmark of kidney injury **(Gyurászová et al., 2020)**. In the present study, in

addition to the higher dose (8 mg/kg bw) CdO-NPs was observed to have effect on the kidney biomarkers at low or medium doses itself however, effect was seen mostly at high dose in case of CuO-NPs.

Heavy metal toxicity has been linked to alterations in lipid profiles in various biological systems. Heavy metal toxicity alters lipid profiles by decreasing HDL-cholesterol and increasing VLDL-cholesterol levels in rats, indicating disruptions in lipid metabolism **(Bekus et al., 2016)**. Cd exposure has been linked to alterations in lipid profiles across various studies. Research indicates that chronic exposure to Cd can lead to liver steatosis and non-alcoholic fatty liver disease (NAFLD) by affecting lipid metabolism **(Ren et al., 2021)**. Studies on rats exposed to cadmium-contaminated food chains show significant changes in plasma lipid profiles, including increased total cholesterol, triglycerides, LDL-cholesterol, and VLDL-cholesterol, along with decreased HDL-cholesterol levels **(Ezedom, 2018; Ovie** and **Asagba, 2019)**. Furthermore, exposure to cadmium has been found to disrupt metabolites, increase serum fatty acids and triglycerides, and elevate serum total cholesterol, triglycerides, and LDL cholesterol levels, indicating a direct impact on lipid metabolism **(Zhu et al., 2024)**. Our study shows increase in the concentration of serum total cholesterol, triglycerides, LDL-cholesterol and decrease in HDL-cholesterol after CdO-NPs treatment indicates deterioration of the lipid profile in mice which may be due to disruption of lipid metabolism.

Exposure to Cu, whether in the form of toxic levels or nanoparticles, has been shown to impact lipid profiles in various ways. Studies have demonstrated that toxic Cu levels can induce lipid peroxidation, affecting RBC membrane deformability and fluidity by altering lipid composition, saturation, and bond configuration **(Adele et al., 2023)**. Additionally, exposure to CuO-NPs has been linked to changes in lipid metabolism, with upregulation of triacylglycerols, phosphatidylcholines, and ceramides, as well as activation of oxidative stress and autophagy pathways **(Sori et al., 2019)**. Furthermore, excessive Cu intake has been associated with hepatic lipo-toxicity disease, where copper promotes the recruitment of Nrf2 to lipogenic gene promoters, ultimately affecting lipid metabolism and potentially leading to obesity and non-alcoholic fatty liver disease **(Zhong et al., 2023)**. Although, our study

reported no significant changes in serum triglycerides concentration but there were rise in the serum levels of cholesterol, LDL-cholesterol and decline in HDL-cholesterol were noticed after CuO-NPs treatment. However, this finding highlights the intricate relationship between Cu exposure and lipid profiles, emphasizing the need for further research to understand the mechanisms underlying these effects.

Data recorded in the present study are in consistent with earlier findings confirming that oxidative stress is a possible mechanism implicated in CdO-NPs and CuO-NPs hepato-, nephron- and neurotoxicity. Increase in the cellular levels of ROS is a result of hinderance mitochondrial electron transport chain (ETC) by Cd uptake by the cells **(Rombel-Bryzek et al., 2018)**. Factors like viral infections, environmental toxins, alcohol, and diet can induce oxidative stress, causing mitochondrial dysfunction, increased ROS expression, and ATP depletion, ultimately leading to liver steatosis, inflammation, fibrosis, cirrhosis, and even liver cancers. Understanding the sources and targets of ROS in liver diseases is crucial, as oxidative stress is intricately linked to cell death mechanisms in hepatocytes, highlighting its pivotal role in liver pathology **(Conde de la Rosa et al., 2022)**. Oxidative stress-induced toxicity in the brain is a common factor in brain disorders **(Pandareesh et al., 2023)**, developmental neurotoxicity, impacting neurodevelopmental and neurobehavioral pathways by disrupting antioxidant systems and mitochondrial function **(Nishimura et al., 2021; Rama** and **García, 2016)**. Studies have demonstrated that exposure to Cd NPs results in a reduction of antioxidant enzyme activity, an increase in ROS, and alterations in oxidative stress markers such as glutathione levels and lipid peroxidation. Cadmium sulfide nanoparticles induce oxidative stress in human lung adenocarcinoma cells, evidenced by ROS generation, reduced GSH levels, and increased lipid peroxidation, leading to cytotoxicity and inflammation **(Alomar, 2015)**. The present study has recorded the elevation in the levels of MDA and degradation of enzymatic and non-enzymatic antioxidants after CdO-NPs administration is aligned with the previous findings. A dose-dependent increase in the MDA levels and decline in the concentration of GSH, GST, SOD and CAT were reported in liver, kidney and brain tissue of CdO-NPs intoxicated mice signifying possible Cd induced toxicity in three major organs. GSH is also thought to be the

primary line of defense towards Cd toxicity **(Singhal et al., 1987)** since it is involved in the chelation of transition metals, which reduces their toxic potential. Furthermore, GSH depletion amplified Cd-induced hepatotoxicity **(Klaassen et al., 1985; Chan** and **Cherian, 1992; Branca et al., 2020)**, nephrotoxicity, and neurotoxicity in rats exposed to Cd.

CuO-NPs induce oxidative stress in cells, leading to apoptotic or autophagic cell death due to surface reactivity generating free radicals and oxidizing macromolecules **(Moschini et al., 2023)**. The present study revealed a significant rise in the concentration of MDA was documented after high dose (10 mg/kg bw) of CuO-NPs treatment and also a decline in the concentration antioxidants such as, GSH, GST, SOD and CAT revealed that short-term consumption of CuO-NPs may cause oxidative stress, inflammation and cellular toxicity in major organs that may remain insensitive for the low doses at the early stage but may have major health consequences in the later stages **(Sajjad et al., 2023)**. SOD and CAT, enzymatic antioxidants, are components of the antioxidant defense system that scavenges free radicals and help to reduce the harmful effects of ROS by converting them to oxygen, which is then transformed to water. The build-up of superoxide and/or hydroxyl radicals in the liver can be determined by measuring the decreased activity of CAT and SOD **(Liu et al., 2020)**. Further, decrease in the concentration of SOD and CAT indicated compromised antioxidant defense mechanism after Cu treatment **(Sajjad et al., 2023)** that aligned with our present study. Thus, imbalance caused between ROS and antioxidants production by CdO-NPs and CuO-NPs treatment contributed to organ toxicity.

The present study hypothesized CdO-NPs and CuO-NPs induces organ toxicity mediated by oxidative stress via histopathological alteration at very low doses. To test this hypothesis, beside the analyses of liver and kidney function biomarkers, lipid and oxidative stress biomarkers, histology of targeted organs i.e., liver, kidney and brain were also performed. Most interestingly, our results of histopathological studies have supported the inferences made on aforementioned analyses. The treatment of Cd and Cu led to marked alterations in the liver tissue architecture with dilation and congestions of vessels, dilation sinusoids, apoptotic nuclei, degeneration

of hepatic cells, vacuolization, and necrosis along with the presence of infiltration of cells signifies occurrence of inflammatory response **(Ibtissem et al., 2017)**. Exposure to Cd leads to various histological changes such as hepatocyte hypertrophy, cytoplasmic vacuolization, pyknotic changes, bile canaliculi dilation, edema, haemorrhage, hypertrophy, hyperplasia, congestion of central vein, and nuclear alterations **(Chandra, 2024)**, disrupted hepatic plates, fibrosis, cellular infiltration, necrotic hepatocytes in the liver of male Swiss albino mice **(Mohapatra et al., 2013)**. Cd exposure induced liver histopathological changes, notably lipid peroxidation-related damage **(Hendrawan et al., 2018)** and DNA methylation in the metabolic pathway **(Ren et al., 2021)**. The studies reported findings such as hepatocyte membrane dissolution, vacuolar degeneration, inflammatory cell infiltration, reduction in hepatocyte size, vacuolization, hypertrophy, and changes in hepatic enzyme activities. Additionally, Cu exposure led to oxidative stress, decreased antioxidant enzyme activities, and increased levels of pro-inflammatory genes in the liver tissues of the exposed organisms. The liver was identified as a crucial target organ for Cu toxicity, showcasing the detrimental effects of Cu exposure on liver histopathology and function in various species **(Liu et al., 2021; Doudi** and **Setorki, 2014; Maharajan et al., 2015)**.

Kidney tissues with dilated vessel, glomerular degeneration with increased glomerular space, vascular congestion, vacuolization, haemorrhage, tubular degeneration, tubule with widened space, fragmentation of tissue, inflammatory infiltration, presence of apoptotic nuclei and cellular of necrosis were noticed in the Cd and Cu treatment animals in our study. Histopathological analysis of the kidney following Cd exposure reveals significant structural disruptions in renal tubules and glomeruli, indicating kidney injury **(Wan et al., 2022)**. Cd accumulation in renal tissues leads to cellular destruction, including collapsed tubular lamina and hypercellularity of glomeruli, highlighting the detrimental effects of Cd on renal morphology **(Al-Gebaly, 2017)**. Additionally, Cd exposure induces oxidative stress and necroptosis, contributing to kidney toxicity and damage **(Tang et al., 2023)**. The combination of Cd with other toxicants exacerbates these effects, leading to acute kidney injury through increased urea nitrogen levels and altered inflammatory

cytokine expression **(Tang et al., 2023)**. Furthermore, Cd exposure triggers the upregulation of genes related to chemical carcinogenesis pathways in the kidney, emphasizing the potential for Cd-induced renal carcinogenesis **(Wan et al., 2022)**. Long-term exposure to Cu in rat kidneys leads to autophagy and apoptosis due to oxidative stress, as indicated by histopathological changes as reported by **Wan et al. (2020)**. Cu treatment in mosaic mice led to severe kidney damage, including karyomegaly, necrosis, lesions, atrophy, sclerosis, and proliferation of epithelial cells, forming carcinoma patterns **(Lenartowicz et al., 2010)**, vacuolated epithelium, tubular degeneration, and reduced haemopoietic tissue volume, potentially impairing kidney function in fishes **(KZ** and **AM, 1998)** and severe necrosis, atrophy, Bowman's capsule damage, and renal architecture disorganization, with increased caspase-3 immunoreactivity in high-dose groups (5, 10 and 25 mg/kg bw/day for a period of 9 days) in male Wistar rats **(Ghonimi et al., 2022)**.

Cd exposure induced histopathological alterations in the cerebral cortex of juvenile mice, including blood vessel changes, leukocyte infiltration, and cellular degeneration **(Yang et al., 2015)**, severe degenerative changes in the cerebral cortex, including cell damage, disrupted myelination, and neuroglial cell accumulation **(Afifi** and **Embaby, 2016)** indicating Cd neurotoxicity effects. In adult male albino rats exposed to copper chloride, histopathological brain changes included increased astrocyte cellularity, neuronal degeneration, and apoptotic bodies, along with elevated serum MDA and decreased CAT levels **(Mostafa, Alaa-Eldin** and **Abouhashem, 2015)** brain edema, and spongiosis with vacuolization in the white matter, altering copper and zinc homeostasis in the brain and other tissues **(Zatta et al., 2005)**. Furthermore, exposure of *Cyprinus carpio* to copper sulfate resulted in brain and spinal cord lesions, including vasogenic edema, inflammatory cell infiltration, and neuronal atrophy, highlighting the neurotoxic effects of Cu in aquatic organisms **(Saied et al., 2022)**. These studies collectively highlight the diverse histopathological effects of Cu and Cd treatment on the brain, ranging from oxidative stress-induced changes and alterations in enzyme activity. In our study, we have found that exposure to Cd and Cu NPs led to production of inflammatory cells, darkly stained neuron, intracytoplasmic vacuolization, cellular vacuolization, cellular

apoptosis, tissue necrosis, fragmentation of tissue, cellular degeneration and congestion of blood vessels which are in agreement with the previous report indicating Cu and Cd mediated neurotoxicity.

Cd induced upregulation of apoptotic markers, BAX and caspase-3 and downregulation of anti-apoptotic marker, BCL-2 in liver, kidney tissue and hepatoma cell line **(Lawal et al., 2018)** suggesting a shift towards promoting cell death was reported in previous studies **(Souza-Arroyo et al., 2022; Fan et al., 2018)**. Intramuscular introduction of Cu NPs resulted in an increase in caspase-3 expression in micro-gliocytes, liver cells, proximal kidney tubules, and spleen cells at different time points and doses **(Sizova et al., 2011)**, and also induces apoptosis in the liver via upregulation of BAX, caspase-3, and downregulation of BCL-2, as implicated by **Liu et al. (2020)**. The present study is in support of the previous studies as administration of CdO-NPs led to the upregulation of the expression of BAX and caspase-3 and downregulation of BCL-2. Cd induces apoptotic cell death by down-regulating BCL-2, activating caspase-3 and BAX, and causing mitochondrial membrane potential loss, implicating similar effects in kidney and brain toxicity **(Lee et al., 2022)**. Similarly, Cu toxicity affects apoptotic pathways, increasing caspase-3 and BAX, and by downregulating BCL-2 levels in the brain, liver, and kidney of mice treated with CuO-NPs.

After Cd treatment, various inflammatory markers are upregulated, indicating pro-inflammatory responses. Studies on inflammatory mediators and markers suggest that Cd, especially in micromolar concentrations, upregulates markers of inflammation like NF-κB, IL-6, TNF-α (**Afolabi et al., 2012)**, IL-1β, and MIP-2 **(Ghosh** and **Indra, 2018)**, iNOS, COX-2, PGE2, and CRP **(Olszowski et al., 2012)** indicating pro-inflammatory properties. Further, upregulation of iNOS, COX-2, and c-Myc, along with downregulation of IL-10 and HO-1 were induced by Cd exposure indicating activation of inflammatory response in cardiac tissue (**Ghosh** and **Indra, 2018)**. TNF-α levels in the liver tissue of rats exposed to Cd increased significantly that plays a crucial role in the inflammatory response **(Kayama et al., 1995)**. For our study, similar interpretation could be made from previous studies as CdO-NPs exposure for 30 days at different doses led to the upregulation of pro-inflammatory

factors IL-1, IL-6, iNOS, NF-κB, COX-2, PGE2, and TNF-α in liver, kidney and brain tissues by increasing ROS production, while inhibiting the anti-inflammatory cytokine, IL-10.

After Cu treatment, various inflammatory markers were found to be expressed in different organs. In the liver and brain, copper overload led to the activation of the NLRP3 inflammasome, resulting in elevated levels of IL-1β, IL-18, IL-6, and TNF-α **(Dong et al., 2021)**. Cu treatment induces inflammatory markers like NOS-II, TNF-α, and COX-2 in liver and lung tissues via NF-κB activation mediated by oxidative stress **(Persichini et al., 2006)**, brain inflammatory markers such as TNF- α, iNOS, and COX-2 were increased in the brain of cholesterol-fed mice, suggesting brain-specific inflammatory responses to copper exposure **(Lu et al., 2009)**. Cu treatment induced deregulation of glial cytoskeleton, NF-kB, and PARP expression in *Capoeta umbla* brain tissue, suggesting astroglial response and DNA damage **(Kirici et al., 2019)**. CuO-NPs treatment resulted in elevation of the levels of IL-1, IL-6, iNOS, NF-κB, COX-2, PGE2, TNF-α and downregulation of IL-10 in different serum and tissue examinations, and this results showed that Cu is also a potential pro-inflammatory factor that can stimulate inflammatory responses in the major organs. Further, uptake of TNF-α, IL-6, and IL-1 resulted in the activation of NF-κB signalling pathways, contributing to the inflammatory response.

Chronic exposure to Cd can negatively impact renal function, with studies showing that Cd induces p53-dependent in proximal tubular cells. Results showed overaccumulation of p53 proteins in the kidney and liver **(Lee et al., 2016)**. Our study suggests Cd and Cu induced apoptosis associated with upregulation of p53 that mediates renal, hepatic and neuro toxicity in mice. Research has shown that upregulation of PPAR-γ activity in hepatocytes can alleviate non-alcoholic fatty liver disease (NAFLD) by influencing the crosstalk between hepatocytes and macrophages, thereby reducing oxidative stress and preventing M1 macrophage polarization **(Li et al., 2022)**. Activation of PPAR-γ reduces pro-inflammatory cytokines, highlighting its anti-inflammatory properties in the context of tuberculosis physiopathology **(Díaz et al., 2023)**. Moreover, in the porcine endometrium, PPAR-γ ligands have been found to influence the expression of genes involved in the DNA

damage response during LPS-induced inflammation, indicating a role in regulating inflammatory processes in the reproductive system **(Mierzejewski et al., 2022)**. PPAR-γ agonist shows protective effects on liver injury **(Elshazly** and **Soliman, 2019)** and plays a crucial role in kidney metabolism, lipid and glucose metabolism, and renal mineral control hence, synthetic agonists of PPAR-γ have reno-protective effects **(Corrales et al., 2018)**. CdO-NPs and CuO-NPs treatment led to the degradation of PPAR-γ in liver, kidney and brain tissue as compared to the normal saline treated groups which indicated that involvement of PPAR-γ in Cd and Cu mediated toxicity.

CHAPTER- 7

SUMMARY

7.1 Summary

- The present study investigated potential organ toxicity of CdO-NPs and CuO-NPs in mice model at low doses. In our study we have used both *in silico* and *in vivo* methods to assess the toxicity of the chemicals.
- *In silico* method of toxicity prediction stands as a very useful tool that helps in the quick assessment of toxicity.
- The physical properties for CdO was found to be safe, but its permeability pattern is below the safety range. Its LD_{50} in animals is low, falling under toxicity class III. CdO is active for neurotoxicity, BBB barrier, ecotoxicity, and Cytochrome CYP2C9.
- Similar predictions were seen for CuO where, physical properties of CuO were predicted within the safety range, but their permeability pattern was below the range. The LD_{50} in animals was 413 mg/kg, falling under toxicity class IV. CuO was found active for neurotoxicity, BBB barrier, ecotoxicity, and Cytochrome CYP2C9.
- ADMET profiling predicted the potential toxicity of CdO and CuO, with water solubility, Caco2 value, intestinal absorption, and skin permeability. CdO was predicted to be negative for all cytochrome P450 inhibitors and substrates. Total clearance was low, and it showed no mutagenic potential. The maximum tolerated dose was low and were not a hERG I and II inhibitor.
- *In vivo* study was carried out with CdO- and CuO-NPs of size < 50 nm, pure crystalline solids were used for the toxicity test, and chemical characteristics were confirmed by using FTIR, FETEM and XRD analyses.
- Acute toxicity test was carried out to determine the LD_{50} for CdO-NPs. Mortality percentages were 33.33% and 66.67% in male and female groups at different doses. The LD_{50} values for male was 63.82 mg/kg and 58.21 mg/kg in female, calculated using OECD 423 guidelines and probit analysis.
- After 30 days of CdO-NPs administration, mice showed a significant decrease in mean body weight, feeding patterns, and water consumption compared to the control group. CdO-NPs intake had a prevailing impact on organ weights in treated female mice, with significant effects on liver, kidney, spleen, colon, lung, ovary, and uterus.
- Hematological parameters revealed major effects of CdO-NPs intoxication in female mice, with depletion of total RBCs count and hemoglobin concentration, and

an increase in total WBCs count. PCV decreased significantly among both control and treated groups.

- The study found a significant increase in cadmium heavy metal levels in liver, kidney, and brain tissues of treatment groups compared to normal mice.
- The study found that CdO-NPs treatment led to significant depletion of protein, albumin, globulin, and increased A/G ratio, total and direct bilirubin in all treated mice compared to normal control mice. The treatment also increased concentrations of kidney function biomarkers, increased ALP, and elevated AST and ALT concentrations. The lipid profile deteriorated, with increased levels of total cholesterol, triglycerides, LDL cholesterol, and decreased HDL cholesterol.
- CdO-NPs administration in female mice for 30 days led to significant oxidative stress in liver, kidney, and brain tissue, with increased malondialdehyde concentrations. The enzymatic and non-enzymatic anti-oxidants, SOD, CAT, GST, and GSH reserves were significantly depleted in these tissues compared to the control group.
- CdO-NPs treatment led to alterations in hepatic tissue architecture, including portal vein congestion, cellular vacuolization, and apoptotic nuclei formation. Kidney tissue sections showed kidney degeneration, glomerular degeneration, vascular congestion, cellular vacuolization, and area of haemorrhage. Histological sections of brain tissue showed normal pyramidal neuronal cells and blood vessels. However, CdO-NPs treatment led to inflammatory infiltration, darkly stained neuron appearance, intracytoplasmic vacuolization, cellular vacuolization, cellular apoptosis, tissue necrosis, tissue fragmentation, cellular degeneration, and congested vessels. The degree of histopathological alterations was more severe at higher doses.
- CdO-NPs increased pro-inflammatory markers in serum, while decreasing anti-inflammatory markers, indicating a potential role in inflammation in the treatment of various diseases. Inflammatory markers like COX-2, TNF-α, NF-κB, IL-6, and iNOS were elevated.
- CdO-NPs treatment significantly altered the expression of apoptotic and anti-apoptotic markers, and tumour-related proteins in liver, kidney, and brain tissues. Pro-apoptotic markers like BAX and active caspace-3 increased, while anti-apoptotic

markers like BCL-2 declined. Tissue suppressor protein P53 expression was also increased, suggesting potential cancer development.

- CuO-NPs intoxication affected female mice's body weight and feeding patterns, leading to a significant decrease in body weight, food, and water consumption compared to the normal control group. Hematological parameters showed decreased RBC counts, hemoglobin concentration, PCV, WBC counts, and MCV, with no significant change in MCH concentration.
- Copper concentration in liver, kidney, and brain increased significantly after consumption, with higher accumulation observed at high doses compared to the normal control group.
- Serological assays showed depletion of protein, globulin, and albumin in treatment groups, increased production of bilirubin, and deterioration of liver and kidney profiles.
- The treatment group showed increased total cholesterol and LDL cholesterol concentrations, while decreasing HDL cholesterol, but no significant changes in triglycerides, serum glucose, chloride, potassium, sodium, or calcium concentrations.
- Regular consumption of CuO-NPs triggers inflammatory and oxidative stress response systems, resulting in elevated levels of IL-6, IL-1, FAD, MPO, prostaglandin B4, leukotriene E2, and a decrease in IL-10 and TAOC.
- Consumption of CuO-NPs led to oxidative stress and depletion of enzymatic and non-enzymatic antioxidants, with elevated MDA levels in liver, kidney, and brain tissues. Enzymatic antioxidants GST, SOD, and CAT were depleted in liver, kidney, and brain tissues.
- The study examined liver, kidney and brain tissue in mice treated with CuO-NPs. Results showed dilation of central veins, sinusoid dilation, apoptotic nuclei, hepatocyte degeneration, tissue fragmentation, congestion, and tissue haemorrhage. Control mice had normal structures, while high-dose CuO-NPs intoxicated mice showed increased changes. In the kidney, CuO-NPs administration led to glomerular degeneration, area of haemorrhage, inflammatory infiltration, and apoptotic nuclei. In the brain, CuO-NPs administration resulted in darkly stained neuron, inflammatory infiltration, cellular vacuolization, apoptosis, necrosis, cellular degeneration, blood vessel congestion, and tissue fragmentation.

- The study investigated the role of pro-apoptotic, anti-apoptotic, and inflammatory markers in CuO-NPs intoxicated female mice. Results showed increased pro-apoptotic markers BAX and active caspace-3 in liver, kidney, and brain tissue, particularly in high dose groups. Inflammatory markers COX-2, IL-6, iNOS, TNF-α, and NF-κB also increased in treatment groups. CuO-NPs intoxication also led to changes in the expression patterns of P^{53} and PPAR-ɣ, with higher doses potentially causing more severe effects.
- Overall, present study suggests that both CdO-NPs and CuO-NPs have the potentiality to cause toxicity when administered regularly even at low doses.

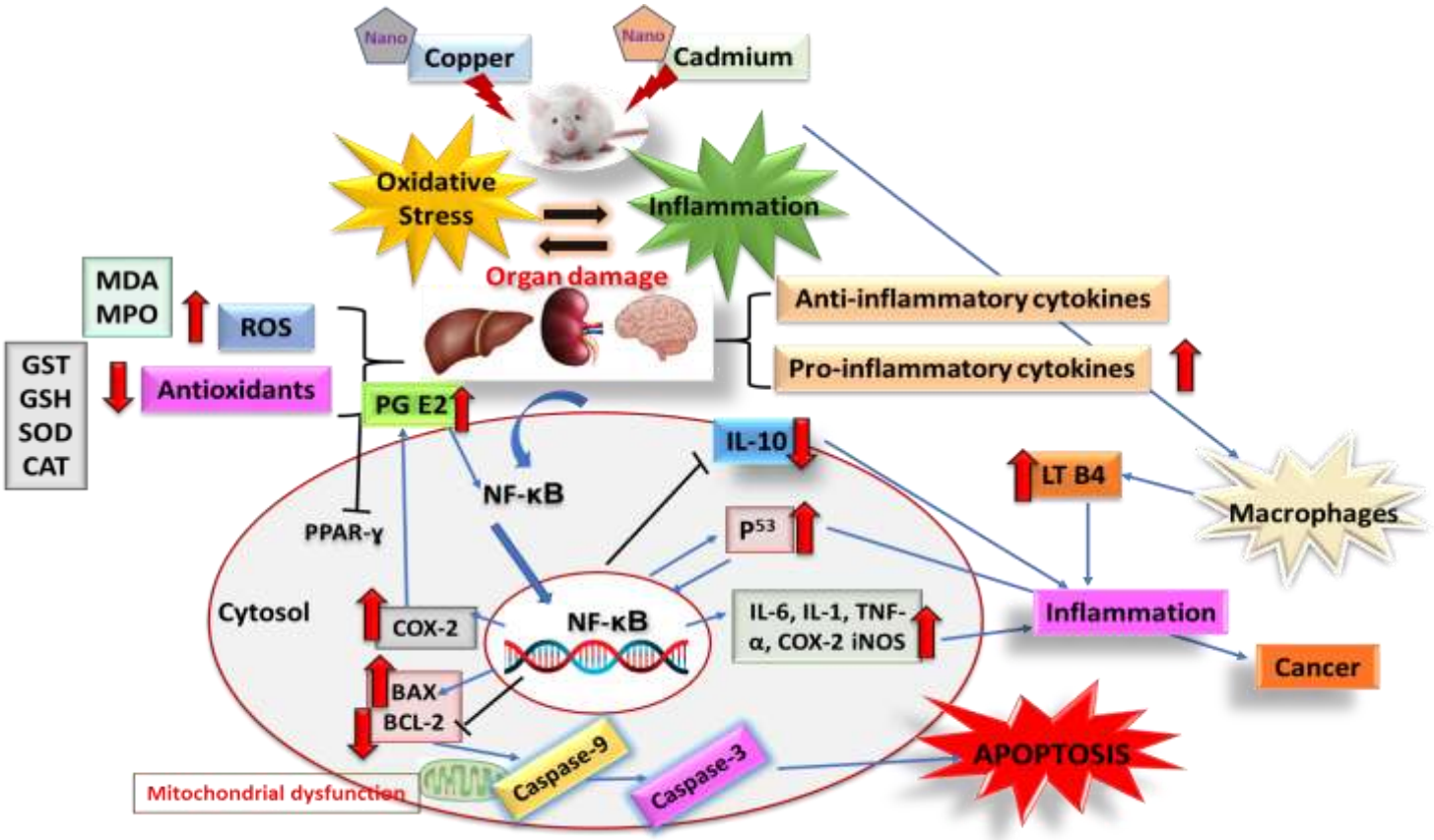

Figure 41 Diagrammatic representation of pathways of organ toxicity induced by CdO-NPs and CuO-NPs in mice.

CHAPTER- 8

CONCLUSION

8.1 Conclusion

The study found that CdO-NPs and CuO-NPs administration in mice significantly triggered oxidative stress in liver, kidney, and brain tissue, alterations in hepatic, renal and brain tissue architecture, and increased pro-inflammatory markers in serum. Cd and Cu metal concentration in liver, kidney, and brain increased after consumption, with higher accumulation observed at high doses. Serological assays showed depletion of protein, globulin, and albumin, increased bilirubin production, and deterioration of liver and kidney profiles. Additionally, the study also addressed that regular consumption of CdO-NPs and CuO-NPs at low doses for short-term triggers inflammatory and oxidative stress response systems.

However, there is an urgent need to address the effects of these metals on different organisms with variable doses in both sexes. More studies uncovering the mechanisms and other target signaling pathways involved in heavy metal organ toxicity are necessary to understand their diverse effects. There is also a vital need to trace the toxicological pathways triggered by these metals on other organs and the endocrine system. Research tracing the relationship between metal accumulation in the brain and cognitive, behavioral, and impact on memory is also of vital need. Additionally, there is a pressing need to conduct research on the gene expression patterns and microbiota profiling, which will further help to understand the potential toxicological outline of the heavy metals and widen the scope of possible treatment options. And lastly, there should be research targeting the possible treatment that will help to ameliorate the toxicity induced by the heavy metals.

REFERENCE

- Abbasi, R., Shineh, G., Mobaraki, M., Doughty, S., & Tayebi, L. (2023). Structural parameters of nanoparticles affecting their toxicity for biomedical applications: a review. *Journal of Nanoparticle Research*, *25*(3), 43.
- Abudayyak, M., Guzel, E., & Özhan, G. (2020). Cupric oxide nanoparticles induce cellular toxicity in liver and intestine cell lines. *Advanced Pharmaceutical Bulletin*, *10*(2), 213.
- Adele, B. O., Idama, C., Ige, A. O., Odetola, A. O., Emediong, I. E., & Adewoye, E. O. (2023). Alterations in plasma and erythrocyte membrane fatty acid composition following exposure to toxic copper level affect membrane deformability and fluidity in female wistar rats. *Journal of Trace Elements in Medicine and Biology*, *80*, 127316.
- Adeyomoye, O. I., & Adewumi, N. A. (2019). Lead exposure causes alteration of haematological indices in adult female Wistar rats. *Asian Journal of Pharmaceutical Research and Development*, *7*(6), 30-34.
- Aebi, H. (1984). Catalase in vitro. In *Methods in enzymology* (Vol. 105, pp. 121-126). Academic press.
- Afifi, O. K., & Embaby, A. S. (2016). Histological study on the protective role of ascorbic acid on cadmium induced cerebral cortical neurotoxicity in adult male albino rats. *Journal of microscopy and ultrastructure*, *4*(1), 36-45.
- Afolabi, O. K., Oyewo, E. B., Adekunle, A. S., Adedosu, O. T., & Adedeji, A. L. (2012). Impaired lipid levels and inflammatory response in rats exposed to cadmium. *EXCLI journal*, *11*, 677.
- Aghababa, H., Taei, S., & Nahid, G. A. (2017). The effect of cadmium nanoparticles on hepatic enzymes variation in blood of Rattus. *International journal of progressive sciences and technologies*, *5*.
- Ahmadi, I., & Foruozandeh, H. (2020). Evaluation the multi-organs toxicity of methamphetamine (METH) in rats. *Toxicologie Analytique et Clinique*, *32*(1), 4-11.
- Ajarem, J. S., Hegazy, A. K., Allam, G. A., Allam, A. A., Maodaa, S. N., & Mahmoud, A. M. (2023). Impact of petroleum industry on goats in Saudi

Arabia: heavy metal accumulation, oxidative stress, and tissue injury. *Environmental Science and Pollution Research*, *30*(2), 2836-2849.

- Al Kahtani, M. A. (2020). Effect of both selenium and biosynthesized nanoselenium particles on cadmium-induced neurotoxicity in albino rats. *Human and experimental toxicology*, *39*(2), 159-172.
- Al-Abdan, M. A., Bin-Jumah, M. N., & Alarifi, S. (2020). Exploration of Cadmium Dioxide Nanoparticles on Bioaccumulation, Oxidative Stress, and Carcinogenic Potential in Oreochromis mossambicus L. *Oxidative Medicine and Cellular Longevity*, *2020*(1), 5407159.
- Alam, S. I., Kim, M. W., Shah, F. A., Saeed, K., Ullah, R., & Kim, M. O. (2021). Alpha-linolenic acid impedes cadmium-induced oxidative stress, neuroinflammation, and neurodegeneration in mouse brain. *Cells*, *10*(9), 2274.
- Al-Bairuty, G. A., Taha, M. N., & Taha, M. N. (2016). Effects of copper nanoparticles on reproductive organs of male albino rats. *International Journal for Sciences and Technology*, *11*(3), 17-24.
- Al-Gebaly, A. S. (2017). Ameliorative effect of arctium lappa against cadmium genotoxicity and histopathology in kidney of wistar rat.
- Alissa, E. M., & Ferns, G. A. (2011). Heavy metal poisoning and cardiovascular disease. *Journal of toxicology*, *2011*(1), 870125.
- Al-Musawi, M. M., Al-Shmgani, H., & Al-Bairuty, G. A. (2022). Histopathological and biochemical comparative study of copper oxide nanoparticles and copper sulphate toxicity in male albino mice reproductive system. *International journal of biomaterials*, *2022*(1), 4877637.
- Alomar, S. (2015). Cadmium sulfide nanoparticle induces oxidative stress and pro-inflammatory effects in human lung adenocarcinoma epithelial cells. *Toxicological and Environmental Chemistry*, *97*(5), 619-633.
- Alvarez, A. M., DeOcesano-Pereira, C., Teixeira, C., & Moreira, V. (2020). IL-1β and TNF-α modulation of proliferated and committed myoblasts: IL-6 and COX-2-derived prostaglandins as key actors in the mechanisms involved. *Cells*, *9*(9), 2005.

- Andjelkovic, M., Buha Djordjevic, A., Antonijevic, E., Antonijevic, B., Stanic, M., Kotur-Stevuljevic, J., ... & Bulat, Z. (2019). Toxic effect of acute cadmium and lead exposure in rat blood, liver, and kidney. *International journal of environmental research and public health*, *16*(2), 274.
- Annie, L., Gurusubramanian, G., & Roy, V. K. (2019). Estrogen and progesterone dependent expression of visfatin/NAMPT regulates proliferation and apoptosis in mice uterus during estrous cycle. *The Journal of Steroid Biochemistry and Molecular Biology*, *185*, 225-236.
- Anreddy, R. N. R. (2018). Copper oxide nanoparticles induces oxidative stress and liver toxicity in rats following oral exposure. *Toxicology Reports*, *5*, 903-904.
- Ansari, M. N., Rehman, N. U., Karim, A., Imam, F., & Hamad, A. M. (2021). Protective effect of Thymus serrulatus essential oil on cadmium-induced nephrotoxicity in rats, through suppression of oxidative stress and downregulation of NF-κB, iNOS, and Smad2 mRNA expression. *Molecules*, *26*(5), 1252.
- Apykhtina, O. L., & Kozlov, K. P. (2017). Dynamics of cadmium acclumulation in the internal organs of rats after exposure to cadmium chloride and cadmium sulphide nanopartiles of various sizes. *Medicni perspektivi*, *22*(2), 4-9.
- Apykhtina, O. L., Dybkova, S. M., Sokurenko, L. M., & Chaikovsky, Y. B. (2018). Cytotoxic and genotoxic effects of cadmium sulfide nanoparticles. *Experimental Oncology*.
- Araya, M., Koletzko, B., & Uauy, R. (2003). Copper deficiency and excess in infancy: developing a research agenda. *Journal of pediatric gastroenterology and nutrition*, *37*(4), 422-429.
- Assadian, E., Zarei, M. H., Gilani, A. G., Farshin, M., Degampanah, H., & Pourahmad, J. (2018). Toxicity of copper oxide (CuO) nanoparticles on human blood lymphocytes. *Biological trace element research*, *184*, 350-357.
- ATSDR U. 2004. Toxicological profile for copper.

- Awwad, A. M., Albiss, B. A., & Salem, N. M. (2015). Antibacterial activity of synthesized copper oxide nanoparticles using Malva sylvestris leaf extract. *SMU Medical Journal*, 91-101.
- Aziz, S., & Abdullah, S. (2023). Evaluation of toxicity induced by engineered CuO nanoparticles in freshwater fish, Labeo rohita. *Turkish Journal of Fisheries and Aquatic Sciences*, *23*(8).
- Bachmanov, A. A., Reed, D. R., Beauchamp, G. K., & Tordoff, M. G. (2002). Food intake, water intake, and drinking spout side preference of 28 mouse strains. *Behavior genetics*, *32*(6), 435–443. https://doi.org/10.1023/a:1020884312053
- Balamurugan, S., Balu, A. R., Usharani, K., Suganya, M., Anitha, S., Prabha, D., & Ilangovan, S. (2016). Synthesis of CdO nanopowders by a simple soft chemical method and evaluation of their antimicrobial activities. *Pacific Science Review A: Natural Science and Engineering*, *18*(3), 228-232.
- Banerjee, P., Eckert, A. O., Schrey, A. K., & Preissner, R. (2018). ProTox-II: a webserver for the prediction of toxicity of chemicals. *Nucleic acids research*, *46*(W1), W257–W263. https://doi.org/10.1093/nar/gky318
- Barua, C. C., Barbhuiya, S. M. A. A., Buragohain, L. I. P. I. K. A., Kakati, A. J. A. Y., & Barua, A. G. (2020). Investigating the Role of Nf-Kb, Cox-1, Cox-2, Comt, IL-10, IL-6 And TNF-α In Modulating Anti-Nociceptive Activity of Methanolic Extract of Entada Phaseoloides. *Int J Pharm Pharm Sci*.
- Bedia, C. (2022). Metabolomics in environmental toxicology: Applications and challenges. *Trends in Environmental Analytical Chemistry*, *34*, e00161.
- Bekus, I. R., Kyryliv, M. V., Ivanusa, I. B., Furka, O. B., Krynytska, I. Y., & Marushchak, M. I. (2016). Biochemical parameters of lipid metabolism in animals affected by heavy metal salts and treated with carnitine chloride and sodium alginate. *International journal of medicine and medical research*, (2, Iss. 2), 42-46.
- Bernhoft, R. A. (2013). Cadmium toxicity and treatment. *The Scientific World Journal*, *2013*.

- Berthelot, M.P.E. (1859). Berthelot's Reaction Mechanism. *Report de Chimie Applique*, *2884*.
- Bhattacharya, P. T., Misra, S. R., & Hussain, M. (2016). Nutritional aspects of essential trace elements in oral health and disease: an extensive review. *Scientifica*, *2016*.
- Bidanchi, R. M., Lalrindika, L., Khushboo, M., Bhanushree, B., Dinata, R., Das, M., ... & Gurusubramanian, G. (2022). Antioxidative, anti-inflammatory and anti-apoptotic action of ellagic acid against lead acetate induced testicular and hepato-renal oxidative damages and pathophysiological changes in male Long Evans rats. *Environmental Pollution*, *302*, 119048.
- Binns, H. J., Campbell, C., Brown, M. J., & Advisory Committee on Childhood Lead Poisoning Prevention. (2007). Interpreting and managing blood lead levels of less than 10 μg/dL in children and reducing childhood exposure to lead: Recommendations of the Centers for Disease Control and Prevention Advisory Committee on Childhood Lead Poisoning Prevention. *Pediatrics*, *120*(5), e1285-e1298.
- Blum, J. L., Edwards, J. R., Prozialeck, W. C., Xiong, J. Q., & Zelikoff, J. T. (2015). Effects of maternal exposure to cadmium oxide nanoparticles during pregnancy on maternal and offspring kidney injury markers using a murine model. *Journal of Toxicology and Environmental Health, Part A*, *78*(12), 711-724.
- Bonizzi, G., & Karin, M. (2004). The two NF-κB activation pathways and their role in innate and adaptive immunity. *Trends in immunology*, *25*(6), 280-288.
- Bonsnss, R. W., & Taussky, H. H. (1945). On the colorimetric determination of creatinine by the Jaffe reaction. *Journal of biological chemistry*, *158*, 581-591.
- Borm, P. J., Robbins, D., Haubold, S., Kuhlbusch, T., Fissan, H., Donaldson, K., ... & Oberdorster, E. (2006). The potential risks of nanomaterials: a review carried out for ECETOC. *Particle and fibre toxicology*, *3*, 1-35.
- Borobia, M., Villanueva-Saz, S., Ruiz de Arcaute, M., Fernández, A., Verde, M. T., González, J. M., ... & Ortín, A. (2022). Copper poisoning, a deadly hazard for sheep. *Animals*, *12*(18), 2388.

- Bradford M. M. (1976). A rapid and sensitive method for the quantitation of microgram quantities of protein utilizing the principle of protein-dye binding. *Analytical biochemistry*, *72*, 248–254.
- Braga, M. M., Dick, T., de Oliveira, D. L., Scopel-Guerra, A., Mussulini, B. H. M., Souza, D. O., & da Rocha, J. B. T. (2015). Evaluation of zinc effect on cadmium action in lipid peroxidation and metallothionein levels in the brain. *Toxicology reports*, *2*, 858-863.
- Branca, J. J. V., Fiorillo, C., Carrino, D., Paternostro, F., Taddei, N., Gulisano, M., Pacini, A., & Becatti, M. (2020). Cadmium-Induced Oxidative Stress: Focus on the Central Nervous System. *Antioxidants (Basel, Switzerland)*, *9*(6), 492. https://doi.org/10.3390/antiox9060492
- Bugata, L. S. P., Pitta Venkata, P., Gundu, A. R., Mohammed Fazlur, R., Reddy, U. A., Kumar, J. M., ... & Mahboob, M. (2019). Acute and subacute oral toxicity of copper oxide nanoparticles in female albino Wistar rats. *Journal of Applied Toxicology*, *39*(5), 702-716.
- Cao, X., Fu, M., Bi, R., Zheng, X., Fu, B., Tian, S., ... & Liu, J. (2021). Cadmium induced BEAS-2B cells apoptosis and mitochondria damage via MAPK signaling pathway. *Chemosphere*, *263*, 128346.
- Carageorgiou, H., & Katramadou, M. (2012). Aspects of cadmium neurotoxicity. *Metal ion in stroke*, 703-749.
- Castagnetto, J. M., Hennessy, S. W., Roberts, V. A., Getzoff, E. D., Tainer, J. A., & Pique, M. E. (2002). MDB: the metalloprotein database and browser at the Scripps Research Institute. *Nucleic acids research*, *30*(1), 379-382.
- Chan, H. M., & Cherian, M. G. (1992). Protective roles of metallothionein and glutathione in hepatotoxicity of cadmium. *Toxicology*, *72*(3), 281–290. https://doi.org/10.1016/0300-483x(92)90179-i
- Chan, P., Yuen, T., Ruf, F., Gonzalez-Maeso, J., & Sealfon, S. C. (2005). Method for multiplex cellular detection of mRNAs using quantum dot fluorescent in situ hybridization. *Nucleic acids research*, *33*(18), e161-e161.

- Chandra, R. (2024). Histopathological Effects of Cadmium Chloride (CdCl2) Exposure on the Liver of Freshwater Fish *Heteropneustes fossilis*. *Knowledgeable Research: A Multidisciplinary Journal*, *2*(06), 74-78.
- Charkiewicz, A. E., Omeljaniuk, W. J., Nowak, K., Garley, M., & Nikliński, J. (2023). Cadmium Toxicity and Health Effects—A Brief Summary. *Molecules*, *28*(18), 6620.
- Chen, W. W., Yan, L. C., Cao, M. Y., Li, X. Y., Pang, S. L., Wang, Y., & Zhang, Y. S. (2019). Effect of lead exposure on the accumulation of copper and iron in central nervous system of rats. *Zhonghua lao Dong wei Sheng zhi ye Bing za zhi= Zhonghua Laodong Weisheng Zhiyebing Zazhi= Chinese Journal of Industrial Hygiene and Occupational Diseases*, *37*(3), 179-185.
- Chen, Z., Meng, H., Xing, G., Chen, C., Zhao, Y., Jia, G., ... & Wan, L. (2006). Acute toxicological effects of copper nanoparticles in vivo. *Toxicology letters*, *163*(2), 109-120.
- Cirillo, T., Amodio Cocchieri, R., Fasano, E., Lucisano, A., Tafuri, S., Ferrante, M. C., ... & Isani, G. (2012). Cadmium accumulation and antioxidant responses in Sparus aurata exposed to waterborne cadmium. *Archives of environmental contamination and toxicology*, *62*, 118-126.
- Conde de la Rosa, L., Goicoechea, L., Torres, S., Garcia-Ruiz, C., & Fernandez-Checa, J. C. (2022). Role of oxidative stress in liver disorders. *Livers*, *2*(4), 283-314.
- Corrales, P., Izquierdo-Lahuerta, A., & Medina-Gómez, G. (2018). Maintenance of kidney metabolic homeostasis by PPAR gamma. *International journal of molecular sciences*, *19*(7), 2063.
- Cory, S., & Adams, J. M. (2002). The Bcl2 family: regulators of the cellular life-or-death switch. *Nature Reviews Cancer*, *2*(9), 647-656.
- Cruces-Sande, A., Rodríguez-Pérez, A. I., Herbello-Hermelo, P., Bermejo-Barrera, P., Méndez-Álvarez, E., Labandeira-García, J. L., & Soto-Otero, R. (2019). Copper increases brain oxidative stress and enhances the ability of 6-hydroxydopamine to cause dopaminergic degeneration in a rat model of Parkinson's disease. *Molecular Neurobiology*, *56*, 2845-2854.

- Cupertino, M. C., Novaes, R. D., Santos, E. C., Neves, A. C., Silva, E., Oliveira, J. A., & Matta, S. L. (2017). Differential susceptibility of germ and leydig cells to cadmium-mediated toxicity: impact on testis structure, adiponectin levels, and steroidogenesis. *Oxidative medicine and cellular longevity*, *2017*.
- Das, S. C., & Al-Naemi, H. A. (2019). Cadmium toxicity: Oxidative stress, inflammation and tissue injury.
- De Jong, W. H., De Rijk, E., Bonetto, A., Wohlleben, W., Stone, V., Brunelli, A., ... & Cassee, F. R. (2019). Toxicity of copper oxide and basic copper carbonate nanoparticles after short-term oral exposure in rats. *Nanotoxicology*, *13*(1), 50-72.
- Demir, E., Qin, T., Li, Y., Zhang, Y., Guo, X., Ingle, T., ... & Chen, T. (2020). Cytotoxicity and genotoxicity of cadmium oxide nanoparticles evaluated using in vitro assays. *Mutation Research/Genetic Toxicology and Environmental Mutagenesis*, *850*, 503149.
- Díaz, A., D'Attilio, L., Penas, F., Bongiovanni, B., Massa, E., Cevey, A., ... & Bay, M. L. (2023). Studies on the contribution of PPAR Gamma to tuberculosis physiopathology. *Frontiers in Cellular and Infection Microbiology*, *13*, 1067464.
- Dong, J., Wang, X., Xu, C., Gao, M., Wang, S., Zhang, J., ... & Han, Y. (2021). Inhibiting NLRP3 inflammasome activation prevents copper-induced neuropathology in a murine model of Wilson's disease. *Cell death and disease*, *12*(1), 87.
- Doudi, M., & Setorki, M. (2014). Acute effect of nano-copper on liver tissue and function in rat. *Nanomedicine Journal*, *1*(5).
- Doumas, B. T., Watson, W. A., & Biggs, H. G. (1971). Albumin standards and the measurement of serum albumin with bromcresol green. *Clinica chimica acta; international journal of clinical chemistry*, *31*(1), 87–96.
- Du Sert, N. P., Ahluwalia, A., Alam, S., Avey, M. T., Baker, M., Browne, W. J., ... & Würbel, H. (2020). Reporting animal research: Explanation and elaboration for the ARRIVE guidelines 2.0. *PLoS biology*, *18*(7), e3000411.

- Du, H., Zheng, Y., Zhang, W., Tang, H., Jing, B., Li, H., ... & Shu, G. (2022). Nano-Selenium Alleviates Cadmium-Induced Acute Hepatic Toxicity by Decreasing Oxidative Stress and Activating the Nrf2 Pathway in Male Kunming Mice. *Frontiers in Veterinary Science*, *9*, 942189.
- Dudley, R. E., Svoboda, D. J., & Klaassen, C. D. (1984). Time course of cadmium-induced ultrastructural changes in rat liver. *Toxicology and applied pharmacology*, *76*(1), 150-160.
- El Bialy, B. E., Hamouda, R. A., Abd Eldaim, M. A., El Ballal, S. S., Heikal, H. S., Khalifa, H. K., & Hozzein, W. N. (2020). Comparative toxicological effects of biologically and chemically synthesized copper oxide nanoparticles on mice. *International journal of nanomedicine*, 3827-3842.
- El Sayed, A. M., El-Sayed, S., Morsi, W. M., Mahrous, S., & Hassen, A. (2014). Synthesis, characterization, optical, and dielectric properties of polyvinyl chloride/cadmium oxide nanocomposite films. *Polymer composites*, *35*(9), 1842-1851.
- El-Atrash, A., Zaki, S., Tousson, E., & Negm, M. (2022). Copper Oxide Nanoparticles Induced Liver and Kidney Toxicity in Rat. *Asian Journal of Biochemistry, Genetics and Molecular Biology*, *12*(4), 154-160.
- Elmore, S. (2007). Apoptosis: a review of programmed cell death. *Toxicologic pathology*, *35*(4), 495-516.
- Elshamaa, S. M., Taha, N. M., Lebda, M. A., Hashem, A. E., & Elfeky, M. S. (2022). Zinc Oxide Nanoparticles Alleviated Hepatic Oxidative Stress Induced by Cadmium Chloride Toxicity in Rats. *Alexandria Journal of Veterinary Sciences*, *73*(1).
- Elshazly, S., & Soliman, E. (2019). PPAR gamma agonist, pioglitazone, rescues liver damage induced by renal ischemia/reperfusion injury. *Toxicology and applied pharmacology*, *362*, 86-94.
- El-Sherbiny, E. M., Abdel-Gawad, E. I., & Osman, H. F. (2022). Impact of nano silver composite structure on cadmium neurotoxicity in albino rats. *Applied Biological Chemistry*, *65*(1), 70.

- Engström, B. (1981). Influence of chelating agents on toxicity and distribution of cadmium among proteins of mouse liver and kidney following oral or subcutaneous exposure. *Acta Pharmacologica et Toxicologica*, *48*(2), 108-117.
- Ezedom, T. (2018). Cadmium and arsenic induced toxicity through a controlled food chain on plasma lipid profile and endogenous metabolites of rats. *Annals of Biomedical Sciences*, *17*(1).
- Fan, R., Hu, P. C., Wang, Y., Lin, H. Y., Su, K., Feng, X. S., ... & Yang, F. (2018). Betulinic acid protects mice from cadmium chloride-induced toxicity by inhibiting cadmium-induced apoptosis in kidney and liver. *Toxicology Letters*, *299*, 56-66.
- FAO/WHO (2015). Codex Committee on Food Additives and Contaminants; Adopted in 1995 Revised in 1997, 2006, 2008, 2009 Amended in 2010, 2012, 2013, 2014, 2015, 2016, 2017; World Health Organization: The Hague, The Netherlands, 2017.
- Faroon, O., Ashizawa, A., Wright, S., Tucker, P., Jenkins, K., Ingerman, L., et al. (2012) Toxicological Profile for Cadmium. Agency for Toxic Substances and Disease Registry (US), Atlanta.
- Fergusson, J.E. (1990). The Heavy Elements: Chemistry, Environmental Impact and Health Effects. *Pergamon Press, Oxford*, 85-547.
- Ferlazzo, N., Micali, A., Marini, H. R., Freni, J., Santoro, G., Puzzolo, D., Squadrito, F., Pallio, G., Navarra, M., Cirmi, S., & Minutoli, L. (2021). A Flavonoid-Rich Extract from Bergamot Juice, Alone or in Association with Curcumin and Resveratrol, Shows Protective Effects in a Murine Model of Cadmium-Induced Testicular Injury. *Pharmaceuticals (Basel, Switzerland)*, *14*(5), 386.
- Finney, D.J. (1971). Probit Analysis. 3rd Edition, Cambridge University Press, London.
- Friedewald, W. T., Levy, R. I., & Fredrickson, D. S. (1972). Estimation of the concentration of low-density lipoprotein cholesterol in plasma, without use of the preparative ultracentrifuge. *Clinical chemistry*, *18*(6), 499–502.

- Gaetke, L. M., & Chow, C. K. (2003). Copper toxicity, oxidative stress, and antioxidant nutrients. *Toxicology*, *189*(1-2), 147-163.
- Galhardi, C. M., Diniz, Y. S., Faine, L. A., Rodrigues, H. G., Burneiko, R. C., Ribas, B. O., & Novelli, E. L. (2004). Toxicity of copper intake: lipid profile, oxidative stress and susceptibility to renal dysfunction. *Food and chemical toxicology*, *42*(12), 2053-2060.
- Garber C. C. (1981). Jendrassik--Grof analysis for total and direct bilirubin in serum with a centrifugal analyzer. *Clinical chemistry*, *27*(8), 1410–1416.
- Gathwan, K. H., & Albir, A. A. (2020). Quantitative and Histological Study of the Effect of Cadmium Oxide on Both Body and Kidney of Mice. *Indian Journal of Forensic Medicine and Toxicology*, *14*(3), 1186-1189.
- Genchi, G., Sinicropi, M. S., Lauria, G., Carocci, A., & Catalano, A. (2020). The effects of cadmium toxicity. *International journal of environmental research and public health*, *17*(11), 3782.
- Ghonimi, W. A., Alferah, M. A., Dahran, N., & El-Shetry, E. S. (2022). Hepatic and renal toxicity following the injection of copper oxide nanoparticles (CuO NPs) in mature male Westar rats: histochemical and caspase 3 immunohistochemical reactivities. *Environmental Science and Pollution Research*, *29*(54), 81923-81937.
- Ghosh, K., & Indra, N. (2018). Cadmium treatment induces echinocytosis, DNA damage, inflammation, and apoptosis in cardiac tissue of albino Wistar rats. *Environmental Toxicology and Pharmacology*, *59*, 43-52.
- Gitelman, H.J. (1967). An improved automated procedure for the determination of calcium in biological specimens. *Analytical Biochemistry*, *18,* 521-531.
- Gluhcheva, Y., Ivanov, I., Atanasov, V., Antonova, N., Ivanova, J., & Mitewa, M. (2011). Hematological changes in case of chronic cadmium intoxication and monensin detoxication. Relationship with rheological variables. *Clinical hemorheology and microcirculation*, *49*(1-4), 417-422.
- Goracci, L., Valeri, A., Sciabola, S., Aleo, M. D., Moritz, W., Lichtenberg, J., & Cruciani, G. (2019). A novel lipidomics-based approach to evaluating the

risk of clinical hepatotoxicity potential of drugs in 3D human microtissues. *Chemical Research in Toxicology*, *33*(1), 258-270.

- Gornall, A. G., Bardawill, C. J., & David, M. M. (1949). Determination of serum proteins by means of the biuret reaction. *The Journal of biological chemistry*, *177*(2), 751–766.
- Grigore, M. E., Biscu, E. R., Holban, A. M., Gestal, M. C., & Grumezescu, A. M. (2016). Methods of synthesis, properties and biomedical applications of CuO nanoparticles. *Pharmaceuticals*, *9*(4), 75.
- Guidance, O. E. C. D. (2001). Document on acute oral toxicity. *Environmental Health and Safety Monograph Series on Testing and Assessment*, *24*.
- Guo, H., Wang, Y., Cui, H., Ouyang, Y., Yang, T., Liu, C., ... & Deng, H. (2022). Copper induces spleen damage through modulation of oxidative stress, apoptosis, DNA damage, and inflammation. *Biological Trace Element Research*, 1-9.
- Gupta, G., Cappellini, F., Farcal, L., Gornati, R., Bernardini, G., & Fadeel, B. (2022). Copper oxide nanoparticles trigger macrophage cell death with misfolding of Cu/Zn superoxide dismutase 1 (SOD1). *Particle and Fibre Toxicology*, *19*(1), 33.
- Gupta, R. (2019). Cadmium nanoparticles and its toxicity. *Journal of Critical Reviews*, *6*(5), 1-7.
- Gyurászová, M., Gurecká, R., Bábíčková, J., & Tóthová, Ľ. (2020). Oxidative Stress in the Pathophysiology of Kidney Disease: Implications for Noninvasive Monitoring and Identification of Biomarkers. *Oxidative medicine and cellular longevity*, *2020*, 5478708. https://doi.org/10.1155/2020/5478708
- Habig, W. H., Pabst, M. J., & Jakoby, W. B. (1974). Glutathione S-transferases. The first enzymatic step in mercapturic acid formation. *The Journal of biological chemistry*, *249*(22), 7130–7139.
- Hadwan M. H. (2018). Simple spectrophotometric assay for measuring catalase activity in biological tissues. *BMC biochemistry*, *19*(1), 7.

- Hager K. K. (2016). Management of Weight Loss in People With Cancer. *Journal of the advanced practitioner in oncology*, *7*(3), 336–338. Hager K. K. (2016).
- Hahn, K., Kanbay, M., Lanaspa, M. A., Johnson, R. J., & Ejaz, A. A. (2017). Serum uric acid and acute kidney injury: A mini review. *Journal of advanced research*, *8*(5), 529–536. https://doi.org/10.1016/j.jare.2016.09.006
- Hamza, R. Z., Al-Eisa, R. A., & El-Shenawy, N. S. (2022). Possible ameliorative effects of the royal jelly on hepatotoxicity and oxidative stress induced by molybdenum nanoparticles and/or cadmium chloride in male rats. *Biology*, *11*(3), 450.
- Han, J. M., Yee, J., Cho, Y. S., & Gwak, H. S. (2020). Factors Influencing Imatinib-Induced Hepatotoxicity. *Cancer research and treatment*, *52*(1), 181–188. https://doi.org/10.4143/crt.2019.131
- Hashish, E. A., & Elgaml, S. A. (2016). Hepatoprotective and nephroprotective effect of curcumin against copper toxicity in rats. *Indian journal of clinical biochemistry*, *31*, 270-277.
- Hassan, L., Hasan, I. M., Al-Amgad, Z., & Ahmed, H. (2024). Acute exposure to copper oxide nanoparticles impairs testicular function and sperm quality in adult male albino rats. *SVU-International Journal of Veterinary Sciences*, *7*(1), 1-21.
- Hassanen, E. I., Tohamy, A. F., Issa, M. Y., Ibrahim, M. A., Farroh, K. Y., & Hassan, A. M. (2019). Pomegranate juice diminishes the mitochondria-dependent cell death and NF-kB signaling pathway induced by copper oxide nanoparticles on liver and kidneys of rats. *International journal of nanomedicine*, 8905-8922.
- Hendrawan, V. F., Purwantari, K. E., Wajdi, S. A., Zulfarniasyah, A. B., Putri, A. S., Rahmawati, M. A., & Al Ilmi, M. F. (2018). Histopathologic changes in liver tissue from cadmium intoxicated mice and treated with curcumin during pregnancy. *Research Journal of Pharmacy and Technology*, *11*(3), 863-866.

- Henson, M. C., & Chedrese, P. J. (2004). Endocrine disruption by cadmium, a common environmental toxicant with paradoxical effects on reproduction. *Experimental biology and medicine, 229*(5), 383-392.
- Hocaoğlu-özyiğit, A., & Genç, B. N. (2020). Cadmium in plants, humans and the environment. *Frontiers in Life Sciences and Related Technologies, 1*(1), 12-21.
- Hoffbrand, V., & Provan, D. (1997). ABC of clinical haematology: macrocytic anaemias. *Bmj*, *314*(7078), 430.
- IARC (International Agency for Research on Cancer), Monographs on the Evaluation of the Carcinogenic Risk of Chemicals to Humans: Arsenic and Arsenic Compounds (Group 1), World Health Organization, Lyon, France, 1987; 7: 100–106.
- Ibrahim, D., Froberg, B., Wolf, A., & Rusyniak, D. E. (2006). Heavy metal poisoning: clinical presentations and pathophysiology. Clinics in laboratory medicine, *26*(1), 67-97.
- Ibtissem, B. A., Hajer, B. S., Ahmed, H., Awatef, E., Choumous, K., Ons, B., ... & Najiba, Z. (2017). Oxidative stress and histopathological changes induced by methylthiophanate, a systemic fungicide, in blood, liver and kidney of adult rats. *African Health Sciences*, *17*(1), 154-163.
- Inaba, S., Sautin, Y., Garcia, G. E., & Johnson, R. J. (2013). What can asymptomatic hyperuricaemia and systemic inflammation in the absence of gout tell us?. *Rheumatology (Oxford, England)*, *52*(6), 963–965. https://doi.org/10.1093/rheumatology/ket001
- Isaac, L. J., Abah, G., Akpan, B., & Ekaette, I. U. (2013, September). Haematological properties of different breeds and sexes of rabbits. In *Proceedings of the 18th annual conference of animal science association of Nigeria* (Vol. 6, pp. 24-7).
- Ismail, S. M., Ismail, H. A., & Al-Sharif, G. M. (2015). Neuroprotective effect of barley plant (Hardeum Valgara) against the changes in MAO induced by lead and cadmium administration in different CNS regions of male guinea pig. *Journal of Life Sciences Research, 2*(2), 53-60.

- Jagadeesan, G., & Kavitha, A. V. (2006). Recovery of phosphatase and transaminase activity of mercury intoxicated Mus musculus (Linn.) liver tissue by Tribulus terrestris (Linn.) (Zygophyllaceae) extract. *Tropical biomedicine*, *23*(1), 45–51.
- Jain, M., Yadav, M., & Chaudhry, S. (2021). Copper oxide nanoparticles for the removal of divalent nickel ions from aqueous solution. *Toxin Reviews*, *40*(4), 872-885.
- Jaishankar, M., Tseten, T., Anbalagan, N., Mathew, B. B., & Beeregowda, K. N. (2014). Toxicity, mechanism and health effects of some heavy metals. *Interdisciplinary toxicology*, *7*(2), 60–72.
- Järup, L. (2002). Cadmium overload and toxicity. *Nephrology Dialysis Transplantation*, *17*(suppl_2), 35-39.
- Järup, L., & Åkesson, A. (2009). Current status of cadmium as an environmental health problem. *Toxicology and applied pharmacology*, *238*(3), 201-208.
- Jensen, K.C. (2008). Theory and Practice of Histological Techniques, 6th Edition. *Journal of Neuropathology and Experimental Neurology*, *67*, 633-633.
- Jia, X., Wang, S., Zhou, L., & Sun, L. (2017). The potential liver, brain, and embryo toxicity of titanium dioxide nanoparticles on mice. *Nanoscale research letters*, *12*, 1-14.
- Jomova, K., Makova, M., Alomar, S. Y., Alwasel, S. H., Nepovimova, E., Kuca, K., ... & Valko, M. (2022). Essential metals in health and disease. *Chemico-biological interactions*, *367*, 110173.
- Joseph, P., Muchnok, T. K., Klishis, M. L., Roberts, J. R., Antonini, J. M., Whong, W. Z., & Ong, T. M. (2001). Cadmium-induced cell transformation and tumourigenesis are associated with transcriptional activation of c-fos, c-jun, and c-myc proto-oncogenes: role of cellular calcium and reactive oxygen species. *Toxicological sciences*, *61*(2), 295-303.
- Kadhim, Z. A., & Abbar, A. H. (2022). A Novel Bio-electrochemical Cell with Rotating Cylinder Cathode for Cadmium Removal from Simulated Wastewater. *Egyptian Journal of Chemistry*, *65*(132), 769-778.

- Kakkar, P., Das, B., & Viswanathan, P. N. (1984). A modified spectrophotometric assay of superoxide dismutase. *Indian journal of biochemistry and biophysics*, *21*(2), 130–132.
- Kanbay, M., Siriopol, D., Nistor, I., Elcioglu, O. C., Telci, O., Takir, M., Johnson, R. J., & Covic, A. (2014). Effects of allopurinol on endothelial dysfunction: a meta-analysis. *American journal of nephrology*, *39*(4), 348–356. https://doi.org/10.1159/000360609
- Karnam, S. S., Ghosh, R. C., & Mondal, S. (2014). Effect on body weight and feed consumption of bisphenol-A induced subacute toxicity in rats.
- Karthik, K., Dhanuskodi, S., Gobinath, C., Prabukumar, S., & Sivaramakrishnan, S. (2018). Multifunctional properties of CdO nanostructures Synthesised through microwave assisted hydrothermal method. *Materials Research Innovations*.
- Kayama, F., Yoshida, T., Elwell, M. R., & Luster, M. I. (1995). Role of tumour necrosis factor-α in cadmium-induced hepatotoxicity. *Toxicology and applied pharmacology*, *131*(2), 224-234.
- Keeble, J. A., & Gilmore, A. P. (2007). Apoptosis commitment–translating survival signals into decisions on mitochondria. *Cell research*, *17*(12), 976-984.
- Kelada, S. N., Aylor, D. L., Peck, B. C., Ryan, J. F., Tavarez, U., Buus, R. J., Miller, D. R., Chesler, E. J., Threadgill, D. W., Churchill, G. A., Pardo-Manuel de Villena, F., & Collins, F. S. (2012). Genetic analysis of hematological parameters in incipient lines of the collaborative cross. *G3 (Bethesda, Md.)*, *2*(2), 157–165. https://doi.org/10.1534/g3.111.001776
- Kesari, A., & Noel, J. Y. (2022). Nutritional assessment. Treasure Island (FL): StatPearls Publishing.
- Khan, Z., Elahi, A., Bukhari, D. A., & Rehman, A. (2022). Cadmium sources, toxicity, resistance and removal by microorganisms-A potential strategy for cadmium eradication. *Journal of Saudi Chemical Society*, 101569.
- Khatami, M., Ebrahimi, K., Galehdar, N., Moradi, M. N., & Moayyedkazemi, A. (2020). Green synthesis and characterization of copper nanoparticles and

their effects on liver function and hematological parameters in mice. *Turkish Journal of Pharmaceutical Sciences*, *17*(4), 412.

- Kind, P. R., & King, E. J. (1954). Estimation of plasma phosphatase by determination of hydrolysed phenol with amino-antipyrine. *Journal of clinical pathology*, *7*(4), 322–326.
- Kini, R. D., Arunkumar, N., & Gokul, M. (2019). Potential Protective Role of Beta Carotene on Cadmium Induced Brain and Kidney Damage. *Indian Journal of Public Health Research and Development*, *10*(9).
- Kirici, M., Nedzvetsky, V. S., Agca, C. A., & Gasso, V. Y. (2019). Sublethal doses of copper sulphate initiate deregulation of glial cytoskeleton, NF-kB and PARP expression in Capoeta umbla brain tissue. *Regulatory Mechanisms in Biosystems*, *10*(1), 103-110.
- Klaassen, C. D., Bracken, W. M., Dudley, R. E., Goering, P. L., Hazelton, G. A., & Hjelle, J. J. (1985). Role of sulfhydryls in the hepatotoxicity of organic and metallic compounds. *Fundamental and applied toxicology: official journal of the Society of Toxicology*, *5*(5), 806–815. https://doi.org/10.1016/0272-0590(85)90164-2
- Klinova, S. V., Minigalieva, I. A., Katsnelson, B. A., Solovyeva, S. N., Privalova, L. I., Gurvich, V. B., ... & Sutunkova, M. P. (2020). General Toxic and Cardiovascular Toxic Impact of Cadmium Oxide Nanoparticles.
- Kong, L., Tang, M., Zhang, T., Wang, D., Hu, K., Lu, W., ... & Pu, Y. (2014). Nickel nanoparticles exposure and reproductive toxicity in healthy adult rats. *International journal of molecular sciences*, *15*(11), 21253-21269.
- Kong, Z., Liu, C., & Olatunji, O. J. (2023). Asperuloside attenuates cadmium-induced toxicity by inhibiting oxidative stress, inflammation, fibrosis and apoptosis in rats. *Scientific Reports*, *13*(1), 5698.
- Koohi, M. K., Hejazy, M., Najafi, D., & Sajadi, S. M. (2017). Investigation of hematotoxic effect of nano ZnO, nano Fe3O4 and nano SiO2 in vitro. *Nanomedicine Research Journal*, *2*(2), 93-99.
- Kostić, M. M., Ognjanović, B., Dimitrijević, S., Zikić, R. V., ZSCtajn, A., Rosić, G. L., & Zivković, R. V. (1993). Cadmium-induced changes of

antioxidant and metabolic status in red blood cells of rats: in vivo effects. *European Journal of Haematology*, *51*(2), 86-92.

- Kumar, V., Kalita, J., Misra, U. K., & Bora, H. K. (2015). A study of dose response and organ susceptibility of copper toxicity in a rat model. *Journal of Trace Elements in Medicine and Biology*, *29*, 269-274.
- KZ, H., & AM, C. (1998). The pollutant effects of copper, zinc and lead on the histological patterns of fish kidney. *Egyptian Journal of Aquatic Biology and Fisheries*, *2*(3), 15-41.
- Laha, D., Pramanik, A., Maity, J., Mukherjee, A., Pramanik, P., Laskar, A., & Karmakar, P. (2014). Interplay between autophagy and apoptosis mediated by copper oxide nanoparticles in human breast cancer cells MCF7. *Biochimica et biophysica acta*, *1840*(1), 1–9. https://doi.org/10.1016/j.bbagen.2013.08.011
- Laios, K., Michaleas, S. N., Tsoucalas, G., Papalampros, A., & Androutsos, G. (2021). The ancient Greek roots of the term *Toxic*. *Toxicology reports*, *8*, 977–979.
- Lawal, A. O., Marnewick, J. L., & Ellis, E. M. (2015). Heme oxygenase-1 attenuates cadmium-induced mitochondrial-caspase 3-dependent apoptosis in human hepatoma cell line. *BMC Pharmacology and Toxicology*, *16*, 1-13.
- L'Azou, B., Passagne, I., Mounicou, S., Tréguer-Delapierre, M., Puljalté, I., Szpunar, J., ... & Ohayon-Courtès, C. (2014). Comparative cytotoxicity of cadmium forms (CdCl2, CdO, CdS micro-and nanoparticles) in renal cells. *Toxicology Research*, *3*(1), 32-41.
- Lebedová, J., Bláhová, L., Večeřa, Z., Mikuška, P., Dočekal, B., Buchtová, M., ... & Hilscherová, K. (2016). Impact of acute and chronic inhalation exposure to CdO nanoparticles on mice. *Environmental Science and Pollution Research*, *23*, 24047-24060.
- Lech, T., & Sadlik, J. K. (2017). Cadmium concentration in human autopsy tissues. *Biological Trace Element Research*, *179*, 172-177.
- Lee, H. J., Lee, J. H., Lee, S. M., Kim, N. H., Moon, Y. G., Tak, T. K., ... & Heo, J. D. (2022). Cadmium induces cytotoxicity in normal mouse renal

MM55. K cells. *International Journal of Environmental Health Research*, *32*(1), 131-140.

- Lee, J., & Lim, K. T. (2011). Preventive effect of phytoglycoprotein (27 kDa) on inflammatory factors at liver injury in cadmium chloride-exposed ICR mice. *Journal of cellular biochemistry*, *112*(2), 694-703.
- Lei, R., Yang, B., Wu, C., Liao, M., Ding, R., & Wang, Q. (2015). Mitochondrial dysfunction and oxidative damage in the liver and kidney of rats following exposure to copper nanoparticles for five consecutive days. *Toxicology Research*, *4*(2), 351-364.
- Leiva, J., Palestini, M., Infante, C., Goldschmidt, A., & Motles, E. (2009). Copper suppresses hippocampus LTP in the rat, but does not alter learning or memory in the morris water maze. *Brain research*, *1256*, 69-75.
- Lenartowicz, M., Windak, R., Tylko, G., Kowal, M., & Styrna, J. (2010). Effects of copper supplementation on the structure and content of elements in kidneys of mosaic mutant mice. *Biological trace element research*, *136*, 204-220.
- Li, M., Han, R., Li, J., Wu, W., & Gu, J. (2024). Research Progress in Acute Oral Toxicity Testing Methods. *International Journal of Biology and Life Sciences*, *6*(1), 19-22.
- Li, T., Yang, C., Hu, H., Zhang, B., & Ma, L. (2021). The toxico-transcriptomic analysis of nano-copper oxide on gazami crab: especially focus on hepatopancreas and gill. *Food Science and Technology*, *42*, e03521.
- Li, X. Y., Ji, P. X., Ni, X. X., Chen, Y. X., Sheng, L., Lian, M., ... & Hua, J. (2022). Regulation of PPAR-γ activity in lipid-laden hepatocytes affects macrophage polarization and inflammation in nonalcoholic fatty liver disease. *World Journal of Hepatology*, *14*(7), 1365.
- Li, X., Sun, W., & An, L. (2018). Nano-CuO impairs spatial cognition associated with inhibiting hippocampal long-term potentiation via affecting glutamatergic neurotransmission in rats. *Toxicology and Industrial Health*, *34*(6), 409-421.

- Lin, J. P., O'Donnell, C. J., Jin, L., Fox, C., Yang, Q., & Cupples, L. A. (2007). Evidence for linkage of red blood cell size and count: Genome-wide scans in the Framingham Heart Study. *American journal of hematology*, *82*(7), 605-610.
- Liu, F., Wang, X. Y., Zhou, X. P., Liu, Z. P., Song, X. B., Wang, Z. Y., & Wang, L. (2017). Cadmium disrupts autophagic flux by inhibiting cytosolic Ca^{2+}-dependent autophagosome-lysosome fusion in primary rat proximal tubular cells. *Toxicology*, *383*, 13–23. https://doi.org/10.1016/j.tox.2017.03.016
- Liu, H., Guo, H., Jian, Z., Cui, H., Fang, J., Zuo, Z., ... & Zhao, L. (2020). Copper induces oxidative stress and apoptosis in the mouse liver. *Oxidative medicine and cellular longevity*, *2020*.
- Liu, H., Guo, H., Jian, Z., Cui, H., Fang, J., Zuo, Z., ... & Zhao, L. (2020). Copper induces oxidative stress and apoptosis in the mouse liver. Oxidative medicine and cellular longevity, 2020(1), 1359164.
- Liu, L., Sun, M., Li, Q., Zhang, H., Alvarez, P. J., Liu, H., & Chen, W. (2014). Genotoxicity and cytotoxicity of cadmium sulfide nanomaterials to mice: comparison between nanorods and nanodots. *Environmental Engineering Science*, *31*(7), 373-380.
- Liu, L., Zhou, Q., Lin, C., He, L., & Wei, L. (2021). Histological alterations, oxidative stress, and inflammatory response in the liver of swamp eel (Monopterus albus) acutely exposed to copper. *Fish Physiology and Biochemistry*, *47*, 1865-1878.
- Liu, T., Liang, X., Lei, C., Huang, Q., Song, W., Fang, R., Li, C., Li, X., Mo, H., Sun, N., Lv, H., & Liu, Z. (2020). High-Fat Diet Affects Heavy Metal Accumulation and Toxicity to Mice Liver and Kidney Probably via Gut Microbiota. *Frontiers in microbiology*, *11*, 1604. https://doi.org/10.3389/fmicb.2020.01604
- Lomer, M. C., Thompson, R. P., & Powell, J. J. (2002). Fine and ultrafine particles of the diet: influence on the mucosal immune response and association with Crohn's disease. *Proceedings of the Nutrition Society*, *61*(1), 123-130.

- Lopez, E., Figueroa, S., Oset-Gasque, M. J., & Gonzalez, M. P. (2003). Apoptosis and necrosis: two distinct events induced by cadmium in cortical neurons in culture. *British journal of pharmacology*, *138*(5), 901-911.
- Lopotych, N., Panas, N., Datsko, T., & Slobodian, S. (2020). Influence of heavy metals on hematologic parameters, body weight gain and organ weight in rats. *Ukrainian Journal of Ecology*, *10*(1), 175-179.
- Lotfi, H., & Rezazadeh, H. (2018). Hematological and hepatic alterations among copper mine workers and office employees in a copper mine in the west of Iran, 2015. *Journal of Occupational Health and Epidemiology*, *7*(1), 30-36.
- Lu, J., Wu, D. M., Zheng, Y. L., Sun, D. X., Hu, B., Shan, Q., ... & Fan, S. H. (2009). Trace amounts of copper exacerbate beta amyloid-induced neurotoxicity in the cholesterol-fed mice through TNF-mediated inflammatory pathway. *Brain, behavior, and immunity*, *23*(2), 193-203.
- M. Nordberg & G. F. Nordberg. (2002). Heavy Metals in the Environment. "Chapter 8," in B. Sarkar, Marcel Dekker, New York, NY, USA, Ed., pp. 231–270.
- Madan, A. K., Bajaj, S., & Dureja, H. (2013). Classification models for safe drug molecules. *Computational Toxicology: Volume II*, 99-124.
- Maharajan, A., Kitto, M. R., Paruruckumani, P. S., & Ganapiriya, V. (2016). Histopathology biomarker responses in Asian sea bass, Lates calcarifer (Bloch) exposed to copper. *The Journal of Basic and Applied Zoology*, *77*, 21-30.
- Malomo, S. O. (2000). Toxicological implication of ceftriaxone administration in rats. *Nig J Biochem Mol Biol*, *15*(1), 33-8.
- Malvy, E., Thiébaut, R., Marimoutou, C., Dabis, F., & Groupe d'Epidemiologie Clinique du Sida en Aquitaine (2001). Weight loss and body mass index as predictors of HIV disease progression to AIDS in adults. Aquitaine cohort, France, 1985-1997. *Journal of the American College of Nutrition*, *20*(6), 609–615. https://doi.org/10.1080/07315724.2001.10719065
- Mannhold, R., Poda, G. I., Ostermann, C., & Tetko, I. V. (2009). Calculation of molecular lipophilicity: State-of-the-art and comparison of log P methods on

more than 96,000 compounds. *Journal of pharmaceutical sciences*, *98*(3), 861-893.

- Manyasree, D., Peddi, K. M., & Ravikumar, R. (2017). CuO nanoparticles: synthesis, characterization and their bactericidal efficacy. *Int J Appl Pharmaceut*, *9*(6), 71-74.
- Markiewicz-Górka, I., Chowaniec, M., Martynowicz, H., Wojakowska, A., Jaremków, A., Mazur, G., ... & Gać, P. (2022). Cadmium body burden and inflammatory arthritis: a pilot study in patients from lower silesia, Poland. *International Journal of Environmental Research and Public Health*, *19*(5), 3099.
- Markiewicz-Górka, I., Pawlas, K., Jaremków, A., Januszewska, L., Pawłowski, P., & Pawlas, N. (2019). Alleviating effect of α-lipoic acid and magnesium on cadmium-induced inflammatory processes, oxidative stress and bone metabolism disorders in Wistar rats. *International journal of environmental research and public health*, *16*(22), 4483.
- Maruna, R. F. (1957). Serum sodium determination; critical study on colorimetric determination and method. *Clinica chimica acta; international journal of clinical chemistry*, *2*(6), 581-585.
- Matović, V., Buha, A., Bulat, Z., & Đukić-Ćosić, D. (2011). Cadmium toxicity revisited: focus on oxidative stress induction and interactions with zinc and magnesium. *Arhiv za higijenu rada i toksikologiju*, *62*(1), 65-75.
- Matović, V., Buha, A., Đukić-Ćosić, D., & Bulat, Z. (2015). Insight into the oxidative stress induced by lead and/or cadmium in blood, liver and kidneys. *Food and chemical toxicology: an international journal published for the British Industrial Biological Research Association*, *78*, 130–140. https://doi.org/10.1016/j.fct.2015.02.011
- Matović, V., Dukić-Ćosić, D., Buha, A., & Bulat, Z. (2013). Route, dose and duration of exposure to cadmium-relevance to oxidative stress induction. *Peroxidases: Biochemical Characteristics, Functions and Potential Applications*, 159-175.

- Mazzali, M., Kanellis, J., Han, L., Feng, L., Xia, Y. Y., Chen, Q., Kang, D. H., Gordon, K. L., Watanabe, S., Nakagawa, T., Lan, H. Y., & Johnson, R. J. (2002). Hyperuricemia induces a primary renal arteriolopathy in rats by a blood pressure-independent mechanism. *American journal of physiology. Renal physiology*, *282*(6), F991–F997.
- Mendes de Oliveira, E., Silva, J. C., Ascar, T. P., Sandri, S., Marchi, A. F., Migliorini, S., Nakaya, H. T. I., Fock, R. A., & Campa, A. (2022). Acute Inflammation Is a Predisposing Factor for Weight Gain and Insulin Resistance. *Pharmaceutics*, *14*(3), 623. https://doi.org/10.3390/pharmaceutics14030623
- Micali, A., Pallio, G., Irrera, N., Marini, H., Trichilo, V., Puzzolo, D., ... & Minutoli, L. (2018). Flavocoxid, a natural antioxidant, protects mouse kidney from cadmium-induced toxicity. *Oxidative medicine and cellular longevity*.
- Mierzejewski, K., Paukszto, Ł., Kurzyńska, A., Kunicka, Z., Jastrzębski, J. P., Makowczenko, K. G., ... & Bogacka, I. (2022). PPARγ regulates the expression of genes involved in the DNA damage response in an inflamed endometrium. *Scientific Reports*, *12*(1), 4026.
- Miller, A. (1987). IARC monographs on the evaluation of the carcinogenic risk of chemicals to humans. Vol. 38. Tobacco smoking: International Agency for Research on Cancer, Lyon, 1986. pp. 421.
- Mire, S. E., & Snow, L. D. (1986). Evaluation of the polyethylene glycol precipitation method for the estimation of chicken high density lipoprotein cholesterol. *Comparative Biochemistry and physiology. B, Comparative Biochemistry*, *84*(1), 105-110.
- Mitra, S., Chakraborty, A. J., Tareq, A. M., Emran, T. B., Nainu, F., Khusro, A., ... & Simal-Gandara, J. (2022). Impact of heavy metals on the environment and human health: Novel therapeutic insights to counter the toxicity. *Journal of King Saud University-Science*, *34*(3), 101865.
- Mohapatra, A. K., Datta, S. H. I. V. I. K. A., & Kumari, P. O. O. N. A. M. (2013). Genotoxic and histopathological effects of cadmium in male swiss albino mice, Mus musculus. *The Bioscan*, *8*(2), 391-401.

- Moron, M. S., Depierre, J. W., & Mannervik, B. (1979). Levels of glutathione, glutathione reductase and glutathione S-transferase activities in rat lung and liver. *Biochimica et biophysica acta*, *582*(1), 67–78.
- Moschini, E., Colombo, G., Chirico, G., Capitani, G., Dalle-Donne, I., & Mantecca, P. (2023). Biological mechanism of cell oxidative stress and death during short-term exposure to nano CuO. *Scientific Reports*, *13*(1), 2326.
- Mostafa, H., Alaa-Eldin, E., & Abouhashem, N. (2015). Neurotoxic and Genotoxic Potentials of Short-Term Copper Exposure in Adult Male Albino Rats (Biochemical, Histopathological, Immunohistochemical and Genotoxic Study). *Ain Shams Journal of Forensic Medicine and Clinical Toxicology*, *24*(1), 21-30.
- National Institutes of Health (NIH). (2023). Apoptosis. *National Human Genome Research Institute*.
- Nawrot, T. S., Staessen, J. A., Roels, H. A., Munters, E., Cuypers, A., Richart, T., ... & Vangronsveld, J. (2010). Cadmium exposure in the population: from health risks to strategies of prevention. *Biometals*, *23*, 769-782.
- Nawrot, T., Plusquin, M., Hogervorst, J., Roels, H. A., Celis, H., Thijs, L., ... & Staessen, J. A. (2006). Environmental exposure to cadmium and risk of cancer: a prospective population-based study. *The lancet oncology*, *7*(2), 119-126.
- Naz, S., Gul, A., & Zia, M. (2020). Toxicity of copper oxide nanoparticles: a review study. *IET nanobiotechnology*, *14*(1), 1-13.
- Naz, S., Gul, A., Zia, M., & Javed, R. (2023). Synthesis, biomedical applications, and toxicity of CuO nanoparticles. *Applied Microbiology and Biotechnology*, *107*(4), 1039-1061.
- Nechytailo, L., Danyliv, S., Kuras, L., Shkurashivska, S., & Buchko, A. (2023). Dynamics of changes in cadmium levels in environmental objects and its impact on the bio-elemental composition of living organisms. *Brazilian Journal of Biology*, *84*, e271324.
- Nedzvetsky, V. S., Gasso, V. Y., Hahut, A. M., & Hasso, I. A. (2020). Glial cytotoxicity of low doses of cadmium as a model of heavy metal pollution influence on vertebrates. *Ecology and Noospherology*, *31*(1), 3-10.

- Nikolić, R., Krstić, N., Jovanović, J., Kocić, G., Cvetković, T. P., & Radosavljević-Stevanović, N. (2015). Monitoring the toxic effects of Pb, Cd and Cu on hematological parameters of Wistar rats and potential protective role of lipoic acid and glutathione. *Toxicology and Industrial Health*, *31*(3), 239-246.
- Nishimura, Y., Kanda, Y., Sone, H., & Aoyama, H. (2021). Oxidative stress as a common key event in developmental neurotoxicity. *Oxidative medicine and cellular longevity*, *2021*(1), 6685204.
- Nordberg, M., & Nordberg, G. F. (2022). Metallothionein and cadmium toxicology—Historical review and commentary. *Biomolecules*, *12*(3), 360.
- Noureen, A., Jabeen, F., Tabish, T. A., Yaqub, S., Ali, M., & Chaudhry, A. S. (2018). Assessment of copper nanoparticles (Cu-NPs) and copper (II) oxide (CuO) induced hemato-and hepatotoxicity in Cyprinus carpio. *Nanotechnology*, *29*(14), 144003.
- Nwokocha, C. R., Nwokocha, M. I., Owu, D. U., Edidjana, E., Nwogbo, N., Ekpo, U., & Ufearo, C. S. (2011). Estimation of absorbed cadmium in tissues of male and female albino rats through different routes of administration. *Nigerian Journal of Physiological Sciences*, *26*(1).
- Oberdörster, G., Oberdörster, E., & Oberdörster, J. (2005). Nanotoxicology: an emerging discipline evolving from studies of ultrafine particles. *Environmental health perspectives*, *113*(7), 823-839.
- OECD. (1992). OECD Guidelines for the testing of chemical substances, No. 420 Acute oral toxicity - fixed dose method. Paris: Organisation for Economic Co-operation and Development.
- OECD. (1996). OECD Guidelines for Testing of Chemicals, No 423: Acute Oral Toxicity-Acute Toxic Class Method. Paris: Organisation for Economic Co-operation and Development.
- OECD. (2001). OECD Guidelines for Testing of Chemicals, No 425: Up-and-Down Procedure. Paris: Organisation for Economic Co-operation and Development.

- Ognik, K., Cholewińska, E., Tutaj, K., Cendrowska-Pinkosz, M., Dworzański, W., Dworzańska, A., & Juśkiewicz, J. (2020). The effect of the source and dosage of dietary Cu on redox status in rat tissues. *Journal of animal physiology and animal nutrition*, *104*(1), 352-361.
- Ognjanović, B. I., Marković, S. D., Đorđević, N. Z., Trbojević, I. S., Štajn, A. Š., & Saičić, Z. S. (2010). Cadmium-induced lipid peroxidation and changes in antioxidant defense system in the rat testes: Protective role of coenzyme Q10 and Vitamin E. *Reproductive Toxicology*, *29*(2), 191-197.
- Ohkawa, H., Ohishi, N., & Yagi, K. (1979). Assay for lipid peroxides in animal tissues by thiobarbituric acid reaction. *Analytical biochemistry*, *95*(2), 351–358.
- Ojo, O. A., Rotimi, D. E., Ojo, A. B., Ogunlakin, A. D., & Ajiboye, B. O. (2023). Gallic acid abates cadmium chloride toxicity via alteration of neurotransmitters and modulation of inflammatory markers in Wistar rats. *Scientific Reports*, *13*(1), 1577.
- Olson, S. H., Xu, Y., Herzog, K., Saldia, A., DeFilippis, E. M., Li, P., ... & Kurtz, R. C. (2016). Weight loss, diabetes, fatigue, and depression preceding pancreatic cancer. *Pancreas*, *45*(7), 986-991.
- Olszowski, T., Baranowska-Bosiacka, I., Gutowska, I., & Chlubek, D. (2012). Pro-inflammatory properties of cadmium. *Acta Biochimica Polonica*, *59*(4), 475-482.
- Orr, S. E., & Bridges, C. C. (2017). Chronic kidney disease and exposure to nephrotoxic metals. *International journal of molecular sciences*, *18*(5), 1039.
- Ovie, R. O., & Asagba, S. O. (2019). Effects of Food-Chain Mediated Metal Exposures on Lipid Profile in Rats. *Asian Journal of Research in Biochemistry*, *4*(2), 1-8.
- Oyewo, E. O., & Don-Pedro, K. N. (2006). Acute toxicity and induced weight changes in laboratory tests with Mn and Cu against Tilapia guineensis(Dumeril) and Tympanotonus fuscatus(Linne). *Journal of Environmental Biology*, *37*(2), 327-334.

- Oyinloye, B. E., Adenowo, A. F., Osunsanmi, F. O., Ogunyinka, B. I., Nwozo, S. O., & Kappo, A. P. (2016). Aqueous extract of Monodora myristica ameliorates cadmium-induced hepatotoxicity in male rats. *SpringerPlus*, *5*, 641. https://doi.org/10.1186/s40064-016-2228-z
- Özçelik, D., Toplan, S., Özdemir, S., & Akyolcu, M. C. (2002). Effects of excessive copper intake on hematological and hemorheological parameters. *Biological Trace Element Research*, *89*, 35-42.
- Padilla, M. A., Elobeid, M., Ruden, D. M., & Allison, D. B. (2010). An examination of the association of selected toxic metals with total and central obesity indices: NHANES 99-02. *International journal of environmental research and public health*, *7*(9), 3332–3347. https://doi.org/10.3390/ijerph7093332
- Paesano, L., Perotti, A., Buschini, A., Carubbi, C., Marmiroli, M., Maestri, E., ... & Marmiroli, N. (2016). Markers for toxicity to HepG2 exposed to cadmium sulphide quantum dots; damage to mitochondria. *Toxicology*, *374*, 18-28.
- Palipoch, S., & Koomhin, P. (2015). Oxidative stress-associated pathology: a review. *Sains Malaysiana*, *44*(10), 1441-1451.
- Pan, J., Plant, J. A., Voulvoulis, N., Oates, C. J., & Ihlenfeld, C. (2010). Cadmium levels in Europe: implications for human health. *Environmental geochemistry and health, 32*, 1-12.
- Pandareesh, M. D., Babu, M. R., Vijayalakshmi, K., & Titus, D. J. (2023). Oxidative stress and neuroinflammatory responses associated with metal toxicity in brain disorders. *Frontiers in Neurology*, *14*, 1283653.
- Pandey, V., Polaka, S., Nalla, L. V., Tekade, M., Sharma, M. C., & Tekade, R. K. (2022). Excipient toxicity and safety. In *Pharmacokinetics and Toxicokinetic Considerations* (pp. 487-511). Academic Press.
- Pantic, S., Radojevic Skodric, S., Loncar, Z., & Pantic, I. (2019). Neurotoxocity, nephrotoxicity, and hepatotoxicity of copper-based nanoparticles: potential implications in molecular medicine and neurosciences. *Reviews on Advanced Materials Science*, *58*(1), 201-205.

- Papp, A., Oszlánczi, G., Horváth, E., Paulik, E., Kozma, G., Sápi, A., ... & Szabó, A. (2012). Consequences of subacute intratracheal exposure of rats to cadmium oxide nanoparticles: electrophysiological and toxicological effects. *Toxicology and Industrial Health*, *28*(10), 933-941.
- Parthasarathi, R., & Dhawan, A. (2018). In silico approaches for predictive toxicology. In *In vitro toxicology* (pp. 91-109). Academic Press.
- Pelegrino, M. T., Kohatsu, M. Y., Seabra, A. B., Monteiro, L. R., Gomes, D. G., Oliveira, H. C., ... & Lange, C. N. (2020). Effects of copper oxide nanoparticles on growth of lettuce (Lactuca sativa L.) seedlings and possible implications of nitric oxide in their antioxidative defense. *Environmental Monitoring and Assessment*, *192*, 1-14.
- Pereira, T. C. B., Campos, M. M., & Bogo, M. R. (2016). Copper toxicology, oxidative stress and inflammation using zebrafish as experimental model. *Journal of Applied Toxicology*, *36*(7), 876-885.
- Perelshtein, I., Lipovsky, A., Perkas, N., Gedanken, A., Moschini, E., & Mantecca, P. (2015). The influence of the crystalline nature of nano-metal oxides on their antibacterial and toxicity properties. *Nano Research*, *8*, 695-707.
- Persichini, T., Percario, Z., Mazzon, E., Colasanti, M., Cuzzocrea, S., & Musci, G. (2006). Copper activates the NF-κB pathway in vivo. *Antioxidants and redox signaling*, *8*(9-10), 1897-1904.
- Pires, D. E., Blundell, T. L., & Ascher, D. B. (2015). pkCSM: Predicting Small-Molecule Pharmacokinetic and Toxicity Properties Using Graph-Based Signatures. *Journal of medicinal chemistry*, *58*(9), 4066–4072. https://doi.org/10.1021/acs.jmedchem.5b00104
- Prasanna, S., & Doerksen, R. J. (2009). Topological polar surface area: a useful descriptor in 2D-QSAR. *Current medicinal chemistry*, *16*(1), 21–41. https://doi.org/10.2174/092986709787002817
- Raehsler, S. L., Marietta, E. V., & Murray, J. A. (2018). Accumulation of heavy metals in people on a gluten-free diet. *Clinical Gastroenterology and Hepatology*, *16*(2), 244-251.

- Rafati Rahimzadeh, M., Rafati Rahimzadeh, M., Kazemi, S., & Moghadamnia, A. A. (2017). Cadmium toxicity and treatment: An update. *Caspian journal of internal medicine*, *8*(3), 135–145. https://doi.org/10.22088/cjim.8.3.135
- Rafati Rahimzadeh, M., Rafati Rahimzadeh, M., Kazemi, S., & Moghadamnia, A. A. (2024). Copper Poisoning with Emphasis on Its Clinical Manifestations and Treatment of Intoxication. *Advances in Public Health*, *2024*(1), 6001014.
- Raies, A. B., & Bajic, V. B. (2016). In silico toxicology: computational methods for the prediction of chemical toxicity. *Wiley Interdisciplinary Reviews: Computational Molecular Science*, *6*(2), 147-172.
- Rajkumar, V., & Gupta, M. (2021). Heavy metal toxicity. *StatPearls.*
- Rama, R., & García, J. C. (2016). Excitotoxicity and oxidative stress in acute stroke. *Ischemic Stroke Updates*, 17-33.
- Ramos-Zúñiga, J., Bruna, N., & Pérez-Donoso, J. M. (2023). Toxicity mechanisms of copper nanoparticles and copper surfaces on bacterial cells and viruses. *International Journal of Molecular Sciences*, *24*(13), 10503.
- Rana, K., Verma, Y., & Rana, S. V. S. (2021). Possible mechanisms of liver injury induced by cadmium sulfide nanoparticles in rat. *Biological Trace Element Research*, *199*(1), 216-226.
- Raul, P. K., Senapati, S., Sahoo, A. K., Umlong, I. M., Devi, R. R., Thakur, A. J., & Veer, V. (2014). CuO nanorods: a potential and efficient adsorbent in water purification. *RSC Advances*, *4*(76), 40580-40587.
- Reed, J. C. Proapoptotic multidomain Bcl-2/Bax-family proteins: mechanisms, physiological roles, and therapeutic opportunities. Cell Death Difer. 13, 1378–1386 (2006)
- Reitman, S., & Frankel, S. (1957). A colorimetric method for the determination of serum glutamic oxal-acetic and glutamic pyruvic transaminases. *American journal of clinical pathology*, *28*(1), 56–63.
- Ren, C., Ren, L., Yan, J., Bai, Z., Zhang, L., Zhang, H., ... & Li, X. (2021). Transcription profiling of cadmium-exposed livers reveals alteration of lipid metabolism and predisposition to hepatic steatosis. *Xenobiotica*, *51*(11), 1271-1281.

- Ren, C., Ren, L., Yan, J., Bai, Z., Zhang, L., Zhang, H., ... & Li, X. (2021). Cadmium causes hepatopathy by changing the status of DNA methylation in the metabolic pathway. *Toxicology Letters*, *340*, 101-113.
- Rhodes, C., Thomas, M., Athis, J., Ballantyne, B., Marrs, T., & Turner, P. (1993). Principles of testing for acute toxic effects. *Stockton Press, New York, NY(USA). 1993.*
- Rombel-Bryzek, A., Rajfur, M., Żuk, O., & Zając, P. (2018). The Effect of Cadmium on Oxidative Stress in. *Ecological Chemistry and Engineering S*, *25*(3), 457-467.
- Rossman, T. G., Roy, N. K., & Lin, W. C. (1992). Is cadmium genotoxic?. *IARC scientific publications*, (118), 367–375.
- Ruczaj, A., & Brzóska, M. M. (2023). Environmental exposure of the general population to cadmium as a risk factor of the damage to the nervous system: A critical review of current data. *Journal of Applied Toxicology*, *43*(1), 66-88.
- Saha, P., Talukdar, A. D., & Nath, R. (2022). Oxidative Stress as a Detrimental Factor in Various Clinical Pathology. In *Biotechnological Advances for Microbiology, Molecular Biology, and Nanotechnology* (pp. 227-243). Apple Academic Press.
- Saied, A. F., Al-Taee, S. K., & Al-Taee, N. T. (2022). Morphohistopathological alteration in the gills and central nervous system in Cyprinus carpio exposed to lethal concentration of copper sulfate. *Iraqi Journal of Veterinary Sciences*, *36*(4), 981-989.
- Sajjad, H., Sajjad, A., Haya, R. T., Khan, M. M., & Zia, M. (2023). Copper oxide nanoparticles: In vitro and in vivo toxicity, mechanisms of action and factors influencing their toxicology. *Comparative Biochemistry and Physiology Part C: Toxicology and Pharmacology*, 109682.
- Sanjeev, S., Bidanchi, R. M., Murthy, M. K., Gurusubramanian, G., & Roy, V. K. (2019). Influence of ferulic acid consumption in ameliorating the cadmium-induced liver and renal oxidative damage in rats. *Environmental Science and Pollution Research*, *26*(20), 20631-20653.

- Sarkar, A., Das, J., Manna, P., & Sil, P. C. (2011). Nano-copper induces oxidative stress and apoptosis in kidney via both extrinsic and intrinsic pathways. *Toxicology*, *290*(2-3), 208-217.
- Satarug, S., Vesey, D. A., & Gobe, G. C. (2017). Current health risk assessment practice for dietary cadmium: Data from different countries. *Food and Chemical Toxicology*, *106*, 430-445.
- SC, Bondy. (1997). Free-radical-mediated toxic injury to the nervous system. *Free radical toxicology*, 221-248.
- Schlesinger, P. H. (2023). *Apoptosis*. *Encyclopedia Britannica*.
- Schoenfeld, R. G., & Lewellen, C. J. (1964). A colorimetric method for determination of serum chloride. *Clinical chemistry*, *10*, 533–539.
- Serasanambati, M., & Chilakapati, S. R. (2016). Function of nuclear factor kappa B (NF-kB) in human diseases-a review. *South Indian Journal of Biological Sciences*, *2*(4), 368-87.
- Shafaei, N., Barkhordar, S. M. A., Rahmani, F., Nabi, S., Idliki, R. B., Alimirzaei, M., ... & Oskoueian, E. (2020). Protective effects of Anethum graveolens seed's oil nanoemulsion against cadmium-induced oxidative stress in mice. *Biological trace element research*, *198*, 583-591.
- Shelley, J. M. (2005). In Vitro Toxicity of Cadmium Oxide Particles in BRL 3A Rat Liver Cells.
- Shojaei, A., Semnanian, S., Janahmadi, M., Moradi-Chameh, H., Firoozabadi, S. M., & Mirnajafi-Zadeh, J. (2014). Repeated transcranial magnetic stimulation prevents kindling-induced changes in electrophysiological properties of rat hippocampal CA1 pyramidal neurons. *Neuroscience*, *280*, 181-192.
- Singhal, R. K., Anderson, M. E., & Meister, A. (1987). Glutathione, a first line of defense against cadmium toxicity. *FASEB journal: official publication of the Federation of American Societies for Experimental Biology*, *1*(3), 220–223. https://doi.org/10.1096/fasebj.1.3.2887478

- Sizova, E., Miroshnikov, S., Polyakova, V., Gluschenko, N., & Skalny, A. (2011). Copper nanoparticles as modulators of apoptosis and structural changes in tissues.
- Smoke, T., & Smoking, I. (2004). IARC monographs on the evaluation of carcinogenic risks to humans. *IARC, Lyon*, *1*, 1-1452.
- Solenkova, N. V., Newman, J. D., Berger, J. S., Thurston, G., Hochman, J. S., & Lamas, G. A. (2014). Metal pollutants and cardiovascular disease: mechanisms and consequences of exposure. *American heart journal*, *168*(6), 812-822.
- Song, G., Lin, L., Liu, L., Wang, K., Ding, Y., Niu, Q., ... & Guo, S. (2017). Toxic Effects of Anatase Titanium Dioxide Nanoparticles on Spermatogenesis and Testicles in Male Mice. *Polish Journal of Environmental Studies*, *26*(6).
- Song, M. F., Li, Y. S., Kasai, H., & Kawai, K. (2012). Metal nanoparticle-induced micronuclei and oxidative DNA damage in mice. *Journal of clinical biochemistry and nutrition*, *50*(3), 211-216.
- Soria, N. C., Aga, D. S., & Atilla-Gokcumen, G. E. (2019). Lipidomics reveals insights on the biological effects of copper oxide nanoparticles in a human colon carcinoma cell line. *Molecular Omics*, *15*(1), 30-38.
- Souza-Arroyo, V., Fabián, J. J., Bucio-Ortiz, L., Miranda-Labra, R. U., Gomez-Quiroz, L. E., & Gutiérrez-Ruiz, M. C. (2022). The mechanism of the cadmium-induced toxicity and cellular response in the liver. *Toxicology*, *480*, 153339.
- Stepankov, M. S., Zemlyanova, M. A., Zaitseva, N. V., Ignatova, A. M., & Nikolaeva, A. E. (2021). Features of bioaccumulation and toxic effects of copper (II) oxide nanoparticles under repeated oral exposure in rats. *Pharmaceutical Nanotechnology*, *9*(4), 288-297.
- STEVENS, K. R. (1982). Practical considerations in the conduct of chronic toxicity studies. *Principles and methods of toxicology*.
- Stogdale, L. (1978). Chronic copper poisoning in dairy cows. *Australian Veterinary Journal*, *54*(3), 139-141.

- Sun, X., Wang, Y., Jiang, T., Yuan, X., Ren, Z., Tuffour, A., ... & Shi, H. (2021). Nephrotoxicity profile of cadmium revealed by proteomics in mouse kidney. *Biological Trace Element Research*, *199*, 1929-1940.
- Sutton, D. J., & Tchounwou, P. B. (2007). Mercury induces the externalization of phosphatidyl-serine in human renal proximal tubule (HK-2) cells. *International journal of environmental research and public health*, *4*(2), 138-144.
- Świergosz-Kowalewska, R. (2001). Cadmium distribution and toxicity in tissues of small rodents. *Microscopy research and technique*, *55*(3), 208-222.
- Taha, M. M., Mahdy-Abdallah, H., Shahy, E. M., Ibrahim, K. S., & Elserougy, S. (2018). Impact of occupational cadmium exposure on bone in sewage workers. *International journal of occupational and environmental health*, *24*(3-4), 101-108.
- Tai, Y. T., Chou, S. H., Cheng, C. Y., Ho, C. T., Lin, H. C., Jung, S. M., ... & Ko, F. H. (2022). The preferential accumulation of cadmium ions among various tissues in mice. Toxicol Rep 9: 111–119.
- Tang, H., Xu, M., Luo, J., Zhao, L., Ye, G., Shi, F., ... & Li, Y. (2019). Liver toxicity assessments in rats following sub-chronic oral exposure to copper nanoparticles. *Environmental Sciences Europe*, *31*(1), 1-14.
- Tang, J., Zhang, N., Chen, S., Hu, K., Li, Y., Fang, Y., ... & Xu, L. (2023). Cadmium (Cd) and 2, 2′, 4, 4′-tetrabromodiphenyl ether (BDE-47) co-exposure induces acute kidney injury through oxidative stress and RIPK3-dependent necroptosis. *Environmental Toxicology*, *38*(10), 2332-2343.
- Tatiana, R. (2018). Proinflammatory Cytokines IL-2, IL-6 and TNF Alpha as Immunoseralogic Indicators of Chronic Viral Hepatitis B and C in Children. *Universal Journal of Medical Science* *6*(1), 1–7. https://doi.org/10.13189/ujmsj.2018.060101
- Tchounwou, P. B., Ishaque, A. B., & Schneider, J. (2001). Cytotoxicity and transcriptional activation of stress genes in human liver carcinoma cells (HepG2) exposed to cadmium chloride. *Molecular and Cellular Biochemistry*, *222*, 21-28.

- Teeri, A. E., & Sesin, P. G. (1958). Determination of potassium in blood serum. *American journal of clinical pathology*, *29*, 86-89.
- Thévenod, F. (2003). Nephrotoxicity and the Proximal Tubule Insights from Cadmium. *Nephron Physiology*, *93*(4), p87-p93.
- Thévenod, F. (2009). Cadmium and cellular signaling cascades: to be or not to be?. *Toxicology and applied pharmacology*, *238*(3), 221-239.
- Thrall, M. A., & Weiser, M. G. (2002). Laboratory procedures for veterinary technicians. *Missouri: Mosby Inc*.
- Tinkov, A. A., Gritsenko, V. A., Skalnaya, M. G., Cherkasov, S. V., Aaseth, J., & Skalny, A. V. (2018). Gut as a target for cadmium toxicity. *Environmental Pollution*, *235*, 429-434.
- Titov, E. A., Sosedova, L. M., Kapustina, E. A., Yakimova, N. L., Novikov, M. A., Lisetskaya, L. G., & Lizarev, A. V. (2021). Analysis of the toxicity of a Cu 2 O nanocomposite encapsulated in a polymer matrix of arabinogalactan. *Nanobiotechnology Reports*, *16*, 537-542.
- Todić, M., Bakić, S., Begović, B., Krošnjar, S., & Zulić, I. (2003). Food and water consumption in assessment of acute oral toxicity of HEPALIP FORTE in rats. *Biomolecules and Biomedicine*, *3*(4), 47-53.
- Tokino, T., & Nakamura, Y. (2000). The role of p53-target genes in human cancer. *Critical reviews in oncology/hematology*, *33*(1), 1-6.
- Toxicity–Up, A. O. (2001). OECD guideline for testing of chemicals. Organisation for Economic Co-Operation and Development: Paris, France.
- Trinder, P. (1952). The determination of cholesterol in serum. *Analyst 77*, 321.
- Trinder, P. (1969a). Enzymatic Calorimetric Determination of Triglycerides by GOP-PAP Method. *Annals of Clinical Biochemistry*, *6*, 24-27.
- Trinder, P. (1969b). Enzymatic determination of glucose in blood serum. *Annals of Clinical Biochemistry*, *6*, 24.
- Tulinska, J., Mikusova, M. L., Liskova, A., Busova, M., Masanova, V., Uhnakova, I., ... & Mikuska, P. (2022). Copper oxide nanoparticles stimulate the immune response and decrease antioxidant defense in mice after six-week inhalation. *Frontiers in Immunology*, *13*, 874253.

- Ungureanu, E. L., & Mustatea, G. (2022). Toxicity of heavy metals. *Environmental Impact and Remediation of Heavy Metals*. IntechOpen.
- Valko, M. M. H. C. M., Morris, H., & Cronin, M. T. D. (2005). Metals, toxicity and oxidative stress. *Current medicinal chemistry*, *12*(10), 1161-1208.
- Venugopal, K., Rather, H. A., Rajagopal, K., Shanthi, M. P., Sheriff, K., Illiyas, M., ... & Maaza, M. (2017). Synthesis of silver nanoparticles (Ag NPs) for anticancer activities (MCF 7 breast and A549 lung cell lines) of the crude extract of Syzygium aromaticum. *Journal of Photochemistry and Photobiology B: Biology*, *167*, 282-289.
- Vijaya, P., Kaur, H., Garg, N., & Sharma, S. (2020). Protective and therapeutic effects of garlic and tomato on cadmium-induced neuropathology in mice. *The Journal of Basic and Applied Zoology*, *81*, 1-11.
- Vijayakumar, T. P., Benoy, M. D., Duraimurugan, J., Suresh Kumar, G., Shanavas, S., Maadeswaran, P., ... & Acevedo, R. (2022). A comparative study on visible-light-driven photocatalytic activity of CdO nanowires and gC 3 N 4/CdO hybrid nanostructure. *Journal of Materials Science: Materials in Electronics*, 1-9.
- Walum, E. (1998). Acute oral toxicity. *Environmental health perspectives*, *106*(suppl 2), 497-503.
- Wan, F., Zhong, G., Ning, Z., Liao, J., Yu, W., Wang, C., ... & Hu, L. (2020). Long-term exposure to copper induces autophagy and apoptosis through oxidative stress in rat kidneys. *Ecotoxicology and environmental safety*, *190*, 110158.
- Wan, X., Xing, Z., Ouyang, J., Liu, H., Cheng, C., Luo, T., ... & Huang, S. (2022). Histomorphological and ultrastructural cadmium-induced kidney injuries and precancerous lesions in rats and screening for biomarkers. *Bioscience Reports*, *42*(6), BSR20212516.
- Wang, B., & Du, Y. (2013). Cadmium and its neurotoxic effects. *Oxidative medicine and cellular longevity*, *2013*.
- Wang, K., Ning, X., Qin, C., Wang, J., Yan, W., Zhou, X., ... & Feng, Y. (2022). Respiratory exposure to copper oxide particles causes multiple organ

injuries via oxidative stress in a rat model. *International Journal of Nanomedicine*, *17*, 4481.

- Wang, M., Guckland, A., Murfitt, R., Ebeling, M., Sprenger, D., Foudoulakis, M., & Koutsaftis, A. (2019). Relationship between magnitude of body weight effects and exposure duration in mammalian toxicology studies and implications for ecotoxicological risk assessment. *Environmental Sciences Europe*, *31*, 1-7.
- Wang, X., Wang, H., Li, J., Yang, Z., Zhang, J., Qin, Z., ... & Kong, X. (2014). Evaluation of bioaccumulation and toxic effects of copper on hepatocellular structure in mice. *Biological trace element research*, *159*, 312-319.
- Wang, Z., Sun, Y., Yao, W., Ba, Q., & Wang, H. (2021). Effects of cadmium exposure on the immune system and immunoregulation. *Frontiers in Immunology*, *12*, 695484.
- Weydert, C. J., & Cullen, J. J. (2010). Measurement of superoxide dismutase, catalase and glutathione peroxidase in cultured cells and tissue. *Nature protocols*, *5*(1), 51-66.
- Winiarska-Mieczan, A., & Kwiecień, M. (2016). The effect of exposure to Cd and Pb in the form of a drinking water or feed on the accumulation and distribution of these metals in the organs of growing Wistar rats. *Biological Trace Element Research*, *169*, 230-236.
- Wu, B., Yang, A., Yan, J., Liu, Z., Sun, X., Zhou, L., & Zhang, G. (2019). Effects of Acute Low-Salinity Stress on the Activities of Catalase (CAT), Superoxide Dismutase (SOD) and Glutathiones-Transferase (GST) in Scapharca broughtonii. *Journal of Molecular Biology Research*, *9*(1), 172-172.
- Xie, G., Sun, J., Zhong, G., Shi, L., & Zhang, D. (2010). Biodistribution and toxicity of intravenously administered silica nanoparticles in mice. *Archives of toxicology*, *84*, 183-190.
- Xiong, G., Wu, Z., Yi, J., Fu, L., Yang, Z., Hsieh, C., Yin, M., Zeng, X., Wu, C., Lu, A., Chen, X., Hou, T., & Cao, D. (2021). ADMETlab 2.0: an integrated online platform for accurate and comprehensive predictions of ADMET

properties. *Nucleic acids research*, *49*(W1), W5–W14. https://doi.org/10.1093/nar/gkab255

- Xu, J., Song, M., Fang, Z., Zheng, L., Huang, X., & Liu, K. (2023). Applications and challenges of ultra-small particle size nanoparticles in tumour therapy. *Journal of Controlled Release*, *353*, 699-712.
- Yadav, R. S., Kant, S., Tripathi, P. M., Pathak, A. K., & Mahdi, A. A. (2022). Transcription factor NF-κB, interleukin-1β, and interleukin-8 expression and its association with tobacco smoking and severity in chronic obstructive pulmonary disease. *Gene Reports*, *26*, 101453.
- Yah, C. S., Iyuke, S. E., & Simate, G. S. (2012). A review of nanoparticles toxicity and their routes of exposures. *Iranian Journal of Pharmaceutical Sciences*, *8*(1), 299-314.
- Yahia, S. H. (2019). Measurement of Serum Uric Acid Pre and Post Hemodialysis.
- Yahya, R. A., Attia, A. M., El-Banna, S. G., El-Trass, E. E., Azab, A. E., Jbireal, J. M., & Shkal, K. E. M. (2019). Hematotoxicity induced by copper oxide and/or zinc oxide nanoparticles in male albino rats. *J Biotechnol*, *3*(4), 1-7.
- Yakubu, M. T., Adesokan, A. A., & Akanji, M. A. (2006). Biochemical changes in the liver, kidney and serum of rat following chronic administration of cimetidine. *African Journal of Biomedical Research*, *9*(3).
- Yan, L. J., & Allen, D. C. (2021). Cadmium-induced kidney injury: Oxidative damage as a unifying mechanism. *Biomolecules*, *11*(11), 1575.
- Yang, B., Bai, Y., Yin, C., Qian, H., Xing, G., Wang, S., ... & Lu, R. (2018). Activation of autophagic flux and the Nrf2/ARE signaling pathway by hydrogen sulfide protects against acrylonitrile-induced neurotoxicity in primary rat astrocytes. *Archives of Toxicology*, *92*, 2093-2108.
- Yang, B., Wang, Q., Lei, R., Wu, C., Shi, C., Wang, Q., ... & Liao, M. (2010). Systems toxicology used in nanotoxicology: mechanistic insights into the hepatotoxicity of nano-copper particles from toxicogenomics. *Journal of nanoscience and nanotechnology*, *10*(12), 8527-8537.

- Yang, H., & Shu, Y. (2015). Cadmium transporters in the kidney and cadmium-induced nephrotoxicity. *International journal of molecular sciences*, *16*(1), 1484-1494.
- Yang, H., Lou, C., Sun, L., Li, J., Cai, Y., Wang, Z., ... & Tang, Y. (2019). admetSAR 2.0: web-service for prediction and optimization of chemical ADMET properties. *Bioinformatics*, *35*(6), 1067-1069.
- Yang, X. F., Fan, G. Y., Liu, D. Y., Zhang, H. T., Xu, Z. Y., Ge, Y. M., & Wang, Z. L. (2015). Effect of cadmium exposure on the histopathology of cerebral cortex in juvenile mice. *Biological trace element research*, *165*, 167-172.
- Yaqub, A., Anjum, K. M., Munir, A., Mukhtar, H., & Khan, W. A. (2018). Evaluation of acute toxicity and effects of sub-acute concentrations of copper oxide nanoparticles (CuO-NPs) on hematology, selected enzymes and histopathology of liver and kidney in Mus musculus. *Indian Journal of Animal Research*, *52*(1), 92-98.
- Yedjou, C. G., & Tchounwou, P. B. (2006). Oxidative stress in human leukemia (HL-60), human liver carcinoma (HepG2), and human (Jurkat-T) cells exposed to arsenic trioxide. In *Metal ions in biology and medicine: proceedings of the... International Symposium on Metal Ions in Biology and Medicine held...= Les ions metalliques en biologie et en medecine: Symposium international sur les ions metalliques...* (Vol. 9, p. 298). NIH Public Access.
- Yoshida, K., & Miki, Y. (2010). The cell death machinery governed by the p53 tumour suppressor in response to DNA damage. *Cancer science*, *101*(4), 831-835.
- Youle, R. J., & Strasser, A. (2008). The BCL-2 protein family: opposing activities that mediate cell death. *Nature reviews Molecular cell biology*, *9*(1), 47-59.
- Young, J. L., Yan, X., Xu, J., Yin, X., Zhang, X., Arteel, G. E., ... & Freedman, J. H. (2019). Cadmium and high-fat diet disrupt renal, cardiac and hepatic essential metals. *Scientific reports*, *9*(1), 14675.

- Zaghloul, G. Y., Eissa, H. A., Zaghloul, A. Y., Kelany, M. S., Hamed, M. A., & Moselhy, K. M. E. (2024). Impact of some heavy metal accumulation in different organs on fish quality from Bardawil Lake and human health risks assessment. *Geochemical Transactions*, *25*(1), 1.
- Zatta, P., Raso, M., Zambenedetti, P., Wittkowski, W., Messori, L., Piccioli, F., ... & Beltramini, M. (2005). Copper and zinc dismetabolism in the mouse brain upon chronic cuprizone treatment. *Cellular and Molecular Life Sciences CMLS*, *62*, 1502-1513.
- Zhang, C. H., Wang, Y., Sun, Q. Q., Xia, L. L., Hu, J. J., Cheng, K., ... & Gu, H. (2018). Copper nanoparticles show obvious in vitro and in vivo reproductive toxicity via ERK mediated signaling pathway in female mice. *International Journal of Biological Sciences*, *14*(13), 1834.
- Zhang, H., Yan, J., Xie, Y., Chang, X., Li, J., Ren, C., ... & Li, X. (2022). Dual role of cadmium in rat liver: Inducing liver injury and inhibiting the progression of early liver cancer. Toxicology Letters, *355*, 62-81.
- Zhang, J., Wang, Y., Fu, L., Wang, B., Ji, Y. L., Wang, H., & Xu, D. X. (2019). Chronic cadmium exposure induced hepatic cellular stress and inflammation in aged female mice. *Journal of Applied Toxicology*, *39*(3), 498-509.
- Zhang, S. S., Noordin, M. M., Rahman, S. O., & Haron, J. (2000). Effects of copper overload on hepatic lipid peroxidation and antioxidant defense in rats. *Veterinary and human toxicology*, *42*(5), 261-264.
- Zhang, X. D., Wu, H. Y., Wu, D., Wang, Y. Y., Chang, J. H., Zhai, Z. B., Meng, A. M., Liu, P. X., Zhang, L. A., & Fan, F. Y. (2010). Toxicologic effects of gold nanoparticles in vivo by different administration routes. *International journal of nanomedicine*, *5*, 771–781.
- Zhao, Q., Yang, Z. S., Cao, S. J., Chang, Y. F., Cao, Y. Q., Li, J. B., ... & Wu, Y. (2019). Acute oral toxicity test and assessment of combined toxicity of cadmium and aflatoxin B1 in kunming mice. *Food and Chemical Toxicology*, *131*, 110577.

- Zhong, C. C., Zhao, T., Hogstrand, C., Song, C. C., Zito, E., Tan, X. Y., ... & Luo, Z. (2023). Copper induces liver lipotoxicity disease by up-regulating Nrf2 expression via the activation of MTF-1 and inhibition of SP1/Fyn pathway. *Biochimica et Biophysica Acta (BBA)-Molecular Basis of Disease*, *1869*(6), 166752.
- Zhou, H., Yao, L., Jiang, X., Sumayyah, G., Tu, B., Cheng, S., ... & Chen, C. (2021). Pulmonary exposure to copper oxide nanoparticles leads to neurotoxicity via oxidative damage and mitochondrial dysfunction. *Neurotoxicity Research*, *39*, 1160-1170.
- Zhou, Q. H., Song, Z. H., Jin, X. D., Liu, Y. H., Qian, Z. Y., & Wang, C. Y. (2023). Study on reproductive toxicity of nano-cadmium sulfide with different particle sizes on male mice. *Zhonghua lao Dong wei Sheng zhi ye Bing za zhi= Zhonghua Laodong Weisheng Zhiyebing Zazhi= Chinese Journal of Industrial Hygiene and Occupational Diseases*, *41*(12), 887-892.
- Zhou, Q., Zhu, J., Liu, B., Qiu, J., Lu, X., Curtin, B., Ji, F., & Yu, D. (2021). Effects of High-Dose of Copper Amino Acid Complex on Laying Performance, Hematological and Biochemical Parameters, Organ Index, and Histopathology in Laying Hens. *Biological trace element research*, *199*(8), 3045–3052. https://doi.org/10.1007/s12011-020-02406-2
- Zhu, Y., Cheng, P., Peng, J., Liu, S., Xiang, J., Xu, D., ... & Sheng, J. (2024). Cadmium exposure causes transcriptomic dysregulation in adipose tissue and associated shifts in serum metabolites. *Environment International*, *185*, 108513.
- Zinia, S. S., Yang, K. H., Lee, E. J., Lim, M. N., Kim, J., & Kim, W. J. (2023). Effects of heavy metal exposure during pregnancy on birth outcomes. *Scientific Reports*, *13*(1), 18990.
- Zuckerman, M., Greller, H. A., & Babu, K. M. (2015). A review of the toxicologic implications of obesity. *Journal of Medical Toxicology*, *11*, 342-354.

Brief Biodata of the Candidate

Name : Bhanushree Baishya

Father's name : Nanda Baishya

Date of Birth : 07/11/1994

Marital status : Unmarried

Nationality : Indian

Religion : Hindu

Contact : 6001034747

Email ID : bhanushreebaishya55@gmail.com

Address : Chapanala, Nagaon, Assam, India-782135.

Educational qualification:

Name of exam	Year	Board/University	Subject	Percentage	Division
B.SC	2016	Gauhati University	Zoology	90.00	1st
M.SC	2018	Gauhati University	Zoology	83.10	1st

CONFERENCE/WORKSHOP/

SEMINAR

Conference/workshop/seminar attended

- **Oral presentation** in "International conference on Biodiversity, Food Security, Sustainability & Climate Change (ICBFSCC-2023)" on **"ROS-dependent BAX/BCL-2 and Caspase-3 pathway-mediated apoptosis in liver and kidney induced by copper nanoparticles in Swiss albino mice,"** on 24th to 28th April, 2023, organized by Assam Agriculture University (AAU), Jorhat and Prof. H. S Srivastava Foundation for Science, Lucknow.

- **Oral presentation** in "Indian Conference on Bioinformatics 2021 (InBix2021)" on **"*In silico* screening of potent bioactive compounds from Manuka honey as an alternative drug to control SARS-CoV-2,"** on 11th to 13th November, 2021, organized by CSIR-North East Institute of Science and Technology, Jorhat, Assam.

- Participated in National workshop on **"One-week training program on Instruments in Biotechnology: Theories and practices,"** from 30th May to 5th June, 2022, organized by STUTI (DST) in collaboration with Department of Biotechnology, Mizoram University, Aizawl.

- Participated in UGC STRIDE workshop on **"Basic and advanced molecular biology techniques,"** from 7th to 11th June, 2021, organized by Mizoram University, Aizawl.

- Participated in UGC STRIDE workshop on **"Sequence to Database & Database to Sequence,"** from 6th to 12th January, 2021, organized by Mizoram University, Aizawl-796004, Mizoram.

- Participated in UGC STRIDE workshop on **"Statistical Data Analysis and Interpretation,"** from 13th to18th January, 2021, organized by Mizoram University, Aizawl-796004, Mizoram.

- Participated in UGC STRIDE workshop on **"Molecular Phylogeny and Molecular Docking,"** from 19th to 27th January, 2021, organized by Mizoram University, Aizawl-796004, Mizoram.

RESEARCH PUBLICATIONS

Research publications

- Bidanchi, R. M., Lalrindika, L., Khushboo, M., **Bhanushree, B.,** Dinata, R., Das, M., ... & Gurusubramanian, G. (2022). Antioxidative, anti-inflammatory and anti-apoptotic action of ellagic acid against lead acetate induced testicular and hepato-renal oxidative damages and pathophysiological changes in male Long Evans rats. *Environmental Pollution*, *302*, 119048.

- Lalrinzuali, S., Khushboo, M., Dinata, R**., Bhanushree, B.,** Nisa, N., Bidanchi, R. M., ... & Gurusubramanian, G. (2023). Long-term consumption of fermented pork fat-based diets differing in calorie, fat content, and fatty acid levels mediates oxidative stress, inflammation, redox imbalance, germ cell apoptosis, disruption of steroidogenesis, and testicular dysfunction in Wistar rats. *Environmental Science and Pollution Research*, *30*(18), 52446-52471.

- Khushboo, M., Sanjeev, S., Murthy, M. K., Sunitadevi, M., Dinata, R., **Bhanushree, B.,** ... & Gurusubramanian, G. (2023). Dietary phytoestrogen diosgenin interrupts metabolism, physiology, and reproduction of Swiss albino mice: Possible mode of action as an emerging environmental contaminant, endocrine disruptor and reproductive toxicant. *Food and Chemical Toxicology*, *176*, 113798.

- Nisa, N., Dinata, R., Arati, C., Abdelgani-Baraka, G. A., **Bhanushree, B.,** Bidanchi, R. M., ... & Gurusubramanian, G. (2023). Computational toxicology and food safety assessment of Parkia timoriana phytoconstituents using quantitative structure-activity relationship (QSAR) modeling approaches. *Indian Journal of Biochemistry and Biophysics (IJBB)*, *60*(12), 896-918.

- Roy, D., Arati, C., Manikandan, B., Abinash, G., Nisa, N., **Bhanushree, B.,** ... & Gurusubramanian, G. (2023). Pharmacological and therapeutic potential of honey bee antimicrobial peptides. *Indian Journal of Biochemistry and Biophysics (IJBB)*, 60, 365-384.

PLAGIARISM CERTIFICATE

turnitin

Similarity Report ID: oid:10015:63760270

PAPER NAME	AUTHOR
Core Bhanushree thesis.docx	Bhanu Shree

WORD COUNT	CHARACTER COUNT
28794 Words	152346 Characters
PAGE COUNT	**FILE SIZE**
140 Pages	21.0MB
SUBMISSION DATE	**REPORT DATE**
Aug 1, 2024 5:33 PM GMT+5:30	Aug 1, 2024 5:35 PM GMT+5:30

0% Overall Similarity

This submission did not match any of the content we compared it against.

- 0% Internet database
- 0% Publications database
- Crossref database
- Crossref Posted Content database
- 0% Submitted Works database

Excluded from Similarity Report

- Bibliographic material
- Quoted material
- Cited material
- Small Matches (Less then 14 words)

turnitin

Similarity Report ID: oid:10015:63760661

PAPER NAME	AUTHOR
Non-core Bhanushree thesis.docx	Bhanu Shree

WORD COUNT	CHARACTER COUNT
11742 Words	65644 Characters
PAGE COUNT	**FILE SIZE**
31 Pages	64.5KB
SUBMISSION DATE	**REPORT DATE**
Aug 1, 2024 5:34 PM GMT+5:30	Aug 1, 2024 5:35 PM GMT+5:30

9% Overall Similarity

The combined total of all matches, including overlapping sources, for each database.

- 4% Internet database
- 3% Publications database
- Crossref database
- Crossref Posted Content database
- 5% Submitted Works database

Excluded from Similarity Report

- Bibliographic material
- Quoted material
- Cited material
- Small Matches (Less then 14 words)

PARTICULARS OF THE CANDIDATE

NAME OF THE CANDIDATE	: BHANUSHREE BAISHYA
DEGREE	: DOCTOR OF PHILOSOPHY
DEPARTMENT	: ZOOLOGY
TITLE OF THESIS	: Organ specific toxicity of copper and cadmium nanoparticles in Swiss albino mice
DATE OF ADDIMISSION	: 04.11.2020

APPROVAL OF RESEARCH PROPOSAL

1. D.R.C.	: 16.04.2021
2. B.O.S.	: 20.04.2021
3. SCHOOL BOARD	: 29.04.2021
MZU REGISTRATION No.	: 2010618
Ph.D. REGISTRATION No. & DATE	: MZU/Ph.D/1540 of 04.11.2020
EXTENSION (IF ANY)	: Nil

(**Prof. H.T. Lalremsanga**)

Head
Department of Zoology
Mizoram University

ABSTRACT

ORGAN SPECIFIC TOXICITY OF COPPER AND CADMIUM NANOPARTICLES ON SWISS ALBINO MICE

AN ABSTRACT SUBMITTED IN PARTIAL FULFILLMENT OF THE REQUIREMENTS FOR THE DEGREE OF DOCTOR OF PHILOSOPHY

BHANUSHREE BAISHYA
MZU REGISTRATION NO.: 2010618
Ph.D. REGISTRATION NO.: MZU/Ph.D./1540 of 04.11.2020

DEPARTMENT OF ZOOLOGY
SCHOOL OF LIFE SCIENCES
AUGUST, 2024

ORGAN SPECIFIC TOXICITY OF COPPER AND CADMIUM NANOPARTICLES ON SWISS ALBINO MICE

By

BHANUSHREE BAISHYA

Department of Zoology

Name of the Supervisor

Prof. GURUSWAMI GURUSUBRAMANIAN

Submitted

In partial fulfillment of the requirement of the Degree of Doctor of Philosophy in Zoology of Mizoram University, Aizawl.

Abstract

1.1 Introduction

The English word **'toxic'** is a Greek derivative of the term *'toxikon'*, which in the context of medical sciences means any substance that can harm animals as well as humans. In Greek, the word *'toxon'* means 'bow' or 'arrow', and later from this term came the word *'toxikon',* which means 'a poison in which arrows are dipped' **(Laios et al., 2021)**. Hence, the adjective **toxicity** can be defined as the degree to which a substance can harm our environment, animals, humans, etc. The study of all noxious substances that have detrimental impacts on organisms and the environment is known as **toxicology (Naz, et al., 2020)**.

Naturally occurring elements having a density at least five times greater than that of water and a high atomic weight usually 5 g cm^{-3} are known as **heavy metals**. There are more than sixty elements in the periodic table which are regarded as heavy metals **(Hocaoğlu-özyiğit and Genç, 2020)**. In the developing era of science and technology, the utilization of nanoparticles, in particular Metal Oxide Nanoparticles (MO-NPs), has received a lot of attention and relevance in recent years due to their diverse structural characteristics and special abilities that make them valuable for a number of applications **(Zhang et al., 2010; Yaqub et al., 2018)**.

Cadmium (Cd) is ranked as the seventh most toxic heavy metal in accordance with the rating provided by the Agency for Toxic Substances and Disease Registry (ATSDR; **Jaishankar et al., 2014; Young et al., 2019**). In contemporary times, it is also used to make specialized alloys, rechargeable batteries, coatings, pigments, and platings, as a plastic stabilizer, and additionally, their presence was detected in cigarette smoke **(Jaishankar et al., 2014)**. Cadmium oxide nanoparticles (CdO-NPs) were used in the initial manufacturing process of quantum dots, which are becoming more and more prominent in targeted therapeutics and medical diagnostic imaging **(Demir et al., 2020)**. In human, inhalation or ingestion are the main ways that leads to Cd exposure. Depending on the size of the particles, 10-50% of the Cd dust that is inhaled is absorbed. Skin contact has very little impact on absorption **(Bernhoft, 2013)**. Smoking of cigarette is one of the major sources of Cd exposure in human. A

cigarette contains about 1-2 µg of Cd and a person smoking 20 cigarettes in a day may absorb nearly 1 µg Cd **(Taha et al., 2018; Genchi et al., 2020)**.

In the era of technology and development, the application of CdO-NPs is opening new doors for researchers as it is used to treat deadly diseases, such as cancer. Although the nanoparticles have been useful to mankind in various ways, it will be ingenious to ignore the other side of the nanoparticles, which is their toxicological insight. So, there is an urgent need to understand the physiological mechanism and molecular and inflammatory pathways by which CdO-NPs induce toxicity at the cellular, tissue, and organ level. It is also thought that tracing the actual toxicological pathways may lead to the uncovering of complex effects and may help provide remedies for Cd toxicity.

Since ancient times, **copper (Cu)** has been used for various purposes in the field of electronics technology, including semiconductors, electronic chips, metal catalysts, and heat transfer nanofluids, due to their superior thermophysical properties. Additionally, the nanoparticles of copper (CuO-NP) are used in fracture and osteoporosis-treatment drugs, additives in livestock and poultry feed, intrauterine contraceptive devices, and as an alternative antimicrobial agent in many biomedical applications **(Yang et al., 2010; Assadian et al., 2017; Bugata et al., 2019)**.

CuONP have a number of interesting applications in nano-medicine, due to their outstanding antibacterial activity and promise as nosocomial infection-preventing disinfectants. These have potent antibacterial properties against several Gram +ve and Gram -ve bacterial strains, which are utilized in wound dressings **(Grigore et al., 2016; Naz et al., 2023)**. It is also known that CuONP have fungicidal effect against some fungal strains. For sensing glucose, dopamine, cholesterol, lactate, DNA, and other biomarkers, CuO-NPs are frequently utilized. Additionally, they could be quite helpful in the management of lung, breast, prostate, kidney, and glioma cancers due to their potential as antitumor agents (**Naz et al., 2023**). CuO-NPs are also used as one of the key elements of fertilizers **(Pelegrino et al., 2020; Tulinska et al., 2022)**, algaecide, fungicides, and herbicides, however they can also harm cells by oxidizing DNA and causing genotoxicity **(Song et al., 2012; Ghonimi et al., 2022)**. They are

additionally employed to remove heavy metals from waste water **(Jain et al., 2021; Li et al., 2021; Tulinska et al., 2022)**. *In vitro* and *in vivo* studies have shown that exposure to CuO-NPs induces cytotoxicity **(Assadian et al., 2018)**, genotoxicity **(Song et al., 2012; Ghonimi et al., 2022)**, apoptosis, inflammation, oxidative damage, and histopathological changes in various organs like the liver, kidney, stomach, bone **(De Jong et al., 2019; Anreddy, 2018; Tulinska et al., 2022),** and brain **(Naz et al., 2020)**.

The present study emphasized upon the toxic nature of Cd and Cu, significance of understanding the absorbed dose, route of exposure, and duration of exposure in determining the toxic effects, and also assess their ability to induce oxidative stress, apoptosis and inflammation in mice model. Understanding the distribution and effects of these heavy metals is crucial for mitigating their harmful consequences on the environment, animals and human health as a whole.

2.1 Objectives

- Computational toxicological profiling of CdO and CuO: An *in-silico* approach.
- Acute oral toxicity of CdO-NPs in Swiss albino mice
- To assess antioxidant status, oxidative stress parameter, histopathology, and pathways of organ toxicity induced by cadmium nanoparticles in adult mice.
- Evaluation of oxidative stress, antioxidant status, molecular mechanism and toxicological pathways that governs the organ specific toxicity in mice intoxicated with copper nanoparticles.

3.1 Materials and methods

I. *In silico* study

Computational toxicological profiling of CdO and CuO: An in-silico approach.

3.1.1 Retrieval of canonical SMILES

The canonical SMILES (Simplified Molecular-Input Line-Entry System) of Copper (II) oxide (CuO; compound ID, CID: 14829) and Cadmium (II) oxide (CdO; compound ID, CID: 14782) were retrieved from PubChem (https://pubchem.ncbi.nlm.nih.gov/) database.

3.1.2 LD_{50} dose and pathway prediction by using ProTox-II online software

ProTox-II provides us with the information on organ toxicity, toxicity endpoints, nuclear receptors signaling pathways, stress response pathways, molecular initiating events and metabolism of a chemical. The software is freely accessible for the users at http://tox.charite.de/protox_II **(Banerjee et al., 2018)**. The simple procedure to use the software is to click on the link that takes us to the homepage of the software. Then clicking on the TOX PREDICTION dialogue box, paste either PubChem name or canonical SMILES followed by clicking on the parameters that we would like to predict and finally on Tox-prediction. The results for the prediction parameters will appear on the screen.

3.1.3 ADMET profiling using pkCSM online software

pkCSM, a graph-based signature was used to know about the absorption, distribution, metabolism, excretion, and toxicity (ADMET) properties of CdO and CuO. The pkCSM is a freely usable software and it was accessed using the https://biosig.lab.uq.edu.au/pkcsm/prediction **(Pires et al., 2015)**. The canonical SMILES format was pasted in the input file section and after that clicking on the predict gave us with a link, which further showed the result of the predictions.

II. *In vivo* study

3.1.4 Animal ethics

This study was performed in strict accordance with the guiding principles approved by ARRIVE guidelines **(Du Sert et al., 2020)** for the care and use of Laboratory animals. The whole experimental procedure of using animal was approved by the Institutional Animal Ethical Committee, Mizoram University, Aizawl, Mizoram, India, bearing Approval No. MZU/IAEC/2021-22/07 dt. September 03, 2021. All the necessary measures and care were taken during and prior to the experiment to reduce the suffering and distress of the animals.

3.1.5 Test Chemical

a) Cadmium oxide nanoparticle (CdO-NPs)

CdO nano powder (size < 50 nm) was commercially purchased from Nanoshel, India (CAS No: 1306-19-0; Purity 99.9%). The particles were crystalline in structures and brown colour in appearance.

b) Copper oxide nanoparticle (CuO-NPs)

CuO-NPs purchased as black powder from Sigma-Aldrich (St. Louis, MO 63103, USA), product number 544868 and CAS number 1317-38-0. The particles were crystalline in structures having average particle size range < 50 nm (TEM).

3.1.6 Characterization of NPs

Fourier Transform Infra-Red (FTIR) spectrometry was performed using IR Affinity 1s (00703, Shimadzu, Japan) to study about the functional group **(Raul et al., 2014)**. Particle size and shape of the compound was studied by generating high resolution (HR) images under Field Emission Transmission Electron Microscopy (FETEM) **(Vijayakumar et al., 2022)** (JEOL 2100 F HR, Japan) at 200kV. Selected-area electron diffraction (SAED) pattern was investigated to find out the physical nature of the particle using TEM **(Balamurugan et al., 2016)**. The structure of the test compound was studied using X-ray diffraction (XRD- Smartlab, Rigaku, Japan) with

Cu Kα radiation operating at a wavelength (λ) of 1.5406 Å, and at a voltage (V) of 40 kV and current (A) 125 mA setting.

3.1.7 Preparation of test solution

The test solution was prepared by dissolving required amount of the test chemical in 0.9% saline solution. The solution was vigorous sonicated (PCI Analytics, India, model: 500F) so as to suspend the test chemical uniformly. Every day prior to the treatment, the test solution was sonicated for 10-15 minutes.

3.1.8 Animal maintenance

Swiss albino mice, weighing 25±5 g of the age group 2-3 weeks old and a total of thirty male and eighty female mice, were collected from the Animal Care and Housing facility, Mizoram University, Aizawl, Mizoram. The male and female mice were housed separately, five per cages, in clean and hygienic polypropylene cages and maintained in the air-conditioned set up at a temperature range of 20 ± 2 ºC, 50-70% relative humidity and under a 12-hour dark/12-hour light cycle. The mice were fed daily at regular interval with a standard commercial mouse pellet feed and ultra-pure water ad libitum. Cleaning of the cages and housing area, and monitoring of the heath conditions of mice were performed daily.

Experiment-I- Acute oral toxicity of CdO-NPs in Swiss albino mice

Acute oral toxicity test was performed in accordance with the guiding principle described by the OECD 423 guidelines **(**Acute Oral Toxicity-Acute Toxic Class Method) **(OECD, 2001)**.

3.1.9 Dosage selection, experimental groups and LD_{50} calculation

In compliance with the OECD 423 Guidelines **(OECD, 2001)**, the starting dose was selected as 5 mg/kg b.w, one of the doses from the four fixed doses (5, 50, 300 and 2000 mg/kg b.w).

Group	Dose (p.o., 1 mL/100 g b.w)	Male + Female (number; n)
I (Control)	Vehicle only	06 + 06

II	CdO-NPs 5 mg/kg b.w	06 + 06
III	CdO-NPs 25 mg/kg b.w	06 + 06
IV	CdO-NPs 50 mg.kg b.w	06 + 06
V	CdO-NPs 75 mg/kg b.w	06 + 06

The doses of CdO-NPs were increased based on the behavioral changes and moribund status of the subsequent lower doses. The acute oral toxicity for calculating lethal dose 50 (LD_{50}) was done using probit analysis **(Finney, 1971)**.

3.1.10 Sample collection

After the completion of 14^{th} day, mice were fasted for 3-4 hours and sacrificed after application of mild anesthesia, 90 mg/kg Ketamine (50-150 mg/kg b.w) and 5 mg/kg Xylazine (5-10 mg/kg b.w) with a 27G needle IP **(Shojaei et al., 2014)**. Blood and tissue sample were immediately excised, and collected for future analysis. A part of the tissue samples was fixed in Bouin's fixative containing saturated picric acid (75%), formaldehyde (25%) and glacial acetic acid (5%), and others kept for the estimation of oxidative stress, antioxidant parameters and inflammatory markers at -20°C.

3.1.11 Daily monitoring-clinical signs and symptoms, body weight, food and water consumption, rectal temperature, and organ indices

Animals were monitored closely just after treatment for 30 mins then for 4 hrs and 6-8 hrs for any sign or symptom of abnormality. And then, monitoring was done in every 24 hrs for remaining 14 days. During the period of treatment, from 1^{st} day to day 14^{th}, body weight (g), food consumption (g), water consumption (mL) and rectal temperature (°C) of each individual of the groups were measured once daily between 06:00 am to 06:00 pm. Rectal temperature was computed using a greased metallic thermocouple.

3.1.12 Hematological analysis

Blood levels of hemoglobin (Hb) was estimated by acid hematin method using Sahli's hemoglobinometer. Total red blood cell (RBC), total white blood cell

(WBC) and packed cell volume (PVC) were computed using hemocytometer **(Thrall, & Weiser, 2002)**. Additionally, RBC related indices such as mean corpuscular volume (MCV), mean corpuscular hemoglobin concentration (MCHC), and mean corpuscular hemoglobin (MCH) were calculated by following standard formulas.

3.1.13 Serum biochemical analysis

Serum sample stored at -20 °C were used for the analysis of various markers of hepato-renal functions and lipid profiles. The sample were thawed to the room temperature and various serological assays were performed both for male and female separately in triplet. Serum levels of total protein **(Gornall, et al., 1949)**, albumin **(Doumas et al., 1971)**, alkaline phosphatase (ALP, **Kind, & King, 1954)**, alanine amino-transferase (ALT, **Reitman, & Frankel, 1957)**, aspartate amino-transaminase (AST, **Reitman, & Frankel, 1957)**, creatinine **(Bonsnss, & Taussky, 1945)**, urea **(Berthelot, 1859)**, uric acid **(Yahia, 2019)** were estimated using commercially available kits (Coral Clinical systems, Goa, India) and, total and direct bilirubin **(Garber, 1981)** were quantified using diagnostic kit manufactured by Asritha Diatech India Pvt. Ltd (Euro Diagnostic systems, Chennai, India), according to the manufacturer protocol. Blood urea nitrogen (BUN), and globulin levels were computed. Similarly, ratios of AST and ALT and albumin and globulin were also measured by diving former by the latter. Further, the markers of lipid profile such as triglycerides **(Trinder, 1969a)**, cholesterol **(Trinder, 1952)**, high density lipoprotein (HDL) cholesterol **(Mire & Snow, 1986)**, were estimated by using commercial diagnostic kits (Coral Clinical systems, Goa, India), where as low density lipoprotein (LDL) cholesterol was calculated in accordance to the formula by **Freidewald et al. (1972)**. Levels of blood glucose **(Trinder, 1969b)**, calcium ion **(Gitelman, 1967)**, sodium ion **(Maruna, 1957)**, potassium ion **(Teeri & Sesin, 1958)** and chloride ion **(Schoenfeld & Lewellen, 1964)** were also assessed individually in all the groups using Coral clinical kits (Coral Clinical systems, Goa, India) following the manufacturer protocol.

3.1.14 Oxidative stress and antioxidant enzyme status

a) Tissue homogenate preparation

Tissue samples were homogenized in ice cold 1× phosphate buffer saline (PBS) constituting 137 mM sodium chloride (NaCl), 2.7 mM potassium chloride (KCl), 10 mM sodium phosphate dibasic (Na_2HPO_4), and 1.8 mM potassium phosphate monobasic (KH_2PO_4) dissolved in distilled water to produce 10% homogenate (w/v).

b) Quantification of protein in the tissue sample

Protein quantification was done by Bradford's method **(Bradford, 1976)**.

c) Measurement of tissue lipid peroxidation (LPO) and malondialdehyde (MDA) levels

MDA is the end product of LPO at cellular or tissue level, therefore the levels of LPO is directly proportionate to the concentration of MDA. The presence of MDA was detected according to the procedure described by **Ohkawa et al. (1979)**.

d) Glutathione reduced (GSH) assay

GSH was estimated based on a method described earlier by **Moron et al. (1979)** with a slight modification. It was expressed as Unit (U)/mg of protein.

e) Glutathione-S-Transferase (GST) assay

GST assay was performed by the procedure explained by **Habig et al. (1974)**. Concentration of the GST was expressed as U/mg of protein.

f) Catalase (CAT) assay

The catalase assay was carried out based on the method and principle described earlier by **Hadwan (2018)**, a slight modification from the method of **Aebi et al. (1984)**. CAT was expressed as U/ mg of protein.

g) Superoxide dismutase (SOD) assay

The tissue level of SOD was quantified based on the procedure formulated by **Kakkar et al. (1984)**. Value of SOD was expressed as U/mg of protein.

3.1.15 Histopathological analysis

The tissue sample, pre-fixed in Bouin's fixative for 24 hours and preserved in 70% alcohol (v/v) were processed for the histopathological study. Liver, kidney, brain, heart, lung, spleen, colon, ovaries, uterus and testis were cut into small sections, dehydrated with the grades of alcohol, embedded in paraffin block and cut into sections of 5 µm thickness (Leica, RM 2125 RTS, Leica systems, Mumbai, India).

3.1.16 Experimental design

Experiment-II To assess antioxidant status, oxidative stress parameter, histopathology, and pathways of organ toxicity induced by cadmium nanoparticles in adult mice: A study on the neuro-hepato-renal axis.

In this experiment, a total of 24 female Swiss albino mice in the age group of 2-3 months, weighing 25 ± 5 g, were allocated into four different groups (n = 6) by random sampling method. As mentioned earlier, CdO-NPs was prepared in 0.9% saline solution and sonicated vigorously for proper mixing in the solution. The animals were administered with the test chemical orally (p. o.) for 30 days. The dosage selected for the experiment are mentioned below-

Group	Dose (p.o., 1 mL/100 g b.w)	Female (number; n)
I (Control)	Vehicle only	06
II	CdO-NPs 2 mg/kg b.w	06
III	CdO-NPs 5 mg/kg b.w	06
IV	CdO-NPs 8 mg/kg b.w	06

Experiment-III Evaluation of oxidative stress, antioxidant status and to trace the molecular mechanism and toxicological pathways that governs the organ specific toxicity in mice intoxicated with copper nanoparticles.

Twenty-four female Swiss albino mice (2-3 months old, weighing 25 ± 5 g) were randomly distributed into four groups (n = 6) of which, one group was control and

other three were treated with CuO-NPs. The period of experiment was 30 days and during that period all the animals were treated daily with the test solution orally (p.o.), according to the plan mentioned below-

Group	Dose (p.o., 1 mL/100 g b.w)	Female (number; n)
I (Control)	Vehicle only	06
II	CuO-NPs 1 mg/kg b.w	06
III	CuO-NPs 5 mg/kg b.w	06
IV	CuO-NPs 10 mg/kg b.w	06

All the animals were observed routinely and body weight, food and water consumption were recorded daily. At the end of the experiment all the animals were sacrificed by decapitation after the intra peritoneal (IP) application of mild anesthesia.

Methodology applied in experiment-II and III

3.1.17 Daily monitoring- body weight, food and water consumption

Body weight of each individual animals were recorded every day before the treatment. In the similar way every day, the animals were fed with a 100 mL of ultrapure water and 50 g of food (dry weight).

3.1.18 Sample collection and organ weight

At the end of the 30^{th} day, all the animals were fasted for 12 hours followed by weighing each animal individually. All the animals were sacrificed by following the IAEC guidelines. Blood samples were collected and stored at -20ºC. Immediately after sacrificing the animals, all the organs were excised and washed in ice-cold saline buffer. Weight of each organs were recorded and later, relative organ weights were computed based on the earlier mentioned formula. Liver, kidney and brain tissue were cut into equal parts carefully, a part of it were fixed in Bouin's fixative

for histopathological study and the other parts were stored at -20 ºC for western blotting.

3.1.19 Hematological assay

The various hematological parameters namely, total RBC, total WBC, concentration of haemoglobin and PCV were measured using the procedure mentioned in earlier section. From the above computed values, various other related hematological parameters (MCV, MCHC and MCH) were calculated.

3.1.20 Estimation of metal accumulation in tissue

Heavy metal accumulation in liver, kidney and brain (cortex) tissue was estimated by using atomic absorption spectrometry (AAS). For the analysis, wet digestion of the tissue sample in nitric acid (HNO_3) and H_2O_2 medium was carried out based on the earlier described method by **Jia et al. (2017**) with minor modification.

3.1.21 Liver and kidney function test, lipid profiles

The markers related to the liver and kidney functions including ALP, AST, ALT, total protein, bilirubin (total and direct), albumin, globulin, urea, uric acid and creatinine were estimated in the serum sample. Lipid profiles parameters including triglyceride, cholesterol, HDL cholesterol and LDL cholesterol, and blood glucose, Na^+, K^+, Cl^+ and Ca^+ ion concentrations were also assessed. All the tests were performed using commercially available kits according to the manufacturer protocol.

3.1.22 Quantification of inflammatory markers

Different biomarkers of inflammatory response were assayed by Enzyme linked immunosorbent assay in serum sample. Various interleukins (IL) namely IL-1, IL-6 and IL-10, leukotriene B4 (LTB4), Prostaglandin E2 (PG E2) and additionally myeloperoxidase (MPO) and total antioxidant capacity (TOAC) were measured using commercially available ELISA kits (Bioassay Technology Laboratory, China) by following manufacturer instructions.

3.1.23 Oxidative stress and antioxidant enzyme assay

Levels of antioxidant (GSH, GST, SOD and CAT) and oxidative stress (MDA) biomarkers were evaluated in liver, kidney, and brain tissues.

3.1.24 Histopathological study

Histological studies were carried out on liver, kidney and brain (cortex) tissues, based on the protocol mentioned in the above section

3.1.25 Western blotting

a) Preparation of tissue homogenate

Tissue homogenate was prepared for the protein estimation and western blot analysis in a sample buffer (lysis buffer) containing 100µL of 100 mM sodium chloride (NaCl), 10 µL of 10 mM Tris-Hydrochloric acid (Tris HCl; pH 7.6), 10 µL of 1 mM Ethylenediaminetetraacetic acid (EDTA; pH 8.0), 10µL of 1 mM Phenylmethylsulfonyl fluoride (PMSF), 10 µL of 1 µg/mL aprotinin and finally the volume was adjusted to 1mL. Then, the tissue samples were thawed to the room temperature and 10% homogenate (w/v) was prepared in the lysis buffer. The sample mixture was centrifuged at 10,000 × g for 15 minutes at 4 ºC.

b) Quantification of apoptotic, anti-apoptotic and inflammatory response markers

The protein sample was denatured and then run in 10% SDS-polyacrylamide gel electrophoresis (PAGE) to separate them based on molecular weight. The separated proteins were transferred to nitrocellulose membranes, blocked for non-specific binding of antibodies, and then incubated with primary antibodies. The antibodies targeting BAX, BCL-2, caspase-3, NF-κB, TNF-α, P^{53}, COX-2, PPARɣ, IL-6 and iNOS were probed into membranes separately and detected by using HRP-conjugated secondary antibodies followed by ECL detection method. The membranes were developed onto X-ray film and analyzed quantitatively using ImageJ software **(Annie et al., 2019)**.

4.1 Summary

- The present study investigated potential organ toxicity of CdO-NPs and CuO-NPs in mice model at low doses. In our study we have used both *in silico* and *in vivo* methods to assess the toxicity of the chemical.
- *In silico* method of toxicity prediction stands as a very useful tool that helps in the quick assessment of toxicity.
- The physical properties for CdO was found to be safe, but its permeability pattern is below the safety range. Its LD_{50} in animals is low, falling under toxicity class III. CdO is active for neurotoxicity, BBB barrier, ecotoxicity, and Cytochrome CYP2C9.
- Similar predictions were seen for CuO where, physical properties of CuO were predicted within the safety range, but their permeability pattern was below the range. The LD_{50} in animals was 413 mg/kg, falling under toxicity class IV. CuO was found active for neurotoxicity, BBB barrier, ecotoxicity, and Cytochrome CYP2C9.
- ADMET profiling predicted the potential toxicity of CdO and CuO, with water solubility, Caco2 value, intestinal absorption, and skin permeability. CdO was predicted to be negative for all cytochrome P450 inhibitors and substrates. Total clearance was low, and it showed no mutagenic potential. The maximum tolerated dose was low and were not a hERG I and II inhibitor.
- *In vivo* study was carried out with CdO- and CuO-NPs of size < 50 nm, pure crystalline solids were used for the toxicity test, and chemical characteristics were confirmed by using FTIR, FETEM and XRD analyses.
- Acute toxicity test was carried out to determine the LD_{50} for CdO-NPs. Mortality percentages were 33.33% and 66.67% in male and female groups at different doses. The LD_{50} values for male was 63.82 mg/kg and 58.21 mg/kg in female, calculated using OECD 423 guidelines and probit analysis.
- After 30 days of CdO-NPs administration, mice showed a significant decrease in mean body weight, feeding patterns, and water consumption compared to the control group. CdO-NPs intake had a prevailing impact on organ weights in treated female mice, with significant effects on liver, kidney, spleen, colon, lung, ovary, and uterus. Hematological parameters revealed major effects of CdO-NPs intoxication in female

mice, with depletion of total RBCs count and hemoglobin concentration, and an increase in total WBCs count. PCV decreased significantly among both control and treated groups.

- The study found a significant increase in cadmium heavy metal levels in liver, kidney, and brain tissues of treatment groups compared to normal mice.
- The study found that CdO-NPs treatment led to significant depletion of protein, albumin, globulin, and increased A/G ratio, total and direct bilirubin in all treated mice compared to normal control mice. The treatment also increased concentrations of kidney function biomarkers, increased ALP, and elevated AST and ALT concentrations. The lipid profile deteriorated, with increased levels of total cholesterol, triglycerides, LDL cholesterol, and decreased HDL cholesterol.
- CdO-NPs administration in female mice for 30 days led to significant oxidative stress in liver, kidney, and brain tissue, with increased malondialdehyde concentrations. The enzymatic and non-enzymatic anti-oxidants, SOD, CAT, GST, and GSH reserves were significantly depleted in these tissues compared to the control group.
- CdO-NPs treatment led to alterations in hepatic tissue architecture, including portal vein congestion, cellular vacuolization, and apoptotic nuclei formation. Kidney tissue sections showed kidney degeneration, glomerular degeneration, vascular congestion, cellular vacuolization, and area of hemorrhage. Histological sections of brain tissue showed normal pyramidal neuronal cells and blood vessels. However, CdO-NPs treatment led to inflammatory infiltration, darkly stained neuron appearance, intracytoplasmic vacuolization, cellular vacuolization, cellular apoptosis, tissue necrosis, tissue fragmentation, cellular degeneration, and congested vessels. The degree of histopathological alterations was more severe at higher doses.
- CdO-NPs increased pro-inflammatory markers in serum, while decreasing anti-inflammatory markers, indicating a potential role in inflammation in the treatment of various diseases. Inflammatory markers like COX-2, TNF-α, NF-κB, IL-6, and iNOS were elevated.
- CdO-NPs treatment significantly altered the expression of apoptotic and anti-apoptotic markers, and tumor-related proteins in liver, kidney, and brain tissues. Pro-apoptotic markers like BAX and active caspace-3 increased, while anti-apoptotic

markers like BCL-2 declined. Tissue suppressor protein P53 expression was also increased, suggesting potential cancer development.

- CuO-NPs intoxication affected female mice's body weight and feeding patterns, leading to a significant decrease in body weight, food, and water consumption compared to the normal control group. Hematological parameters showed decreased RBC counts, hemoglobin concentration, PCV, WBC counts, and MCV, with no significant change in MCH concentration.
- Copper concentration in liver, kidney, and brain organs increased significantly after consumption, with higher accumulation observed at high doses compared to the normal control group.
- Serological assays showed depletion of protein, globulin, and albumin in treatment groups, increased production of bilirubin, and deterioration of liver and kidney profiles.
- The treatment group showed increased total cholesterol and LDL cholesterol concentrations, while decreasing HDL cholesterol, but no significant changes in triglycerides, serum glucose, chloride, potassium, sodium, or calcium concentrations.
- Regular consumption of CuO-NPs triggers inflammatory and oxidative stress response systems, resulting in elevated levels of IL-6, IL-1, FAD, MPO, prostaglandin, leukotriene, and a decrease in IL-10 and TAOC.
- Consumption of CuO-NPs led to oxidative stress and depletion of enzymatic and non-enzymatic antioxidants, with elevated MDA levels in liver, kidney, and brain tissues. Enzymatic antioxidants GST, SOD, and CAT were depleted in liver, kidney, and brain tissues.
- The study examined liver, kidney and brain tissue in mice treated with CuO-NPs. Results showed dilation of central veins, sinusoid dilation, apoptotic nuclei, hepatocyte degeneration, tissue fragmentation, congestion, and tissue hemorrhage. Control mice had normal structures, while high-dose CuO-NPs intoxicated mice showed increased changes. In the kidney, CuO-NPs administration led to glomerular degeneration, area of hemorrhage, inflammatory infiltration, and apoptotic nuclei. In the brain, CuO-NPs administration resulted in darkly stained neuron, inflammatory infiltration, cellular vacuolization, apoptosis, necrosis, cellular degeneration, blood vessel congestion, and tissue fragmentation.

- The study investigated the role of pro-apoptotic, anti-apoptotic, and inflammatory markers in CuO-NPs intoxicated female mice. Results showed increased pro-apoptotic markers BAX and active caspace-3 in liver, kidney, and brain tissue, particularly in high dose groups. Inflammatory markers COX-2, IL-6, iNOS, TNF-α, and NF-κB also increased in treatment groups. CuO-NPs intoxication also led to changes in the expression patterns of P^{53} and PPAR-ɣ, with higher doses potentially causing more severe effects.
- Overall, present study suggests that both CdO-NPs and CuO-NPs have the potentiality to cause toxicity when administered regularly even at low doses.

5.1 References

- Aebi, H. (1984). Catalase in vitro. In *Methods in enzymology* (Vol. 105, pp. 121-126). Academic press.
- Annie, L., Gurusubramanian, G., & Roy, V. K. (2019). Estrogen and progesterone dependent expression of visfatin/NAMPT regulates proliferation and apoptosis in mice uterus during estrous cycle. *The Journal of Steroid Biochemistry and Molecular Biology*, *185*, 225-236.
- Anreddy, R. N. R. (2018). Copper oxide nanoparticles induces oxidative stress and liver toxicity in rats following oral exposure. *Toxicology Reports, 5*, 903-904.
- Assadian, E., Zarei, M. H., Gilani, A. G., Farshin, M., Degampanah, H., & Pourahmad, J. (2018). Toxicity of copper oxide (CuO) nanoparticles on human blood lymphocytes. *Biological trace element research*, *184*, 350-357.
- Balamurugan, S., Balu, A. R., Usharani, K., Suganya, M., Anitha, S., Prabha, D., & Ilangovan, S. (2016). Synthesis of CdO nanopowders by a simple soft chemical method and evaluation of their antimicrobial activities. *Pacific Science Review A: Natural Science and Engineering*, *18*(3), 228-232.
- Banerjee, P., Eckert, A. O., Schrey, A. K., & Preissner, R. (2018). ProTox-II: a webserver for the prediction of toxicity of chemicals. *Nucleic acids research*, *46*(W1), W257–W263. https://doi.org/10.1093/nar/gky318
- Berthelot, M.P.E. (1859). Berthelot's Reaction Mechanism. *Report de Chimie Applique, 2884*.
- Bonsnss, R. W., & Taussky, H. H. (1945). On the colorimetric determination of creatinine by the Jaffe reaction. *Journal of biological chemistry*, *158*, 581-591.
- Bradford M. M. (1976). A rapid and sensitive method for the quantitation of microgram quantities of protein utilizing the principle of protein-dye binding. *Analytical biochemistry*, *72*, 248–254.
- Bugata, L. S. P., Pitta Venkata, P., Gundu, A. R., Mohammed Fazlur, R., Reddy, U. A., Kumar, J. M., ... & Mahboob, M. (2019). Acute and subacute oral toxicity of copper oxide nanoparticles in female albino Wistar rats. *Journal of Applied Toxicology*, *39*(5), 702-716.

- De Jong, W. H., De Rijk, E., Bonetto, A., Wohlleben, W., Stone, V., Brunelli, A., ... & Cassee, F. R. (2019). Toxicity of copper oxide and basic copper carbonate nanoparticles after short-term oral exposure in rats. *Nanotoxicology*, *13*(1), 50-72.
- Demir, E., Qin, T., Li, Y., Zhang, Y., Guo, X., Ingle, T., ... & Chen, T. (2020). Cytotoxicity and genotoxicity of cadmium oxide nanoparticles evaluated using in vitro assays. *Mutation Research/Genetic Toxicology and Environmental Mutagenesis*, *850*, 503149.
- Doumas, B. T., Watson, W. A., & Biggs, H. G. (1971). Albumin standards and the measurement of serum albumin with bromcresol green. *Clinica chimica acta; international journal of clinical chemistry*, *31*(1), 87–96.
- Du Sert, N. P., Ahluwalia, A., Alam, S., Avey, M. T., Baker, M., Browne, W. J., ... & Würbel, H. (2020). Reporting animal research: Explanation and elaboration for the ARRIVE guidelines 2.0. *PLoS biology*, *18*(7), e3000411.
- Finney, D.J. (1971). Probit Analysis. 3rd Edition, Cambridge University Press, London.
- Friedewald, W. T., Levy, R. I., & Fredrickson, D. S. (1972). Estimation of the concentration of low-density lipoprotein cholesterol in plasma, without use of the preparative ultracentrifuge. *Clinical chemistry*, *18*(6), 499–502.
- Garber C. C. (1981). Jendrassik--Grof analysis for total and direct bilirubin in serum with a centrifugal analyzer. *Clinical chemistry*, *27*(8), 1410–1416.
- Genchi, G., Sinicropi, M. S., Lauria, G., Carocci, A., & Catalano, A. (2020). The effects of cadmium toxicity. *International journal of environmental research and public health*, *17*(11), 3782.
- Gitelman, H.J. (1967). An improved automated procedure for the determination of calcium in biological specimens. *Analytical Biochemistry*, *18*, 521-531.
- Gornall, A. G., Bardawill, C. J., & David, M. M. (1949). Determination of serum proteins by means of the biuret reaction. *The Journal of biological chemistry*, *177*(2), 751–766.
- Grigore, M. E., Biscu, E. R., Holban, A. M., Gestal, M. C., & Grumezescu, A. M. (2016). Methods of synthesis, properties and biomedical applications of CuO nanoparticles. *Pharmaceuticals*, *9*(4), 75.

- Guidance, O. E. C. D. (2001). Document on acute oral toxicity. *Environmental Health and Safety Monograph Series on Testing and Assessment*, *24*.
- Habig, W. H., Pabst, M. J., & Jakoby, W. B. (1974). Glutathione S-transferases. The first enzymatic step in mercapturic acid formation. *The Journal of biological chemistry*, *249*(22), 7130–7139.
- Hadwan M. H. (2018). Simple spectrophotometric assay for measuring catalase activity in biological tissues. *BMC biochemistry*, *19*(1), 7.
- Jain, M., Yadav, M., & Chaudhry, S. (2021). Copper oxide nanoparticles for the removal of divalent nickel ions from aqueous solution. *Toxin Reviews*, *40*(4), 872-885.
- Jaishankar, M., Tseten, T., Anbalagan, N., Mathew, B. B., & Beeregowda, K. N. (2014). Toxicity, mechanism and health effects of some heavy metals. *Interdisciplinary toxicology*, *7*(2), 60–72.
- Jia, X., Wang, S., Zhou, L., & Sun, L. (2017). The potential liver, brain, and embryo toxicity of titanium dioxide nanoparticles on mice. *Nanoscale research letters*, *12*, 1-14.
- Kakkar, P., Das, B., & Viswanathan, P. N. (1984). A modified spectrophotometric assay of superoxide dismutase. *Indian journal of biochemistry & biophysics*, *21*(2), 130–132.
- Kind, P. R., & King, E. J. (1954). Estimation of plasma phosphatase by determination of hydrolysed phenol with amino-antipyrine. *Journal of clinical pathology*, *7*(4), 322–326.
- Laios, K., Michaleas, S. N., Tsoucalas, G., Papalampros, A., & Androutsos, G. (2021). The ancient Greek roots of the term *Toxic*. *Toxicology reports*, *8*, 977–979.
- Li, T., Yang, C., Hu, H., Zhang, B., & Ma, L. (2021). The toxico-transcriptomic analysis of nano-copper oxide on gazami crab: especially focus on hepatopancreas and gill. *Food Science and Technology*, *42*, e03521.
- Maruna, R. F. (1957). Serum sodium determination; critical study on colorimetric determination and method. *Clinica chimica acta; international journal of clinical chemistry*, *2*(6), 581-585.

- Mire, S. E., & Snow, L. D. (1986). Evaluation of the polyethylene glycol precipitation method for the estimation of chicken high density lipoprotein cholesterol. *Comparative Biochemistry and physiology. B, Comparative Biochemistry*, *84*(1), 105-110.
- Moron, M. S., Depierre, J. W., & Mannervik, B. (1979). Levels of glutathione, glutathione reductase and glutathione S-transferase activities in rat lung and liver. *Biochimica et biophysica acta*, *582*(1), 67–78.
- Naz, S., Gul, A., & Zia, M. (2020). Toxicity of copper oxide nanoparticles: a review study. *IET nanobiotechnology*, *14*(1), 1-13.
- Naz, S., Gul, A., Zia, M., & Javed, R. (2023). Synthesis, biomedical applications, and toxicity of CuO nanoparticles. *Applied Microbiology and Biotechnology*, *107*(4), 1039-1061.
- Ohkawa, H., Ohishi, N., & Yagi, K. (1979). Assay for lipid peroxides in animal tissues by thiobarbituric acid reaction. *Analytical biochemistry*, *95*(2), 351–358.
- Pelegrino, M. T., Kohatsu, M. Y., Seabra, A. B., Monteiro, L. R., Gomes, D. G., Oliveira, H. C., ... & Lange, C. N. (2020). Effects of copper oxide nanoparticles on growth of lettuce (Lactuca sativa L.) seedlings and possible implications of nitric oxide in their antioxidative defense. *Environmental Monitoring and Assessment*, *192*, 1-14.
- Pires, D. E., Blundell, T. L., & Ascher, D. B. (2015). pkCSM: predicting small-molecule pharmacokinetic and toxicity properties using graph-based signatures. *Journal of medicinal chemistry*, *58*(9), 4066-4072.
- Raul, P. K., Senapati, S., Sahoo, A. K., Umlong, I. M., Devi, R. R., Thakur, A. J., & Veer, V. (2014). CuO nanorods: a potential and efficient adsorbent in water purification. *RSC Advances*, *4*(76), 40580-40587.
- Reitman, S., & Frankel, S. (1957). A colorimetric method for the determination of serum glutamic oxal-acetic and glutamic pyruvic transaminases. *American journal of clinical pathology*, *28*(1), 56–63.
- Schoenfeld, R. G., & Lewellen, C. J. (1964). A colorimetric method for determination of serum chloride. *Clinical chemistry*, *10*, 533–539.

- Shojaei, A., Semnanian, S., Janahmadi, M., Moradi-Chameh, H., Firoozabadi, S. M., & Mirnajafi-Zadeh, J. (2014). Repeated transcranial magnetic stimulation prevents kindling-induced changes in electrophysiological properties of rat hippocampal CA1 pyramidal neurons. *Neuroscience*, *280*, 181-192.
- Song, M. F., Li, Y. S., Kasai, H., & Kawai, K. (2012). Metal nanoparticle-induced micronuclei and oxidative DNA damage in mice. *Journal of clinical biochemistry and nutrition*, *50*(3), 211-216.
- Taha, M. M., Mahdy-Abdallah, H., Shahy, E. M., Ibrahim, K. S., & Elserougy, S. (2018). Impact of occupational cadmium exposure on bone in sewage workers. *International journal of occupational and environmental health*, *24*(3-4), 101-108.
- Teeri, A. E., & Sesin, P. G. (1958). Determination of potassium in blood serum. *American journal of clinical pathology*, *29*, 86-89.
- Thrall, M. A., & Weiser, M. G. (2002). Laboratory procedures for veterinary technicians. *Missouri: Mosby Inc*.
- Trinder, P. (1952). The determination of cholesterol in serum. *Analyst 77*, 321.
- Trinder, P. (1969). Enzymatic Calorimetric Determination of Triglycerides by GOP-PAP Method. *Annals of Clinical Biochemistry*, *6*, 24-27.
- Trinder, P. (1969). Enzymatic determination of glucose in blood serum. *Annals of Clinical Biochemistry*, *6*, 24.
- Tulinska, J., Mikusova, M. L., Liskova, A., Busova, M., Masanova, V., Uhnakova, I., ... & Mikuska, P. (2022). Copper oxide nanoparticles stimulate the immune response and decrease antioxidant defense in mice after six-week inhalation. *Frontiers in Immunology*, *13*, 874253.
- Vijayakumar, T. P., Benoy, M. D., Duraimurugan, J., Suresh Kumar, G., Shanavas, S., Maadeswaran, P., ... & Acevedo, R. (2022). A comparative study on visible-light-driven photocatalytic activity of CdO nanowires and gC 3 N 4/CdO hybrid nanostructure. *Journal of Materials Science: Materials in Electronics*, 1-9.
- Yahia, S. H. (2019). Measurement of Serum Uric Acid Pre and Post Hemodialysis.

- Yang, B., Wang, Q., Lei, R., Wu, C., Shi, C., Wang, Q., ... & Liao, M. (2010). Systems toxicology used in nanotoxicology: mechanistic insights into the hepatotoxicity of nano-copper particles from toxicogenomics. *Journal of nanoscience and nanotechnology*, *10*(12), 8527-8537.
- Yaqub, A., Anjum, K. M., Munir, A., Mukhtar, H., & Khan, W. A. (2018). Evaluation of acute toxicity and effects of sub-acute concentrations of copper oxide nanoparticles (CuO-NPs) on hematology, selected enzymes and histopathology of liver and kidney in Mus musculus. *Indian Journal of Animal Research*, *52*(1), 92-98.
- Young, J. L., Yan, X., Xu, J., Yin, X., Zhang, X., Arteel, G. E., ... & Freedman, J. H. (2019). Cadmium and high-fat diet disrupt renal, cardiac and hepatic essential metals. *Scientific reports*, *9*(1), 14675.
- Zhang, X. D., Wu, H. Y., Wu, D., Wang, Y. Y., Chang, J. H., Zhai, Z. B., Meng, A. M., Liu, P. X., Zhang, L. A., & Fan, F. Y. (2010). Toxicologic effects of gold nanoparticles in vivo by different administration routes. *International journal of nanomedicine*, *5*, 771–781.